DYEING PROPERTIES OF EXTRACTS FROM *Prosopis juliflora* AND *Aloe succotrina* AND EVALUATION OF REMEDIATION POTENTIALS OF THEIR WASTE BIOMASS

BY

ODERO MARK PETER

B.Sc. Analytical Chemistry (UoE), MSc. Analytical Chemistry (Moi)

A THESIS SUBMITTED TO THE SCHOOL OF SCIENCES AND AEROSPACE STUDIES, DEPARTMENT OF CHEMISTRY AND BIOCHEMISTRY IN PARTIAL FULFILLMENT OF THE REQUIREMENT FOR THE AWARD OF DOCTOR OF PHILOSOPHY DEGREE IN ANALYTICAL CHEMISTRY, MOI UNIVERSITY

OCTOBER 2021

DECLARATION

Declaration by the Candidate

This research thesis is my original work and has not been presented for the award of any degree course in any other University. No part of this thesis may be reproduced without the prior written permission of the author and/or Moi University.

Odero Peter Mark ……. Date: . …….....

PHD/ACH/02/18

Declaration by Supervisors

This thesis has been submitted for examination with our approval as University supervisors.

Prof. Ambrose K. Kiprop: ……..… Date: ……..

Department of Chemistry and Biochemistry

Moi University, Eldoret, Kenya

Dr. Isaac O. K'Owino: ……..….. Date:…….…….....

Department of Pure and Applied Chemistry

Masinde Muliro University of Science and Technology, Kakamega, Kenya

Adjunct Senior Lecturer Moi University

Dr. Milton Arimi: …… Date: ……..…….

Department of Chemical Engineering

Moi University, Eldoret, Kenya

DEDICATION

This thesis is dedicated to my dear parents Florence Midega Odero and Pius Kita Odero for the sacrifices they made to ensure that I get quality education. And to Beatrice Abidha, Joyce Aluchio and Arianna Kita Odero.

ACKNOWLEDGEMENT

First, to God almighty the giver of life and who granted me favour and grace to be where I am today. Special appreciations to the World Bank Group through the African Centre of Excellence II in Phytochemicals Textile and Renewable Energy (ACE II-PTRE) who awarded me a scholarship towards the attainment of this PhD degree.

My most sincere appreciations go to my supervisors namely Prof. Ambrose K. Kiprop, Dr. Isaac K'Owino and Dr. Milton Arimi who have been insightful, helpful and invaluable during the course of this work. Together, they have mentored and moulded me into a better analytical chemist. My appreciation also goes to Prof. Fredrick Keng'ara, Dr. Phanice T. Wangila and Dr. Jackson Cherutoi for their helpful input and critique during this learning process. I am equally grateful to Mr. John Khafafa of Moi University Textile Engineering department and Paul Kipkorir of the department of chemistry and biochemistry for their unwavering help and commitment during the course of this work.

My appreciation goes to my colleagues and fellow ACE II - PTRE PhD and MSc colleagues at the Department of Chemistry and Biochemistry especially Samuel Baker Obakiro, Scolastica Manyim, Calvince Ondijo and Micah Omari for their collective efforts, wisdom and friendship. Finally, I am grateful to Prof. Stephen Ojwach of University of Kwa-Zulu natal for his expertise and for giving me access to several equipment.

ABSTRACT

In the last two decades, natural dyes have increasingly become popular over their synthetic counterparts due to their environmental friendliness and biodegradability. Whereas synthetic dyes are persistent, allergy inducing and carcinogenic, natural dyes are eco-friendly with no side effects. The main objective of this study, was to assess the potential of *Aloe succotrina* leaves and the heartwood of *Prosopis juliflora* as sources of natural dyes and the potential of their waste biomass as modified adsorbents for the removal of synthetic dyes. The specific objectives of the study were to evaluate the dyeing properties of *A. succotrina* and *P. juliflora*, to identify the compounds responsible for the dyeing properties and to determine the remediation potential of their waste biomass. Maceration was used in the extraction of *P. juliflora* while solvent extraction was used for extracting *A. succotrina*. These were used for dyeing cotton fabrics using pre-mordanting, simultaneously mordanting and post mordanting techniques. The dyed fabrics, were then tested for their suitability using wash, light and rub fastness. Gas chromatography tandem Mass spectroscopy (GC-MS) and Fourier transformed Infrared (FTIR) spectroscopy were used for evaluation of dyeing compounds. Biochar derived from the waste biomass were characterized by X-ray Diffractometer (XRD) for their crystalline properties, FTIR for their functional groups and scanning electron microscope (SEM) for surface properties. Batch adsorption experiments were conducted for the removal of synthetic dyes. The waste biomass, were transformed into biochar at pyrolysis temperatures of 300℃ and 500℃. The dye from *P. juliflora*, had good fastness results with the additions of mordants improving both colour and wash fastness. Dyes from *A. succotrina*, had good colour and light fastness with poor wash fastness. Except for the case of pre-mordanting, the use of mordants did not improve the wash fastness. The GC-MS analysis of *A. succotrina* revealed the presence of 27 compounds among them the dyeing compound orcinol, which could be the main source of colour. For *P. juliflora*, 16 compounds were identified among them catechol, a naturally occurring benzenediol resulting from the pyrolysis of catechin, a flavonoid responsible for yellow pigment in natural dyes. The XRD, FTIR and SEM results showed, a difference in physical and chemical properties with the biochar pyrolyzed at 300℃ being organic and amorphous while the biochar prepared at 500℃ being less organic and porous. For the adsorption of reactive red 120 (RR120), the q_{max} calculated for the most effective biochar PJ300 was 20.643 mg/g against that of the commercially activated carbons of 243.5 mg/g. For methyl violet 2b (MV2b), the q_{max} calculated for most effective biochar was 82.530 mg/g against the commercially activated carbons 504 mg/g. The experimental data fitted into Freundlich isotherm for RR120, which indicates that the process is heterogenous and Langmuir for MV2B, which indicates monolayer adsorption. In conclusion, the extracts from both plants showed potentials to be used as natural dyes. The biochar derived from the waste biomass of the two plants are recommended as alternatives to commercially activated carbon in the remediation of textile effluents.

TABLE OF CONTENTS

LIST OF TABLES

LIST OF FIGURES

LIST OF EQUATIONS

DEFINITION OF TERMS AND ABBREVIATIONS

A. succotrina- Aloe succotrina

AS 300 - Biochar derived from *Aloe succotrina* pyrolyzed at 300 ℃

AS 500 - Biochar derived from *Aloe succotrina* pyrolyzed at 500 ℃

ASAL - Arid Semi-Arid Lands

ATR - Attenuated total reflectance

BC - Before Christ

CIE- Commission International de L'eclairage /International commission of illumination

EDX - Energy Dispersive X-Ray

ESI - Electron Spray Ionization

FTIR - Fourier Transformed Infrared

GC-MS - Gas Chromatography coupled with a Mass Spectrometer

GAE- Gallic acid equivalent

ISO - International standards organization

IUCN- International Union for Conservation of Nature

K/S - Colour strength

M/Z ratio - Mass to charge ratio

Mordants - Binders between fabric and natural dye

MV 2b- Methyl violet 2b

Natural dyes- Dyes from natural sources

Phytochemicals- Biologically active chemicals naturally synthesized by plants

PJ 300- Biochar derived from *Prosopis juliflora* pyrolyzed at 300 ℃

PJ 500- Biochar derived from *Prosopis juliflora* pyrolyzed at 500 ℃

P. juliflora- Prosopis juliflora

Remediation- removal from a matrix

R.I - Retention Index

RR120 - Reactive red 120

R_t - Retention Time

SEM - Scanning electron microscope

TEM - Transmission electron microscope

TFC - Total flavonoid content

TIC - Total ion chromatogram

TPC - Total Phenolic content

UV-VIS- Ultraviolet Visible

XRD - X Ray Diffractometer

CHAPTER ONE

INTRODUCTION

1.1 Background of the study

The distinct art of dyeing has been historically passed on from one generation to another having been previously used in its primitive forms from as early as 3500 BC (Kant, 2012). Historically, it has been a symbol of art in various societies and a medium of visual communication linked with the cognitive and cultural evolution of humanity (Ardila-Leal *et al*., 2021). Colourants i.e substances that give colour, exist in two broad categories namely dyes and pigments. Dyes, are coloured compounds owing to their inherent possession of chromophores and auxochromes which are functional groups such as hydroxyl (OH), sulphonic acid (SO_3H), amino (NH_2) groups that absorb and reflect light in the process imparting colour (Kumar *et al.,* 2021). These polar auxochromes and chromophores together confer upon dyes their solubility in water, enabling them to bind to the fabric through interactions with oppositely charged groups of the fabric structure (Sharma *et al.,* 2021).

Pigments on the other hand are organic or inorganic compounds, that are coloured but insoluble in water. The first forms of natural dyeing processes were primitive, time-consuming and involved basic applications such as rubbing and boiling with fabric with varying success (Kant, 2012; Key Colour, 2016). The dyes, were principally obtained from natural sources such as plants, insects or sea animals and extracted with water or oil, and then used to decorate substances such as fabric, skin, jewellery, clothing and caves. For example, some of the oldest known natural dyes known are alizarin (a red dye derived the madder plant and scale insects: kermes and *Dactylopius coccus*), indigo (derived from the

leaves of *Indigofera tinctoria* and *Isatis tinctoria*) and tyrian purple extracted from glands of snails (Benkhaya, El Harfi, & El Harfi, 2017; Gupta, 2019; Key Colour, 2016).

Dyes from natural sources were cheap, environmentally friendly, locally available but unsustainable. This is because, despite its advantages, natural dyes were limited in the ranges of shades they could produce, they were not easily reproducible and they had poor fastness to wash, light and rub (Kant, 2012). Thus, over time, the primitive methods of dyeing have transformed to more sophisticated methods that involve the use of organic and inorganic binders known as mordants. Presently, more advanced and sophisticated techniques are being used to make the dyeing process of both natural and synthetic dyes not only successful but also appealing to the eye. This has led to the suggestion that the main attraction of any piece of fabric is the colour so that most commercial fabrics are bound to fail no matter how excellent they are if they are unsuitably coloured (Guha, 2019; Jothi, 2008; Kant, 2012).

Over the past century, both the textile and the dye industries have grown massively with an excess of 8×10^5 metric tonnes of dyes globally manufactured annually owing to the extensive range of colour pigments and consistent colours produced (Slama *et al.*, 2021). This, is evidenced by dyed garments becoming more affordable, a phenomenon which truly coincides with the Industrial Revolution and the rise of the middle class. The increased production of dyed textiles is to fulfil the ever-increasing need for suitable cloth materials which are suitably dyed due to the increasing world human population and the ever-increasing need for industries that also consume the various forms of dyes such as food, tannery, cosmetic, paper, plastics, paint, ink, photographic and agricultural industries (Sharma *et al.*, 2021; Shindhal *et al.*, 2021).

Presently there are over 100,000 known variation of commercially available colour shades (Benkhaya, El Harfi, & El Harfi, 2017; Dwivedi & Tomar, 2018). Previously, dyes were extracted from different parts of the tree such as the bark, roots, leaves and flowers which were in turn used for dyeing clothes, skins and fabric using simple and archaic techniques. This, later changed in the mid-19th century as the first synthetic dyes was accidentally discovered by William Perkins in 1856 (Abuamer, Maihub, & El-ajaily, 2014; Kant, 2012). The first synthetic dye, endeared many in the industries as it had a brilliant colour when applied to silk, was easily reproducible and could be produced cheaply (Singh, & Singh, 2015). Soon after, more synthetic dyes were industrially synthesised marking the beginning of technology shift from natural dyes to synthetic dyes in what was referred to as the "dyes revolution" (Slama *et al.,* 2021). This was fuelled by the fact that synthetic dyes were readily available at economical prices and also they could easily produce a wide variety of colours, reproducible shades and dyes that were reliable in terms of fastness to light, wash and colour (Abuamer *et al*., 2014).

Since the invention of Perkin's Mauveine dye in 1856, numerous developments have been witnessed in the dyeing industry such as the development and the publication of the first edition of the Colour Index in 1924, which is a numerical system of classification of dyes based on their application and chemical classes. Presently, there are tens of thousands of synthetic organic colourants that have flooded the global markets which have been adopted to varying degrees. While other dyes, have been commercially successful and embraced, others are rarely used or have been discontinued mainly due to their high costs, low fastness or potential toxic effects (Hagan, & Poulin, 2021).

Synthetically manufactured dyes have not only been invaluable in the textile industry, but they also have found importance in other dyeing intensive industries such as the food, pharmaceutical, beauty and leather industries. As the synthetic dyes gained more use courtesy of the industrialization and the rapid increase in population of different nations, so did its adverse effects on the environment and health begin to manifest (Lellis, Fávaro-Polonio, Pamphile, & Polonio, 2019). This is because, potentially up to between 10 % - 15 % percent of toxic unspent dyes and dye auxiliaries, are usually discharged directly to the environment especially in third world countries where effluent treatment methods are often costly or non-existent with another 2 % making its way as direct effluent discharge even after remediation techniques have been employed (Dwivedi & Tomar, 2018; Elango, Rathika, & Elango, 2017; Jadhav, & Jadhav, 2021).

The toxicity of most synthetic dyes is because these dyes are manufactured mainly from petrochemical sources that contain amine groups and also because mordants used to fix the dyes to the fabric are based on certain heavy metals such as chromium, lead, nickel and tin (Affat, 2021). The most common forms of synthetic dyes currently being used in the textile industries are azo based which constitute more than 60% of total dyes used in the textile industry. This dyes, have the common functional group -N=N- which unites two symmetrical (or asymmetrical), identical or non-azo alkyl and aryl radicals and are easily manufactured by simple diazotization and coupling reactions (Benkhaya, M'rabet, & El Harfi, 2020; Khan *et al.*, 2021).

More recent research suggests that some of these dyes are not only persistent and recalcitrant in the environment but also carcinogenic, mutagenic and harmful to human beings and to other life forms such as the aquatic habitat (Almeida *et al*., 2014; Benkhaya

et al., 2019; Elshaarawy, Sayed, Khalifa, & El-Sawi, 2017). The carcinogenicity of azo dyes has been studied since 1979 when it was first reported in Shanghai China after a group of people working in the textile industry were reported to have cancer of the bladder (You *et al*., 1990). Presently, quite a number of synthetic dyes have been linked to not only bladder cancer, but also to other forms of cancers such as cancers of the rectum, stomach, ovaries and prostates. Apart from their perceived carcinogenicity, azo based dyes have also been proven to be mutagenic and teratogenic to various organisms and forms of life. Other negative effects that have also been recorded concerning this type of dyes include severe allergic reactions, asthma and bronchitis (Khan *et al.*, 2021).

As a result of health and environmental concerns, present research has shifted back to the possible development and use of natural dyes as viable alternatives to synthetic dyes. This is due to their perceived safety, environmental friendliness and potential medicinal values. Presently, both large scale and small scale manufactures have begun adopting natural dyes with an estimated worldwide demand of approximately 100,000 tonnes especially used for the making sportswear, lingerie and other high demand market products (Gao & Cranston, 2008).

Although useful and often presented as an alternative to synthetic dyes, quite a few natural dyes can be made reproducibly with stability and with colourfast that rivals synthetic dyes. Thus, in most cases they require mordants to assist in the dyeing processes the advantage being that it’s possible to have both natural and synthetic mordants in natural dyeing processes. Mordants are found in nature in various forms such as wood ash, acidic fruits like lime, stale urine and plants extracts such as those of *Aloe vera*. Synthetically they can be manufactured as aluminium chloride, salts of iron, copper, nickel, chromium etc

(Zubairu & Mshelia, 2015). The application of mordants have not only helped the binding of dyes to clothes but it has also been proven that different mordants can yield different colours and shades at different temperatures and pH (Samanta & Agarwal, 2009; Samanta & Konar, 2011).

Synthetic mordants are often poisonous to human beings and harmful to the environment especially because most of them are based on salts of heavy metals like chromium, lead, zinc and copper among others (Abuamer *et al*., 2014; Shweta Singh & Singh, 2018). It is for this reason that a number of research have been done also for development of more eco-friendly alternatives to synthetically manufactured mordants such as the use of tannins, alum and natural essential oils as potential natural mordants(Freeman, 2017; Rossi, Araújo, Brito, & Freeman, 2015). Another possible alternative is to remove the excess heavy metals present in the effluents and dyes before they are released into the environment.

There are several processes that have been used to attempt to remove and eliminate the presence of dyes and heavy metals in textile effluents. They include methods such as microfiltration, ultrafiltration, reverse osmosis, chemical precipitation, centrifugation, ion exchange adsorption etc. Most of the above said methods are very costly to industries especially those in third world countries as the prerequisite for each method is that they must be able to separate the aqueous phase from the dyes (Malik, Lata, & Singhal, 2015). Sorption processes such as biosorption and adsorption, have slowly become a choice of removal for most industrial and agricultural wastes as it is cheaper, reliable and readily available.

Biosorption, is a general term used to mean that a biological compound has been used for the removal of metals or compounds of interests such as dyes through a metabolically

mediated process. This is not only limited to the use of plants only but can also be algae, fungi and even activated enzymes (Carmen & Daniela, 2012; Dan, 2001). Although, not traceable to any particular source or time, the general idea of adsorption has been present for a long time (Raskin & Ensley, 1999). Apart from sorption processes being cheap, they also have a major advantage of being very efficient and are more importantly they are considered to be essentially "green". Meaning that, when compared to conventional methods that often involve the process of chemical treatments, this processes more often than not require no chemicals and are mostly *in situ* i.e. remediation is done directly without the need for being taken to another site (Chuluun *et al*., 2009). For example, there has been a wide spread use of forest wastes as bio sorbents to remove a variety of heavy metals such as lead (Pb), arsenic (Ar) and Chromium (Cr) (Yu *et al.,* 2015).

1.2 Statement of the Problem

The last century has seen a rapid growth in the dye and textile industries as a result of the corresponding rapid human population growth. Presently, synthetic dyes have been used not only for the textile industry, but they have also found a place in the agro, pharmaceutical, food, cosmetic and other industries for the purposes of colouring. An estimated 10% -15 % of dyes and mordants used in the textile industry are lost during the process of dyeing as unused waste waters with an estimated 2% making its way into the environment as direct discharge in the form of aqueous effluents (Dwivedi & Tomar, 2018).

Most of this dye and effluents, are composed of both organic and inorganic substances which are toxic and persistent in the environment. In fact, according to (WHO, 2002), textile waste effluents from factories can be a direct health risk to the environment and to

humans because exposure to such waters have been suggested to cause a myriad of health problems such as cancer, allergies, immune suppression, respiratory disorders, circulatory disorders, problems with the central nervous system among many other diseases. This especially when the dyes and the mordants used in the industrial process, escape to the environment even in small portions and are drank or are used domestically for other purposes.

These waste waters are not only toxic to the environment but are also persistent in the environment and therefore not easily decomposed. For example, dyes such as reactive blue dye have been shown to have a half-life of about 46 years at pH 7 and at a temperature of 25 °C (Carmen & Daniela, 2012) with the effects of such dyes being felt even at concentrations as low as 1 mg/L presenting visual pollution to waterbodies in return affecting light penetration and biological life forms in water. This, has led to several research attempts first to develop environmentally friendly dyes such as natural dyes and secondly to develop appropriate methods for the removal and reduction of dyes in textile effluents (Garg, 2018; Jothi, 2008).

Despite most researchers attempting to focus on the development of natural dyes as viable alternatives to the toxic synthetic dyes, more often than not the dyes developed have poor fastness, lack reliability and cannot be standardized. Equally, with the existence of many remediation techniques such as coagulation, ultrafiltration, bioremediation and others which are often specific and expensive, there is need for the development of not only dyes of reliable shades but also remediation techniques that are not only cheap, but also reliable and non-selective.

In this research study, we have developed natural dyes of reliable shades of colour from *Prosopis juliflora* and the *Aloe succotrina* plants with potential benefits to the communities where this plants freely grow. This is because, the *P. juliflora* exist in abundance as an invasive in many arid and semi-arid regions of Kenya, while *A. succotrina* grows freely in the Kerio valley. Subsequently, the waste biomass from this research, have also been developed into potential adsorbents for environmental remediation. This study aims to address these problems by producing natural dyes from the leaves of *Aloe succotrina* and *Prosopis juliflora* and to evaluate their dyeing properties on cotton fabric for their possible potentials as future sources of natural dyes. The plant extracts were studied for their chemical compositions and properties that give them their dye giving properties. Finally, the remaining biomass of the plants after extraction of the dyes, were transformed into biochar and their properties studied and used to remove selected environmental pollutants commonly present in textile effluents.

1.3 Significance of the study

The study will result to the development of natural dyes that are ecofriendly, of reliable shade and biodegradable from two plants namely *Prosopis juliflora* which is a noxious weed and *Aloe succotrina*. Equally, the waste biomass from the extraction process, will be pyrolyzed in biochar which will in turn be used as a cheap and non-selective alternative remediation process for the adsorption of the anionic dye reactive red 120 and the cationic dye methyl violet 2b.

1.4 Objectives of the study

1.4.1 Main objective

The main objective of this study was to assess the dyeing properties of *Aloe succotrina* leaves and the heartwood of *Prosopis juliflora* both as sources of natural dyes and the potentials of their subsequent waste biomass as modified adsorbents.

1.4.2 Specific objectives

The specific objectives of this study were to;

i) Assess and optimize dyeing conditions of extracts from *Aloe succotrina* leaves and the heartwood of *Prosopis juliflora*.

ii) Identify compounds responsible for the dyeing properties of the *Aloe succotrina* and *Prosopis juliflora*.

iii) Evaluate the sorption potentials of pyrolytically derived biochar from *Aloe succotrina* and *Prosopis juliflora* against reactive red 120 and methyl violet 2b.

1.5 Justification

Currently, most research on the dye and textile industries have shifted back to natural dyes that are eco-friendly and not as hazardous to the environment as their synthetic counterparts in what is referred to as “back to nature” research. This is because, most synthetic dyes are toxic with adverse effects on almost all forms of life. The toxic effects of synthetic dyes have been studied since the 1970’s when they were first shown to cause cancer of the bladder (You *et al*., 1990). Presently, research on the same has shown that these dyes not only cause cancer of the bladder, but also cancer of the rectum, stomach and ovaries. Apart

from being carcinogenic, they are also allergy inducing causing irritations of the skin and lungs especially to children (Chengaiah, Rao, Kumar, Alagusundaram, & Chetty, 2010). Approximately 10 % - 15 % of dyes in the textile dyeing industry are lost in the dyeing process with about 2 % being directly dumped into the environment with the world health organisation (WHO), stating that the direct release of dyes into the environment causes a direct human risk. Dyes such as RR120 and MV2B despite being commonly used, are serious pollutants with brilliant colours with visible colouration to water and wastewater bodies at concentrations as low as 1ppm. With the problems associated with synthetic dyes, natural dyes have been suggested as a potential substitute for them. This is because, as opposed to their synthetic counterparts, natural dyes are considered safe, environmentally friendly with little side or no effects. This is because they occur naturally in the plants and the environment and are easily degradable (Chengaiah *et al*., 2010; Shachi Singh & Verma, 2011).

Recent studies on several properties of natural dyes show that dyes extracted from plants such as those from turmeric not only impart dyes to fabric, but also medicinal properties such as antiseptic properties, antimicrobial properties and antifungal properties (Chengaiah *et a*l., 2010; Shachi Singh & Verma, 2011). Despite the disadvantage of synthetic dyes and the advantages of natural dyes, the dye industry still relies heavily on synthetic dyes and because most of these effluents are harmful, most industries in developed nations have set systems for the removal and remediation of the said textile effluents with varied success depending on the method of removal (Dwivedi & Tomar, 2018).

Most of the methods used for the removal of dyes from textile effluents, are very expensive and once they reach municipal wastewater treatment plants, the methods used are not

sufficiently efficient to remove them. For this reason, adsorption has been mooted as a potentially cheap, available and effective technique (Garg, 2018). This is because, depending on the type of adsorbent, adsorption is very effective and can be customized for intended use especially when the dyes are too stable for conventional methods (Tim Robinson, McMullan, Marchant, & Nigam, 2001).

Presently, adsorption is considered among the cheapest and the most effective of the removal methods for dyes in the treatment of textile effluent (Yagub, Sen, Afroze, & Ang, 2014). Where-as commercial adsorbents like activated charcoal and synthetic zeolites are costly, present research has shifted to cheaper adsorbents through the valorisation of agricultural wastes, the use of composite materials and the use of locally available soils as probable sources of adsorbents.

This research, has developed natural dyes of reliable sheds of colour from the *Prosopis juliflora* and *Aloe succotrina* plants with potential benefits to the communities where this plants freely grow. This is because, the *P. juliflora* plant, exist freely as an invasive weed in several parts of the country with adverse effects on animals with little or no use to humans. On the other hand, dyes from *A. succotrina* plant, have also been developed, this possibly providing a source of income to the communities. The waste biomass from this research has also been developed into potential adsorbents for environmental clean-up.

1.6 Scope of the study

This research work, covers the extraction of natural dyes from the heartwood of *P.julilfora* and the leaves of *A. succotrina* and their application on cotton fabric. Optimization of dyeing parameters such as temperature, pH, time, concentration, mordanting techniques and colour strength (K/S) were done. Equally, the research covers the pyrolysis of the waste

biomasses of the two plants into biochar at two different temperatures and the subsequent use for the removal of two synthetic dyes namely reactive red 120 and methyl violet 2b.

1.7 Hypothesis of the study

i) Extracts of *Prosopis juliflora* and *Aloe succotrina* will not dye fabric

ii) Pyrolyzed waste extracts of the waste biomasses of both *Prosopis juliflora* and *Aloe succotrina* will not adsorb reactive red 120 and methyl violet 2b.

CHAPTER TWO

LITERATURE REVIEW

2.1 Introduction to dyes, pigments and the theory of colourants

2.1.1. Dyes and pigments

Colour, as it is now known has been a source of fascination to humankind, on both social and aesthetic grounds (Kumar *et al.,* 2021). The incredible and adept nature of the human eyes in recognizing even the most miniscule colours difference cannot be overemphasized (Dassanayake, Acharya, & Abidi, 2021). Throughout human history therefore, dyes, pigments and other colourants have continued to be the prominent impression in various articles of commerce wherein the manufacture of nearly all known commercial products incorporates colour at one or more of its stages. Today, the world has more than 9,000 colourants registered under 50,000 trade names and more are being used for various industrial applications. This is due to the wide range of tints and hues that have been achieved through synthesis of different chemical dyes, given the fact that colour observed is directly related to the molecular structure of the dye.

Dyes are natural or synthetic substances that are used to impart colour to or change the colour of materials (leather, textiles, paper, and other materials that are otherwise collectively called substrates) by physically or chemically bonding to them (Dutta *et al.,* 2021). The colourings are such that they are not easily altered by light, heat, washing, or other such factors which the coloured materials are likely to be exposed to (Mustroph, 2014). The entomology of the word ‘‘dye’’ is from the Middle age English word ‘‘deie’’ and the old English word ‘‘dag’’ and ‘‘dah’’. The first known use of modern form of the word ‘‘dye’’ is historically traced to before the 12th century.

Dyes, are characteristically distinguishable from pigments which are finely ground solids dispersed in a liquid (for example ink and paint), and do not chemically bond to the substrate (Kumar *et al.,* 2021). In addition, dyes are principally organic compounds usually ringed or aromatic compounds of carbon while pigments are either inorganic compounds (devoid of carbon atoms) or organic compounds which possesses brighter colours than the former. Ochres (coloured clays that are present as soft deposits within the earth crusts) are a representative example of one of the oldest known pigments used in early cave walls to impart yellow and red colour in combination with white chalks (Kumar *et al.,* 2021).

Dyes are also distinguished by their ability to dissolve in aqueous systems (water) or other organic solvents. On the other hand, pigments are significantly insoluble in water, inorganic and organic media; hence they are instead suspended in solvents to be used as application media or as the carrier liquids (Pittis *et al.,* 2018). Additionally, dyes are applied onto substrates to which they have affinity to, unlike pigments which can only impart colour to polymeric substrates through a mechanism not comparable to that of dyes because the surface-only colouration entails mixing the pigment with the polymer prior to fibre or moulded article formation.

Dyes, impart colour to their substrates owing to their ability to selectively absorb certain wavelengths of light, which on the other hand, determines the colour of the dye i.e. the specific wavelength(s) of light that are reflected or transmitted by the dye, and not those that are absorbed determine their colours (Beaver, 2018; Van der Kooi, Elzenga, Staal, & Stavenga, 2016). Another point of difference between dyes and the pigments is that the particle size of pigments are much larger than that of dyes and for this reason, the latter are

not stable to ultraviolet light whereas the former are markedly stable to ultraviolet light (Kumar *et al.*, 2021).

Dyeing, one of the oldest aspects in the world of fashion, is historically dated to as far back as the Neolithic period (between 10,000 BC to 4,000 BC). Evidences of dyed fabric came into better recognition when man shifted from living in the embellished caves and adopted a sedentary lifestyle with the domestication of animals, growing crops and building civilization (MSK, 2021). In Chinese history for example, evidences of dyeing processes that utilize utilize plant materials, rocks as well as insects have been traced back to more than five centuries ago and the earliest script in the history of dyeing fabric claims to be about 2600 BC from China (MSK, 2021).

Application of dyes onto textiles is referred to as dyeing. Another synonymous term used in the textile industry is printing. However, printing is a different application in that the colour is applied to a localized area with the desired patterns unlike in normal dyeing where colour is applied to the entire textile (Gooby, 2020). Digitized textile printing came into the lime lights in the 1990s strictly as a prototyping tool as well as the vehicle for printing smaller batches of fabric solely for special market articles (Koseoglu, 2019; Tyler, 2005). With the nascent paradigm shift and the introduction of synthetic dyes and pigments, digital textile printing (DTP) has boasted of a more creative potential and entrepreneurial business models in textile design that offers unprecedented opportunity for designers to offer bespoke products with superior customization of designs (Polston, Parrillo-Chapman, & Moore, 2015).

2.1.2. Structures and properties of colours and pigment

The hues of dyes are invariably contingent on the wavelength of the light that they absorb (Gupta., 2019; Selim, & Mohamed, 2017). Since the wavelengths of light (in the electromagnetic spectrum) that a dye absorb depends on its structure, it is plausible that any change which affects the pie-electron system will affect the hue. Thus, structural changes that causes the absorption band to shift to longer wavelengths (that is yellow > orange > red > violet > blue > green) are termed as a bathochromic shifts. The reverse of this shift i.e. the shifting of the absorption band from a longer to a shorter wavelengths) is referred to as hypsochromic shift (Maltanava, Poznyak, Belko, & Samtsov, 2021; Tanaka *et al.*, 2021).

Just as there is a relationship between the physical and chemical properties of organic compounds, there should exist definite relationships between the colour and constitution of dyes. For example, the commonly known hexacyclic benzene is a colourless compound but its isomer (fulvene; a cyclic cross-conjugated molecule) is a yellow compound. At least four different theories have been advanced to explain and correlate the colour of dyes with their molecular structures (Nidhi, 2020). One such earlier attempts by Otto Witt (a German Chemist) in the year 1876 led to the popular Witt's theory or the Chromophore-Auxochrome theory. In his theory, Witt postulated that the colour of a dye is attributable to certain chemical groups (colour-bearing groups) with multiple bonds, collectively known as chromophores (from Greek *chroma*-colours and *phores*-bearing) and auxochromes. Compounds with a chromophore are thus called chromogens (Nidhi, 2020). The chromophores are unsaturated groups that absorbs light and reflects the same at specific angles to give the hue (Chakraborty, 2014). Representative examples of

chromophores include the quinonoid group, ethylenic bond (-C=C), nitroso group (-N=O), acetylenic bond (C≡C), carbonyl group (-C=O), azo group (-N=N-), the nitro group (O=N=O). Thus, dyes are coloured, ionising, aromatic organic compounds based fundamentally on the cyclic structure of benzene (aryl rings with delocalised electron systems).

Chromophore groups, are divided into two major groups i.e those in which a single chromophore can impart colour to the compound as in the cases of compounds containing -N=N, -N=O, $-NO_2$, =N=N-N, -N=N→O and the phenyl-quinonoid, and those with more than one chromophore that impart the colour such as in >C=O and >C=C< groups. A typical example is seen in acetone (with a single >C=O group, a potential chromophore but is colourless) and biacetyl (in which two >C=O groups are present and therefore imparts a yellow colour). In this context, it was concluded that as the number of chromophores increases for a particular dye, so does the depth of the shade of the dye increase (Kumar *et al.*, 2021; Nidhi, 2020).

Witt went ahead to substantiate that the auxochromes (salt-forming groups) complemented the chromophores in deepening the colour of dyes (Nidhi, 2020). Examples of auxochromes are include the hydroxyl (-OH), amino ($-NH_2$), halogen (chloride, bromide or iodide) and carboxylic acid (-COOH) groups. Most auxochromes are either acidic or basic. For example, the pale yellow of the dye 1,3-dinitronapthalene deepens to orange red when an hydroxyl group is introduced to the ring to form the dye Martius yellow (2,4-dinitro-1-naphthol). Within this frame of reference, the hydroxyl group acts as an auxochrome whose presence deepened the colour of 1,3-dinitronapthalene (Kumar *et al.*, 2021). In other words, an auxochrome modifies the ability of the chromophore to absorb

light, altering the wavelength or intensity of the absorption. Because of their salt-forming nature, auxochromes readily form salts with basic or acidic groups, and their presence can also chemically transform a coloured compound (without any salt-forming groups) into a dye that can be fixed more or less permanently onto a fiber. Thus, the Witt's theory advances that permanent fixing of dyes onto textile fibers is plausibly triggered by chemical bond formation between the fiber and the auxochrome.

Witt's theory underwent modification following more probing research which unravelled that chromophores in dyes are chemically electron-withdrawing groups on the one hand, and the auxochromes are, on the other hand, electron-donating groups. These studies shone further light that the two groups in any typical dye are connected by a conjugated system (Lech, 2020).

Another colour and constitution theory is the Armstrong Theory (Quinonoid theory). In 1885, Armstrong postulated that all colouring matters may be represented by quinonoid structures (*p*-or o-). He therefore held that if a particular compound can be formulated into a quinonoid form, it is coloured. Otherwise, it is not coloured. Using this theory, benzene is colourless (which is true in practice) while benzoquinones are typically coloured compounds. However, this theory fails to explain the colour observed in all known compounds. For instance, iminoquinone and diiminoquinone which are chemically made up of a typical quinoid structure are colourless compounds (Nidhi, 2020).

The most recent, non-empirical and plausible explanation for the existence of colour in dyes is provided by Modern Theories: Valence Bond Theory (VBT) and Molecular Orbital Theory (MOT). The two theories understand the colour of dyes from molecular and optical viewpoints. The major point of divergence between them is that in the former, electrons

are treated in pairs while in the latter electrons are treated singly (Kumar *et al.,* 2021). The Valence Bond Theory (or the Resonance Theory) holds it that chromophores are groups of atoms which contain π-electrons. Thus, it postulates that in the ground state, the electron pairs of a molecule are in a state of oscillation and absorbs photons of appropriate energy (when positioned in the path of a beam of light) and gets excited (Goel, 2020).

The wavelength of the photon of light adsorbed is contingent on the energy difference between the ground and the excited states. Thus, in transferring from ground to excited states by the absorption of radiation, specific colours are given off. Auxochromes on the other end of the spectrum are visualized as groups that tend to foster electronic resonance through their interaction with the unbonded electrons of the π-electron system in the aromatic ring. By so increasing resonance, auxochromes ultimately augments the intensity and the absorption of specific wavelengths of light and conjointly shifts the optical phenomenon to a longer wavelength, resulting in the deepening of the dye colour. This therefore reasonably implies that increment in resonance (owing to the presence of auxochromes) deepens the colour of dyes (Goel, 2020).

The theory also suggests that the dipole moment changes as a result of oscillation of electron pairs. The observed order for the excitation of the different groups is: N=O > C=S > N=N > C=O >C=N >C=C (Goel, 2020). The Valence Bond Theory also expounds the relationship between colour and the symmetry of the dye molecule or its transition dipole to be as a result of increment in the number of charged canonical structures which subsequently deepens the colour of the dye. Consequently, higher possibilities and longer paths for a change to oscillate in a compound translates into longer wavelengths of light being absorbed and thus deepening of the colour of the dye (Goel, 2020).

The Molecular Orbital Theory on the other hand posits that whenever a molecule absorbs a photon of light, an electron is transferred from the bonding (non-bonding) orbital to an antibonding orbital. The electrons are essentially σ (sigma), π (pie) or n (non-bonding) electrons, with the higher energy states being anti-bonding orbitals. In association with the anti-bonding orbitals (σ and π bonds) respectively are the σ* and π* orbitals. Based on the different types of electron present in a molecule, different types of electronic transitions are possible which are usually accompanied by release of light of some colour (Goel, 2020).

Despite the diverse structures and colours produced by different dyes, the broadest classification system categorizes dyes into synthetic and natural dyes as elaborated in the subsequent sections. These may be further divided into different groups basing on certain features such as chemical classes and methods of application (Bonetto *et al*., 2015; Selim, & Mohamed, 2017).

2.2 Synthetic dyes

The term synthetic dyes is used to refer to industrially manufactured dyes produced by large scale industries, originating mainly from petrochemicals and organic sources. They are less commonly referred to as ‘‘coal tar dyes’’, alluding to the fact that they used to be manufactured from substances which, until lately, were only derived from coal tar and petroleum (Kumar *et al.,* 2021). Before the discovery of synthetic dyes, the dyeing industry at large relied heavily on the use of natural dyes. Earlier strides in pursuit of manufacturing both synthetic and semi-synthetic dyes were made by Barth on the dye indigo carmine in 1743 (De Keijzer *et al.,* 2012), Woulfe on picric acid in 1771, and later Scheele on murexide in 1776 and finally Runge on aurin in 1834 (Polston *et al.,* 2015). The first

successful synthetic dye was accidentally produced by William Henry Perkins in the year 1856 as he was trying to synthesize quinine, the main ingredient in most medicines used for the treatment of malaria during that era.

Perkins discovery was made after he realized that the compound aniline, could be oxidized and used to colour silk. He synthesized a brilliant purple colour that was named mauveine thus opening doors for the idea to synthesize different colours (Kant, 2012; Mościpan, Zarębska, & Kulesza, 2016; Samanta & Agarwal, 2009). Figure 2.1 below shows the molecular structure of mauveine i.e the first synthetic dye.

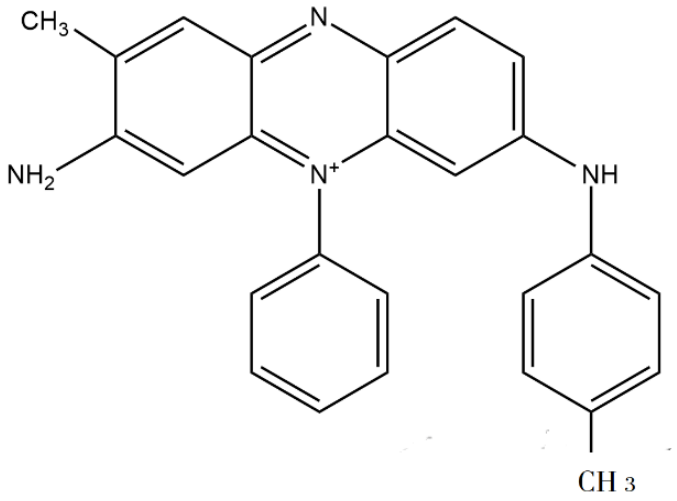

Figure 2.1: Structure of mauveine (the first synthetic dye)

Presently, most synthetic dyes are of the form of aromatic organic compounds that are azo based or contain the -N=N- bond. Recent studies show that there exists in excess of over 100,000 commercial dyes available in the world markets with an estimated amount of approximately 10,000,000 tons of dyes being produced to meet the ever-increasing demand in the textile, leather, cosmetic and pharmaceutical industries (Dwivedi & Tomar, 2018; Gao & Cranston, 2008). This coupled with the fact that the global apparel market is worth well above the 1.5 trillion USD mark. These dyes have not only been used in the textile

industry, but they have also found a prominent place in inks, in biomedicine as biological stains, in the pharmaceutical industry as colourants for medicine, in sweets for colouring and in foods and drinks industries as food colours.

The introduction of computers (following the industrial revolution) and the growth of computer colour matching (CCM) systems i.e processes where colours can be closely monitored from the manufacturing to the dyeing process in a method that produces identical shades from batch to batch has made significantly increased the reliability of shades and colours of synthetic colours. In addition, chemists have invented and continue to invent various methods and strategies to facilitate the synthesis of other complex synthetic dyes for specific applications (Ziarani, Moradi, Lashgari, & Kruger, 2018).

All these industrial processes have led to the continuous discharge of these harmful synthetic dyes into the environment hence becoming an environmental nuisance, especially in places where they previously did not exist. This has led to colouration of water bodies such as rivers, streams and lakes which sometimes reduces the amount of sunlight penetration leading to death of photosynthetic aquatic plants. Research suggests that reduction in the quality and colour of water, occurs at very low dye concentrations such as 1 mg/L and directly impacts the aesthetic merit, transparency and solubility of gases in water with some of the dyes having an extended half-life of more than 45 years (Bonetto *et al*., 2015).

Additionally, some of the dyes are poisonous and therefore can exert acute and/or chronic effects on organisms (contingent on their concentrations and the exposure time) and in some cases they are lethal to aquatic organisms especially when untreated effluents are discharged into such water bodies (Lellis *et al.,* 2019; Berradi *et al.,* 2019). Up to 60 % of

commercially used synthetic aromatic dyes used in various commercial applications are azo type dyes. Recent research on azo type dyes shows that they are stable in their states and very persistent in the environment meaning that they are very difficult to biodegrade. The major problem being that they are not only persistent in the environment but also carcinogenic (Almeida *et al*., 2014; Yaseen, & Scholz, 2018). In fact, the carcinogenicity of azo dyes has been studied since the early 1979 when they were first reported among a group of textile workers in Shanghai China when it was first shown to cause cancer of the bladder (You *et al*., 1990).

Presently, synthetic dyes and their derivatives have been linked to not only bladder cancer, but to also other forms of cancers such as cancer of the rectum, stomach, ovaries and prostates. This is because when they are ingested even in low concentrations, they form active metabolites such as aromatic amines especially when they get into contact with the intestinal microflora (Almeida *et al.,* 2014). Other negative side effects that have also been recorded concerning this dyes include severe allergic and respiratory reactions, asthma, bronchitis, itching among others (Hassaan & Nemr, 2017).

It is estimated that the textile industry worldwide has a consumption of approximately 10,000 tonnes/year of dyes with a possibility of about 100 tonnes/year of dyes being discharged into the environment as direct textile effluents. Textile effluents, are sources of organic and inorganic compounds due to the fact that quite a number of dyes require fixative i.e. mordants which are mostly heavy metals that are not only environmental hazards even in trace amounts but also bio accumulators leading to long term harm (Hassaan & Nemr, 2017).

Synthetic dyes, have been classified by their compositions and the specific type of material that it can be applied to. For example, acidic dyes which are majorly used for nylon, silk and modern polyesters. Such types of dyes cannot be used for cellulosic fabrics that cannot withstand acidic dyes. Azo types of dyes, basic dyes which are sometimes used for wool and silk etc. Synthetically manufactured dyes, have since become invaluable in the food, textile, leather and pharmaceutical industries due to their economical prices, light fastness and colour fastness as compared to their natural counterparts and their wide arrays of colours which are more than 10, 000 variants (Hassaan & Nemr, 2017).

2.2.1 Classification of Synthetic Textile dyes

Synthetic dyes can be categorized based on two major classifications i.e. based on their application and chemical structures. The classes based on their structures include azo dyes, anthraquinone dyes, nitro and nitroso dyes, sulphur dyes and xanthene dyes. While those dyes based on their application include acidic dyes, basic dyes, reactive dyes, disperse dyes, reactive dyes (Abuamer *et al*., 2014; Chavan, 2011; Yagub *et al*., 2014).

2.2.1.1 Dyes based on their method of application

Synthetic dyes can be classified based on their method of application. Table 2.1 below shows a table of classification of dyes based on their method of application.

Table 2.1: Classification of dyes based on their method of application adopted from Hunger (2007).

Class	Method of application	Chemical types
Acid	Starting from neutral to acidic bath.	Anthraquinone, xanthene, azo, nitro, and triphenylmethane.
Basic	From acidic dye baths.	Hemicyanine, azo, oxazine, cyanine, azine diazahemicyanine, xanthene, diphenylmethane, triarylmethane, acridine, anthraquinone and
Direct	From neutral/ mildly alkaline bath with electrolytes.	Phthalocyanine, azo, oxazine, and stilbene.
Disperse	Thermofixation or padding	Benzodifuranone, azo, anthraquinone, nitro, and styryl.
Reactive	Reaction with active sights on the dye with functional groups on fabric under the influence of both heat and pH.	Anthraquinone,formazan, azo, oxazine phthalocyanine, and basic.
Sulphur	Aromatic substrate vatted with sodium sulphide and reoxidised to insoluble sulphur-containing products on fibre	Indeterminate structures
Vat	Water-insoluble dyes solubilised by dropping in sodium hydrogen sulphite, then exhausted on re-oxidised and fibre.	Indigoids and anthraquinone.

2.2.1.2 Dyes based on chemical structure

These are dyes that have their building blocks based on functional groups classified as nitro, xanthene, sulphur, anthraquinones, indigoids, azo and nitroso. These are represented in Figures 2.2 - 2.7 below.

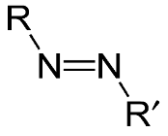

Figure 2.2: Azo functional group

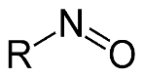

Figure 2.3: Nitroso functional group

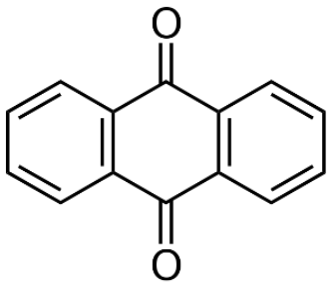

Figure 2.4: Anthraquinone functional group

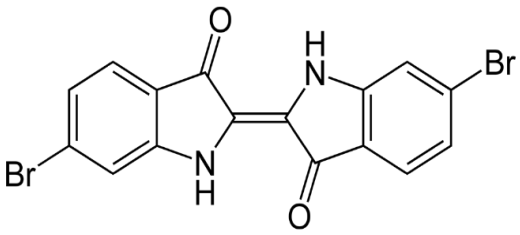

Figure 2.5: Indigoid functional group

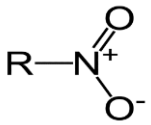

Figure 2.6: Nitro dyes

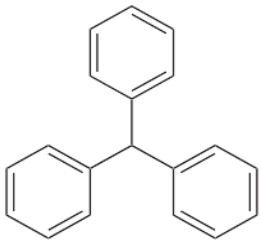

Figure 2.7: Triaryl methane dyes

2.3 Natural Dyes

The terms natural dyes or pigment, are generic terms that are used to refer to dyes that are extracted from several parts of the plant like the leaves, the roots, the bark and the wood or from living organisms such as fungi, molluscs and insects (Chengaiah *et al*., 2010; Kasiri & Safapour, 2014; Pervaiz, Mughal, & Khan, 2016). History records the use of natural dyes to be as early as during the Bronze Age, where they employed archaic methods of extraction and application to ensure that the dyes stick onto the respective fabric materials. For example, naturally coloured plants were used for dyeing via rubbing to the respective fabric. From the madder dyed robes made specifically for King Tut who reigned in the years 1332-1323 BC up to the biblical account of scarlet linens that were dyed with insects, natural dyes have been used time in memorial for the purpose of colouring of linen (Ford, 2017).

Because of the increased concerns about the toxicity of synthetic dyes to the environment and to various forms of life, several interests have risen on the suitability of natural dyes as an authentic substitute to synthetic dyes based on the assumption that they are actually derived from the environment hence they are safe (Guha, 2019; Shweta Singh & Singh, 2018). This, has been proven though to not always be the case as natural dyes from the plants such as *Haematoxylum campechianum* commonly referred to as logwood have been shown to contain the compound hematoxylin and hematein which are toxic and can enter the body through several means including absorption by the skin causing serious irritation and allergic reactions.

This notwithstanding, it is generally accepted that most natural dyes are safe to use. This coupled with the matchless appearance of natural dyed fabric, natural dyes now appear to be favoured especially by the green and environmentally minded consumers. In fact, there is a new niche market for such natural dyed textile this is especially with the rich who love unique products (Gokhale, Tatiya, Bakliwal, & Fursule, 2004; Jihad, 2014). The major disadvantages of most natural dyes is that it is practically impossible to reproduce a shade and to standardize a certain colour (Samanta & Konar, 2016).

Natural dyes also have very poor colourfastness, wash fastness and lightfastness. In fact quite a large number of them have medium to very low colour and lightfastness meaning that for them to be effectively used as dyes for fabric material, special binders that bind the dyes to the fabric commonly referred to as mordants have to be used (Jihad, 2014). These mordants will vary greatly for different natural dyes based on their modes of actions and bonding, this is based on the fact that most natural dyes are complex organic structures and

how they interact with the mordants will result to how the dyes will bind itself to the fabric (Ferreira, Hulme, Quye, & Ferreira, 2004).

2.3.1 Classifications of natural dyes

Natural dyes have been classified in several ways depending on their unique chemical structure and particular way of bonding that is, chemically where the substrate bonds strongly with the dye compounds or held by physical forces. Unlike synthetic dyes with a single entity, the structure of natural dyes comprises of complex chemical constitutions with mixtures of closely related chemical compounds.

2.3.1.1 Classification based on the method used in application of the dye

They include acid dyes, mordant dyes and direct dyes. Acidic dyes are those dyes that are applied at acidic pH of below 7, and mainly used for dyeing fabrics made from wool e.g. dyes from anthraquinone structure. Direct dyes are those that are water soluble, and generally sold cheaply. They stick directly to the cloth and do not necessarily need a mordant or anything to make them stick. Most direct dyes are bright with poor wash fastness. Mordant dyes on the other hand, entails the vast majority of dyes known to man, these are dyes that would otherwise not stick to fabric unless mixed with a mordant or a fixer mostly metallic salt. The major advantage of mordant dyes being that they have a better wash, colour and light fastness compared to acidic or direct dyes (Samanta & Konar, 2011).

2.3.1.2 Classification based on chromophore type

Natural dyes can also be categorized based on their chromophoric structures into seven subgroups i.e chlorophyll dyes, carotenoids dyes, anthraquinone dyes, flavonoid dyes,

curcuminoid dyes, naphthoquinone dyes and indigoid dyes (İşmal & Yildirim, 2018; Samanta & Agarwal, 2009). Their basic structures are as in the figures 2.8 – figure 2.13 below.

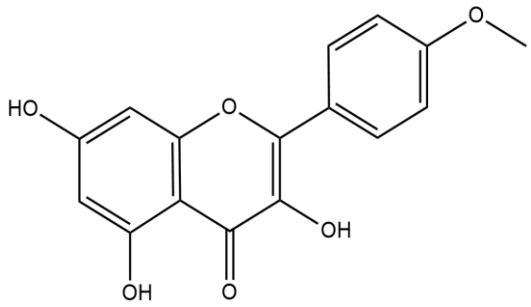

Figure 2.8: Kaemferol- A flavanoid

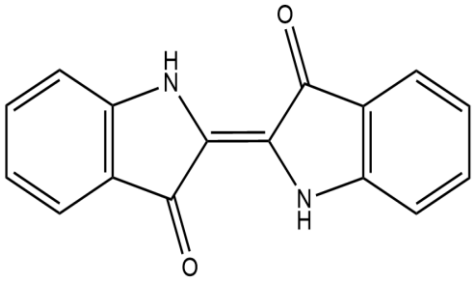

Figure 2.9: Indigoid structure

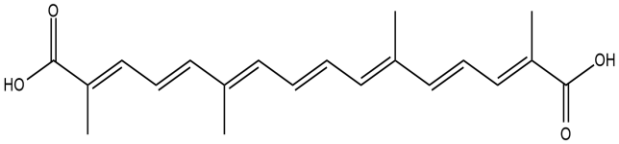

Figure 2.10: Crocetin a carotenoid

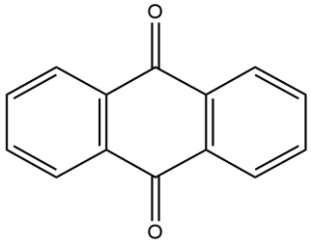

Figure 2.11: Anthraquinone structure

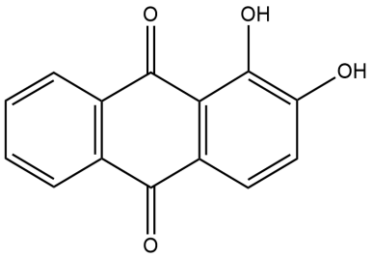

Figure 2.12: Alizarin, an anthraquinone

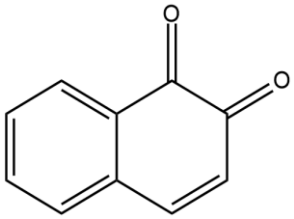

Figure 2.13: Naphthoquinone

2.3.2 Medicinal properties of natural dyeing plants

Previous research shows that natural dyes are not only useful for imparting colour but also, they have been shown to be medically useful. For example, the dyeing plant *Punica granatum* has been reported to have potent antimicrobial activities due to tannins that are

present in it in large numbers. The *Lawsone* spp commonly referred to as henna plant also has antimicrobial activities majorly due the presence of naphthoquinones (Singh, Jain, Panwar, Gupta, & Khare, 2005). They tested four dyeing plants i.e. *Acacia catechu, Kerria lacca, Quercus infectoria, Rubia cordifolia* and *Rumex maritimus* against several common pathogens after impartation of the said dyes on fabric and found them to have antimicrobial activity although at lesser intensities when compared to the raw dyes.

Clothes dyed with *Aloe vera* and neem tree were evaluated for their antibacterial and antifungal properties and were found to be very effective with the antibacterial properties being very good and durable even after the cloths were washed severally with soap and water.

2.3.3 Extraction methods for natural dyes

Extraction is hailed as the first and most important procedure in recovering dyes from natural sources and in any natural products research (Chemat *et al.*, 2019). The methods used for extraction are usually termed sample preparation techniques. They principally involve the process of separating the compounds of interest from the natural product matrices. Thus, extraction is the most important step towards obtaining high quality dye from the plant/animal products. This is because with the right methods, there is a maximization of the possible yields. This is important because in the end, the extraction yields determines whether the method that is used to extract the dye can be of economic value or not hence utilization in the dye industry.

Extraction methods will vary greatly depending on the nature of the source i.e. whether it is from the plant root, bark, stem, mineral or animal source (Butnariu, 2016; Manhita, Ferreira, Candeias, & Barrocas Dias, 2011). Thus, for any extraction purpose to be counted

as successful, the method/ technique used plays a big role. In the end the solvents and the technique used should at least be able to retain the integrity of the needed extracts, it should be green where possible, of low toxicity, simple and evaporates easily.

Advances in analytical techniques have recently improved the accuracy and time with which analysis of phytochemicals are performed but they still rely on the choice of the appropriate extraction methods, input parameters and the exact nature of natural product being investigated (Altemimi, Lakhssassi, Baharlouei, Watson, & Lightfoot, 2017). Some of the salient factors that influences the efficiency of extraction are the matrix properties of the part used, the extracting solvent(s) used, temperature and the extraction time used (Nawaz, Shad, Rehman, Andaleeb, & Ullah, 2020).

Various extraction techniques are used for recovering dyes from plant matrices but are dictated by the extracting power of solvents, the required phytochemical group and the effect of using heat and/or mixing to perfect the recovery. For this reason, multiple solvents may be mixed in varying proportions to enable the extraction of dyes from dry pulverized materials (powder of plants) to overcome the interference of water as an inherent constituent of plant cells (Altemimi *et al.,* 2017). A recently growing extraction procedure centers on using multiple solvents sequentially so as to limit the number of analogous compounds in the desired yield of the extracted dyes. The common solvents used in serial extraction in order of their increasing polarity are hexane < chloroform < ethyl acetate < acetone < methanol < ethanol < water (Altemimi *et al.,* 2017). The precise extraction techniques used in recovering dyes from natural sources are discussed in the penultimate subsections. The crude extracts obtained from such extraction procedures maybe further concentrated on a rotary evaporator.

2.3.3.1 Aqueous extraction method

This is done by finely reducing the plant parts of interest into small pieces by mechanical grinding. This is done so as to increase surface area to volume ratio, and heated together for given amounts of time of extraction via any optimum method (Samanta & Konar, 2011).

2.3.3.2 Solvent extraction

Because some compounds cannot be extracted by water only such as phenolics and aglycones which also contribute to colour, then sometimes it is necessary to use a mixture of solvents such as water: alcohols or methanol: ethanol mixtures in different ratios sometimes acidified to prevent degradation (Samanta & Agarwal, 2009)**.**

2.3.3.3 Extraction by non-aqueous and other solvent-assisted methods

This includes methods such as, solid phase microextraction and supercritical fluid extraction (SFE) which have recently gained preference due to several environmental concerns on solvent use. SFE has been proven to be very effective as a method of extraction of organic compounds such that it has been touted to soon be a standard for extraction techniques of plant materials and food items. Other modern methods used for extraction include ultrasound-assisted extraction method and the microwave-assisted extraction method (Ford, 2017; Samanta & Agarwal, 2009; Biesaga, 2011; Chemat *et al*., 2019).

2.4 Phytochemical screening of natural dyes

Phytochemical screening is a classical qualitative technique that is relatively simple, fast and cheap. It entails subjecting preparations of aqueous and organic extracts from natural products (for example heartwood, sap, leaves, stems, whole plant, roots, root bark, stem

bark, fruits and exudates) that acts as reservoirs of secondary metabolites in plants (Chiocchio *et al.*, 2021). The extracts are usually screened for the presence of secondary metabolites such as flavonoids, terpenes, glycosides, saponins, volatile oils, anthraquinones, terpenoids, alkaloids, tannins and phenols. Standard test procedures are usually employed during phytochemical screening and these are available in literature for each secondary metabolite (Suleiman & Ateeg, 2020).

2.5 Mordants and Mordanting

Derived from the latin word modere, meaning to bite, mordants are special binders or substances that fix dyes on to a respective substrate that would otherwise not easily bind, hence increasing the colour fastness, wash fastness and lightfastness. In principle, mordants will bind to the substrate or fabric on one end and bind with the dye on the other hence making the dye process possible (Teli, Sheikh, & Shastrakar, 2013). Most natural dyes are very unstable when dyed on fabric, this is because due to their phytochemistry, they are readily oxidizable in the presence of air hence easily losing their colours and shades.

Equally most dyes naturally don't easily combine readily with fabric and will therefore need a medium of making them bind onto the fabric hence the need for mordants which assist the binding process making them more stable to environmental conditions such as light, sweat, rub and wash (Chao, Ho, Cheng, Kao, & Tsai, 2017). The figure 2.14 below, shows an example of the natural dye alizarin and how it binds to fabric with the assistance of a mordant.

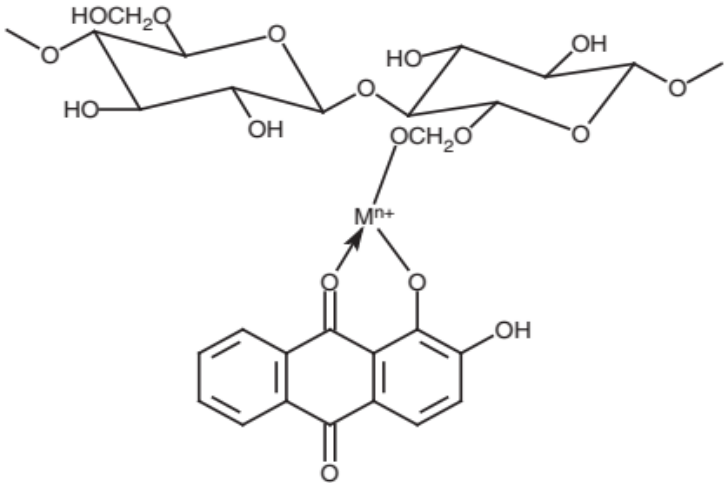

Figure 2.14: A natural dye (alizarin) bonding with the assistance of a mordant (M^{n+})

Traditionally and industrially, the mordanting process has been primarily achieved through three major methods i.e. by pre mordanting, simultaneous or meta mordanting and post mordanting. In pre mordanting technique, the fabric is mordanted in a separate bath prior to being dyed while in simultaneous mordanting, the fabric is dyed simultaneously in the same dye bath. For post mordanting, the fabric is dyed first in the dye bath then afterwards it is mordanted. Mordants, are broadly classified as metallic mordants, natural mordants or oil mordants. (Samanta & Agarwal, 2009).

2.6 Optimization of dyeing parameters

Optimization refers to the process of improving of system performance by obtaining the maximum benefits from it or the discovering of conditions that give a procedure the best possible response (Almeida, Erthal, Padua, Silveira, & Am, 2008). In analytical chemistry, optimization of process variables and parameters has always been done traditionally by using the one variable at a time technique. In this method, one parameter is changed at a time while all the other factors are kept constant (Almeida *et al*., 2008). For textile dyeing, various parameters such as pH, dye concentration, dyeing time and dyeing temperature

greatly affect the dyeing quality of the fabric and therefore must first be optimized prior to the dyeing process (Siddiqua *et al.,* 2021).

The classical optimization method that assesses each factor at a time with other dyeing parameters kept constant at a specific level complicates the optimization process. Ultimately, it will require adequate time and repeated experimental runs to arrive at the optimal conditions for dyeing. However, the interactive effects of such parameters on the responses are hardly reached through the classical method. Yet it is important that during the optimization study the most influential variable is identified, its effect on the behaviour and performance of dyeing should also be considered. These drawbacks associated with the classical approach has led to the introduction of a more efficient statistical response surface methodological approach (Siddiqua *et al.,* 2021). This includes many statistical or mathematical procedures that are valuable even in the presence of multivariate interactions and helpful for developing, improving, and optimizing different processes (Rehman, Adeel, Ahmad, Mateen, & Amin, 2021).

2.7 Analytical techniques for characterization of natural dyes

There is a myriad of analytical techniques utilized in characterization of natural dyes and other organic compounds (Lee, Kang, Lee, & Lee, 2013; Lech, 2020). This includes traditionally spectrophotometric methods such as ultraviolet-visible (UV-Vis) spectroscopy, Fourier transform infrared spectroscopy (FTIR), mass spectrometry (MS), Nuclear magnetic resonance (NMR) spectroscopy and chromatographic techniques such as gas chromatography (GC), thin layer chromatography (TLC) and High performance liquid chromatography (HPLC) which are useful for both qualitative and quantitative

analyses. In recent past, more and more of this techniques have been combined into one instrument for more efficiency in what are referred to as hyphenated techniques such as GC-MS, LC-MS etc.

2.7.1 Gas chromatography-Mass Spectrometry

A gas chromatography-mass spectrometer commonly referred to just as GC-MS is a hyphenated technique combining two very reliable analytical chemistry machines namely the Gas chromatography and the Mass spectrometer. Whereas the gas chromatograph part is very effective in the separation and analysis of complex matrixes, the mass spectrometer on the other hand is able to distinctly identify a compound based on the mass to charge ratios of different fragments of a compound often denoted as (*m/z*). Because of its sensitivity, simplicity and accuracy in resolving and measuring different mixtures of compounds, the GC-MS is now considered one of the most powerful, important and widely used instrument in analytical chemistry (Al-rubaye, Hameed, & Kadhim, 2017).

Recently, the GC-MS has gained use in the chemistry of natural products to resolve compounds that are volatile and of low molecular weight in mixtures and in complicated matrix, especially in dereplication studies. This, entails identifying a previously identified compound or as it is commonly named “finding known unknowns ” (Bouslimani, Sanchez, Garg, & Dorrestein, 2014). Due to the costs related to extraction, isolation and characterization of compounds, the MS has been proven to be very useful in dereplication studies as compounds, can be rapidly and efficiently analysed saving money and time (Yang, Zhang, & Ju, 2019).

The GC-MS was used by (Jayakumari, Ram, Rao, Kumaran, & Ramesh, 2017), to determine the compounds present in *Aloe barbadensis*, in turn getting 15 compounds.

Equally (Pakkirisamy, Kalakandan, & Ravichandran, 2017) used a GC-MS to identify bioactive compounds from *Curcuma caesia* Roxb commonly referred to as black turmeric, affording a total of 15 bio-active compounds. Extracts of *Acacia nilotica* were evaluated for their dye giving abilities with 12 compounds being identified (Jamadar & Sannapapamma, 2018).

All this, showing that indeed the GC-MS coupled with other analytical instruments act as a very strong instrument for the identification of compounds especially when matched with libraries such as the NIST library for matching of fragmentation patterns, similarities and retention indexes.

2.7.2 Ultraviolet-Visible Spectroscopy

The Ultra-violet visible spectroscopic technique commonly referred to as UV-Vis, is both a qualitative and quantitative analysis technique commonly used in analytical chemistry for measurement of colour and to characterize molecular species. The technique harnesses the absorption spectroscopy in the ultraviolet light region i.e from 180 nm to 380 nm and the visible light wavelength region i.e 380 nm to 750 nm to characterize dyes and colourants. It is considered as one of the most basic analytical techniques that is important for identification of major classes of biomolecules which possesses certain light-absorbing functional groups (chromophores). Upon absorbing UV-Vis light, such chromophores get excited from the ground state to excited states and in the process gives characteristic spectra which are used in the identification of the specific group of chromophores (Kalaichelvi & Dhivya, 2017).

In quantitative analysis, the scan is done at a fixed wavelength and the absorbances obtained are used in quantification of the desired compound or group of compounds based

on a linear line of absorbance vs a series of known standards. In a UV-Visible spectrum of a dye or any colourant, the maximum wavelength (λ_{max}) is usually indicative of the main hue or colour in that compound (Samanta & Agarwal, 2009). For most natural dyes, the spectra will not have just one peak but several peaks. This is because these dyes are usually made up of not just one colour but a group of several organic compounds each with a characteristic functional group responsible for giving the dye its colour. For example, UV spectra of colourants extracted from the neem plant showed two absorption peaks at 275 and 374 nm (Samanta & Agarwal, 2009) while those extracted from the *Trigonella foenum* plant, had several absorption peaks around 259.2, 265.6, 358.4, 371.2 and 396.8nm (Selvam *et al*., 2015).

2.7.3 Fourier Transform Infrared spectroscopy

The Fourier Transform Infrared spectroscopy (FTIR) is a powerful qualitative analytical technique used to obtain the infrared spectrum of absorption and emission of dyes by using the mathematical process (Fourier transform) to translate the interferogram into the actual spectrums. It fundamentally identifies the chemical bonds and/or functional groups in dyes. Here, infrared red (IR) bands, are commonly used to identify functional groups based on their excitations in the fingerprint region (Deena, Jebaseelan, & Roopan, 2019; Ezyanie Safie *et al*., 2015; Nema, Khare, Pradhan, & Gupta, 2012). The technique, relies on the principle that different functional groups absorb at different wavelengths of light. The bands are usually between the regions 4000 to 400 cm^{-1} and are characteristic of certain bonds.

2.8 Textile effluents and their effects on the environment

With the increase in population and the need for more textile products to serve the populace, the textile industry has grown exponentially over the past 50 years. This means that there has also been a rapid increase in the use of complex synthetic-coloured dyes used to impart colour onto fabric. It has been shown that the textile industry is one of the industries that releases a high volume of waste waters (Carmen & Daniela, 2012).

These waste waters are not only toxic but are also persistent in the environment. For example, the reactive blue dye has been shown to have a half-life of about 46 years at pH 7 and at a temperature of 25 °C (Carmen & Daniela, 2012). Also, textile effluents carry a large degree of organic compounds ranging from the carcinogenic azo based dyes to organochlorines and heavy metals that are generally used as mordants for the stabilization of colour. Their effects being felt due to the fact that most dyes are easily visible in water even at concentrations of 1 mg/L presenting visual pollution to waterbodies hence affecting light penetration and biological life forms in water.

Visual pollution, affects the aquatic biota, hindering both the processes of photosynthesis and oxygenation. Most dyes being azo based have been proven scientifically to be carcinogenic, persistent, allergens and mutagenic. Heavy metals present in textile effluents such as cadmium, Iron, Zinc, Cobalt are not only toxic to the environment but also to human beings causing a wide variety of health complications such as cancer, diabetes, kidney problems etc (Ram & Sonia, 2017).

2.9 Research overview of dyes selected for removal from aqueous solution

2.9.1 Methyl Violet 2b

Methyl violet dyes represent a group of intensely coloured synthetic organic dyes that are cationic and basic in nature. They are dark green crystals, which when dissolved in water, have a brilliant purple colour and intensity belonging to the triphenyl methane class (Dahri, Raziq, Kooh, & Lim, 2013; Raziq, Kooh, Dahri, & Lim, 2017). This classification is due to the presence of three aryl groups that are individually bonded to a nitrogen atom (that otherwise interacts with one or two other methyl groups). Their basicity is due to the existence of a positive charge on the amino group.

Methyl violet 2b, is one of the most common shades of methyl violet dyes heavily used in industries such as textile, rubber, paint and petroleum industries (Raziq, Kooh, & Lim, 2017). The other two common dyes that are listed under methyl violet dyes are Methyl Violet 6B and Methyl Violet 10B (crystal violet) which are hexamethyl and pentamethyl pararosaniline chlorides, respectively i.e. the three dyes differ only in the number of methyl groups attached to the amine functional group.

This group of dyes are revered for their broad application in textiles (for dyeing of silk, leather, straw, paper, bamboo and cotton), paints, print inks (Ofomaja, Ukpebor, & Uzoekwe, 2011) and bacteriological gram staining (Bonetto *et al*., 2015). Methyl violet 2b (IUPAC name: N-(4-(bis(4-(dimethylamino)phenyl)methylene) cyclohexa-2,5-dien-1-ylidene) methanaminium chloride) is soluble in both water and ethanol. It is a yellow dye in solutions of lower pH but changes its colour to violet with increase in pH to about 3.2. Figure 2.15 below, shows the molecular structure of the methyl violet 2b dye.

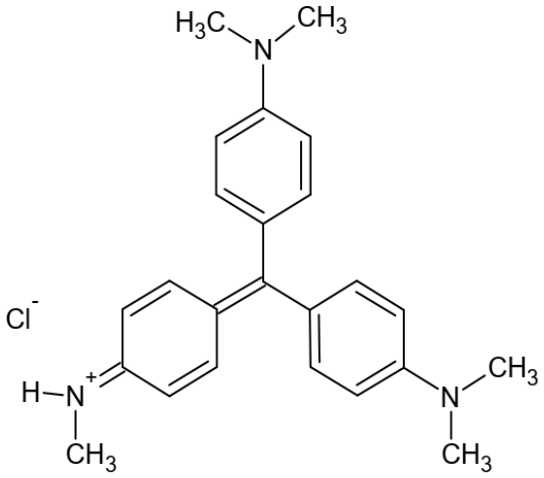

Figure 2.15: Molecular structure of Methyl violet 2b

When released untreated into the environment, Methyl violet 2b has been shown to be toxic, interfering with the growth of bacteria in water and other natural processes such as photosynthesis. Equally, when long term exposure is involved, it has also been suggested to be not only carcinogenic but also mutagenic, mitotic and allergenic, inducing severe skin and eye irritations especially to children. Its toxicity is indicated to be due to the release of its decomposition products such as carbon monoxide, nitrogen monoxide and carbon dioxide among other products (Ofomaja *et al*., 2011).

2.9.2 Reactive red dye 120

Reactive dyes is a group of important commercial dyes that owing to their superior binding ability through forming covalent bonds between their reactive groups and the surface groups of the textile and cellulose fibers i.e. they impart colour to fabric through the process of reacting directly with fabric molecules (Kim Y, Kim, Moon, & Shin, 2018). Reactive red 120 is a dye from the largest family of dyes (azo dyes), which are well recognized by the presence of the azo group (-N=N-). Broadly, the dye falls under a broad grouping of reactive dyes which owe their name to the presence of the reactive chemical function of

triazine or vinylsulfone type (Oueslati, Lima, Ayachi, Cunha, & Lamine, 2020). The molecular structure of RR 120 is as shown in Figure 2.16 below.

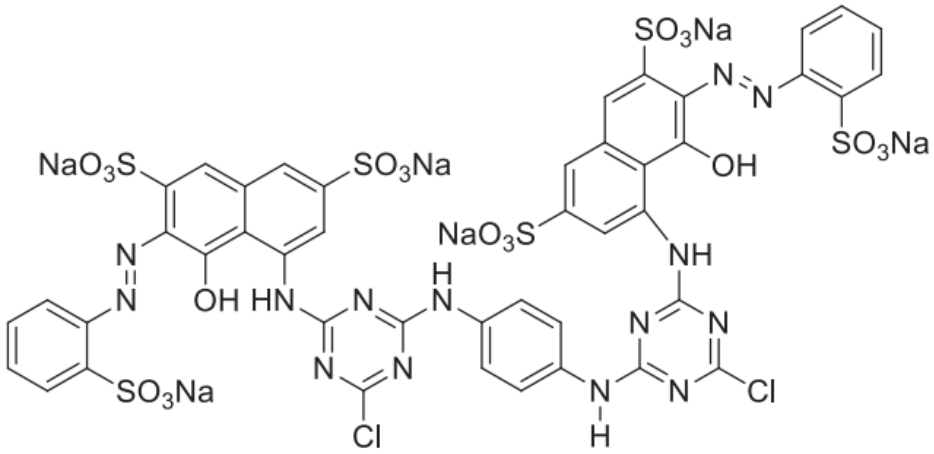

Figure 2.16: Molecular structure of Reactive red 120

Reactive red 120 is a commonly used dye in the textile industry. However, use of reactive dyes present increasing environmental threats owing to their marked toxicity, mutagenicity and poor biodegradation profile. This is exacerbated by the fact that most dyes from this family are not readily removed by use of conventional treatment systems and their proven resistance to natural biodegradation owing to their complex aromatic structure. In addition to the aforementioned environmental effects, Reactive red 120 is also reported to be an allergen (Bazrafshan *et al*., 2013).

2.10 Methods of removal of pollutants from waste water

Despite the continuous research indicating that synthetic dyes exert deleterious effects on both humans and the environment alike, their use has continued year after year due to the fact that they are reliable, cheap and can be mass produced easily in different shades. Presently, synthetic dyes have remained an integral ingredient demanded in many

industries such as the tanning, paper and pulp, ink, textiles, pharmaceuticals and food sectors (Dassanayake, Acharya, & Abidi, 2021). The textile industry which is the largest end user of dyes have reportedly low efficiency as regards to textile dyeing processes. Where-as most dyeing processes have lead to a dye loss of about 10 % to 15 % as unspent dyes due to poor exhaustion and fixation of dyes onto textile substrates, most industries have tried to reduce the amounts of textile effluents by use of several remediation techniques such as chemical, physical and biological techniques that reduce the amounts of dyes in the textile effluents by degrading them (Dassanayake, Acharya, & Abidi, 2021). Even with advanced industrial remediation techniques in some industries in developed nations, a cumulative 2 % of the dyes still make their way into effluents culminating into voluminous quantities of wastes thus making the textile industry the core producer of dye effluents. Such wastes, in addition to just the dyes, include more than 8000 supplementary chemicals (dye auxiliaries) such as mordants which exist in form of salts, alkalis, acids, surfactants and heavy metals (Dwivedi & Tomar, 2018; Elango *et al*., 2017) .

Table 2.2 below shows the international permissible standards for textile effluents showing the permissible levels of colour, pH, biological oxygen demand, chemical oxygen demand, suspended solids and temperature of the dye effluents.

Table 2.2: International standard of dye effluent discharge into the environment adapted from Katheresan *et al*. (2018).

S/N	Factor	Permissible limit
1.	Colour	Below 1 ppm or 1 mg/L
2.	Biological oxygen demand (BOD)	Below 30 mg/L
3.	Temperature	Below 42 °C
4.	pH	Between 6–9
5.	Chemical oxygen demand (COD)	Below 50 mg/L
6	Toxic pollutants	Not allowed to be released into environment
7.	Suspended solids	Below 20 mg/L

Consequently, research efforts are now being directed towards addressing the challenge of removing unspent dyes from wastewater (or treating them) before such wastes are purged into the environment. At present, the methods being employed for removal of dyes from effluents can be grossly divided into three categories namely: physical, chemical and biological methods. Because of the chemical diversity of synthetic dyes and type of methods and adsorbents, the foregoing methods have both advantages and their limitations as regards to one or more groups of dyes (Aruna, Bagotia, Sharma, & Kumar, 2021; Dutta *et al*., 2021).

2.10.1 Physical methods

By far, the explicit choice of method used in the remediation of dyes from textile house effluents relies mainly on the costs, the efficiencies and the ease with which they can be performed. Accordingly, physical methods for the removal of dyes are at the forefront owing to their simplicity, flexibility, non-selectivity and efficiency (Dutta *et al.,* 2021; Saharan, Sharma, Kumar, & Kaushal, 2019). Under this category, conventional removal of

unwanted dyes are effected by mass transfer and entails the use of techniques such as ion exchange, coagulation or flocculation, irradiation, reverse osmosis, nano filtration or ultra-filtration, adsorption and membrane filtration.

In ion exchange technique, the chemical process is entirely reversible and involves ions from the dye wastewater being swapped with similar ions on a stationary solid surface. It is advantageous in that the regeneration of the adsorbent material used is possible and therefore the process is considered cheap. Equally the method affords good percentage dye removal and produces high quality water. The major disadvantage of this technique is that its use is limited to few types of dyes depending on the functional groups (Yagub *et al*., 2014, Gürses, Güneş, & Şahin, 2021).

Coagulation or flocculation uses selected chemicals that upon addition to the dye effluents results in clumping and cleaving together between the coagulant and the dye particles. The clumps, are then eliminated by simple techniques such as filtration. The advantage of this method is that it is relatively cheap, robust and effective for removal of several groups of dyes such as disperse, sulphur and vat dyes from the dye effluents. Nonetheless, its disadvantage is that it leads to the generation of copious quantities of concentrated sludge and does not remove azo, basic, acid and reactive dyes from textile effluents. Equally the process is highly reliant on the pH of the systems making it slightly expensive owing to the requirement to use special chemicals that are needed to adjust the pH of the solution (Katheresan *et al*., 2018).

Another physical technique used for the removal of dyes from water is irradiation. Though the method is very effective in most laboratory-based environments, a prohibitively high quantity of dissolved oxygen is required for the method to successfully work which makes

it equally expensive and limited in use (Katheresan *et al*., 2018). Membrane filtration and other associated technologies such as reverse osmosis, microfiltration/ultrafiltration and nanofiltration are by far the fastest techniques that are effective in removing nearly all known types of dyes. In nanofiltration and ultra-filtration unlike with membrane filtration, dye effluents are channeled through more thin-pored membranes that separates dye particles from clean water (Abid, Zablouk, & Abid-Alameer, 2012).

Reverse osmosis is the most advanced of these techniques in that it is a more pressure-driven system where water is passed through ultra-thin membranes that snuggly separates dyes on one side and clean microbial-free water on the other end (Katheresan *et al*., 2018). The major drawback is that these techniques generate concentrated sludge that creates disposal challenges and subsequently increases the overall remediation costs (Abid, Zablouk, & Abid-Alameer, 2012). In addition, membrane filtration cannot be used in the treatment of large volumes of dye wastewater due to the possible incidences of membrane fouling or blocking that ultimately makes the process not only tedious but also expensive. Also, the methods requires high pressure and the initial costs are fairly high.

Adsorption is the considered the most effective and inexpensive treatment methods for removing dyes from wastewater (Dutta *et al*., 2021). It involves use of adsorbents made from high adsorption capacity materials such as activated carbon, nanotube materials among others to adsorb dyes from textile waste water. The cost of adsorption is highly dependant on the choice of adsorbent used with the method being not only having high removal efficiencies but because the process is physical, the possibilities for regeneration for most adsorbents is possible cheaply (Katheresan *et al.*, 2018).

2.10.2 Chemical methods

As the name suggests, these methods involve the use of chemicals that react with the dyes to convert them to harmless or less toxic chemicals. The well-known commonly used methods under this are ozonation, electrochemical destruction, oxidation, advanced oxidation process, fenton reaction dye removal, photochemical and ultraviolet irradiation. In ozonation, gaseous ozone which uses an extremely reactive species of oxygen which has of its powerful oxidation ability and shorter half-life of about 20 minutes is reacted with the effluent in a batch reactor. This, is highly efficient for decolourizing textile wastewater but is an expensive technology that in addition to being unstable, yields toxic by-products (Yang, & Yuan, 2016). Interestingly, the ozone can just be used in its gaseous state which in turn, does not increase the volume of the wastewater, but quickens the reaction. Thus, it is usually sought of as a pre-treatment strategy for efficient chemical oxidation of recalcitrant textile dye wastewater through improving the wastewater's biodegradability and minimizing risks of acute ecotoxicity prior to complete removal of the dyes via serial biological treatment methods (Punzi *et al*., 2015; Ledakowicz, & Paździor, 2021; Venkatesh, Venkatesh, & Quaff, 2017).

For electrochemical destruction, electrocoagulation or non-soluble anodes are used to chemically reduce the dye molecules. The chemicals used are not consumed and therefore no sludge is formed. The major disadvantage of this method is that the process is only applicable to dyes that are soluble in water, and the process is not only expensive but it is also produces hazardous by products (Punzi *et al*., 2015; Ledakowicz, & Paździor, 2021; Venkatesh, Venkatesh, & Quaff, 2017).

Oxidation uses oxidizing agents to effect removal of dyes from dye effluents. The process, usually performed in the presence of a catalyst, causes the decomposition of complex dye molecules to produce carbon dioxide and water. It is the most common chemical method because it is fast and can completely degrade dyes. However, its use by limited by the cost of the chemicals and catalysts required, pH fluctuations as well as the challenges with activating hydrogen peroxide agent. Advanced oxidation process on the other hand uses various oxidation processes concomitantly in eliminating dye particles. For this reason, they can remove even toxic substances and even dyes in otherwise unusual states. Despite its excellent dye removal potential, this technique is expensive, not very flexible, is affected by pH fluctuations and may produce undesirable byproducts (Punzi *et al*., 2015; Ledakowicz, & Paździor, 2021; Venkatesh, Venkatesh, & Quaff, 2017).

Chemical and (electro)coagulation, involve the use of chemicals or electricity to destabilize charged suspended colloidal impurities and dyes in effluents, especially high oxygen demanding chemicals. This approach has received industrial credit and is the most preferred treatment method in large industries because it involves the formation of little or no harmful byproducts or toxic intermediates. Nevertheless, coagulation process results in the formation of sludge whose disposal poses the utmost challenge as it increases the overall treatment cost (Dutta *et al*., 2021; (Punzi *et al*., 2015; Ledakowicz, & Paździor, 2021; Venkatesh, Venkatesh, & Quaff, 2017).

The Fenton's process is tagged as environmentally friendly but like the foregoing techniques usually results in the production of large volumes of iron sludge (Nidheesh *et al.*, 2013), may not be used to remove disperse and vat dyes, requires longer reaction times and can only be performed at low pH. Its uses Fenton's reagent (a mixture of catalyst and

hydrogen peroxide) to eliminate dyes from dye effluents. The advantages include complete removal of all toxins from the waste water, possibility of removing even dyes from dyes wastewater with solid content.

Ultraviolet irradiation method uses ultraviolet light to decompose dye particles in the waste effluents. Though the radiation itself is hazardous, no toxic chemicals are required no sludge is generated but the overall foul odour of the wastewater can be significantly reduced. The method is not widely embraced due to its high energy consumption, high cost of setting up the facilities and limited treatment times. An advanced form of this method is called the photochemical method and it involves Fenton reaction coupled with ultraviolet light. It is advantageous in that it is very effective in removing dyes, does not generate foul odors or iron sludge (Katheresan *et al*., 2018).

Overall, chemical methods are very effective for the removal of dye species from water although they have the major disadvantages such as copious demand for chemicals as well as reagents, high costs towards precipitation, sludge generation and its difficulty in disposal. Equally, most of the chemical dye removal methods are expensive in comparison to biological and physical dye removal methods (Katheresan *et al*., 2018). Therefore in most industrial setups, they are are commercially unattractive as they require high electrical energy to power equipment or reactors in which chemical dye removal progresses (Yagub *et al.*, 2014, Gürses, Güneş, & Şahin, 2021).

2.10.3 Biological methods

In this method, degradation or removal of dyes is achieved using biological phenomenon such as bioremediation. It is considered a consortium of green techniques for treating textile wastewater at the lowest possible cost but at optimum operating times (Bhatia,

Sharma, Singh, & Kanwar, 2017). They are generally efficient in reducing the chemical oxygen demanding chemicals and turbidity but may not remove the colour of dyes. Under this head, the available techniques include aerobic-anaerobic combination (conventional method), adsorption by microbial biomass, fungal remediation (fungal cultures), enzyme degradation, algal degradation, microbial cultures and pure and mixed cultures (Katheresan *et al.*, 2018; Piaskowski, Świderska-Dąbrowska, & Zarzycki, 2018).

The conventional method of biological treatment of textile dye wastewater is the aerobic-anaerobic combination. It uses specially formulated sludge to degrade dyes. It is advantageous in that it decolourizes most dyes and it is cheap although it may not completely degrade the dyes. The release of methane and hydrogen sulphide from this method, extensive space required, and production of iron sludge makes the process less attractive (Katheresan *et al.*, 2018). Algae degradation is considered unstable and slow as it depends on algae that consumes the dye particles for their own growth. The methods is however ecofriendly and cheap (Hernández-Zamora *et al*., 2015).

Enzymatic degradation of dyes, involve the extraction and use of enzymes to remediate dye wastewater. They are comparatively non-toxic, cheap, have high efficiency of removal, reusable but the quantity of potential enzymes realized from extractions limit the sustainability of this technique. Fungal cultures have also been employed to degrade dyes. They excrete extracellular enzymes that digests the dye molecules which are then absorbed by the fungi. This is considered as soft technology, as decoloursizing is mediated by biodegradation of the dye chromophores in addition to absorption and adsorption in tandem (Rani *et al*., 2014). For this reason, this approach can flexibly remove various classes of dyes simultaneously. However, the system is often unstable, may require lengthy growth

phase for the fungi as well as large reactors and nitrogen-confined areas for the growth of fungi (Katheresan *et al*., 2018).

Microbial culture method uses principally bacteria in combination with chemicals or other bacteria to remediate dyes from textile wastewater. Typically, the process may require upto 30 hours to finish the first phase of decoloursizing the dye wastewater. This method is distinctly effective only for a limited number of dye classes but mostly cost-effective on industrial levels only. An extension of this method is called the pure and mixed cultures method. It entails the use of mixtures of bacteria, algae, or fungi with other chemicals to effect dye removal from waste effluents. This implies that the same ingredients can be reused, and this has been indicated to be effective in the removal of azo dyes which are synthetically resistant to biodegradation under natural conditions. The side products produced are colourless (which does not affect the colour of treated water) and can also eliminate toxic byproducts. However, this method results in production of sludge and may require other conventional methods as post-treatment strategies for efficient treatment (Katheresan *et al.*, 2018).

The last and somewhat context-specific preferred biological method involves adsorption of dyes from dye wastewater by use of microbial biomass. Here, a consortium of organic living organisms with tested affinity to adsorb dyes. This is specifically useful for dyes that are known to possess superior affinity towards such microbial biomass. Unfortunately, this technique is not applicable to all classes of dyes but are effective in the removal of azo dyes (Busi, Chatterjee, Rajkumari, & Hnamte, 2016).

2.11 Background of the selected plants used in this study

2.11.1 *Aloe succotrina* Lam.

The plant *Aloe succotrina* Lam. belongs to the genus *Aloe* L. (family: Asphodelaceae; subfamily Asphodeloideae) which has about at least 548 known species in the world (Khaing, 2011; Grace, Simmonds, Smith, & Van Wyk, 2009; Wabuyele, Bjorå, Nordal, & Newton, 2006) and about 63 known and identified species in Kenya alone (Bjorå, Wabuyele, Grace, Nordal, & Newton, 2015). The *Aloe* genus encompasses some of the most cultivated plants for both traditional and industrial (commercial) uses (Nalimu, Oloro, Kahwa, & Ogwang, 2021; Salehi *et al*., 2018). The name of the *Aloe* genus is thought to have derived from "Allaeh" which is Arabic for shining bitter substances (Sánchez, González-Burgos, Iglesias, & Gómez-Serranillos, 2020; Surjushe, Vasani, & Saple, 2008). Of the known 63 species in Kenya, several species have been reported to have medicinal properties such as *Aloe lateritia*, *Aloe barbadenis* and *Aloe secundiflora* while others such as *Aloe ballyi* and *Aloe elata* are very poisonous to the extent that they are often used by different ethnic groups in Kenya as arrow poison due to the presence of the alkaoid γ-coniceine (Waihenya *et al*., 2002). In Morocco, *A. succotrina* has been reported as folk remedy for the treatment and management of diabetes (Fouad, & Lahcen, 2020; Fouad, Fatiha, Larbi, & Lahcen, 2019). The other remaining species have no reported medicinal uses.

The species *Aloe succrotina* Lam (also called the Fynbos aloe) is endemic to South Africa, especially within the regions of Cape town, Cape valley and the south-western corner of the Western Cape. The *A. succotrina* plant occur in clusters of leaves that form dense rosettes with the south African one being reported to annually flower between June and

September to produces a tall raceme with conspicuous red flowers that make it mostly visited by sunbirds (Grace, Simmonds, Smith, van Wyk, 2008).

Within the slopes of Keiyo valley of Kenya in Elgeyo- Marakwet county lies the *Aloe succotrina* species. This species of *Aloe*, is unique in that it exudes a unique royal purple sap that can be harvested from the leaves of the plant (Van Wyk, 2013). Previous work done on other species of *Aloe*, show that some of them possess red and yellow dyes, which have been found to be generally stable to both light and wash when used as natural dyes for different fabric (Annapoorani & Divya, 2015; Srivastava & Singh, 2011). Among the species of *Aloe* that have been evaluated for their dyeing properties is the *Aloe barbadensis* which was tested as a possible source of natural dyes and discovered that in the presence of a drops of nitric acid solution, the plant yielded a beautiful golden yellow colour on both cotton and silk fabric. Equally, it was also realised that with the variations of different mordants, the colours of the dye, greatly varied from yellow, to pink, khaki and brown depending on the mordant of use and application procedure. This, greatly showing the potentials of the *Aloe* species towards imparting of colour (Srivastava & Singh, 2011). This results were similar to other studies done on *Aloe vera* which also showed good fastness to wash and rub on cotton in the presence of metallic mordants such as Alum, ferrous sulphate and copper sulphate (Annapoorani & Divya, 2015).

The purple sap extracted from the leaves of the *Aloe succotrina* plant have long been used by the Marakwet community of Kenya for the dyeing of *kiondos* which are handbags locally made from sisal. Incidentally, little scientific research has been done on the said plant species for the assessment of its phytochemical composition or for the spectral and chromophoric components responsible for its dyeing properties. What makes the plant even

more exciting is the fact that what is harvested is the leaves, unlike other plants whose dyes are extracted from the bark, wood or root that end up destroying the plant. Figure 2.17 below show a picture of A. succotrina in its natural habitat.

Figure 2.17: A picture of *A. succotrina* in its natural habitat (Source: Author 2018)

Some *Aloe* species, have been reported to have a large number and variety of bioactive compounds that can be utilized for a wide range of purposes (Bani, Grossi, Lucini, Pellizzoni, & Minuti, 2016). Apart from dyeing properties, members of the *Aloe* species exhibit other important properties such as antimicrobial, antifungal and antibacterial capabilities that can be exploited in its applications for textile finishes. Like other medicinal plants with dyeing potentials, the *Aloe succotrina* plant can also be exploited for not only its dyeing potentials but also its potential antimicrobial finishing (Joshi, Ali, Purwar, & Rajendran, 2009).

2.11.1.1 *Aloe* species in the remediation of dyes

Research on the remediation potentials of members of the species of *Aloe* genus have been investigated with fairly good results. For example, the rind powder from *Aloe vera* was extracted and heated at 353 K without further modification was used for the evaluation of its adsorption capacity against Methyl violet dyes, proving to be very good adsorbent with very high capacities (Ahmad, Megat, Zubaidah, Jamaludin, & Khalid, 2018). Equally activated carbon from the leaves of *Aloe vera* have been used for the removal of different dyes from different media for example, it has been used for the removal of Rhodamine- B dye, congo red, reactive blue, methyl orange and dyes (Giannakoudakis *et al*., 2018; Kannan, 2014; Khaniabadi, Mohammadi, Shegerd, Sadeghi, & Saeedi, 2017).

2.11.2 *Prosopis juliflora* (Prosopis or Mesquite)

The *Prosopis juliflora* (Sw.) plant is a hard and woody species belong to the genus *Prosopis* that is known to have about 44species. The plant is native to both south and central America and grows to hights of about 18 meters with a diameter of up to 1 meter especially when it is grows in a favourable environment (Patnaik, Abbasi, & Abbasi, 2017; Ilukor, Rettberg, Treydte, & Birner, 2016). World-wide, the plant has been reported to be present in Portugal, India, Peruvian-Ecuador, Uganda, Spain, Sri Lanka, Sudan, Ethiopia, Egypt, Yemen, Tanzania, Hawaii, Kenya, Nigeria, Paraguay, Peru, Senegal, the United States, and Pakistan (Ilukor *et al*., 2016; Kumar, & Tamilarasan, 2013; Prasad, & Tewari, 2016).

In Kenya, the *P.juliflora* is locally referred to as “Mathenge” and it grows on arid and semi-arid areas such as Turkana, Tana river, Baringo Kajiado and Garissa counties having been introduced in Kenya in the late 1970’s for the purposes of afforestation (Chepkwony *et al*., 2020; Khandelwal, Sharma, & Agarwal, 2016; Odero, Munyendo, & Kiprop, 2017; Preeti,

Ram Avatar, & Mala, 2015). The plant is very hardy, being tolerant to various conditions such as drought, soil alkalinity, water logging conditions and little rainfall up to 50 mm. Because of its drought tolerant nature and the ability of its roots to go deep in search of water, the plant is ever an green shrub even in arid and semi-arid regions this attracting livestock to it. When the pods of the plant which are rich in sugar content are eaten, it has been recorded that livestock such as sheep and goats lose their teeth and, in some cases, die due to complications of the digestive tract (Maundu, Kibet, Morimoto, Imbumi, & Adeka, 2009). Figure 2.18 below shows a picture of the *P.juliflora* plant.

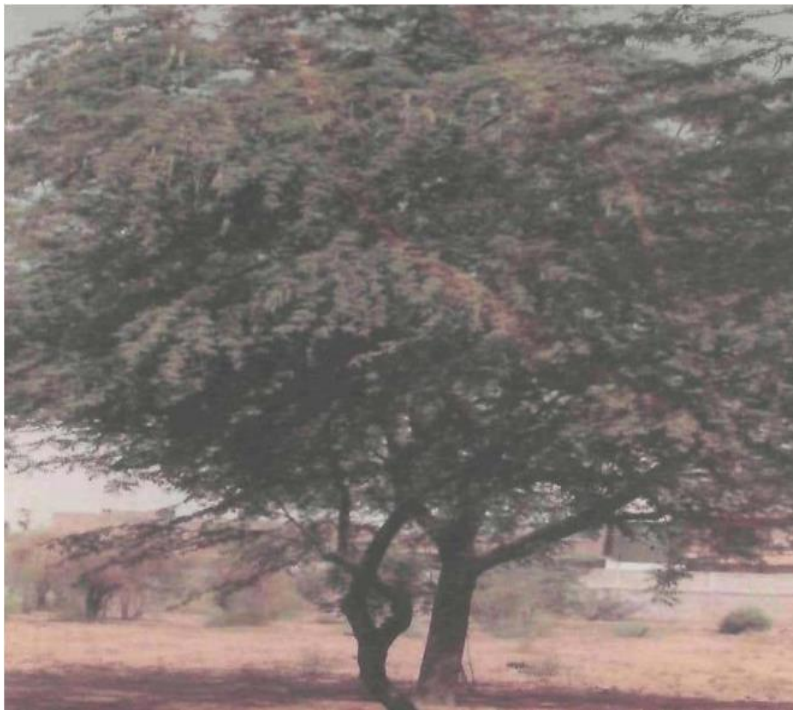

Figure 2.18: A picture of the *P. juliflora* plant (Source: Azam *et al*., 2011)

The phytochemistry of organic and aqueous extracts of *P. juliflora* whole plant, flowers, leaves, pods, stem, roots, and thorns has been evaluated with results showing the presence of several phytochemicals such as phenols, alkaloids, glycosides, coumarins, terpenoids, steroids, tannins, flavonoids and saponins (Mani, 2017; Preeti *et al*., 2015; Ibrahim *et al*.,

2013; Lakshmibai, & Amirtham, 2018; Singh, 2012; Sukirtha, & Gowther, 2012; Sathiya, & Muthuchelian, 2008). Previous studies done on the heartwood of the plant, showed it to be full of flavonoids with potent antioxidant properties such as mesquitol, catechin and epicatechin which gives the heartwood of this plant a characteristic dark brown shade (Chepkwony *et al.*, 2020 ; Sirmah, Mburu, Iaych, Dumarçay, & Gérardin, 2009).

Given its richness in flavonoid contents, and with research on natural dyes of brown origin showing that flavonoids are responsible for brown colours in most natural dyes, the plant was evaluated for its dyeing properties. Other phytochemical investigations on the extracts of different parts of *P. juliflora* have identified majorly phenolic derivatives and alkaloids, some of which were reported for the first time in the literature (Ibrahim *et al.*, 2013). Most of the novel compounds were named after the species itself. For example, juliflorine and julifloricine (Aqeel, Khursheed, Viqaruddin, & Sabiha, 1989), julifloricine, juliflorine and julifloridine which was obtained as a gum (Ahmad, Basha, & Haque, 1978), juliflrosinene (Ahmad, Khursheed, Sabiha, & Viqaruddin, 1989), 3-oxo-juliprosine and 3'-oxo-juliprosine (Nakano *et al*., 2004). Other allelopathic compounds from this species include L-triptophan (Nakano *et al*. 2001), Syringin and (-)-Lariciresinol (Nakano *et al*., 2002).

2.11.2.1 Potential of *P. juliflora* in remediation of dyes

Modified parts of *P. juliflora* plant have been previously developed into low cost adsorbents (Prasad, & Tewari, 2016; Sahithya, & Krishnaveni, 2021). For example, activated carbon from the barks of the plant were used for the adsorption of methyl orange, Victoria blue and basic violet dyes. Kinetic and equilibrium studies on the removal of Victoria Blue using *P. juliflora*-modified carbon/Zn/alginate polymer composite beads reported a percentage removal of 86% of the Direct Yellow 12 dye by *P. juliflora* bark

occurred at pH of 3, at 150 rpm, 100 ppm initial dye concentration and 400 mg/50ml adsorbent dosage in 120 min at 55 ^{o}C temperature (Kumar & Tamilarasan, 2013; Kumar, & Tamilarasan, 2014; Sanghavi and Ranga, 2017). Equally polyaniline-treated activated carbon of the barks of the *P. juliflora* were used for the adsorption of reactive dyes by (Gopal, Asaithambi, Sivakumar, & Sivakumar, 2014). All this showing different potentials of the plant to be used a source of low-cost adsorbent.

2.12 Biochar and its properties

Biochar refers to material that are rich in carbon that are prepared via pyrolysis in limited air or oxygen resulting to a highly compact structure with surface functional groups leading to high adsorption capacity (Kyi, Quansah, Lee, & Moon, 2020). Initial materials used to make biochar vary greatly from agricultural wastes such as melon peels, maize cobs and tassels, mango peels, sugarcane bagasse to sewage sludge, manure etc. These, have been used as sources of low cost adsorbents in environmental clean-up with the major advantages of biochar being that their raw materials are readily available, cheap, have a high cation exchange capacity and they are mostly effective both modified or un modified (He *et al*., 2017; Wang & Wang, 2019).

2.12.1 Effect of Temperature on the properties of biochar

One of the most important aspects of production of biochar is the temperature at which the biochar has been prepared. For example, it has been noted that biochar produced at very high temperatures, are not only rich in carbon content but they also have a higher surface area due to the fact that the higher temperatures ensure that micropore volumes have been increased after the expulsion of organic compounds (Wang & Wang, 2019).

On the other hand, biochars produced at a much lower temperatures have a much higher yield than those produced at a higher temperature with most organic functional groups being present. Since the sorption potentials of the biochars are a direct function of the functional groups present in the biochar, it is of utmost importance that there is a balance between the temperature of preparation of the biochar, the intended yield and the intended purpose (Wang & Wang, 2019).

All biochar derived from plant sources, are made up of three major part; cellulose, hemicellulose and lignin with each part, behaving differently when they are subjected to heat. Of the three, the most reactive part is the hemicellulose part which is made up of polysaccharides with chained structures that decompose at temperatures between 220 °C-315 °C. The cellulosic part of the plant is more stable than the hemicellulose although its also made up of polysaccharides though not branched. It decomposes at temperatures of about 280 °C – 400 °C. The Lignin part decomposes slowly and over a wide range of temperature starting from 160 °C up to around 900 °C. This is because lignin is a macromolecule which is complex and three dimensional (Shaaban, Se, Mitan, & Dimin, 2013; Weber & Quicker, 2018). The figure 2.19 below shows how biochars derived from rubber wood saw dust varied at different temperatures in content (Shaaban *et al*., 2013).

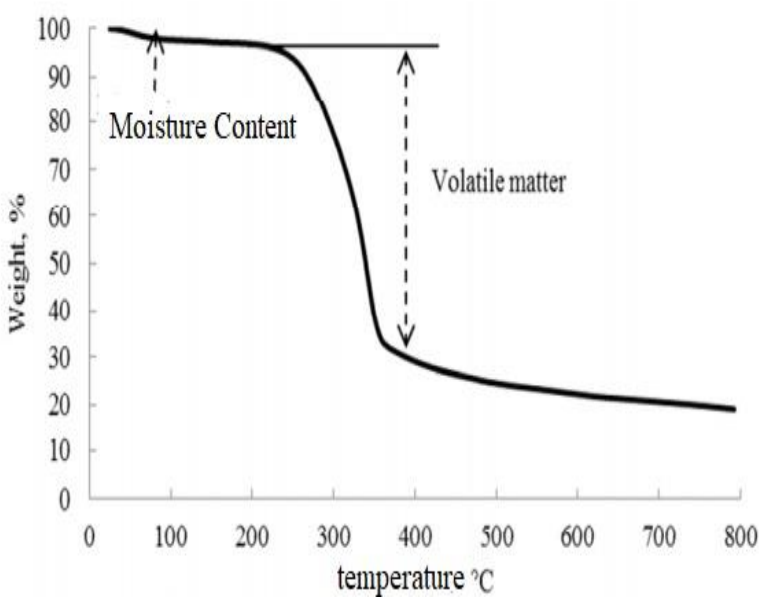

Figure 2.19: Variation of biochar content at different temperatures. Adopted from (Shaaban *et al*., 2013)

2.13 Characterization of biochar

2.13.1 X-ray powder diffraction

X-ray powder diffraction (XRD) is a powerful, rapid and non-destructive crystallographic analytical technique used to analyse crystalline properties, amorphous properties and atomic spacing of different types of materials (Bunaciu, Udriştioiu, & Aboul-enein, 2015). It avails date and information on the structures, crystal orientations (texture), phases, and other structural features such as the strain, average grain size and crystal defects (Toso *et al.,* 2021). Its main advantage being that it is non-destructive, highly accurate and samples can be analysed in situ without much preparation (Holder, & Schaak, 2019).

X-ray analysis is based on the constructive interference between the samples being analysed and monochromatic X-rays (from a cathode ray tube) which are scattered at specific angles from each set of lattice planes in the sample. In other words, XRD analysis relies solely on the dual wave/particle nature of X-rays in pursuit of providing relevant

information pertaining to the structure of crystalline materials (Holder, & Schaak, 2019). The resultant peak intensities are established by the atomic positions within the lattice planes, as both the destructive and constructive diffractions are governed by Braggs law for crystalline structures. Thus, XRD patterns are fingerprints of the periodic atomic arrangements of the materials under analysis and online searching of standard database for X-ray powder diffraction patterns affords quick phase identification where various crystalline materials have been analyzed.

In the characterization of biochar, XRD has been extensively used as a primary analytical technique. This is because, it is able to show the differences in carbon content, it is able to show the level of crystallization, whether or not the biochar is amorphous and structure of biochar (Cuixia *et al*., 2020; Kim, Jae, Cho, & Choi, 2012).

2.13.2 Energy Dispersive X-ray- Scanning Electron Microscopy

Energy Dispersive X-ray-Scanning Electron Microscopy commonly referred to as the EDX-SEM is an analytical technique that combines two analytical instruments namely EDX and SEM. EDX, is an X-ray technique that does elemental analysis of substances based on characteristic X-rays (Scimeca, Bischetti, Lamsira, Bonfiglio, & Bonanno, 2018). It is largely a non-destructive technique which analyses samples *in situ* with little or no sample preparation required. EDX is a qualitative, semi-quantitative and quantitative technique but can also be utilized to furnish information on the spatial distribution of elements through mapping (Scimeca *et al*., 2018).

On the other hand, SEM is a microscopic technique that analyses the surface characteristics of a substance (Fomenko, Yumashev, Kukhtetskiy, Zhizhaev, & Anshits, 2020). It avails detailed high-resolution images of the sample by rastering a focussed electron beam across the surface and detecting secondary or backscattered electron signal (Abd Mutali *et al.,*

2017). Together, the two form an important instrument that is used for elemental analysis and surface properties. EDX systems are usually attached to Electron Microscopy (Scanning Electron Microscopy, SEM or Transmission Electron Microscopy, TEM) in which case the imaging capability of the microscope is harnessed for identification of the sample. Data from EDX analyses are spectra indicating peaks that can be corresponded with the elements contained in the sample under analysis. This feature implies that both image analysis and elemental mapping of samples are feasible in EDX analysis.

In instances where the data obtained from the combination of EDX and microscopy (SEM or TEM) are inadequate to allow for precise identification of a sample a more powerful multi-technique approach may be adopted by use of other complementary techniques such as Surface Analysis (Time-of-Flight Secondary Ion Mass Spectrometry or X-ray photoelectron spectroscopy), Raman Microscopy, FTIR microscopy and Nuclear Magnetic Resonance (NMR) Spectroscopy (Abd Mutali *et al.*, 2017).

2.13.3 Transmission Electron Microscopy

Invented in 1931, the transmission electron Transmission Electron Microscopy (TEM) has become an important microscopy instrument with a myriad of functions ranging from the sizes of nano particles to examining of ultra-fine features to characterize morphology and crystalline structures of up to the atomic scale (Tang & Yang, 2017). It has higher magnification power when compared to SEM and they can additionally be used to elucidate the crystallographic structure and the composition of smaller compounds and substances. TEM essentially works in the same way as SEM i.e. uses electrons as the excitation source. However, specimens to be analyzed are prepared to be very thin to make them semi-

transparent to electrons which implies that sample preparation takes longer than in SEM (Harris, 2018).

Recent developments in this technique has made it very instrumental in assessing nano-reinforcement dispersion in biopolymer composites and microstructural analysis of membranes and biopolymer films that are not possible when SEM is used (Scuderi *et al*., 2021).

2.14 Adsorption

The association of chemicals (liquids or gases) with a solid phase are generally termed as sorption processes. Thus, the two terms i.e., absorption and adsorption are used to delineate the nature of the association. The difference between them is that in absorption, the molecules penetrate a three-dimensional matrix, while in adsorption the molecules are attached to a two-dimensional matrix (Qi *et al*., 2017).

Adsorption therefore refers to the process of removal of substances (adsorbate) from one phase accompanied by a subsequent concentration of the same substance on another substance commonly referred to as the adsorbent (Hamzezadeh, Rashtbari, Afshin, Morovati, & Vosoughi, 2020). According to IUPAC general definition, adsorption refers to the enrichment of molecules, atoms or ions in the vicinity of an interface (Thommes *et al*., 2015). For the case of removal of pollutants from effluents, adsorption has become a method of choice when compared to other methods. This is because the initial cost is cheaper, it is simple to design, does not require skilled labour to operate and it is non-selective. The adsorption characteristics of different types of adsorbents have been studied

and evaluated and even suggested for future use (Hamzezadeh *et al*., 2020; Tim Robinson *et al.*, 2001; Yagub *et al.*, 2014).

Adsorption is a surface phenomenon, which uses surface forces. Whenever a solution containing the absorbable solute (adsorbate or adsorptive) interfaces with a solid (adsorbent) with a sufficiently porous surface structure, liquid-solid intermolecular forces of attraction initiates the concentration of the solute at the solid surface. Adsorbents are of different types but those used in removal of dyes are primarily sourced from sources materials such as charcoal, zeolites, clays, ores and other waste resources of plant and animal origins. Useful dye adsorbents have been prepared from wastes such as rice husk, sugar industry wastes (bagasse), seaweed and algae, sawdust, scrap tyres, fly ash, fruit wastes, coconut shell, fertilizer wastes, petroleum wastes, tannin-rich materials, blast furnace slag, chitosan and seafood processing wastes, peat moss. Adsorption is often described to be either physisorption or chemisorption process, contingent on the interaction strength between the adsorbate and the substrate (Sims, Harmer, & Quinton, 2019; Vital, Saibaba, & Shaik, 2016).

Physisorption (also called physical absorption) is due to weak van der Waals, dipole-dipole and London intermolecular forces of attraction that takes precedence at temperatures below the critical temperature of the adsorbate, resulting into the formation of a monolayer or multilayer (Sims *et al*., 2019). The process in its entirety has low enthalpy, as it progresses at low temperatures well below the adsorbate boiling point and it is freely reversible. Sometimes called van der Waals adsorption, the rates of adsorption and desorption in this form of adsorption are relatively fast because the process is devoid of surface reactions and the bands formed are thus easily broken because of the weak interactions. The Van der

Waals forces are known to arise from the interactions between induced, permanent or transient electric dipoles. As surface coverage is indirectly proportional to temperature in this process, it is frequently used for measuring the total surface area of materials and in pore size analysis of mesopores, micropores and nanopores (Thommes *et al.,* 2015).

Chemisorption i.e chemical adsorption on the other hand is a chemical process characterized by changes in temperature and chemical interactions between the adsorbent and the adsorbate (Yagub *et al.*, 2014). It involves the transfer or sharing of electrons between the adsorbate and adsorbent (atoms or molecules) and the adsorption of adsorbates onto adsorbents is due to the formation of chemical bonds between them (Thommes *et al.,* 2015). The interactions in chemisorption are typically two orders of magnitudes stronger than that of physiosorbed species, and results in the formation of a monolayer of the adsorbate attached to the surface of the adsorbent (Sims *et al*., 2019). This is because the process occurs at very high temperatures and pressures and the energy of adsorption exists between 200 and 400 kJ/mol (Ma, Han, Jia, & Wu, 2020) i.e. chemisorption as a process possess high enthalpy, occurs at all temperatures and it is completely irreversible (Singh, & Kaushal, 2017).

It is worth noting that isosteric heat is one of the basic quantities of adsorption studies. It on the whole relates the ratio of the change in the infinitesimal of the adsorbate enthalpy to the infinitesimal change in the adsorbed amount (Azahar *et al.,* 2018). The significance of the data related to heat released in kinetic studies is explained by the fact that adsorption is typically exothermic which leads to partial absorption of the released energy by the solid adsorbent as well as partial dissipation to the surrounding. In this context, the particle temperature increases by the adsorbed portion of the solid adsorbent which can ultimately

slow down the adsorption kinetics. This is largely triggered by the uptake of mass that is regulated by the cooling rate of the particles in the later adsorption stage (Singh, & Kaushal, 2017).

2.14.1 Factors affecting adsorption of synthetic dyes onto adsorbents

Both physical and chemical adsorptions are processes that are influenced by adsorption parameters such as particle sizes, cationic exchange capacity, contact time, pH, agitation speed, initial concentration and the temperature used (Ma *et al.,* 2020; Radhi, Hussein, & Kadhim, 2019). These parameters exert different effects on adsorption processes, and thus determines the rate of adsorption and desorption of solutes onto the adsorbent. For maximal remove of the dye from wastewater therefore, these factors should be optimized before the process can be recommended for large scale application as a textile wastewater treatment process (Radhi *et al.,* 2019; Rápó, & Tonk, 2021) .

2.14.1.1 Effect of pH of the medium

The pH of aqueous solution is considered as one of the most important parameters that affect the adsorption of dyes. This is because it affects several factors such as the ionization of the dye, solubility of the adsorbent, the response of functional groups in the biochar such as carboxylate, phosphate, hydroxyl and amine groups and the electrostatic charges on the surface of the adsorbent (Albroomi, Elsayed, Baraka, Kazem, & Forces, 2015; Iftekhar, Lakshmi, Srivastava, Bilal, & Sillanp, 2018; Munagapati, Wen, Pan, Gutha, & Wen, 2019). In general, it is expected that for cationic dyes, the adsorption will decrease as a result of a decrease in pH and increase for an increase in pH. On the other hand, for anionic dyes such as reactive red, the adsorption efficiency increases when the pH decreases and vice versa

(Adib, Razi, Nur, & Mohd, 2017). For example, (Verma & Mishra, 2010) showed that for for cationic dyes such as crystal violet and direct orange, there is a direct increase in percent dye removal due to an increase in pH.

A point is reached on the surface of the adsorbent media in which the electric charge density on the surface is equal to zero. This is termed the point of zero charge, defined precisely as that pH value (pH_{pzc}) when the number of cations and anions on the surface of the adsorbent are in equilibrium (Dos Santos Silva *et al.*, 2018). Ideally, the pH_{pzc} is described in terms of the concentration of the solution. When the pH of the solution is lower than the pH_{pzc}, the acidic medium donates more protons than the hydroxide group so that the adsorbent surface is net positively charged. Such surfaces will then favour the adsorption of anions from the solution. On the other hand, when the pH of the solution is above pH_{pzc}, the surface of the adsorbent is negatively charged which favours adsorption of cations from the solution (Hossain, Rahman, Ara, & Alam, 2016; De Farias Silva *et al.*, 2020).

2.14.1.2 Effect of temperature

As most physico-chemical processes are either endothermic or exothermic, temperature usually affects the adsorption processes directly (Smoczyński, Pierożyński, Mikołajczyk, 2020). For example, for endothermic adsorption processes, an increase in temperature usually favours the adsorption process while for exothermic process, an increase in temperature leads to a decrease in adsorption (Yagub *et al.*, 2014; De Farias Silva *et al.*, 2020) . In some cases, temperatures higher than room temperature usually enhance the sorption process as it also increases the kinetic energy within the solute and surface activity. However, at very high temperatures it is possible to damage the adsorbate or to increase the kinetic energy to a point where desorption also occurs.

It is worth emphasizing that the effect of temperature on adsorption is dictated by the nature and the process' mechanism (Smoczyński *et al.,* 2020). On the whole, chemical adsorption tends to report a positive effect when temperature increases while the reverse is true for physical adsorption. In chemical thermodynamics (for the case of chemisorption), the effect of temperature on the rate at which chemical reactions proceed follows the popular empirical rule advanced by Van't Hoff (Smoczyński *et al.,* 2020). This rule states that for every increase in temperature by 10 kelvins, a two to four-fold increase in the reaction rate is recorded. This is indicative that temperature increases as the chemical adsorption reaction proceeds may quicken the process. As observed by other authors such as Abdelwahab *et al*. (2015) and De Farias Silva *et al*. (2020), a decrease in dye adsorption following increase in temperature can equally arise due to the weaker adsorption forces between the active sites of the adsorbent and the molecules of adsorbate.

2.14.1.3 Effect of initial dye concentration

As adsorption is a process that relies on the available binding sites, then it means that it can adsorb only a fixed amount of dye (Banerjee, & Chattopadhyay, 2017). As a result, adsorption is a function of initial concentration thus the higher the concentration, the lower the percentage removal of dye by the adsorbent (Yagub *et al.*, 2014). The initial dye concentration in solution is the sole driving force that overcomes mass transfer resistance of adsorbate between the solid phase and aqueous phases (Radhi *et al*., 2019). Normally, reports from equilibrium studies reveal that adsorption ratio initially decreases with increment in the initial concentration of dye. There is evidently fewer number of free active sites on the surface of the absorbent when the dye is introduced. As the initial concentration of dye is not increased, the amount of dye that can be removed decreases but the actual

amount of dye adsorbed per unit mass of adsorbent increases with increase in dye concentration (Radhi *et al.*, 2019). These observations draws to the conclusion that the fractional removal of dyes from wastewater is more efficient at lower dye concentration ranges for batch laboratory studies and industrial reactors (Kowsalya, Sharmila, & Rebecca, 2020; Al-Ghouti, & Al-Absi, 2020).

2.14.1.4 Effect of agitation speed and technique

In aqueous systems, the adsorption mass transfer is affected by the boundary film thickness (Xu, Cai, & Pan, 2013). During the process of agitation, there is an increase in mass transfer of the dyes into the adsorbent helping the equilibrium to be reached faster. However, this speed has to be optimized as if it is too slow, the equilibrium will take longer to be achieved. If the speed is too high beyond the optimum speed at the equilibrium time, then desorption begins to occur, this is because the speed in the liquid system is strong enough to break the bonds formed between that adsorbing species and the adsorbent (Mubarak, Jawad, & Nawawi, 2017). At higher agitation speed there may be a process of desorption. Thus, the difference in agitation speed affects the kinetics of the adsorption as well as the equilibrium adsorption capacity. In other probing investigations, the agitation techniques employed have also been highlighted to exert a marked effect on dye absorption. For example, the adsorption equilibrium of 4-chlorophenol dyes onto granular activated carbon was reportedly attained faster when using a benchtop Erlenmeyer flask than when the same experiment was done a round-bottomed flask at the same agitation speed. Comparing shaking techniques, better adsorption rates and efficiencies of 4-chlorophenol dyes were achieved when mechanical and magnetic stirrers were used than when a laboratory shaker was used for the same purpose (Kuśmierek, & Świątkowski, 2015).

2.14.1.5 Effect of contact time

Initially, the rate of adsorption is very high, becomes almost constant and then gradually slows down up to a point where an equilibrium is achieved. This is because, in the beginning a lot of adsorption sites are available for adsorption and after a while, they get exhausted. As a result, the adsorption curve is usually sharp initially and there afterwards declines steadily (Robinson, Chandran, & Nigam, 2002). This may also be explained by aggregation of the dye molecules as the time of contact increases, making it almost impossible for the dye molecules to diffuse any further into the adsorbent structure at higher energy sites (Kurniawati, Bahrizal, Sari, Adella, & Salmariza, 2021).

2.14.1.6 Effect of adsorbent dose

The rate of adsorption of dyes onto adsorbents at constant dye concentration tend to increase with increasing dosage of the adsorbent, assuming the other factors are kept constant (Radhi *et al.,* 2019). This can be attributed to increased surface area and availability of more adsorption sites.

2.14.1.7 Effect of adsorption selectivity of the absorbents

Adsorption selectivity refers to the preferential adsorption ability of adsorbents for some substances because of their particular composition and the structure of the adsorbents. For example, activated carbon is composed of covalently linked carbon atoms, and can preferentially adsorb high-molecular-weight organic molecules due to its large aperture.

2.14.2 Adsorption isotherms

The voluminous pollution challenges introduced by dumping of untreated textile effluents,

have necessitated the design of low-cost adsorbents for detoxification, removal or immobilization of such effluents in the field of environmental chemistry. Subsequently, modelling of experimental data from adsorption processes has proven to be important means of predicting the mechanisms of various adsorption systems (Ayawei, Ebelegi, A.N., & Wankasi, 2017). Therefore, this subsection gives an overview of common adsorption isotherms, as well as the application of linear regression analysis, nonlinear regression analysis, and error functions for optimum adsorption data analysis.

Adsorption isotherms are of importance in the understanding of the various interactions between the adsorption site and the compound of interest. This is achieved by taking into consideration the equilibrium data and the adsorption properties of both the adsorbent and the adsorbate. This, allows the environmental chemist to establish and describe the interaction mechanisms between the adsorbent and the adsorbate at constant temperature (Al-Ghouti, & Da'ana, 2020). In the case of batch experiments, adsorption isotherms can also be harnessed for the determination of solid-water distribution coefficient (K_{id}). Adsorption isotherms provides a description of the equilibrium performance of adsorbents at constant temperature. They depend on the adsorbate, adsorbed species, adsorbent, and several other physical properties of the wastewater effluents such as pH, ionic strength, and temperature (Yan, Fan, Wang, & Shen, 2017).

Typically, the adsorption isotherms are determined whenever there is contact between the adsorbate and the adsorbent for a reasonable period of time in which the interface concentration exits in a dynamic balance with the adsorbate concentration existing in the bulk solution. Specifically, adsorption isotherms are useful when designing an industrial adsorption process or characterizing porous solids. A classification availed by the

International Union of Pure and Applied Chemistry (IUPAC) shows that adsorption isotherms can be placed in six different categories according to the isotherm shape of adsorbate-adsorbate pairs (Keller and Staudt, 2005). For Type I isotherms (convex upward), they are characterized by a horizontal plateau in which it maintains for very high gas pressures, and it can be adequately described by Langmuir equation (Inglezakis, Poulopoulos, & Kazemian, 2018).

Type II isotherms precisely describe adsorption on mesoporous monolayer materials at low pressures and on mesoporous multilayer material at high pressures near saturation but with no hysteresis. It has a single inflection point, and is only witnessed in microporous, nonporous, or disperse solids with pore diameters greater than 50 nm (Sultan, Miyazaki, & Koyama, 2018). Type III isotherms (concave upward) are observed where the adsorbate–adsorbate interaction is big compared to adsorbate–sorbent interaction as observed in the adsorption of water on hydrophobic zeolites and activated carbon, bromine and iodine on silica gel, and carbon tetrachloride adsorption on mesoporous gel (Khalfaoui, Knani, Hachicha, & Lamine, 2003). Type IV isotherms, usually with two deflection points, ideally describes specific mesoporous materials adsorption behaviour indicating the pore condensation and the hysteresis which exists between the desorption and the adsorption branch (Inglezakis *et al.,* 2018).

Type V isotherms on the other hand possesses one inflection point and usually indicates the presence of mesopores in circumstances where phase changes like pore condensation could occur. A typical example of this is observed in the adsorption of water on activated carbon fiber or carbon molecular sieves (Inglezakis *et al.,* 2018). The last type of isotherms (Type VI isotherms) follows from the science that adsorption layers become more

pronounced and the isotherms presents stepwise multilayer adsorbates at low temperatures. They usually present several inflections, as exemplified in the adsorption of methane gas onto magnesium oxide and adsorption of noble gases on the surfaces of planar graphite, adsorption of butanol on aluminium silicate (Al-Ghouti, & Da'ana, 2020).

The past two decades have witnessed three fundamental approaches bringing forth a plethora of important isotherm models including the famous Langmuir, Freundlich, Dubinin-Radushkevich, Temkin, and Toth isotherms (Al-Ghouti, & Da'ana, 2020). The very first approach considers closely the kinetics in which the adsorption and desorption rates are equal. In this approach, the adsorption equilibrium is defined as a state of dynamic equilibrium. The second approach centres around the thermodynamics aspect, further availing the framework for deriving various adsorption isotherm models in various forms. The third and last approach, however, distinctly relays a core concept of producing the characteristic adsorption curves (Foo, & Hameed, 2010).

An in-depth survey of the literature reiterates that great strides have been achieved in modelling adsorption isotherms. The Henry, Langmuir and Toth isotherm models are commonly used in the so called ‘‘Henry’s region’’ but are invalid at high pressures (Al-Ghouti, & Da'ana, 2020). In response to this, another isotherm model was advanced by Toth in which the power function of the relation between adsorption capacity and the adsorption potential of adsorbent surface are used. This model preceded the Jaroniec and Marczewksi model following the discovery that the Toth model could not precisely explain the transition to the saturation region. The penultimate model (Dubinin-Radushkevich isotherm model) was hailed for its excellent performance at high pressures but just like

other models with flaws, it failed under low-pressure experimental data (Al-Ghouti, & Da'ana, 2020).

As the adsorbate-adsorbent thermodynamics proved complex due to the influence of adsorbate properties, pore size distributions, site energy distribution and surface heterogeneity (Ng, Burhan, Shahzad, & Ismail, 2017), the Sips, Freundlich, and Jovanovich isotherm models gained prominence peculiarly after Ross and Olivier proposed the Homotattic Patch Approximation (HPA). This approximation sections the surface of heterogeneous adsorbent into small-sized homogenous patches in which the energy distribution of the adsorption energy sites is known (Burhan, Shahzad, & Ng, 2018).

Although numerous adsorption equations and methods exist (with Henry's isotherm model considered the simplest), the Langmuir and Freundlich isotherms have been described as the most effective models for the description of the removal of adsorbates from most aqueous systems. The two have especially gained favour in the description of the relationship between the equilibrium amount adsorbed denoted as q_e (mg/L) and the final concentrations denoted as C_e (mg/L) at equilibrium (Ngeno, Orata, Baraza, & Shikuku, 2016).

2.14.2.1 The Henry's adsorption isotherm model

Henry's isotherm model is revered as the most precise single-parameter adsorption isotherm model because the partial pressure of the adsorptive gas considered is proportional to the amount of surface adsorbate (Ayawei, Ebelegi, & Wankasi, 2017). The model describes the appropriate fit of the adsorbate adsorption at low concentrations, especially where all the adsorbate molecules are secluded from their closest neighbours.

The expression given in the following equation (Equation 2.1) describes the equilibrium concentrations of the adsorbate in the liquid phase and the adsorbed phases.

$$q_e = K_{HE} C_e \quad \ldots\ldots\ldots\ldots\ldots\ldots\ldots\ldots \text{Equation 2.1}$$

From which q_e = equilibrium concentration of the dye being adsorbed in mg/g,

C_e = equilibrium dye concentration in mg/l

K_{HE} = Henry adsorption constant.

The subsequent adsorption models described hereafter are two-parameter isotherm models.

2.14.2.2 The Langmuir adsorption isotherm model

The Langmuir adsorption isotherm model is based on the Langmuir theory (Foo and Hameed, 2010). It assumes that the interaction between the solute molecules and adsorbent is monolayer and homogeneously distributed hence each site can contain only one molecule per site. Therefore once the sites are filled, a point of saturation is reached where no further adsorption can occur (Mourabet, Rhilassi, Boujaady, & Taitai, 2017). Put simply, the rates of adsorption and desorption should be equal. The model has been traditionally used for both quantification and contrasting the adsorption capacities of bio sorbents. Two forms (linear and non-linear mathematical expressions) of the Langmuir adsorption equation exists i.e. the normal and the linearized form which are presented in Equations 2.2 and 2.3, respectively.

$$q_e = \frac{q_{max} K_l C_e}{1 + K_l C_e} \quad \ldots\ldots\ldots\ldots\ldots\ldots\ldots\ldots \text{Equation 2.2}$$

$$\frac{C_e}{q_e} = \frac{1}{q_{max} K_l} + \frac{1}{q_{max}} C_e \quad \ldots\ldots\ldots\ldots\ldots\ldots\ldots \text{Equation 2.3}$$

Where the value q_e =equilibrium concentration of the dye being adsorbed in mg/g,

C_e = equilibrium dye concentration in mg/l

q_{max} = the maximum monolayer capacity in mg/g

K_l = Langmuir adsorption constant in L/mg

The value of q_e is calculated using the equation below

$$q_e = \frac{V(C_i - C_f)}{M} \quad \text{……..……Equation 2.4}$$

Where the value C_i = Initial concentration of metal solution

C_f = the final concentration

M = total dry weight of bio-sorbent used

V = Solution of volume used in litres.

A total of six simple adsorption mechanisms were identified and categorized by Langmuir which takes into close consideration the structural geometry and surface chemistry diversity of solid materials (Swenson, & Stadie, 2019). These include;

1. **Single-site Langmuir adsorption** (the simplest of gas-solid adsorption in which the surface possesses similar elementary adsorption sites capable of containing a single adsorbed molecule),
2. **Multisite Langmuir adsorption** (in which two or more types of elementary adsorption sites are available on the surface and each site might fit for single adsorbed molecule),
3. **The generalized Langmuir adsorption**. This is a scenario in which an amorphous material serving as a continuum can comprise of an intractable number of adsorption sites possessing many adsorbate affinities,
4. **Cooperative adsorption** wherein the binding sites on the surface are identical but can potentially host multiple molecules,

5. **Dissociative adsorption**. This is treated as a two-fold adsorption process viz: (i) chemical bonding which causes residence at the surface adsorption site and molecular dissociation, and (ii) desorption by the same molecules where two neighbouring surface atoms re-associates into diatomic molecules and detaches from the surface,
6. **Multilayer adsorption**. Here, it is considered that all sites of adsorption though identical are independent so that molecules have the freedom to be adsorbed above each other owing to the fact that no limit exists for the number of molecules adsorbed.

As an empirical model, the Langmuir isotherm asserts that the thickness of the adsorbed layer is one molecule (monolayer adsorption) in which adsorption process occurs at identical and equivalent definite localized sites. Thus, no steric hindrance and lateral interaction should exist on adjacent sites, amongst the adsorbed molecules so that the that adsorption is homogenous with all molecules possessing a constant sorption activation energy and constant enthalpies (Vijayarachavan *et al.*, 2006). This on the other hand implies that the adsorption sites will possess comparable affinity towards the adsorbate, translating into little to no possibility of adsorbate transmigration in the surface plane (Kundu and Gupta, 2006).

2.14.2.3 The Freundlich adsorption isotherm equation

As opposed to Langmuir adsorption which is monolayered in its approach, the Freundlich model is a two-parameter isotherm model used for the determination of adsorption capacity of an adsorbent of interest onto a heterogenous surface (Yagub *et al*., 2014). It is described

mathematically in two empirical forms i.e. the normal and the linearized from as in equations 2.5 and 2.6, respectively.

$$Q = K (C_f)^{1/n} \text{ ……...……...……. Equation 2.5}$$

$$\text{Log } Q = \log K + (1/n) \text{ Log } C_f \text{ ……Equation 2.6}$$

Where Q = amount adsorbed per unit mass of adsorbent. And K and n are Freundlich constants.

This model is employed for describing reversible and non-ideal adsorption processes and unlike with the Langmuir adsorption isotherm model, it does not necessitate that the adsorption heat and affinities should as a rule at thumb be uniformly distributed on the heterogeneous surface. Not until recently, the Freundlich isotherm adsorption model was applied primarily to animal charcoal adsorption solely. Currently, the model has found application in multiple heterogeneous systems such as adsorption of organic compounds or species which interact on molecular sieves or activated carbon as it has a small range of pressure owing to the isotherm's tendency to follow Henry's law as the system approaches low pressures (Al-Ghouti, & Da'ana, 2020).

2.14.2.3 Jovanovic monolayer adsorption isotherm model

In addition to the assumptions made in Langmuir model, this model also assumes that for adsorption to occur, there is some mechanical contact between the adsorbent and the adsorbate (Ayawei, Ebelegi, & Wankasi, 2017; Kudzinski & Wojciechowski, 1977). This single allowance of the adsorption surface of Jovanovich adsorption isotherm model makes its equations of little use in physical adsorptions and majorly utilized in mobile and monolayer localized adsorption with no lateral interactions (Saadi, Saadi, & Fazaeli, 2015).

The Jovanovic isotherm equation is described in its linear and nonlinear forms as in equations 2.7 and 2.8, respectively.

$$\ln q_e = \ln q_{max} - K_J C_e \quad \text{..... Equation 2.7}$$

$$q_e = q_{max}(1 - \exp(-K_J C_e) \quad \text{..... Equation 2.8}$$

Where

q_e= equilibrium concentration of the dye being adsorbed in mg/g,

C_e = equilibrium dye concentration in mg/l

q_{max} = maximum capacity (describes the maximum adsorbate uptake), usually in mg/g

K_J = Jovanovic constant

The factors (q_{max} and K_J) can be obtained by plotting a graph of ln q_e versus C_e. The equation of this model is bound to approach the limit of saturation in the event that concentration becomes too high and the reverse is true at low concentrations where it reduces to Henry's law. In comparison to the Langmuir equation, Jovanovich equation has a relatively slower approach towards saturation (Al-Ghouti, & Da'ana, 2020).

Other two-parameter isotherm models which are available but were not discussed in detail in this section include the;

1) Dubinin-Radushkevich adsorption isotherm model (purposefully used for expressing the mechanism of adsorption with the distribution of Gaussian energy onto the heterogeneous surfaces),
2) Temkin adsorption isotherm model (which emphasizes the possible interaction between the adsorbent and the adsorbate by ignoring extremely large and low concentrations),

3) Flory-Huggins adsorption isotherm model (considers the nature of surface coverage degree of the adsorbate on the adsorbent by describing the nature of the adsorption process regarding the feasibility and spontaneity of the process),
4) Hills isotherm model (endeavours to expound the various species' binding mechanism to homogeneous substrates by treating adsorption as a cooperative phenomenon in which adsorbates can bind at a site of an adsorbent which may influence other available sites), and the
5) Halsey isotherm model (as with the Freundlich isotherm model that is best suited for heterogeneous surfaces in which the adsorption heat is not evenly distributed, the model attempts to evaluate multilayer adsorption systems through comprehensive description of its condensation at lager distances from the surface),

Other than these, the BET (Brunauer, Emmett and Teller) isotherm and modified BET isotherms are worth noting because of their wide adoption in the study of equilibrium of gas-solid systems (Al-Ghouti, & Da'ana, 2020). Three-parameter isotherm models such as (i) Redlich–Peterson isotherm model (a hybridized isotherm model incorporating both the Freundlich and Langmuir isotherm models but with three parameters), (iii) Toth isotherm model (principally treated as an empirical modification of Langmuir equation as a strategy to minimize the error between the value of both the experimental and predicted value), (iii) Sips isotherm model (literally a merged form of Langmuir and Freundlich isotherm models which enhances the prediction of the heterogeneity of adsorption systems and gives a way around the limitations introduced by increase in concentrations of the adsorbate in the Freundlich isotherm model) and the (iv) Khan adsorption isotherm model (a generalized model applicable to adsorbate adsorption from pure solutions). Four-parameters isotherm

models are also known. These include the (i) Fritz–Schlunder adsorption isotherm model, (ii) Baudu adsorption isotherm model, (iii) Marczewski-Jaroniec adsorption isotherm model, and the (iv) Weber-Van Vliet adsorption isotherm model. The Fritz–Schlunder isotherm model can also be modified into a five-parameter empirical model specially to provide a precise simulation of the model variations for application to a large set or range of equilibrium data (Ayawei *et al.*, 2017).

Recent developments have afforded the evolution of multi-parametric adsorption isotherm models which are extrapolated from the mono-parametric isotherm models to enhance the study of the expected equilibria and interactions between the different components of adsorption systems. Examples of such adsorption isotherm models include the Modified Redlich–Peterson multiparametric isotherms, Non-modified Redlich– Peterson multi-parametric isotherms, Modified Langmuir isotherm, Non-modified Langmuir model, Extended Langmuir multi-parametric isotherm, Extended selective Langmuir isotherm, Sheindrof–rebuhn–sheintuch isotherm, Extended Freundlich multi- parametric isotherm, Extended sips model and the ideal adsorption solution theory–sips model (Al-Ghouti, & Da'ana, 2020).

2.14.3 Determination of adsorption kinetic parameters

Adsorption equilibrium parameters are readily obtained from experiments. Determination of kinetic parameters such as fluid film mass transfer coefficient (kF) and the intraparticle diffusivity (DS) calls for extra experimental and analytical efforts (Fujiki, Kawakita, Teshima, & Furuya, 2017). For instance, the value of the fluid film mass transfer coefficient is often arrived at through theoretical and/or empirical equations such as the Wilson–Geankoplis correlation.

The study of kinetic parameters is a very important aspect when studying adsorption because they describes the rate of adsorbate uptake hence giving the efficiency of the process which is used to show whether or not the process is cost effective and can be adopted. It is also in charge of the residual time of the whole process (Aljeboree, Alshirifi, & Alkaim, 2017; Harrache, Abbas, Aksil, & Trari, 2019). The two common kinetic modelling studies usually done are the Lagergren's pseudo first order model and the Ho's pseudo second order models (Aljeboree *et al.*, 2017).

2.14.3.1 Pseudo first order kinetic model

The pseudo first order (PFO) kinetic model is commonly used for describing the adsorption kinetics of a solute from a solution on an adsorbent at a specific time. It assumes that the rate of change of solute uptake with time is directly proportional to the difference in saturation concentration and the amount of solid uptake with time, which is generally applicable over the initial stage of the adsorption process. Kinetics usually follows the Lagergren pseudo–first-order rate equation if and only if adsorption occurs by diffusion through the interface. The pseudo first order kinetic model can be described mathematically using equation 2.9 below.

$$\frac{dq_t}{dt} = k_1 (q_e - q_t) \quad \text{..... Equation 2.9}$$

Where the value of q_t refers to amount adsorbed at a given time t, and the value of k_1 being the Lagergren's rate constant for first order adsorptions. The values of q_e and q_t referring to the amounts adsorbed at the point of equilibrium and at a time t.

The equation above can be linearized by integrating and applying the boundary conditions (at t = 0 and t = t) in equation 2.9 (Ji, Wang, Song, & Chen, 2019). This resulting in the equation 2.10 below.

$$\text{Log}\,(q_e - q_t) = \text{Log}\,q_e - \frac{k_1}{2.303}\,t \quad \text{..... Equation 2.10}$$

From the linear graph of log (q_e - q_t) against T, the value of the first order rate constant k_1 is obtained as the slope. For adsorption processes following true first-order kinetics, the intercept of $\log(q_e - q_t)$ versus T plots is usually equal to the log of the experimentally determined q_e or can be adjusted to fit the experimental value. For slow adsorption processes however, true equilibrium are far from reached which complicates accurate measurement of q_e. In some instances, the Lagergren pseudo–first-order equation will not fit well for the whole range of the adsorption time (it is known to be applicable only over the initial 20–30 minutes of the adsorption process). In this regard, extrapolation of the experimental data to infinite time is required if q_e is to be obtained which is often a distant possibility. Hence, q_e becomes an adjustable parameter that can only be estimated by trial and error (Ji *et al*., 2019).

2.14.3.2 Pseudo second order kinetic model

The pseudo second-order (PSO) kinetic model, relies on the assumption that the rate-limiting step for the whole adsorption process is the chemical sorption or chemisorption and predicts the behaviour over the whole range of adsorption. In the pseudo second order equation, the equation is like the first order equation based on the sorption capacity of the adsorbate, but it predicts the behaviour over a range of adsorption. Here, the adsorption rate is dependent on the adsorption capacity and not the concentration of adsorbate. This is given by the differential equation (equation 2.11) below.

$$\frac{dq_t}{d_t} = k_2\,(q_e - q_t)^2 \text{.....} \quad \text{..... Equation 2.11}$$

Where q_e is the amount of the dye adsorbed at equilibrium (mg/g), and k_2 is the equilibrium rate constant of the pseudo–second-order model (g/mg min).

Rearranging the equation and separating the variables, then the equation above can be rewritten as the equation 2.12 below.

$$\frac{dq_t}{(q_e - q_t)^2} = k_2\, t \quad \text{.....Equation 2.12}$$

Where k_2 is rate constant in mg/g, and q_e and q_t are the amounts of dye adsorbed at equilibrium and at a time given time t, respectively. After mathematical development and incorporating the boundary conditions (t = 0, t = t and $q_t = q_t$ and $q_t = 0$), the equation takes the form given by equation 2.13 below.

$$\frac{t}{q_1} = \frac{1}{k_2 q_e^2} + \frac{1}{q_e} t \quad \text{..... Equation 2.12}$$

With $h = k_2 q_e^2$, where h = the initial sorption rate. A plot of t/q_t as a function of time yields a linear relationship. From the slope ($1/q_e$) and the intercept ($1/h$ or $1/(k_2 q_e^2)$), it is possible to compute the amount of adsorbate adsorbed at equilibrium and also gives k_2 (the second-order rate coefficient). The principal advantage of the pseudo second-order kinetic model over Lagergren first order is that computation of the equilibrium adsorption capacity from the model is possible, implying that there is theoretically no need to evaluate adsorption equilibrium capacity from experiment.

2.14.3.3 Elovich Kinetic model

The Elovich kinetic model is applied in the interpretation of the kinetics of adsorption and description of second-order kinetics assuming that the surface is energetically heterogeneous i.e. it is used to analyse chemisorption studies in heterogenous surface.

Sometimes called the Roginsky–Zeldovich kinetic model, the Elovich isotherm model is a model that is more compatible with chemisorption and was first put forward by Roginsky and Zeldovich in 1934. The model was initially used in gaseous systems but has recently gained use in analysis of waste water with the model assuming that adsorption rate decreases exponentially as a function of the increase of adsorbed solute (Ayawei *et al*., 2017; Kajjumba, Emik, Öngen, Özcan, & Aydın, 2018). The linear and non-linear equations are described below in equations 2.14 and equation 2.15, respectively.

$$\frac{q_e}{q_m} = K_e\, C_e\ \ e\ \ \frac{q_e}{q_m} \quad \text{…….……..,……. Equation 2.14}$$

$$\text{In}\ \frac{q_e}{C_e} = \text{In}\, K_e\ \ q_m - \frac{q_e}{q_m} \quad \text{……...Equation 2.15}$$

From a plot of ln t versus qt, the constants can be obtained from the slope and intercept of the plot. The elovich equation with its capacity to explain the chemical nature of adsorption kinetics without desorption makes the elovich isotherm model quite handy in adsorption studies.

2.14.3.4 Weber-Morris intraparticle diffusion model

The intraparticle diffusion model, is used widely to find the rate determining step of an adsorption process and was first predicted by Weber and Morris in 1963. This is achieved through the identification of the diffusion mechanism in the adsorption. The model is given by the equation 2.16 below (Kajjumba *et al.*, 2018).

$$Q_t = K_i\, t^{\frac{1}{2}} + C_i \quad \text{……. Equation 2.16}$$

Where K_i = intraparticle diffusion rate (mg/g min $^{-1/2}$). Whenever intraparticle diffusion is involved in the adsorption process, the plots of Q_t as a function of $t^{1/2}$ should represent straight lines. A plot of Q_t versus K_i passing through the origin also suggests that the intraparticle model controls the adsorption process. The rate constants K_i and C_i (mg/g) are evaluated from the slope and intercept of the regression line. The values of C is informative of the thickness of the boundary layer. The larger the value of C, the greater effect of the boundary layer. It is not uncommon that nonlinearity is observed. Thus, multiple processes may be limiting the overall adsorption rate which can be reflected by the data exhibiting multilinear plots. For such cases, these rate-limiting processes are separated into different linear parts of the data over the time (Ayawei *et al.*, 2017; Kajjumba *et al.*, 2018).

2.14.4 Linear versus non linearized forms of evaluation of isotherms and kinetics

To determine isotherms and kinetics, both linearized and non-linear forms of equations have been used. The linearization version of the isotherms and kinetics have been favoured by most scientists because of its simplicity, relative accuracy and software availability. Where-as linearization was and is still popular, it is often not the most accurate method of adsorption analysis because it propagates errors (Mehdinejadiani, Amininasa, & Manhooei, 2018; Osmari *et al.*, 2013). Presently with the emergence of statistical packages and software, non-linearized have versions of the isotherms and kinetics have been shown to be more accurate and reliable.

Where-as linearized models are direct and use the coefficient of correlation(R^2) as a means of analysis, the non-linear models use a combination of several factors of statistics such as the sum-of-squared errors (SSE), corelation coefficient (R^2), Hybrid fractional error function, minimum square error (MSE), adjusted coefficient of determination R^2_{adj} and

chi-square (Ayawei *et al.*, 2017; Hossain, Ngo, & Guo, 2013; Kajjumba *et al.*, 2018; Mehdinejadiani *et al.*, 2018; Osmari *et al.*, 2013).

2.14.4.1 Sum-of-squared errors (SSE)

Sum of squared errors is considered as one of the most widely used statistical method in the analysis of adsorption. SSE can be represented by the equation 2.17 below (Ayawei *et al.*, 2017; Kajjumba *et al.*, 2018).

$$\sum_{i=1}^{n} (q_{e,i,calc} - q_{e,i,meas})^2 \quad \text{.....Equation 2.17}$$

Where $q_{e,\,i,\,calc}$= theoretical concentration of adsorbate on the adsorbent,

$q_{e,\,i,\,meas}$ = adsorbed concentration of the adsorbate adsorbed on the adsorbent.

2.14.4.2 Coefficient of correlation

The coefficient of correlation is used to represent the variance about the mean. The coefficient of determination (R^2) is defined by the following equation 2.18 below (Kajjumba *et al.*, 2018).

$$R^2 = \frac{\Sigma (q_{e\,cal} - q_{mexp})^2}{\Sigma (q_{e\,cal} - q_{m\,exp})^2 + (q_{e\,cal} - q_{mexp})^2} \quad \text{..... Equation 2.18}$$

Where q_e cal: calculated amount of adsorbate adsorbed onto adsorbent,

q_e exp : experimental amount of adsorbate adsorbed, n: data points,

2.14.4.3 Nonlinear Chi-Square Test (X^2)

Is obtained by the equation below 2.19 below

$$X^2 = \frac{\Sigma (q_{e\,cal} - q_{m\,exp})^2}{\Sigma (q_{e\,cal} - q_{m\,exp})} \quad \text{.....Equation 2.19}$$

Where q_e cal : calculated amount of adsorbate adsorbed onto adsorbent,

q_e exp : experimental amount of adsorbate adsorbed,

2.14.4.4 Marquardt's percent standard deviation

It is an error function, that has been modified from the geometric mean distribution. It uses the degrees of freedom of a system (Ayawei *et al*., 2017; Kajjumba *et al*., 2018).

$$MPSD = \sqrt{\frac{1}{n-p}\sum_{i=l}^{n}\left(\frac{\left(q_{e\,exp}-q_{e\,cal}\right)}{\Sigma\,(q\,exp)}\right)2} \quad \text{..... Equation 2.20}$$

Where $q_{e\,cal}$: calculated amount of adsorbate adsorbed onto adsorbent,

$q_{e\,exp}$: experimental amount of adsorbate adsorbed,

2.14.4.5 Hybrid fractional error function

The Hybrid fractional error function was an improvement of the sum square of errors. And is defined by the equation 2.21 below

$$Hybrid = \frac{100}{n-p}\sum_{i=l}^{n}\frac{(q_{e\,meas}-q_{ecal})\,2}{\Sigma\,(q_{exp})} \quad \text{.....Equation 2.21}$$

Where $q_{e\,cal}$: calculated amount of adsorbate adsorbed onto adsorbent,

$q_{e\,meas}$: experimental amount of adsorbate adsorbed

CHAPTER THREE

MATERIALS AND METHODS

3.1 Research philosophy

This research employed a positivist research paradigm consisting of experimental quantitative and qualitative analysis. In central sciences such as chemistry, positivism research design is usually employed where an assumption that knowledge exist outside and is independent of the researchers.

3.2 Equipment and chemicals

3.2.1 Chemicals and reagents

All the chemicals and reagents used were of analytical grade. Alum ($K_2SO_4.Al_2(SO_4)$. 24 H_2O), ferrous sulphate ($FeSO_4$), potassium dichromate ($K_2Cr_2O_7$), Tin Chloride ($SnCl_2$) were all analytical grade manufactured by Sigma Aldrich and supplied to Moi University by Kobian Kenya Limited, Nairobi, Kenya. The solvents used in extraction such as acetone, dichloromethane, hexane, ethanol, methanol and distilled water were all analytical grade manufactured by Loba Chimie and supplied by Pyrex Laboratories Nairobi Kenya. Methyl Violet 2B ($C_{24}H_{28}N_3Cl$), reactive red 120 ($C_{44}H_{30}Cl_2N_{14}O_{20}S_6$), pure 100% scoured and macarized cotton were provided by Rivatex East Africa Limited, Eldoret (Kenya) and were used without further processing.

3.2.2 Equipment

The following equipment were used; Bruker AXS D2 Phaser SSD 160 X-Ray diffraction machine (America) , Zeiss EVO L 15 ESEM-EDX machine (Germany) , JEOL 1400 transmission electron microscope- brightfield, darkfield, diffraction (Japan) , Mettler

Toledo digital analytical balance (XS204 Delta Range, Switzerland), Beckman Coulter single beam UV Visible Spectrometer (DU 720, Beckham Coulter Inc., USA), Gas chromatography-Mass spectrometer-Shimadzu QP 2010 (Japan) , Hanna 211 digital microprocessor-based bench top pH meter (Hanna instruments, Italy), a wiseman furnace, Nicolet iS50 FTIR spectrometer (Thermo Fisher Scientific, USA), SDL Atlas Launder-o-meter (USA) , SDL ATLAS light fastness tester M237 (USA) and an SDATLAS crock-meter M238 AA (USA). Pure 100% scoured and macarized cotton were purchased from Rivatex East Africa limited (REAL) in Uasin Gishu county, Kenya.

3.3 Materials

3.3.1 Plant materials

The samples used in this study were *Prosopis juliflora* (*P. juliflora*) and *Aloe succotrina* *A. succotrina* were collected on 16th November 2018 and July 14th, 2019, respectively. *P. juliflora* samples were collected from Marigat in Baringo County, Kenya (latitude 0°, 28’ 0.01” N, longitude 35°, 57’ 0.01” E) while samples of *A. succotrina* were collected from Sisiya in Elgeyo Marakwet County on the slopes of Kerio valley, Kenya (latitude 0°, 58’ 56.2” N, longitude 35°, 40’ 0.01” E). The locations where the samples were collected are shown in **Figure 3.1**. The samples were identified and authenticated by a botanist (Mr. Taabu Tepeny) at the Department of Biological Sciences, Moi University, Kenya.

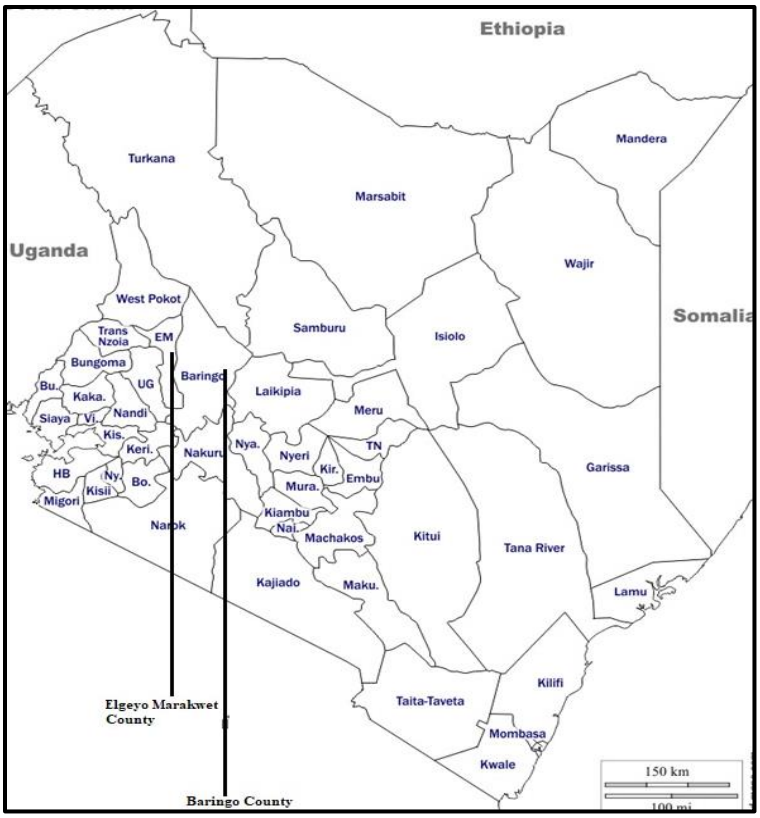

Figure 3.1. Map of Kenya showing the location of Baringo and Elgeyo Marakwet counties where the samples were collected.

3.3.2 Sample preparation

The collected samples of *P. juliflora* were washed under running tap water and put under shade to air dry for three weeks. The heartwood was extracted and later cut into pieces and ground into powder using a locally assembled hammer mill. The ground powder was then extracted using different solvents. For *A. succotrina*, the outer layer of the leaf was first separated from the fleshy latex part manually, and then blended with the desired extraction solvent. The samples were filtered to separate the pulp from the liquid dye before they were transferred to a refrigerator for storage until commencement of analysis. The waste biomass for both plants were transformed into biochar. Sample codes were subsequently assigned

for each of the samples as shown in **Table 3.1** and were henceforth used as unique identifiers for each of the samples used.

Table 3.1: Sample Codes as Unique Identifiers

Plant species	**Unique sample identifier**
Prosopis juliflora	P.J
Aloe succotrina	A.S
P. juliflora biochar prepared at 300 ℃	PJ 300
P. juliflora biochar prepared at 500 ℃	PJ 500
A. succotrina biochar prepared at 300 ℃	AS 300
A. succotrina biochar prepared at 500 ℃	AS 500

3.4 Extraction of dyes

3.4.1 Extraction of dyes from *Prosopis juliflora*

Weighed 500 grams of ground powder of *P. juliflora* heartwood were soaked in 1.5 litres of acetone in 2000 ml beakers for 48 hours with physical agitations at room temperature. The resultant solutions were separately filtered through cotton wool and then Whatmann No. 1 filter paper. The filtrates were concentrated to dryness on a Hahnvapour HS-2005S vacuum rotary evaporator (Hahnshin S&T Limited, Korea) at 40 ℃ under reduced pressure. The concentrated extracts were collected in pre-weighed labelled sample vials and kept in a desiccator containing anhydrous sodium sulphate to remove any traces of water in them.

3.4.2 Extraction of dyes from *Aloe succotrina*

The outer layer of the *A. succotrina* leaves were first separated from the fleshy latex part of the leaves manually. This was the put in a mechanical blender, blended and filtered to remove the pulp from the liquid dye (Khurshid, Muhammad, Asad, & Shah, 2015).

3.5 Phytochemical screening of *P. juliflora* and *A. succotrina* extracts

3.5.1 Classical phytochemical screening

Weighed 0.5 g of the crude plant extracts were dissolved in their respective solvents of extraction in a ratio of 1:20 (w/v). Classical phytochemical screening was performed using standard protocols for the identification of phytochemicals as reported elsewhere (Anyalogbu, Ezeji, & Nwalozie, 2013; Lakshmibai & Amirtham, 2018; Sivanandham, 2016). This provided for testing and detecting the presence of alkaloids, flavonoids, saponins, steroids, tannins and terpenoids.

3.5.1.1 Test for alkaloids (Wagner's test)

To measured 2 mL of the extract, 2 mL of 1% hydrochloric acid was added and steamed. Three drops of Wagner's reagent was added to the resultant solution. Formation of a brown or reddish brown precipitate indicates presence of alkaloids (Sasidharan, Chen, Dharmaraj, & Karupiah, 2011).

3.5.1.2 Test for saponins/saponin glycosides (Froth formation test)

To 1 ml of the extract was added 5 ml of distilled water. The test tube was vigorously shaken for 15 minutes. Formation of a stable foam lasting for 5 minutes indicates presence of saponins in the plant extract.

3.5.1.3 Test for flavonoids (Alkaline reagent test)

To 2 ml of the plant extract in a test tube was added of freshly prepared 2 drops of sodium hydroxide solution. The appearance of a yellow colour which disappear or become colourless after addition of two drops of dilute sulphuric acid indicates the presence of flavonoids in the extract.

3.5.1.4 Test for steroids (Salkowski's test)

To measured 2 ml of the extract in a test tube, 1 ml of concentrated sulphuric acid was added by the side of the test tube. The appearance of a dark reddish colour indicates the presence of steroids in the plant extract.

3.5.1.5 Test for tannins (ferric chloride test)

To measured 2 ml of the plant extract was added 2 ml of 45% ethanol in a test tube. The mixture was then boiled for five minutes and 1 ml of 15% ferric chloride solution was added. The appearance of greenish to black colour indicates the presence of tannins in the plant extract.

3.5.1.6 Test for terpenoids

To 5 ml of the plant extract was added with 2 ml of chloroform and 3 ml of concentrated sulphuric acid. Appearance of a reddish-brown colour at the interface indicates the presence of terpenoids.

3.5.2 Total phenolic content of the dyes

Total phenolic content (TPC) of the extracts was determined spectrophotometrically using Folin-Ciocalteau method as reported by previous authors (Ketema, 2020; Singleton,

Orthofer, & Lamuela-Ravent, 1999). Briefly, the crude extracts (0.01 g) were dissolved in 10 mL of distilled water from which 0.01 mg/mL solutions were prepared by dissolving 0.1 mL of the resultant solutions in 10 mL of distilled water. A measured volume of 0.5 of the resultant extract solutions were separately transferred into vials and mixed with 2.5 mL of Folin-Ciocalteau reagent. After a period of 7 minutes, 2.5 mL of 6% sodium hydrogen carbonate solution was added to the reaction mixture. Blanks were also prepared with 50% methanol, 2.5 ml of 10% Folin-Ciocalteau reagent dissolved in distilled water and 7.5% of sodium hydrogen carbonate solution. The samples were subsequently incubated for 45 minutes at 45 ^{0}C. The absorbances of the assay mixtures were measured at 760 nm a Beckman Coulter single beam UV-Vis spectrophotometer.

The calibration curve used for quantitative analysis of the TPC of the extracts was prepared using gallic acid as the standard. Measured 0.5 mL of prepared gallic acid solutions at concentrations of 10, 20, 40, 60 and 80 ppm were separately transferred into vials and given the same treatment as described for the extracts. Based on the measured absorbances obtained, the TPC of the extracts were expressed in gallic acid equivalent per 100 gram of dry weight (mg of GAE/ 100g DW) of the extracts from the calibration curve (Equation 3.1).

$$TPC = D_f \frac{C\,V}{M} \quad \text{.....(Equation 3.1)}$$

Where D_f = dilution factor

C = concentration of gallic acid established from the calibration curve (in mg/mL)

V = the volume of the extract used

M = the mass of the extract used

3.5.3 Total flavonoid content of the dyes

The Total flavonoid content (TFC) of the extracts were determined using the aluminium chloride coloursimetric assay described by (Hossain *et al*., 2013) with little modifications. Measured 0.25 g of each dyes was taken and dissolved in 1.25 ml of distilled water. A volume of 75 µL of 6% sodium nitrate solution was added and the solution shaken until thoroughly mixed. The resultant mixture was then incubated in a dark oven at room temperature for six minutes.

After, a solution of freshly prepared 10% aluminium chloride was added, and the reaction mixture was further incubated in a dark cabinet for 5 minutes. A calibration curve for quantification of the TFC of the extracts was prepared using standard quercetin at concentrations of 0, 20, 40, 60, 80 and 100 µg/mL using methanol. The absorbances of both the reaction mixtures and quercetin solutions were measured at 510 nm on a Beckman Coulter single beam UV-Vis spectrophotometer using methanol as the blank. The TFC was determined in milligrams quercetin equivalent per gram of dry weight of the extracts (mg QE / g DW) from the quercetin calibration curve using equation 3.2.

$$\text{TFC} = \frac{\text{Absorbance of crude extracts} \times \text{Mass of quercetin in Mg}}{\text{Absorbance of standards} \times \text{Mass of extracts in Mg}} \quad \ldots\ldots \text{(Equation 3.2)}$$

3.6 Spectroscopic and chromatographic characterization of dyes

3.6.1 Ultraviolet-visible spectroscopy analysis

Absorbance spectra, of both dyes were read between 200-800 and the results recorded.

3.6.2 Fourier Transform-Infrared analysis

Dried samples of both *P. juliflora* and *A. succotrina* dyes were scanned at performed at room temperature using an FTIR spectrophotometer for the presence of functional groups. Scanning was done from 500 cm^{-1} to 4000 cm^{-1} with the spectral resolution set at 4 cm^{-1}.

3.6.3 Gas chromatography-mass spectrometry analysis

Extracts of both dyes were initially extracted using C_{18} Solid Phase Extraction cartridges and filtered through 0.45 µm syringe filters. They were then transferred into auto-sampler vials for GC-MS Shimadzu QP 2010 Model for further analysis. Carrier gas used was ultrapure Helium with the flow rate set at 1ml / minute. A BPX5 non-polar column, 30m; 0.25 mm ID; 0.25 µm film thickness, was used for separation.

The GC-MS machine was set and programmed as follows: temperature of 50 ˚C (1 minute). This was subsequently increased at a rate of 5 ˚C /min up to 250 ˚C (9 minutes) with the total run-time being exactly 30 minutes. 1 µL of the sample was injected into the GC at 200 ^{0}C in split mode. This were in split ratios of 10:1 with the interface temperatures set at 250 ^{0}C. The Electron Ionization (E.I) ion source was set at 200 ^{0}C. Mass analysis, was done in full scan mode within the ranges 50-600 m/z and the detected peaks auto-matched against the NIST libraries for possible identification. Both Fragmentation patterns and retention index, were used for matching.

3.7 Optimization of Parameters used for Dyeing

Several experiments were done to optimize dyeing parameters. This were dye concentration, pH, dyeing time and dyeing temperature.

3.7.1 Optimization of dye concentration

Optimization of dye concentration was done as prescribed by (Islam, Hasan, & Deb, 2016) and (Kundal, Singh, & Mc, 2016). The dyeing temperature were held constant at 60 ℃, material to liquor ratio at 1:50 and a dyeing time of 1 hour. For *Prosopis juliflora*, the concentration of the dye was varied at 10 mg/L, 20 mg/L, 30 mg/L 40 mg/L and 50 mg/L and subsequently recorded. For *A. succotrina*, the method was also as above with the dyes being diluted 1:1. 1:2, 1:3 and 1:4.

3.7.2 Optimization of dyeing pH

Optimization of pH was done by methods prescribed by (Islam *et al*., 2016; Kundal *et al*., 2016). The dyeing temperature was held at 60 ℃, material to liquor ratio at 1:50, dyeing time of 1 hour and a concentration of 20 g/L for *P. juliflora* and non-diluted sap from *A. succotrina.* The pH of the dye bath was varied at 3.0, 4.2, 7.1, 8.0 and 9.1 for *P. juliflora* and 3.0, 5.2, 7.1, 9 and 12. The pH was adjusted to the desired value by using HCl and NaOH.

3.7.3 Optimization of dyeing temperature

Optimization of dyeing temperature was done by methods described by (Islam *et al*., 2016; Kundal *et al*., 2016). The dyeing time was held at 1 hour, material to liquor ratio at 1:50, and dye concentration of 20 g/L for *P. juliflora* and non-diluted sap from *A. succotrina.* Five experiments were done at temperatures 25, 40, 60,80 and 100 ℃ and results recorded.

3.7.4 Optimization of dyeing time

Optimization of dyeing time was performed as described by preceding authors (Islam *et al*., 2016; Kundal *et al*., 2016). The dyeing temperature was held at 60 ^{o}C, material to liquor ratio at 1:50, and a concentration of 20 g/L for *P. juliflora* and non-diluted sap from *A. succotrina*. The dyeing time was varied from 10 minutes to 20 minutes, 30 minutes, 40 minutes, 50 minutes and then 60 minutes, and the K/S values calculated.

3.8 Optimization of mordanting method

The following four mordants were used: Alum ($K_2SO_4.Al_2(SO_4).24\ H_2O$), ferrous sulphate ($FeSO_4$), potassium dichromate ($K_2Cr_2O_7$) and stannous chloride ($SnCl_2$). Three mordanting procedures (pre mordanting, post mordanting and simultaneous mordanting) were followed as described by (S. Ali, Hussain, & Nawaz, 2009; Islam, Hasan, & Deb, 2016) with little modifications.

3.8.1 Pre-mordanting

Half a gram of each of the mordants were dissolved in 100 ml of distilled water and then heated to 100°C. The cotton fabric was first dipped into the hot mordant solution at 100 °C and left for 1 hour while occasionally stirring to evenly distribute the mordant into the sample. After mordanting, the fabrics were cooled for five minutes and squeezed several times to remove any excess liquids and mordants. They were immediately inserted into the dye bath at 60 °C and allowed to soak for 1 hour while shaking it occasionally to ensure the dye is evenly distributed onto the cotton fabric. The samples were then washed with 1% non-ionic soap, rinsed and then transferred to a shade to dry awaiting further tests (Islam *et al*., 2016; Janani, Hillary, & Phillips, 2014).

3.8.2 Simultaneous mordanting

Here, accurately measured 0.5 g of the mordants were dissolved in 100 ml of the dye bath while maintaining the material to liquor ratio of 1:50. They were then simultaneously heated to a temperature of 100°C. After, the cotton fabric was then added to the mixture which was then heated together while occasionally stirring for 1 hour. The cotton fabric was then removed, allowed to cool and afterwards washed with 1% non-ionic soap, cooled and put in the shade to dry awaiting further tests (Islam *et al*., 2016; Janani, Hillary, & Phillips, 2014).

3.8.3 Post-mordanting

In this method, the sample cotton fabric was first dyed in the respective dye baths at 60 °C for 1 hour, before being removed and added separately to the solutions of the mordants. The ratio of mordant to solvent was maintained at 1.20 at temperatures of 100°C and the fabric left for 30 minutes. The dyed fabric was then soaked in the mordant solution at 100 °C and the fabric left for 1 hour with occasional stirring to evenly distribute the mordant in the fabric. The samples were allowed to cool before they were washed with 1% non-ionic soap and left to dry in the shade (Islam *et al*., 2016; Janani, Hillary, & Phillips, 2014).

3.9 Determination of fastness of the dyed cotton fabric

The subsequently dyed samples were subjected to fastness tests based on previously prescribed ISO standard tests.

3.9.1. Fastness to washing

The respective dyed fabric was placed with another material of the same kind i.e. cotton and the two stitched together as per ISO 105-C06:1994 specifications. The fabric was then added to a 5 g/L non-ionic detergent maintaining the material to liquor ratio at 1:50, at 50°C for 45 minutes in Launder-o-meter and the samples assessed for colour loss. The difference were assessed using a grey scale ISO 105 A02;1993 for change in colour (Yusuf *et al*., 2015).

3.9.2. Fastness to sunlight

The apparatus used for testing of fastness to sunlight was the exposure rack. Thinly cut fabric of 1 cm by 8 cm were inserted in test tubes and hang on an exposure rack. They were then illuminated using a 500 W SDL ATLAS light fastness tester for 4 hours. Thereafter, they were assessed using grey scale ISO 105 A02;1993 for the evaluation loss of shade depth (Jihad, 2014; Kumaresan, Palanisamy, & Kumar, 2011).

3.9.3 Fastness to rub

Testing of fastness to rub was done using a Crockmeter (AATCC Model, M238AA SDATLAS) as per ISO 105-X12:2001 by mounting the dyed fabric on the crockmeter panel and rubbing it ten times using the stoke both wet and dry. The fabric was then assessed for staining on the special white adjustment fabric on the crockmeter.

3.10 Determination of CIELAB-Colour coordinates of dyed fabric samples

All the dyed fabric were tested for their colour coordinates commonly referred to as the CIE L*, a*, b*, C*, h^0. This was done using a benchtop spectrometer X-rite SP60-

EB05003377 illuminant D65-10 mode by taking three independent points on the fabric and then averaging them for their means (N. F. Ali & El-Mohamedy, 2011; Y. Ding & Freeman, 2017). The value of L* corresponds to either luminosity or lightness, a* corresponds to redness when positive or greenness when negative. The values of b* corresponds to shades of yellow when positive and shades of blue when negative. The Values of Cie c* and h^o correspond each to chroma and hue angle, respectively. The values of cie C and h^o were calculated using equations 3.3 and 3.4, respectively.

$$\text{Chroma } (C^*) = \sqrt{a^2 + b^2} \quad \text{.....(Equation 3.3)}$$

$$\text{Hue Angle}(h) = \tan^{-1}\frac{b}{a} \quad \text{..... (Equation 3.4)}$$

3.11 Evaluation of Colour strength

The colour strength is usually calculated in the form K/S values fitted in the Kubelka - Monk equation of reflectance (Kundal *et al*., 2016; Sarkar, 2004; Yusuf, Mohammad, & Shabbir, 2016). This equation (Equation 3.6) defines a relationship between the percentage reflectance (%) of a given sample, the scattering (S) and the samples absorption (K).

$$\frac{K}{S} = \frac{(1-R)^2}{2R} \quad \text{..... (Equation 3.5)}$$

Three values of the R value of the fabric were taken and their results averaged. This was used to calculate the colour strength based on the formula above.

3.12 Evaluation of chemical properties of biochar

3.12.1 Fourier Transform Infrared analysis

Different FTIR analysis of the produced biochar both before and after adsorption were done using a Nicolet iS-50 FTIR spectrometer within the regions of 400 to 4000 cm^{-1} to

establish the presence of functional groups. For each sample analysed, a total of 32 scans at 0.5 cm^{-1} resolution were done in the attenuated total reflectance mode.

3.12.2 X-ray powder diffraction analysis

The XRD patterns were recorded using an X-ray diffractometer (Bruker D2 phaser SSD 160 Series 2, Bruker Co., Germany) at 2θ values ranging from 5° to 70°. This was used to evaluate mineral composition of the biochar using the scan software, diffract eva and diffract suite match software.

3.12.3 EDX-SEM analysis

A Zeiss EVO LS 15 scanning electron microscope (conventional SEM, low vacuum, ESEM and EDX) operating at 20 kV accelerating voltage was used to carry out microscopic analyses while energy dispersive X-ray (EDX) analyses were carried out using an Oxford make EDX detector.

3.12.4 Transmission electron microscopy

A JEOL 1400 transmission electron microscope (brightfield, darkfield, diffraction, EDX) operating at an accelerating voltage of 200 kV was used to perform transmission electron microscopic data.

3.13 Batch Adsorption Procedures

3.13.1 Preparation of adsorbents for sorption processes

The left-over biomass from the extraction of the samples of both *A. succotrina* and *P. juliflora* were first dried under shade. They were then pyrolyzed at 300 ^{o} C and 500 ^{o} C

respectively using the method prescribed by (Song *et al*., 2012). The starting temperature was 200 ^{0}C in an oven. This was sequentially elevated by temperatures of 50 ^{o} C and held for 1.5 hour at every point, till the final required temperature was attained. Heating above 250 ^{o} C were done in a furnace. The prepared biochar samples were then allowed to cool and later stored in airtight containers and later used for sorption studies.

3.13.2 Optimization of adsorption

Several factors that are known to affect adsorption were optimized and these included pH, contact time, shaking speed, temperature, adsorbent dosage and initial concentration. For all cases, except when the parameter was being optimized, the constant conditions were an initial concentration of 20 ppm, a pH of 7.2 for RR 120, a pH of 6.4 MV2b both ambient pH's, a rotation speed of 420 rpm and a temperature of 25 ℃ with a contact time of 20 minutes.

3.13.2.1 Optimization of pH

To get the best pH for adsorption, the pH was varied at 2, 4.5, 7, 8.2 and 9.5 for RR 120 and 4, 6.2, 7, 8 and 10 for MV 2B while maintaining all other conditions in the experiment constant. 0.1 g of the adsorbent was used while the temperatures was maintained at 25 ^{0} C, a shaking speed of 420 rpm, and a time of 30 minutes and initial concentration of 20 ppm. The samples were then filtered and measured in a UV-Vis spectrophotometer.

3.13.2.2 Optimization of initial concentration

To determine the optimum initial concentration, all the factors were held constant i.e. temperature of 25 ℃, pH of 7.2 for RR120, and pH 6.4 for MV 2b, shaking speed of 420

rpm, and a contact time of 30 minutes. The initial concentrations varied were 1 ppm, 1.5 ppm, 2ppm, 2.5 ppm, 5 ppm, 10 ppm and 20 ppm.

3.13.2.3 Optimization of temperature

To determine the optimum temperature, all the other factors were held constant and the temperature varied in the ranges of 25, 30, 40, 50, 60 and 80 ℃.

3.13.2.4 Optimization of shaking speed

To determine the optimum shaking speed, all the other factors were held constant and the shaking speed varied at 120, 220, 420, 620 and 820 rpm.

3.13.2.5 Optimization of contact time

To determine the optimum contact time, all the other factors were held constant and the contact time varied between 5, 10, 20, 30, 40, 50, 60, 80, 100 and 120 minutes and the results recorded.

3.14 Data Analysis

All experiments were done in triplicates and their results recorded. Data analysis was done with Microsoft Excel (Microsoft Corporation, USA), CAVS adsorption software, FTIR explorer and Sigma plot statistical software for Windows (version 12, Systat Software Inc.)

CHAPTER FOUR

RESULTS AND DISCUSSION

4.1 Phytochemical screening results

Both plants, *A. succotrina* and *P. juliflora* extracts, were analysed for the most common phytochemicals namely; saponins, steroids, tannins, flavonoids, terpenoids, phenolics and alkaloids and the results are presented as follows.

4.1.1 Phytochemical screening of *Aloe succotrina*

Phytochemical screening of the crude ethanolic and water extracts of *Aloe succotrina* plant were found to have saponins, steroids, tannins, flavonoids, terpenoids, phenolics and alkaloids, this agree with results previously obtained from the phytochemical screening of other species of *Aloe* namely *Aloe barbadensis* and *Aloe gilbertii* respectively (Dharajiya, Pagi, Jasani, & Patel, 2017; Yadeta, 2019). Table 4.1 below, shows a summary of qualitative analysis of *A. succotrina* extracts.

Table 4.1: A table of phytochemicals screening of different extracts of *A. succotrina*

Phytochemical components	Ethanolic Extracts	Water Extracts
Saponins	+	+
Steroids	+	+
Tannins	+	+
Flavonoids	-	+
Terpenoids	+	+
Phenolics	+	+
Alkaloids	+	+

Key : + : present –: absent

4.1.2 Phytochemical *Prosopis juliflora*

Various crude extracts of *P. juliflora* showed that different phytochemicals were present. Methanolic extracts were found to have terpenoids, saponins, tannins, alkaloids, flavonoids and steroids with alkaloids being absent. Acetonic extracts yielded for all the above previously stated phytochemicals except for saponins. Hexanolic extracts on the other hand, had only tannins and alkaloids with distilled water extracts having all the phytochemicals present except terpenoids and steroids. These results, are similar to those previously discussed by (Lakshmibai, Mirtham, & Adhika, 2015; Khandelwal, Sharma, & Agarwal, 2016; Preeti, Avatar, & Mala, 2015). Table 4.2 below, shows the results of the phytochemical screening of different extracts of *P. juliflora*.

Table 4.2: A table of phytochemicals screening of different extracts of *P. juliflora*

Phytochemical compound	Methanol	D. Water	Acetone	Hexane
Terpenoids	+	-	+	-
Saponins	+	+	_	-
Tannins	+	+	+	+
Alkaloids	-	+	+	+
Flavonoids	+	+	+	-
Steroids	+	-	+	-

Key: +: present –: absent

The dye extracts chosen for this study, were the flavonoid rich acetonic extracts of the heartwood of *P. juliflora*. This information, was based on previous research that suggested that, the acetonic extracts have an unusually high levels of flavonoids and also on the fact that yellow and brown dyes have been suggested to be mainly flavonoids and its derivatives (Selvam *et al*., 2015; P. K. Sirmah, 2019; Yunus *et al*., 2011).

4.1.3 Total Phenolic Content (TPC)

A majority of natural dyes from plants have their major dyeing compounds being phenolic or polyphenolic compounds (Ford, 2017). The TPC content for the two natural dyes, was therefore done based on a standard calibration curve of absorbance against concentration for gallic acid which was used as a standard. Figure 4.1 below, shows the calibration curve of absorbance against concentration of gallic acid.

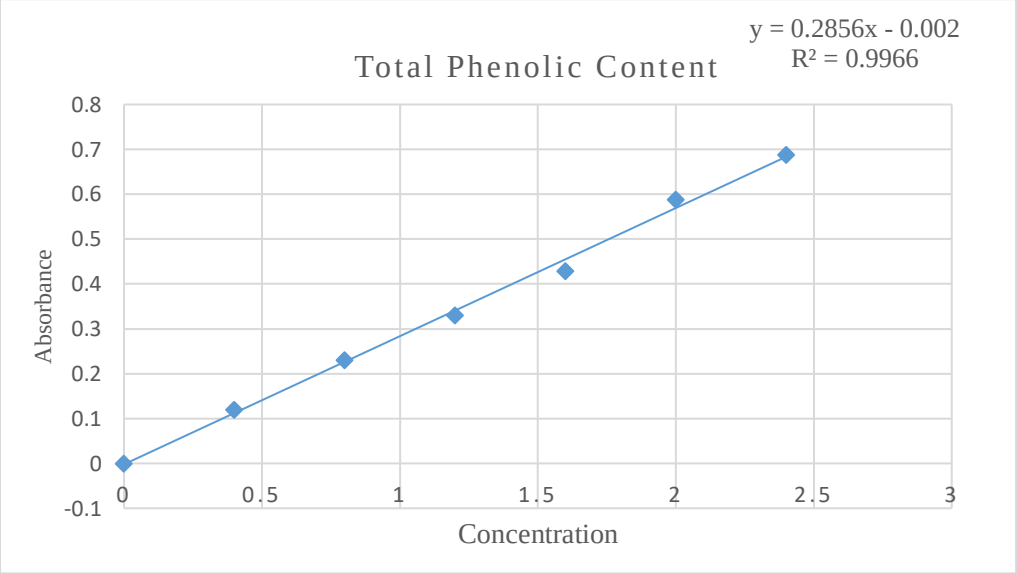

Figure 4.1: A calibration curve of absorbance against concentration for TPC

As shown in the figure 4.1 above, a good correlation coefficient (R^2= 0.9966) was obtained from the standard calibration curve. The total phenolic content for *A. succotrina* leaves and the acetonic extracts of *P. juliflora* were found to be 34.9 ± 1.7 and 53.5 ± 2.6 gallic acid equivalent GAE respectively. Several studies have been done to measure the TPC of other species of *Aloe*, such as ethanolic leaf gel extracts of *Aloe vera* plant which showed slightly higher TPC in the ranges of 40.500 ± 0.041 GAE (Liu, Chen, & Shi, 2013). On the other hand, ethanolic extracts of another species of *Aloe*, *Aloe greatheadii* had slightly lower TPC of 30.9 ± 0.77 GAE (Botes, Westhuizen, & Loots, 2008). The TPC of another species of *Prosopis* i.e *Prosopis cineraria*, was 530 mg/g GAE (Rathore *et al*., 2019).

4.1.4 Total Flavonoid Content (TFC)

As most brown and yellow natural dyes are attributed to flavonoids, the TFC of the dyes, were investigated (Ford, 2017). The figure 4.2 below shows a graph of absorbance against the concentration of quercetin for the quantification of flavonoids.

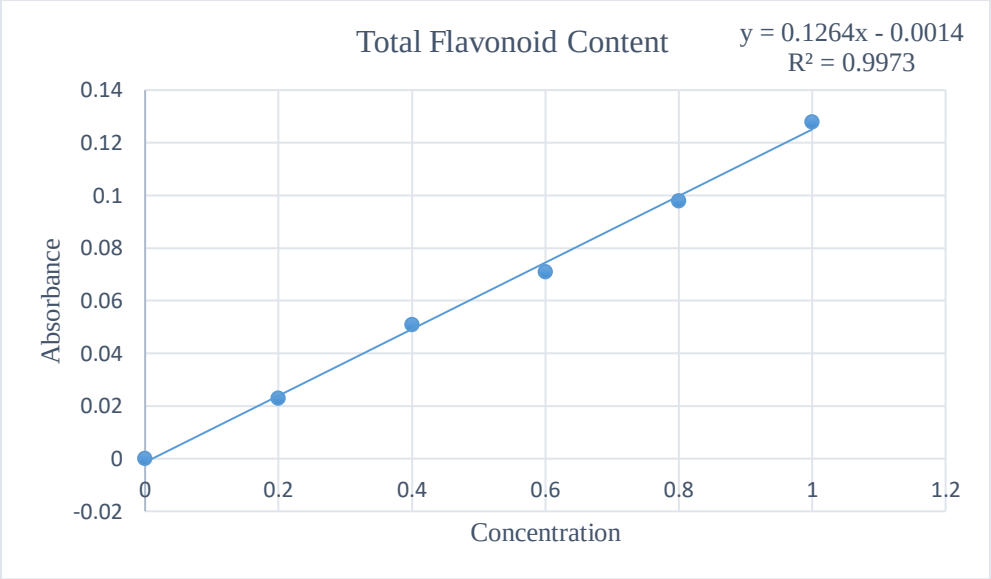

Figure 4.2 A calibration line of Absorbance Vs concentration for TFC

The correlation coefficient of the graph (R^2=0.9973) was obtained for the standard curve. The Total flavonoid content is described in mg of quercetin equivalent per gram of dry weight of the heartwood of *P. juliflora* for the acetonic extract, was found to be 33.7 ± 1.22 while the TFC for extracts of *Aloe Succotrina* were found to be 27.37 ± 1.48.

Other species such as *Aloe vera* in literature, recorded TFC of 138.13±6.63 which are fairly high when compared to this species (Vastrad, Goudar, Byadgi, Devi, & Kotur, 2015). Equally, *Aloe vera* extracted in Iran, showed TFC of 33.6 ± 1.98 (Nejatzadeh-barandozi, 2013). On the other hand, extracts of *Aloe greatheadii*, showed very low amounts of TPC of 2.37 ± 0.06. This perhaps suggesting that different species of Aloe have varying amounts

of extractives, depending on their environment uses and potential medicinal (Botes *et al*., 2008).

4.2 Spectroscopic and chromatographic characterization of chromophores

4.2.1 UV-Vis spectra

4.2.1.1 UV-Vis Spectrum of *Aloe succotrina*

The UV-Vis spectrum for the extracts of *A. succotrina* dye was done between the wavelengths of 200-800. Figure 4.3 below, shows the UV-vis spectrum of the *A. succotrina* dye.

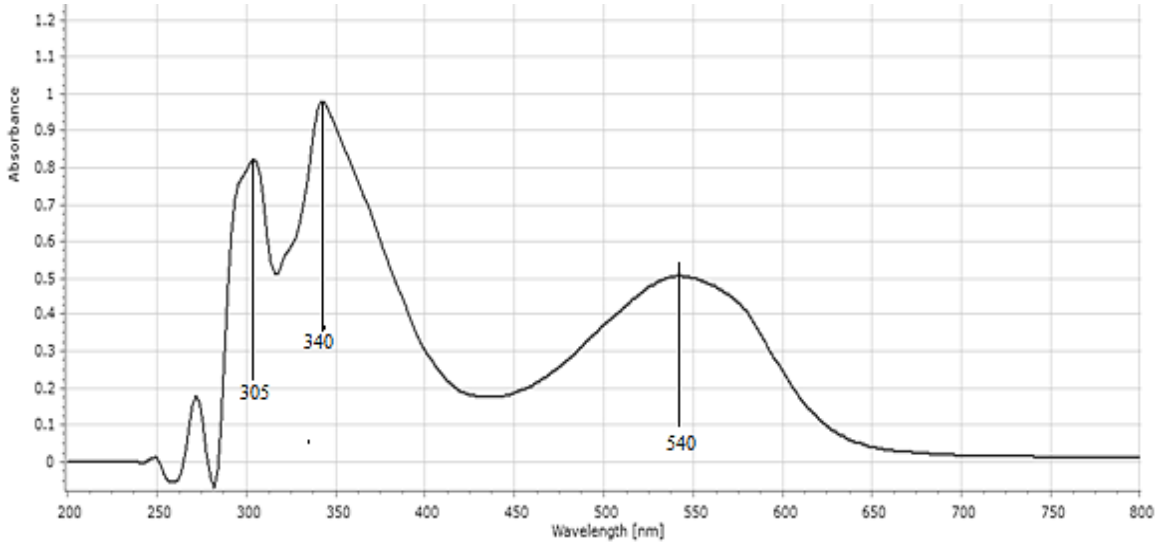

Figure 4.3: UV-VIS spectrum of Aloe dye

The spectrum had three significant peaks. One at around 540 nm and the others at 340 and 305 nm. The peak around 540, is characteristic for purple coloured anthocyanin, whose peaks usually absorb at wavelengths of between the ranges 540-580. Examples of some anthocyanins that absorb around this region include petunidin (λ_{max}=543), malvidin (λ_{max}=

542) and delphinidin (λ_{max}= 546) (Espinosa-Morales, Reyes, Hermosín, & Azamar-Barrios, 2012).

The peaks at 305 and 340 may be due either the presence of flavonoids or to interference as result of co-pigmentation where the λ_{max} is shifted due to the presence of other compounds which can cause a hyperchromic shift in the λ_{max} to a different value. For example previous research showed that in the presence of caffeic acid, delphinidin (λ_{max}= 546), formed a complex with it giving another peak at approximately λ_{max}= 585 (Espinosa-Morales *et al*., 2012).

4.2.1.2 UV Spectrum of *Prosopis juliflora*

Figure 4.4 below, shows the UV-Vis spectrum of *P. juliflora* dye, between the wavelengths of 200-800.

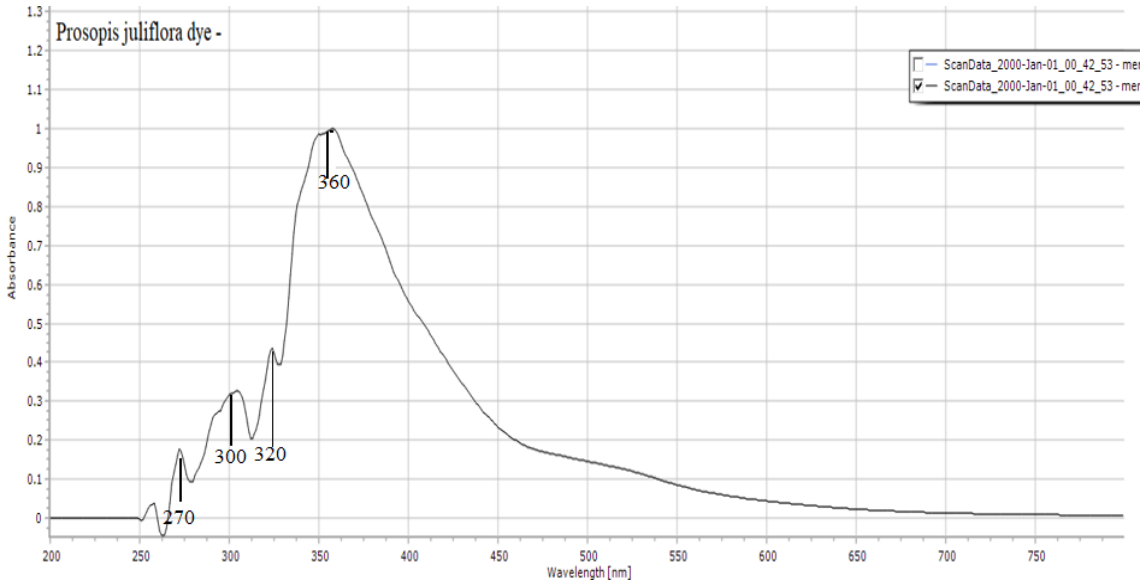

Figure 4.4: UV spectrum of *Prosopis juliflora*

The dye extracted from *P. juliflora*, shows evidence of co-pigmentation with several absorptions of around 250 nm, 270 nm, 300nm, 320 nm and 360 nm meaning that the colour of the dye cannot be attribute to one group but several groups. This is not unique to

this dye as previous brown dyes have also been reported to have multiple absorption peaks (Selvam *et al*., 2015). For example, a brown dye from the *Trigonella foenum* plant, had absorptions of 259.2, 265.6, 358.4, 371.2 and 396.8nm.

The peaks around 250 and 270 nm, are characteristic of flavonoid dyes and can therefore be attributed them (Yunus *et al*., 2011). This can also be corroborated by the presence of flavonoids in the phytochemical screening and also to previous studies that have shown the presence of un usually large amounts of flavonoids such as catechin, epicatechin, mesquitol and gallocatechin in the heartwood of *the P. juliflora* a plant (Chepkwony *et al*., 2020; Odero *et al*., 2017; P. K. Sirmah, 2019). Other brown dyes extracted from the shells of chest nut, showed an absorbance of between 245-265 nm with subsequent mordanting with Al^{3+} and Fe^{2+} leading to changes in shades of colour to brown and dark green respectively. This phenonemenon was also witnessed in this dye which also changed colour to khaki and dark green in the presence of metallic mordants (Yunus *et al*., 2011).

4.2.2 FTIR Spectra of the dyes

FTIR spectroscopy of the two dyes, were done between the wavelengths of 4000 – 500 cm^{-1} for the identification of functional groups present in the dyes and documented below.

4.2.2.1 FTIR spectrum of *Aloe succotrina*

Figure 4.5 below, represents the FTIR spectrum of the *A. succotrina* dye. The FTIR spectrum of the dye showed several peaks such as a broad peak at 3273.20 which is characteristic of O-H for a carboxylic acid or N-H for an amide group or a terminal ≡C-H. The peak at 2927.94 is characteristic of an O-H stretch for carboxylic acid while the peak at 2848.86 is for a C-H bond in an aldehyde (Bartošová, Blinová, Sirotiak, & Michalíková, 2017; Cuixia *et al*., 2020; Hussein, Hadi, & Hameed, 2016).

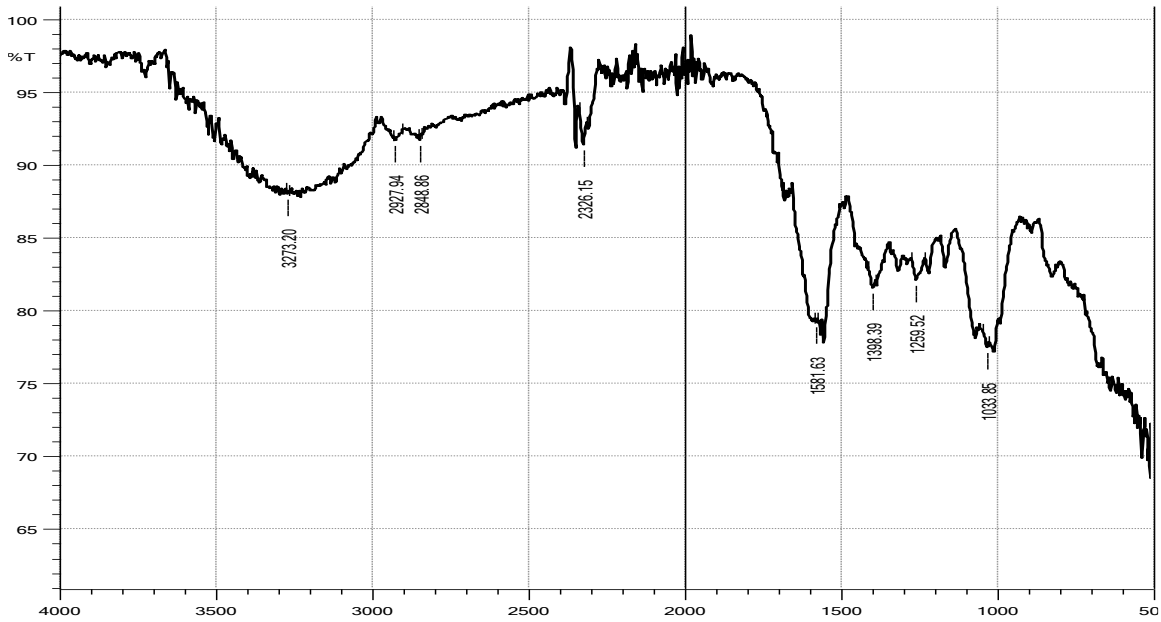

Figure 4.5: FTIR spectrum of *Aloe succotrina* dye

The peak at 2326.15 is for C≡N while the 1581 peak is for C=C, N-H for a primary amine group, or NO_2 for an aliphatic Nitro. The peak for 1398.39 is for C-O-H bond while the peaks for 1259.52 and 1033.85 are for either C-O, C=O respectively. (Bartošová *et al*., 2017; Cuixia *et al*., 2020; Hussein *et al*., 2016).

4.2.2.2 FTIR spectrum of *Prosopis juliflora* dye

Figure 4.6 below shows FTIR spectrum of the *P. juliflora* dye. The dye from *Prosopis juliflora*, also had several notable peaks such as the broad peak at 3228.84 characteristic of a OH group for a carboxylic acid, N-H for an amide group or a terminal ≡C-H. The absorption at 2324.22 is characteristic of C≡N while the absorption band at 1606.70 is for C=C bond, N-H bond and C=O for conjugation of aldehydes with two aromatic rings (Bartošová *et al*., 2017; Cuixia *et al*., 2020; Hussein *et al*., 2016).

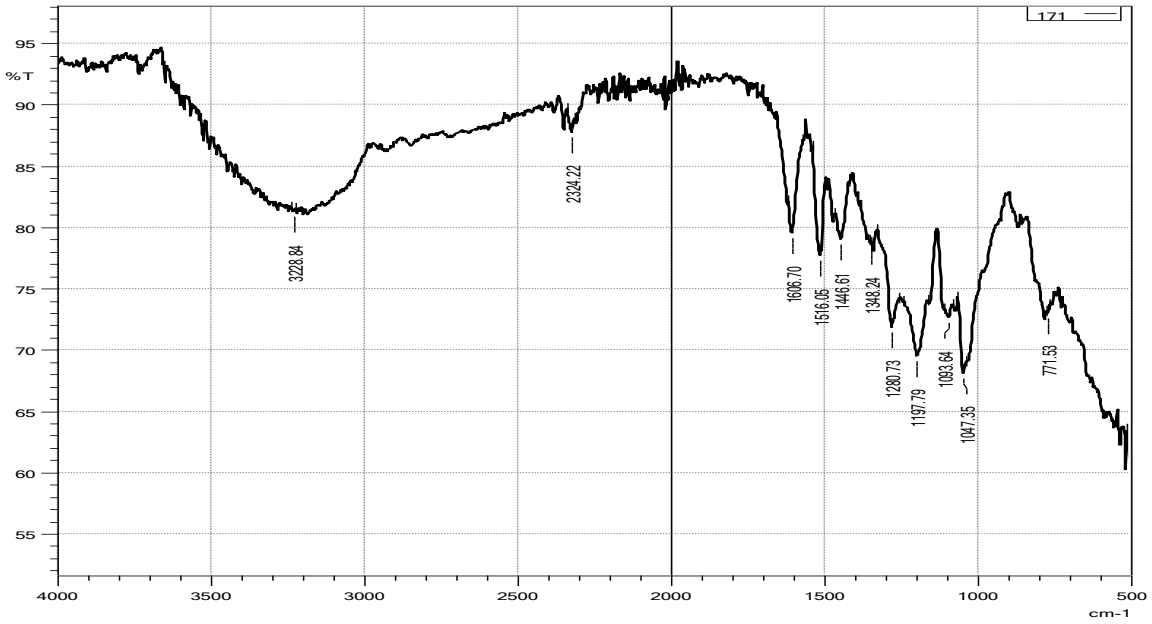

Figure 4.6: FTIR Spectrum of *Prosopis juliflora* dye

The absorption at 1516.05 is for C=C, N-H or NO_2, the peak at 1348.24 is for C-O-H, C-F or NO_2 bond. While the peak at 1280.73 is for C-O-H, C=O or C-O. The peak at 1197.79 1093.64 and 1047.35 both represent C-O for alcohols and ethers while the peak at 771.53 is for N-H, =C-H or C-Cl (Bartošová *et al*., 2017; Cuixia *et al*., 2020; Hussein *et al*., 2016).

4.2.3 GC-MS

GC-MS analysis of the dyes, was done using a Shimadzu QP 2010-SE GC-MS machine.

4.2.3.1 GC-MS results of *Aloe succotrina*

Figure 4.7 below, shows the GC chromatograms of separated compounds with their respective retention times and table 4.3 below, shows a summary of GC retention time (RT) and information obtained from GC-MS showing molecular weights, chemical formulas, names and possible compounds based on compared NIST entries.

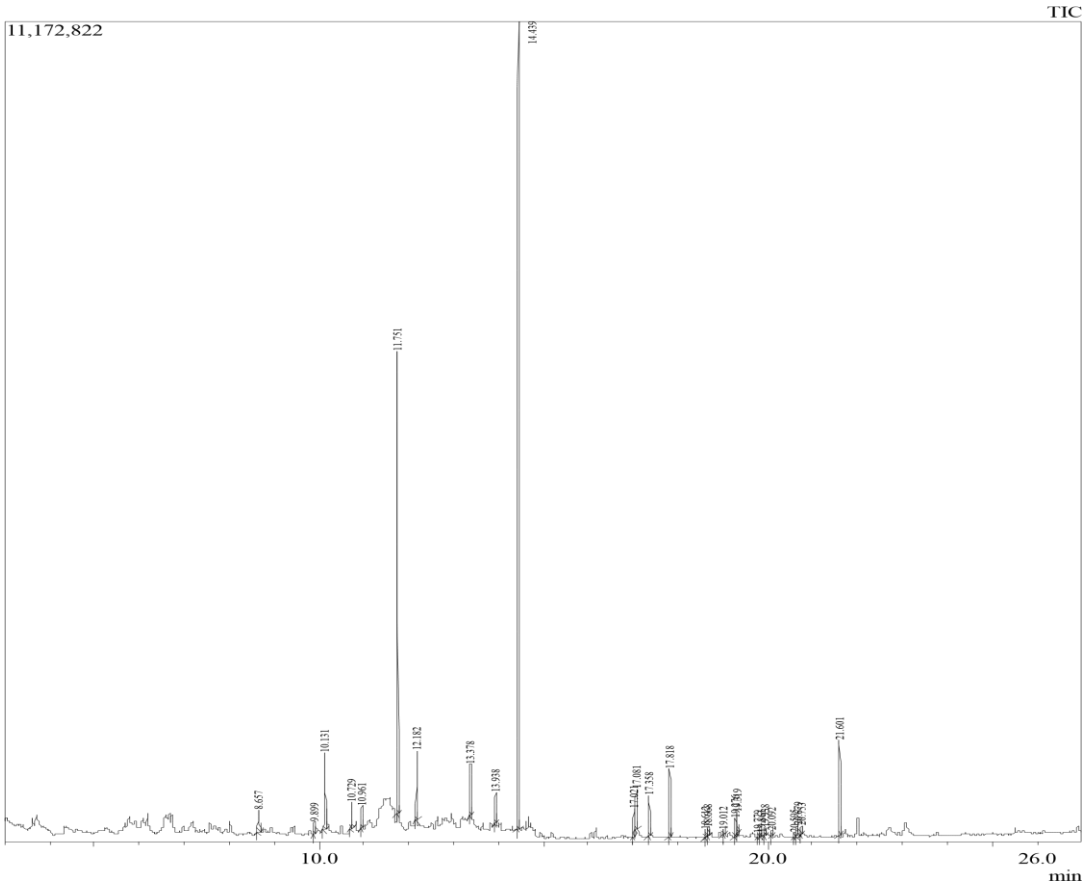

Figure 4.7: GC-MS peak report for *Aloe succotrina* extracts

Table 4.3: A summary of GC retention time (RT) and information obtained from GC-MS showing molecular weights, chemical formulas, names and possible compounds based on compared NIST entries. Each of the structures are attached in the appendix

Peak#	R.Time	Area	Area%	Height	Height%	Molecular Weight	Molecular Formular	Name
1	8.657	703575	1.57	1.57	302482	206	C_6H_4BrClO	2 chloro-4-bromophenol
2	9.899	419276	0.94	0.94	168901	143	$C_6H_9NO_3$	DL-Proline, 5-oxo-, methyl ester
3	10.131	2260286	5.05	5.05	1046915	124	$C_7H_8O_2$	Orcinol
4	10.729	628500	1.41	1.41	362414	172	$C_9H_{20}Si$	1-Methyl-1-n-pentyloxy-1-silacyclobutane
5	10.961	479206	1.07	1.07	306238	256	$C_7H_{21}O_4PSi_2$	Phosphoric acid, bis(trimethylsilyl)mono
6	11.751	9998476	22.35	22.35	6301078	186	$C_{12}H_{26}O$	1-Dodecanol
7	12.182	1412141	3.16	3.16	952032	278	$C_{17}H_{30}OSi$	Phenol, 2,4-bis(1,1-dimethylethyl)-
8	13.378	1135384	2.54	2.54	695058	227	$C_{13}H_{13}N_3O$	Hydrazinecarboxamide, N,N-diphenyl-
9	13.938	737951	1.65	1.65	416022	166	$C_9H_{10}O_3$	2',4'-Dihydroxy-3'-methylacetophenone
10	14.439	17100863	38.23	38.23	11003534	254	$C_{16}H_{30}O_2$	2-Propenoic acid, tridecyl ester
11	17.021	782109	1.75	1.75	378222	270	$C_{17}H_{34}O_2$	Hexadecanoic acid, methyl ester
12	17.081	1430874	3.20	3.20	562232	190	$C_{11}H_{10}O_3$	4H-1-Benzopyran-4-one, 7-hydroxy-2,5-dimethyl
13	17.358	1095071	2.45	2.45	551395	256	$C_{16}H_{32}O_2$	n-Hexadecanoic acid
14	17.818	1497665	3.35	3.35	925826	274	$C_{15}H_{30}O_2S$	Propanoic acid, 3-mercapto-, dodecyl ester
15	18.612	180418	0.40	0.40	108568	242	$C_{16}H_{34}O$	1-Hexadecanol
16	18.668	176639	0.39	0.39	119206	294	$C_{19}H_{34}O_2$	9,12-Octadecadienoic acid, methyl ester
17	19.012	96596	0.22	0.22	66229	296	$C_{19}H_{36}O_2$	Cyclopentanetridecanoic acid, methyl ester
18	19.276	443441	0.99	0.99	255964	374	$C_{11}H_{15}BrClO_3PS$	Profenofos
19	19.319	426885	0.95	0.95	280880	284	$C_{18}H_{36}O_2$	Octadecanoic acid
20	19.779	75464	0.17	0.17	46865	312	$C_{20}H_{40}O_2$	Acetic acid n-octadecyl ester
21	19.861	93182	0.21	0.21	52297	262	$C_{15}H_{22}N_2O_2$	5-(4-Phenyl-piperazin-1-yl)-pentanoate
22	19.938	199626	0.45	0.45	115779	272	$C_{16}H_{32}O_3$	Tetradecanoic acid, 2-hydroxyethyl ester
23	20.092	121682	0.27	0.27	67630	227	$C_{14}H_{29}NO$	N,N-Dimethyldodecanamide
24	20.595	123679	0.28	0.28	54706	196	$C_{14}H_{28}$	ethyl-cyclododecane,
25	20.679	396882	0.89	0.89	156761	456	$C_{30}H_{48}O_3$	10-Hydroxy-2,4a,6a,6b,9,9,12a-heptamethyl-1,2,3,4,4a,5,6,6a,6b,7,8,8a,9,10,11,12,12a,12b,13,14b-icosahydropicene-4a carboxylic acid
26	20.753	196227	0.44	0.44	117724	312	$C_{19}H_{36}O_3$	9-Octadecanoic acid, 12-hydroxy-, methyl
27	21.601	2516585	5.63	5.63	1291233	340	$C_{23}H_{32}O_2$	Phenol, 2,2'-Methylbis [6-(1,1-dimethyethyl)-4-methyl-
		44728683	100.00	100.00	26706191			

Exactly 27 hits matched the NIST 14 library as identified compounds from the *A. succotrina* dye with their respective molecular masses, retention times and retention indexes matching. Some compounds were phytochemicals while others were classified as solvents or contaminants. Only significant phytochemicals or compounds were discussed further in this work.

2 chloro-4-bromophenol, is a synthetic organobromine pesticide, and was therefore not analysed further. The presence of the compound, may be due the use of pesticides in the environment which can bioaccumulate in the plant. The compound DL-Proline, 5-oxo-, methyl ester is a plant flavonoid with antioxidant and anti-inflammatory properties that has been previously been detected using GC-MS from the herbal mixtures of the plants *Terminalia chebula, Phyllanthus emblica* and *Treminalia bellirica* in India (Eugin Amala & Jeyaraj, 2014).

The compound orcinol, of retention time of 10.131 was the first significant phytochemical with potential dyeing properties identified by the GC-MS from the *A. succotrina* plant. This compound, has previously been isolated from *Roccella tinctoria* which is a purple lichens (Poulin, 2018). This compound, has previously been credited with the purple dye from the lichens as a result of the interaction with air to form orcein which is purple in colour (Casselman, 1994; Fisch, Flick, & Ardrttit, 1973). Historically, the purple dyes from this species of lichens, had often been used by the lesser affluent members of the society as an alternative dye to the more expensive tyrian purple dye due to its royal purple colour (Calà *et al*., 2019). As extracts of the *Aloe succotrina* plant are equally royal purple in colour, it can be concluded that the compound orcinol, is partly responsible for the purple colour. The mass spectrum is attached in the appendix.

1-Dodecanol, is plant metabolized 12 carbon fatty acid that exists naturally in plants like coconuts and palm with a floral odour and antimicrobial activities. It has been previously been identified by GC-MS in plants such as *Etlingera elatior* commonly known as the ginger flower (Wijekoon, Bhat, Karim, & Fazilah, 2013). 1-Methyl-1-n-pentyloxy-1 silacyclobutane and Phosphoric acid, bis(trimethylsilyl)mono are solvents and were not analysed further.

Compound 7, Phenol, 2,4-bis(1,1-dimethylethyl), is a naturally occurring phenol that has been reported in at least 169 species of organisms with insecticidal, nematocidal, antiviral, antifungal and antibacterial activities (Zhao, Wang, Lucardi, Su, & Li, 2020). 2',4'-Dihydroxy-3'-methylacetophenone is a secondary metabolite that has been isolated in plants like Trichoderma. Hydrazinecarboxamide, N,N-diphenyl- , 2',4'-Dihydroxy-3'-methylacetophenone and 2-Propenoic acid, tridecyl ester are solvents.

Compound 11, Hexadecanoic acid, methyl ester is a plant metabolite with antifungal potentials. This, has previously been proven by (Abubacker & Deepalakshmi, 2013) who isolated the compound from the leaves of *Annona muricata* Linn. This compound, has previously been evaluated using GC-MS as one of the constituents of the plant *Pterocarpus angolensis* which has a deep red coloured sap that is used as a natural dye.

1-Hexadecanol is a16 carbon fatty alcohol, that was first isolated from whale oil. Previously, it has also been identified through GC-MS of several plants such as *Etlingera elatior* flowers (Flowers, Susanti, Awang, Qaralleh, & Ibrahim, 2013). The compound 16, 9,12 Octadecadienoic acid, methyl ester is a plant metabolite that has been previously isolated from *Elaeis guineensis* fruit (Odion, Ogboru, & Ighene, 2020). Equally, Cyclopentane-tridecanoic acid, methyl ester, is a plant metabolite that has also been

previously identified using GC-MS in methanolic extracts of *Chenopodium album* leaves. Octadecanoic acid, also referred to as stearic acid is a plant metabolite is an 18 carbon straight-chain saturated fatty acid used in the making of soaps plastics, cosmetics etc. It has previously been identified in other species of *Aloe* such as the *Aloe vera* plant (Silva, Mocan, Calhelha, & Sokovi, 2019).

Acetic acid n-octadecyl ester, is a plant metabolite that has been previously identified using a GC-MS from the plant *Trichoderma harzianum*. Tetradecanoic acid, 2-hydroxyethyl ester commonly reffered to as Myristic acid is a fatty acid ester that has been previously extracted from the leaves of *Aloe vera* (Silva *et al*., 2019). N,N- Dimethyldodecanamide, is a plant metabolised alkaloid, that has potential antimicrobial activity. It was previously identified in the medicinal plant *Picralima nitida* (Igwe & Mgbemena,2015).10-Hydroxy2,4a,6a,6b,9,9,12aheptamethyl,1,2,3,4,4a,5,6,6a,6b,7,8,8a, 9,10,11,12,12a, 12b ,13,14b-icosahydropicene-4a carboxylic acid is a terpene that has been previously identified from the plant *Adenanthera pavonine* and *Lantana camara* (Ansari, Sirbaiya, Kumar, & Usmani, 2016; Mariajancyrani, Chandramohan, Brindha, & Saravanan, 2014). Phenol, 2,2'-Methylbis [6-(1,1-dimethyethyl)-4-methyl-**,** is a volatile oil that has previously been isolated from (Wei & Guo, 2020).

Figure 4.8 below, shows the structures of some of the identified compounds from *Aloe succotrina*.

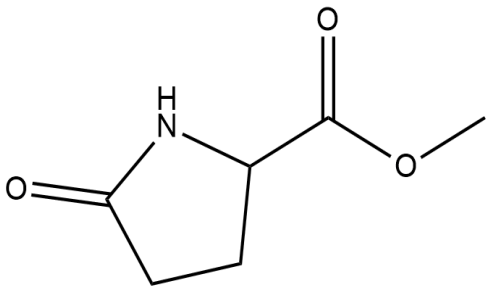

DL-Proline, 5-oxo-, methyl ester

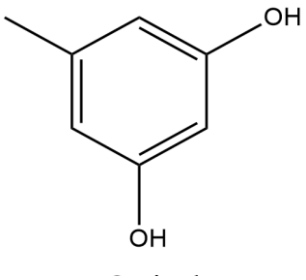

Orcinol

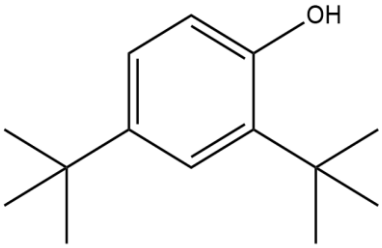

Phenol, 2,4-bis(1,1-dimethylethyl)-

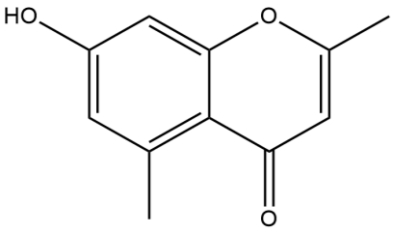

4H-1-Benzopyran-4-one,7-hydroxy-2,5-dimethyl

1-dodecanol

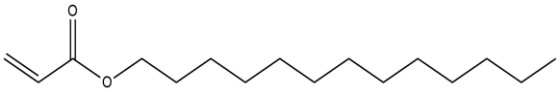

2-Propenoic acid, tridecyl ester

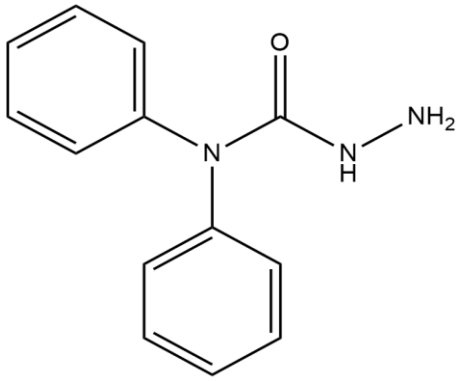

Hydrazinecarboxamide, N,N-diphenyl-

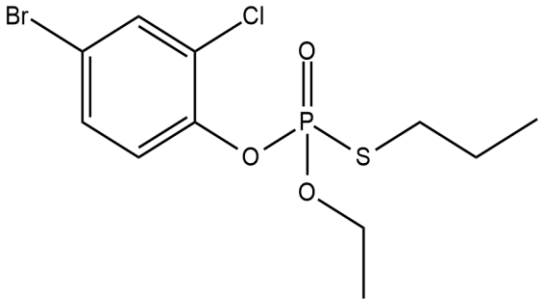

Profenofos

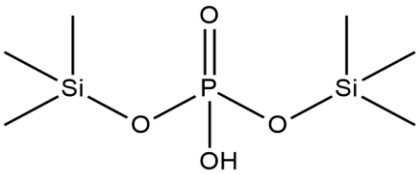

Phosphoric acid, bis(trimethylsilyl)mono

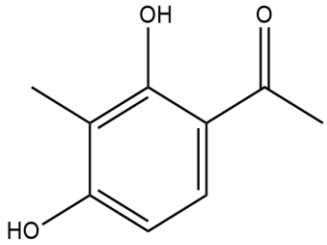

2',4'-Dihydroxy-3'-methylacetophenone

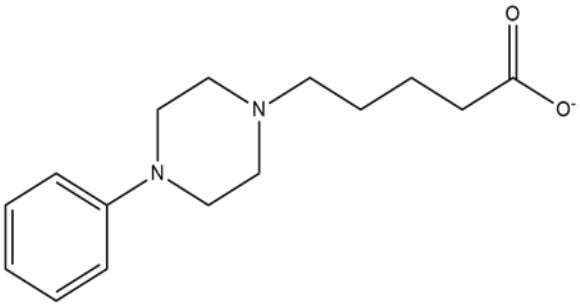

5-(4-Phenyl-piperazin-1-yl)-pentanoate

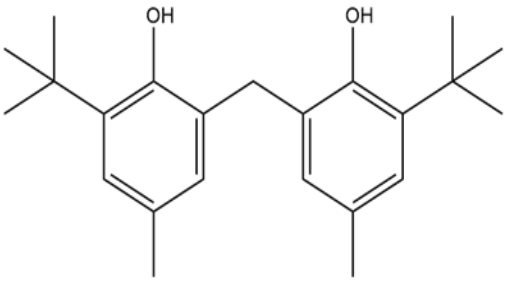

Phenol, 2,2'-Methylbis [6-(1,1-dimethyethyl)-4-methyl-

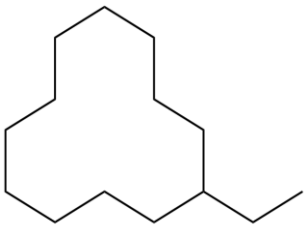

ethyl- cyclododecane

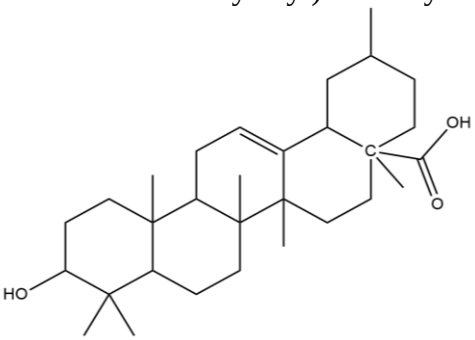

10-Hydroxy-2,4a,6a,6b,9,9,12a-heptamethyl 1,2,3, 4, 4a, 5,6,6a,6b,7,8,8a,9,10,11,12,12a,12b,13,14b -icosahydropicene-4acarboxylic acid

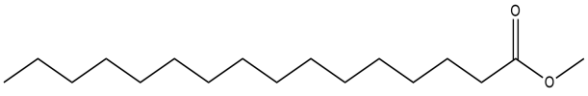

Hexadecanoic acid, methyl ester

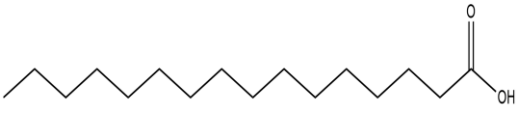

n-Hexadecanoic acid

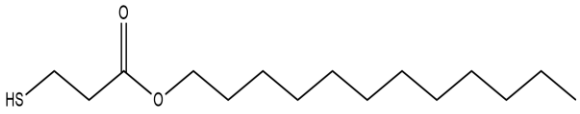

Propanoic acid, 3-mercapto-, dodecyl ester

1-hexadecanol

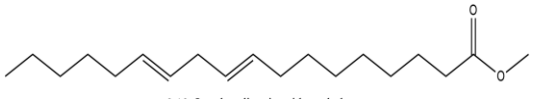

9,12-Octadecadienoic acid, methyl ester

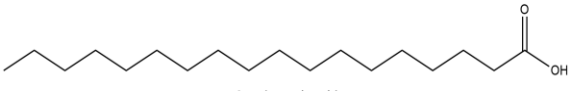

Octadecanoic acid

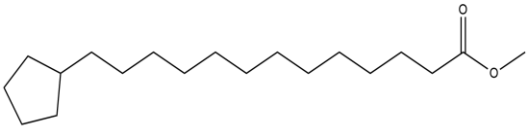

Cyclopentanetridecanoic acid, methyl ester

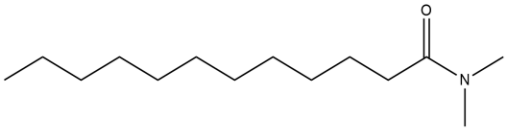

N,N- Dimethyldodecanamide

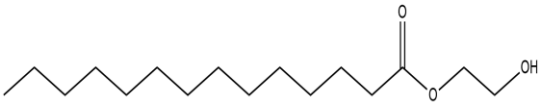

Tetradecanoic acid, 2-hydroxyethyl ester

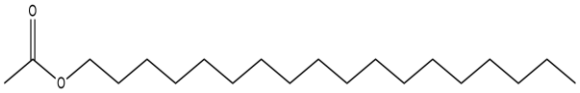

Acetic acid n-octadecyl ester

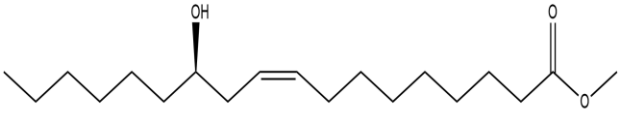

9-Octadecanoic acid, 12-hydroxy-, methyl ester [R-(Z)]-

Figure 4.8: Structures of compounds identified by GC-MS for *Aloe succotrina*

4.2.3.2 GC-MS results of *Prosopis juliflora*

The total run time was 30 minutes. Several compounds were detected and their fragmentation patterns and retention indexes compared to NIST 2014, MS library. The GC chromatogram was as follows in figure 4.9.

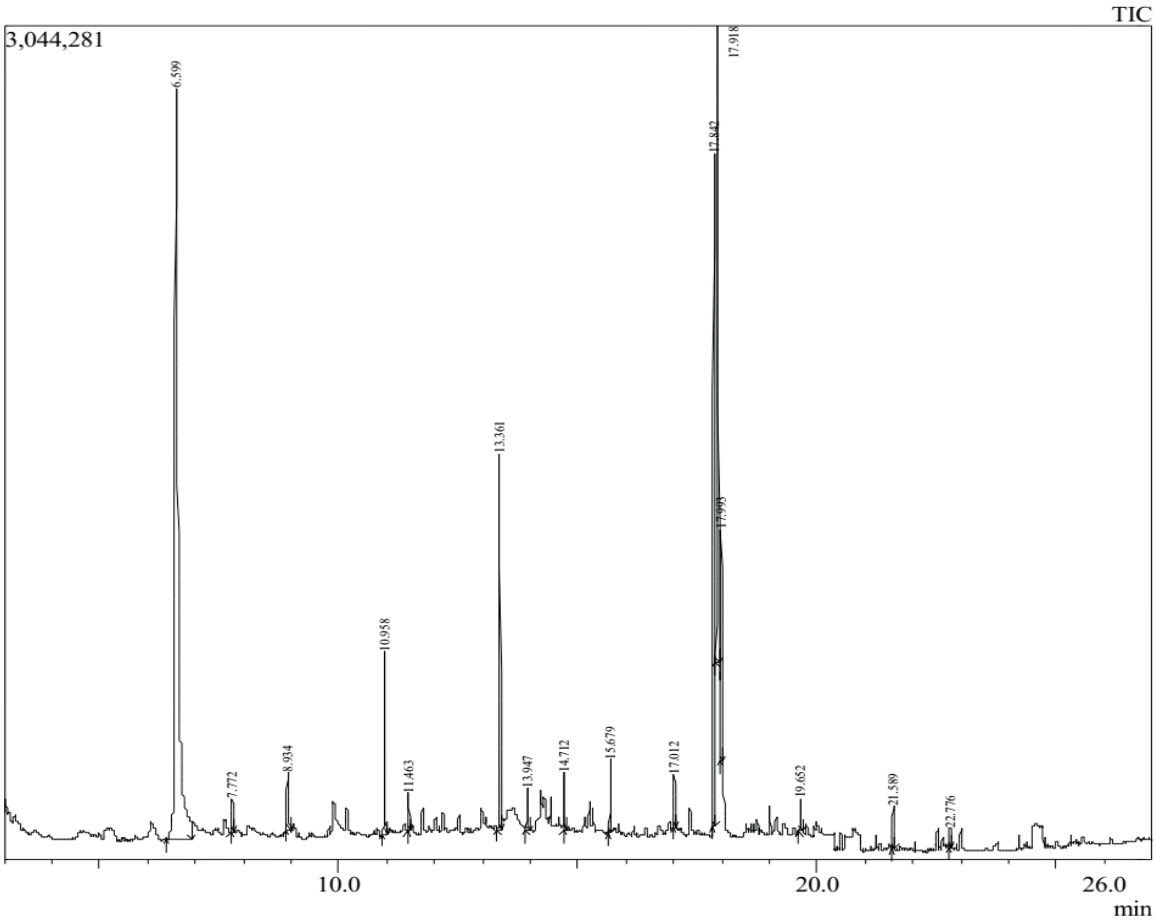

Figure 4.9: GC chromatogram of *Prosopis juliflora* extract

Table 4.4: A summary of GC retention time (RT) and information obtained GC-MS showing molecular weights, chemical formulas, names and possible compounds based on compared NIST entries. Structures are attached in the appendix

Peak#	R.Time	Area	Area%	Height	Height%	Molecular Weight	Molecular formular	Name
1	6.599	12304817	41.11	2743368	22.77	166	$C_9H_{10}O_3$	Ethanone, 1-(2-hydroxy-4-methoxyphenyl)-
2	7.772	241730	0.81	120418	1.00	110	$C_6H_6O_2$	Catechol
3	8.934	526583	1.76	209283	1.74	240	$C_7H_{21}O_3PSi_2$	Phosphonic acid, methyl-, bis(trimethylsilyl)-ester
4	10.958	1151141	3.85	667890	5.54	152	$C_6H_8N_4O$	5-[1,2,4]triazol-1-yl-pyrrolidin-2-one
5	11.463	240335	0.80	136915	1.14	186	$C_{12}H_{26}O$	1-Dodecanol
6	13.361	2300968	7.69	1371981	11.39	374	$C_{24}H_{22}O_4$	Phthalic acid, di(3-ethylphenyl) ester
7	13.947	267068	0.89	154160	1.28	340	$C_{16}H_{28}O_4Si_2$	4-Hydroxymandelic acid, ethyl ester, di-TMS
8	14.712	355248	1.19	211786	1.76			Benzeneacetic acid, 4-(2,2,3,3,3-pentafluoro-
9	15.679	470481	1.57	267685	2.22	266	$C_{17}H_{18}N_2O$	Ethanone,1-[4-[4-(dimethylamino)benzylienamino] phenyl
10	17.012	368135	1.23	192569	1.60	186	$C_{11}H_{22}O_2$	Decanoic acid, methyl ester
11	17.842	5278370	17.64	2458966	20.41	281	$C_{13}H_{19}N_3O_4$	Pendimethalin
12	17.918	4327239	14.46	2321788	19.27			2(4H)-Benzofuranone,5,6,7,7a-tetrahydro-4,4,7a-trimethyl-, (R)-
13	17.993	1520034	5.08	846328	7.02	`		Cyclopentanecarboxylic acid, 3-(3-fluorophenylcarbamoyl)-1,2,2-trimethyl
14	19.652	201596	0.67	122334	1.02	196	$C_{12}H_{20}O_2$	2-Benzofuranmethanol, 2,4,5,6,7,7a-hexahydro 4,4,7a-trimethyl-,cis
15	21.589	286529	0.96	154274	1.28	340	$C_{23}H_{32}O_2$	Phenol,2,2'-Methylbis[6-(1,1-dimethylethyl)-4-methy
16	22.776	90036	0.30	70343	0.58	207	$C_7H_5N_5O_3$	Pterin-6-carboxylic acid
		29930310	100.00	12050088	100.00			

Exactly 16 hits matched the NIST 14 library as identified compounds from the *P. juliflora* dye with their respective molecular masses, retention times and retention indexes matching. A comprehensive detailed Chromatogram and spectra, are in the appendix attached on page. The first significant phytoconstituent was catechol which is a benzenediol that occurs natural in plant and can be as a result of pyrolysis of catechin (Rao & G, 2018).

Decanoic acid, methyl ester is a fatty acid, metabolized by plants that have previously been identified from palm oil plants (Kamatou & Viljoen, 2017). Pterin-6-carboxylic acid, is a plant metabolite that has been extracted from *Foeniculum vulgare* (Hussein *et al*., 2016).

Figure 4.10 below, shows tentative structures of some of the compounds identified by GC-MS .

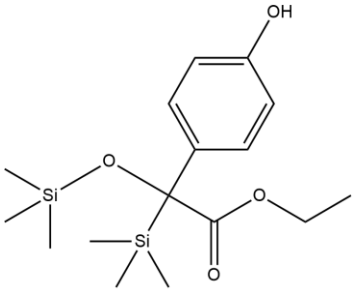

4-Hydroxymandelic acid, ethyl ester, di-TMS

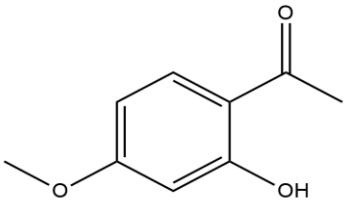

Ethanone, 1-(2-hydroxy-4-methoxyphenyl)

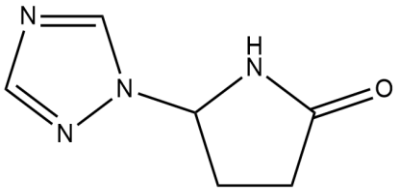

5- [1,2,4] triazol-1-yl-pyrrolidin-2-one

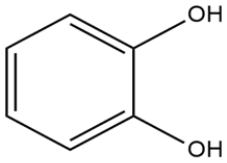

Catechol

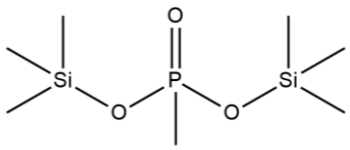

Phosphonic acid, methyl-, bis(trimethylsilyl)-ester

1-Dodecanol

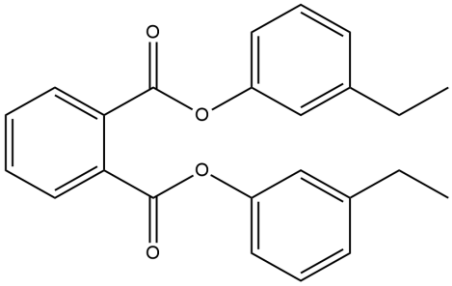

Phthalic acid, di(3-ethylphenyl) ester

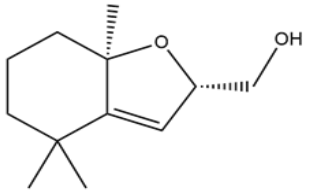

2(4H)-Benzofuranone,5,6,7,7a-tetrahydro-4,4,7a-trimethyl-, (R)-

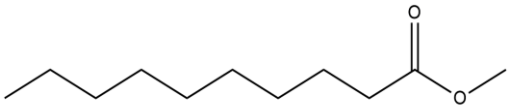

Decanoic acid, methyl ester

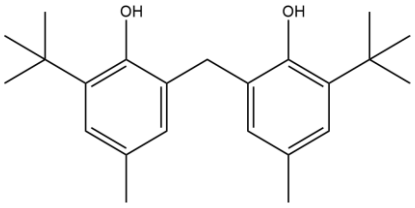

Phenol, 2,2'-Methylbis[6-(1,1-dimethyl ethyl -4-methyl

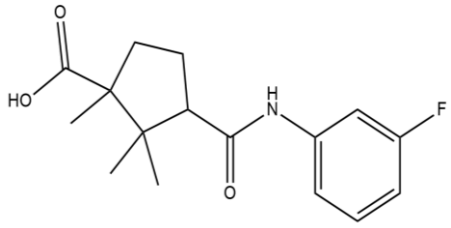

Cyclopentanecarboxylic acid, 3-(3-fluorophenylcarbamoyl)-1,2,2-trimethyl

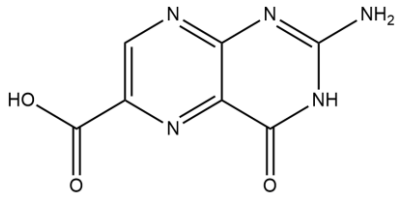

Pterin-6-carboxylic acid

Figure 4.10: Structures of compounds identified by GC-MS from *Prosopis juliflora*

4.3 Optimization of Dyeing Parameters

Several dyeing parameters such as concentration, pH, dyeing time, dye concentration and dyeing temperature were optimized prior to the actual dyeing process. This was done by keeping all the measured parameters constant while varying only one parameter at a time. The most optimum points were calculated based on the colour strength (K/S). For all cases, except when the parameter was being optimized, the constant parameters were dyeing temperature of 60°C, material to liquor ratios of 1:50, dyeing time of 1 h, and a concentration of 20 g/L at pH 7.2 for *P. juliflora* and undiluted for *A. succotrina* (Islam *et al*., 2016b; Kundal *et al*., 2016).

4.3.1 Dyeing with extracts of *A. succotrina*

4.3.1.1 Optimization of dye concentration

The concentrations of *A. succotrina* dye was varied while all the other parameters held constant and the results recorded in table 4.5 below.

Table 4.5: Optimization of dye concentration

Concentration of dye / **Parameter**	**No dilution**	**Diluted 1:1**	**1:2**	**1:3**	**1:4**
L	60.01	62.76	63.06	69.18	72.16
a	10.52	13.16	12.92	12.03	11.61
b	-7.01	-16.78	-16.90	-13.14	-12.98
c	12.6	21.3	21.3	17.8	17.4
H°	326.3	308.1	307.4	312.5	311.8
K/S	0.85	0.53	0.44	0.22	0.12

The optimization of dyeing concentration, showed that the lightness (L) value of the dyed fabric changed as a function of dilution, so that the colour lightness increased as the dye

concentration decreased meaning that the more concentrated the dye is the darker the shade of the dye in the fabric (Yusuf *et al*., 2015). The negative value of b suggests that the colour has a blueish shade.

The non-diluted dye, had the highest K/S value hence suggesting that it is the most effective dyeing condition when the concentrations are optimized. This is because, in its non-diluted state, there are more dye molecules available to bind with the fabric, hence the colour strengths are higher (Paul, Das, Islam, Siddiquee, & Mamun, 2017; Shahid, Hossain, Hossain, & Ali, 2016).

4.3.1.2 Optimization of pH

The pH of the *A. succotrina* dye was varied while all the other parameters held constant and the results recorded in table 4.6 below.

Table 4.6: Optimization of pH

pH of dye / **Parameter**	**3.0**	**5.2**	**7.1**	**9**	**12**
L	70.86	62.57	72.76	73.16	74.11
a	9.95	12.22	7.88	7.87	8.07
b	-3.45	-16.11	-6.02	-9.01	-8.16
c	10.5	20.2	9.9	12.0	11.5
H°	340.9	307.2	322.6	311.1	314.7
K/S	0.71	0.84	0.87	0.75`	0.62

Optimization of pH also shows that as the pH changes from 7.1- 12, there is a steady increase in the L value meaning that as there was an increase in the lightness of the dye as a function the increase in pH this results are consistent with other literature which suggest that pH directly affects the shade of the dye (Souissi, Guesmi, & Moussa, 2018; Yusuf *et*

al., 2015). The K/S value of the dye, increased from 3.0- 7.1 and subsequently decreased towards 12 showing that the optimum pH is 7.

4.3.1.3 Effect of time dyeing

Dyeing time, of *A. succotrina* dye was varied while all the other parameters held constant and the results recorded in table 4.7 below.

Table 4.7: Optimization of time

Time / Parameter	20 MIN	30 MIN	40 MIN	50 MIN	60 MIN
L	72.01	68.98	69.79	66.48	62.57
a	8.72	11.01	11.12	10.62	12.22
b	-4.27	-9.01	-8.05	-7.92	-16.11
c	9.7	14.2	13.7	13.2	20.2
H°	333.9	320.7	324.1	323.3	307.2
K/S	0.16	0.28	0.33	0.83	0.84

Optimization of time shows the highest (L) value was at 20 Min meaning that it had the lightest colour while the lowest L value was at 60 minutes meaning that it had the darkest shade. The highest K/S value was at 60 minutes, meaning that 60 Minutes is the best time for dyeing (N. F. Ali & El-Mohamedy, 2011; Zubairu & Mshelia, 2015). This is because, the more the time the fabric stays in the dye bath, the more the interaction between the dye molecules and the fabric.

4.3.1.4 Optimization of Temperature

The dyeing temperature of *A. succotrina* dye with fabric, was varied while all the other parameters held constant and the results recorded in table 4.8 below.

Table 4.8: Optimization of temperature

Temperature / Parameter	R.T	40 ℃	60℃	80℃	100℃
L	62.57	60.23	64.36	64.01	63.55
a	12.22	12.01	11.15	11.17	11.22
b	-16.11	-10.97	-5.56	-5.01	-4.71
c	20.2	16.3	12.5	12.2	12.5
H°	307.2	317.6	333.5	335.8	333.5
K/S	0.84	0.82	0.88	0.88	0.92

The highest L value was at 60 °C meaning that at this point, it was the lightest. The highest K/S value was at temperatures of 100 °C meaning that it is the optimum dyeing temperature for the dye was at this temperature (N. F. Ali & El-Mohamedy, 2011; Yusuf *et al*., 2015). Previous literature suggests that, as temperature increases, so does the structure of the fabric expand. This in turn, allows for the uptake of more dyes into the fabric hence the possible increase of colour strength as temperature increases (Paul, Das, Islam, Siddiquee, *et al*., 2017; Shahid *et al*., 2016).

4.3.1.5 Dyeing of fabric with the *A. succotrina* dye

The fabric, was dyed using the optimum conditions discussed above and recorded in the table 4.9 below. This was done using three main dyeing techniques namely pre mordanting, simultaneous mordanting and post mordanting in the presence of selected mordants. The fabric was then subjected to ISO standard methods to ascertain the suitability of the dye with respect to wash fastness, light fastness and rub fastness.

Table 4.9: A table of fastness studies, colour coordinates and colour strengths of the *Aloe succotrina* dye with Cotton fabric

Method	Mordant	Wash **ISO 105-C06**	Light **ISO 105-A02**	Rub **ISO 105-X12**	L	a	b	c	h°	K/S
Standard	NONE	**1**	**4**	**5**	62.57	10.6	-5.6	12.0	332.2	0.63
Pre-	Alum	**2**	**4/5**	**5**	57.8	7.7	-4.3	8.8	330.8	0.72
Mordanting	$SnCl_2$	**2**	**4**	**5**	85.13	3.74	9.76	10.5	69.0	0.77
	$FeSO_4$	**2**	**4**	**5**	62.4	6.1	-1.65	6.3	344.9	0.79
	K2Cr2O7	**2**	**4**	**5**	69.19	7.53	-2.56	8.0	341.2	0.69
Simultaneous	Alum	**1**	**4**	**5**	83.9	5.9	6.3	8.6	46.9	0.81
Mordanting	$SnCl_2$	**1**	**4**	**5**	82.8	3.65	15.88	16.3	76.9	0.75
	$FeSO_4$	**1**	**4**	**5**	80.9	1.32	17.14	17.2	85.6	0.79
	$K_2Cr_2O_7$	**1**	**4**	**5**	75.29	7.61	2.66	8.1	340.7	0.66
Post	Alum	**1**	**5**	**5**	89.9	0.7	8.7	8.7	85.4	0.88
Mordanting	$SnCl_2$	**1**	**5**	**5**	81.70	5.3	5.97	8.0	48.4	0.76
	$FeSO_4$	**1**	**5**	**5**	71.3	3.2	6.2	7.0	62.7	0.81
	$K_2Cr_2O_7$	**1**	**5**	**5**	85.9	1.7	8.9	9.1	280.8	0.91

From the table 4.9 above, it can be concluded that except for the case of pre-mordanting, the use of mordants in the *A. succotrina* dye, did not significantly improve the ability of the dye to bind onto the fabric. For the case of pre-mordanting, the presence of the mordant, slightly improved the wash fastness of the dye, this was despite the use of varying mordant types (Kumbhar, Hankare, Sabale, & Kumbhar, 2019; Lee & Kim, 2004). Also, the L values of the fabric, did not follow any particular trend although it can be concluded that when simultaneously and post mordanting techniques were employed, the colour of the dye in the cloth changed totally maybe due to a chemical reaction between the dyes and the mordants which was specifically more pronounced for the mordants $SnCl_2$ and $FeSO_4$. Figure 4.11 below, shows the different dyes and shades that were obtained based on different mordants and mordanting techniques that were used.

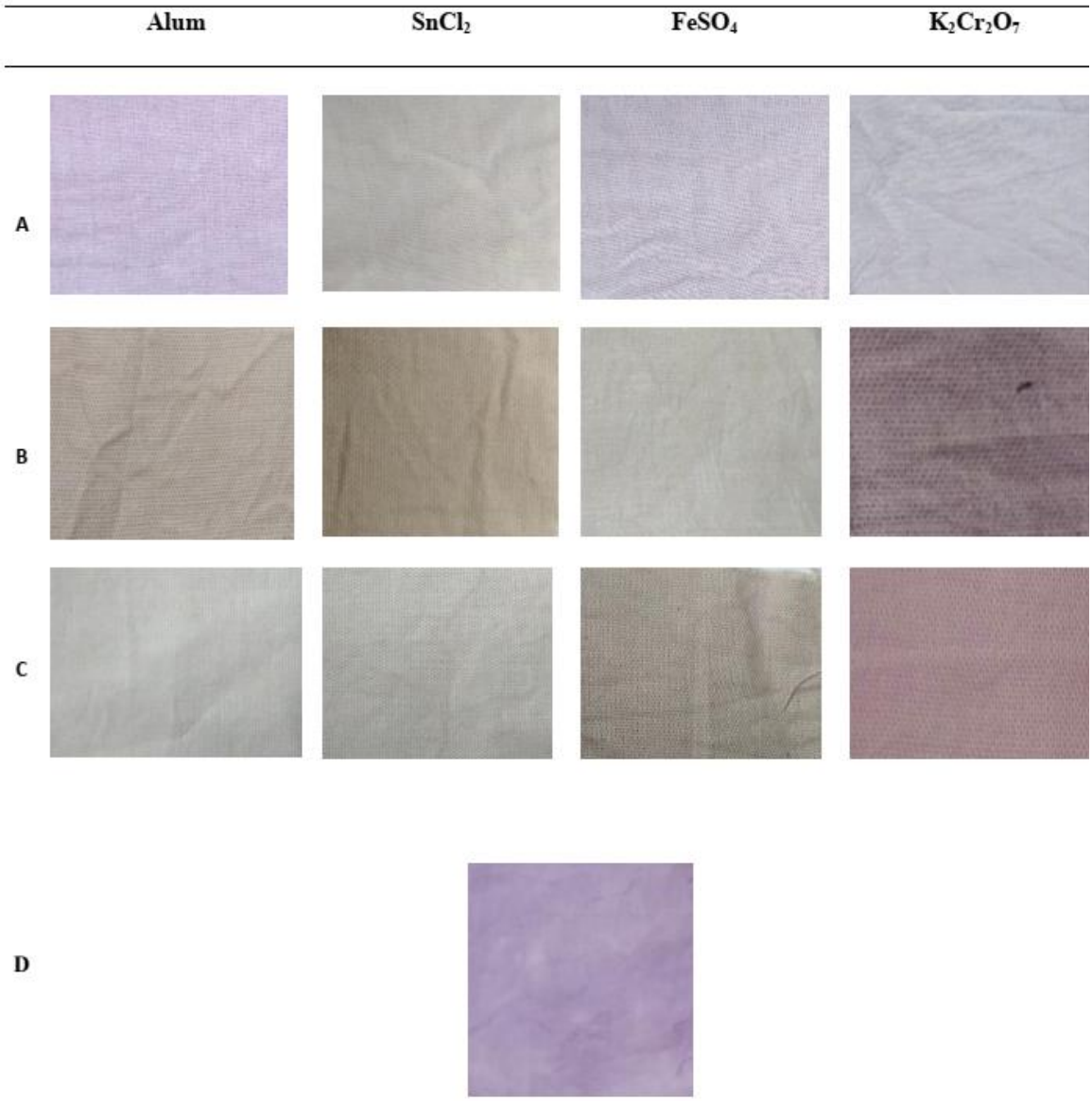

Key: A: Pre mordant, B: Simultaneous mordanting C: Post mordant D: Standard

Figure 4.11: Dyed fabric in combination with different mordants and mordanting techniques

4.3.1.2 FTIR spectra of plain fabric, dye and fabric dyed with *Aloe succotrina*

FTIR, was used to analyse the dyeing properties of the dye imparted on to the fabric and the spectra compared in figure 4.12 below.

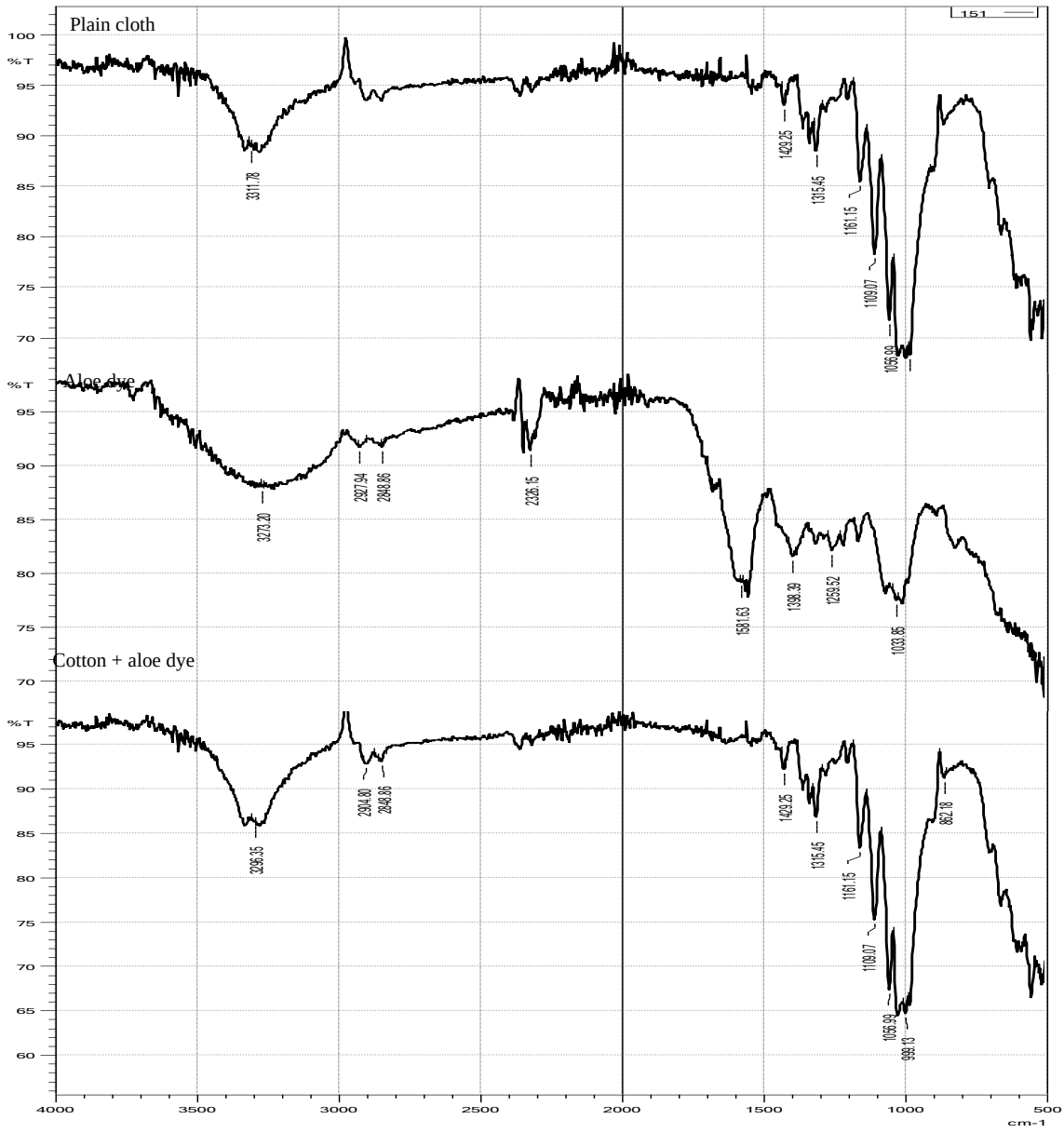

Figure 4.12: FTIR spectra of Fabric, dye and Fabric dyed with *Aloe succotrina*

A careful examination of the three spectra i.e. the plain fabric, dye and dyed fabric, shows slight changes in the FTIR spectrum of the dyed fabric from that of the plain fabric. A

difference in the two, is a sign that dyeing has occurred and as a result, the dye molecules have successfully bonded to the fabric in turn changing the FTIR spectrum. A peak of 3296.35 is predominant in the dyed fabric, as opposed to 3311in the spectrum of the plain fabric. Equally, a new peak of 862.18 appears on the dyed fabric which is absent on the plain fabric. Also, a new peak at 2848.86 which represents O-H stretch for carboxylic acid and CH_2 stretch for a long alkyl chain (Chung, Lee, & Choe, 2004). This, is present in the spectrum of the dye, is in the dyed fabric all this, being proof that the fabric was dyed.

4.3.2 *Prosopis juliflora*

4.3.2.1 Optimization of dye concentration

The concentrations of *P. juliflora,* dye was varied while all the other parameters held constant and the results recorded in table 4.10 below.

Table 4.10: Optimization of dye concentration

Dye Concentration Parameter	10 mg/l	20mg/l	30mg/l	40mg/l	50mg/l
L	72.93	71.78	71.00	72.14	69.77
a	5.95	3.85	5.01	5.15	4.58
b	28.21	24.59	28.21	28.48	27.09
c	28.83	24.9	28.65	28.9	27.5
H°	78.09	81.1	79.94	78.8	80.4
K/S	0.350	0.352	0.365	0.384	0.378

Optimization of dyeing concentrations showed that the lightness (L) value of the dyed fabric changed as a function of the concentration. Such that the higher the concentration of the dye, the lower the value of L meaning that at high concentrations of the dyes, the colours on the fabric became darker or had a darker shade (Yusuf *et al.*, 2015). The highest

K/S value was at 50 mg/L suggesting that the most effective dyeing condition when the concentration is optimized is at this point (N. F. Ali, 2011). This is consistent, with other papers that report the same. This is because, as the concentration increases, there is more dyeing molecules that are free to bind with the fabric hence the subsequent higher colour strengths (Paul, Das, Islam, & Siddiquee, 2017; Shahid *et al*., 2016).

4.3.2.2 Optimization of pH

The pH of the *P. juliflora* dye was varied while all the other parameters held constant and the results recorded in table 4.11 below.

Table 4.11: Optimization of pH

pH / Parameter	3.0	4.2	7.1	8.0	9.1
L	65.77	68.73	65.79	67.56	76.46
a	5.93	4.10	6.15	7.92	5.12
b	28.44	25.84	24.82	27.62	24.90
c	29.1	26.2	26.6	28.8	25.4
H°	78.2	81.0	76.1	74.0	78.4
K/S	0.425	0.373	0.425	0.386	0.311

Optimization of pH showed pH 9.1 as having the lightest colour with pH 7.2 being the darkest shades. A slight difference with the L value at pH 3.0. The K/S values were highest at pH 3 and also at pH 7.1 which is the default pH of the dye bath. The default pH was chosen as the optimum pH based on also its L value being slightly higher than that of pH 3 (Punrattanasin, Nakpathom, Somboon, & Narumol, 2013; F. Ali, 2011).

4.3.2.3 Optimization of time

The dyeing time of the *A. succotrina* dye was varied while all the other parameters held constant and the results recorded in table 4.12 below.

Table 4.12: Optimization of time

Time / Parameter	20 MIN	40 MIN	60 MIN	80 MIN	100 MIN
L	75.56	74.35	73.90	73.73	71.78
a	3.39	3.65	3.71	3.50	3.85
b	24.27	24.17	2413	23.67	24.59
C	24.5	24.4	24.4	23.9	24.9
H	82.0	81.4	81.3	81.6	81.1
K/S	0.321	0.331	0.342	0.351	0.350

Optimization of dyeing time showed the highest value of L at 20 min and the lowest value of at 60 minutes meaning that the lightest and darkest values were at 20 at 100 minutes respectively (Yusuf *et al*., 2015; N F. Ali, 2011). The highest value of K/S was at 80 Minutes and 100 min, meaning that beyond the 80^{th} minute the K/S levels off. This is also in line with other literature which suggest that as time increases, colour strength usually increases because there is more interaction between the dye and the fabric (Paul, Das, Islam, & Siddiquee, 2017; Shahid *et al*., 2016).

4.3.2.4 Optimization of Temperature

Table 4.13: Optimization of temperature

Temperature Parameter	R.T	40	60	80	100
L	74.32	75.37	71.78	71.89	73.42
a	4.31	4.23	3.85	4.10	3.19
b	28.15	26.78	24.59	23.35	22.11
c	28.5	27.1	24.9	23.7	22.3
H°	81.3	81.0	81.1	80.0	81.8
K/S	0.333	0.318	0.348	0.345	0.325

Optimization of dyeing temperatures showed 40 ^{0}C, to have the highest Lightness value, and 60 Minutes to have the lowest Lightness value meaning that this were the darkest and lightest points respectively. Temperature 60 $^{\circ}$C, had the highest value of K/S value suggesting that it was the optimum temperature for dyeing (Yusuf *et al*., 2015; N. F. Ali, 2011). This is because, as temperature increases, the fabric structure also increases allowing more dye to enter it, leading to a higher K/S value.

4.3.2.5 Dyeing of fabric with the *P. juliflora* dye

The fabric, was dyed using the optimum conditions obtained from the experiments above and the results recorded in the table 4.14 below. This, was done using three main dyeing techniques namely pre mordanting, simultaneous mordanting and post mordanting in the presence of selected mordants. The fabric, was then tested for its wash fastness, light fastness and rub fastness using ISO standard methods.

Table 4.14: A table of fastness studies, colour coordinates and colour strengths of *Prosopis juliflora* dye with Cotton fabric

Method	Mordant	Wash **ISO 105-C06**	Light **ISO 105-A02**	Rub **ISO 105-X12**	L	a	b	c	h	K/S
Standard	NONE	3	5	5	63.5	3.3	19.5	19.8	80.4	0.43
Pre-Mordant	Alum	3/5	5	5	62.4	6.3	27.8	28.5	77.1	0.54
	$SnCl_2$	3/5	5	5	57.6	7.1	25.7	26.7	74.7	0.72
	$FeSO_4$	3/5	5	5	46.7	2.6	14.3	14.6	79.7	0.65
	$K_2Cr_2O_7$	3/5	5	5	63.6	5.5	27.1	27.7	78.5	0.63
Sim Mordant	Alum	4	5	5	47.4	6.7	24.5	25.4	74.4	0.64
	$SnCl_2$	4	4/5	5	56.5	7.7	31.7	32.6	76.4	0.68
	$FeSO_4$	4	5	5	46.7	2.6	14.3	14.5	79.7	0.82
	$K_2Cr_2O_7$	4	5	5	55.5	8.1	22.3	23.7	70.0	0.54
Post Mordanting	Alum	5	5	4	58.4	7.7	23.4	24.6	71.8	0.58
	$SnCl_2$	5	5	5	65.0	4.0	29.6	29.8	82.2	0.44
	$FeSO_4$	5	5	5	44.1	1.86	9.2	9.4	78.6	0.86
	$K_2Cr_2O_7$	5	5	4	41.0	6.29	16.71	17.9	69.4	0.74

From the table above, it can concluded that in overall, the use of mordants successfully improved the ability of the dye sticking to the fabric. This can be seen by the general improvements of the wash fastness of the fabric before and after the introduction of mordant. This is often reported as so for most natural dyes (Kumbhar *et al*., 2019; Lee & Kim, 2004). Also, it can be said that of the mordanting techniques employed, post mordanting technique was more effective as a method followed by simultaneous mordanting then pre mordanting.

The Lightness value (L) of the dye, did not show a particular trend as observed in the table. However, significant mordant and effect of mordanting technique on the colour strength was present. Post mordanting had lower L values this suggesting that although the colours had a higher colour strength, they were duller. The effects of mordants was evident with the stannous chloride and potassium dichromate mordants, producing brighter shades tending towards a bright shade of brown and with Ferrous Sulphate dulling the shades to shades of green, this effects of the said mordants are similar to those reported by other studies of yellowish, brownish dyes (Janani *et al*., 2014; Ugya & Priatamby, 2016; Wanyama, Kiremire, Ogwok, & Murumu, 2010; Yunus *et al*., 2011).

Figure 4.13 below, shows the different dyes and shades that were obtained based on different mordants and mordanting techniques that were used for the *P. juliflora* dye.

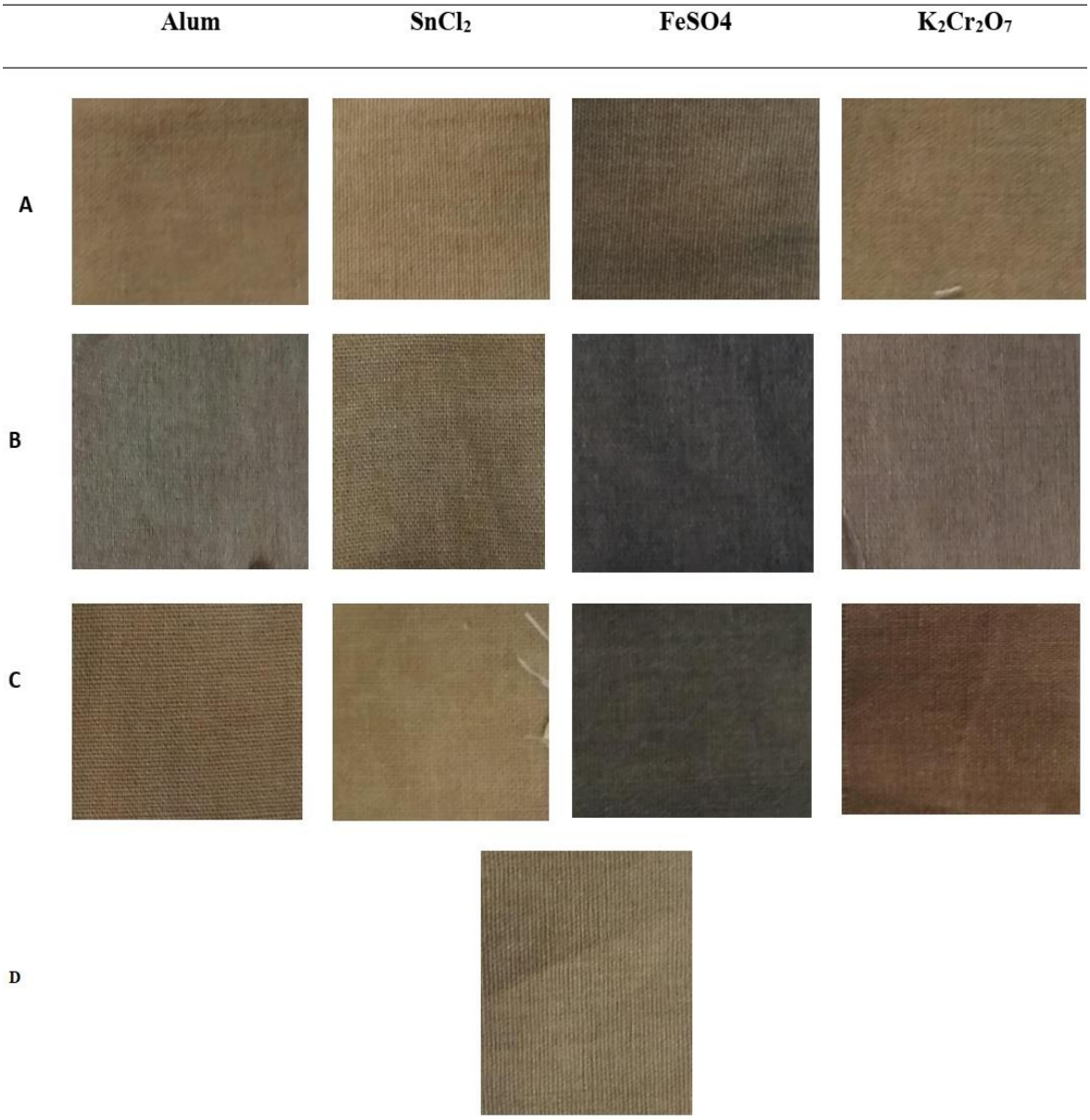

Figure 4.13: Dyed fabric in combination with different mordants and mordanting techniques

Key A: Pre mordant, B: Simultaneous mordanting C: Post mordant D: Standard

4.3.3 FTIR spectra of Plain Fabric, dye and fabric dyed with *Prosopis juliflora*

FTIR, was used to analyse the dyeing properties of the dye imparted on to the fabric and the spectra compared in figure 4.14 below

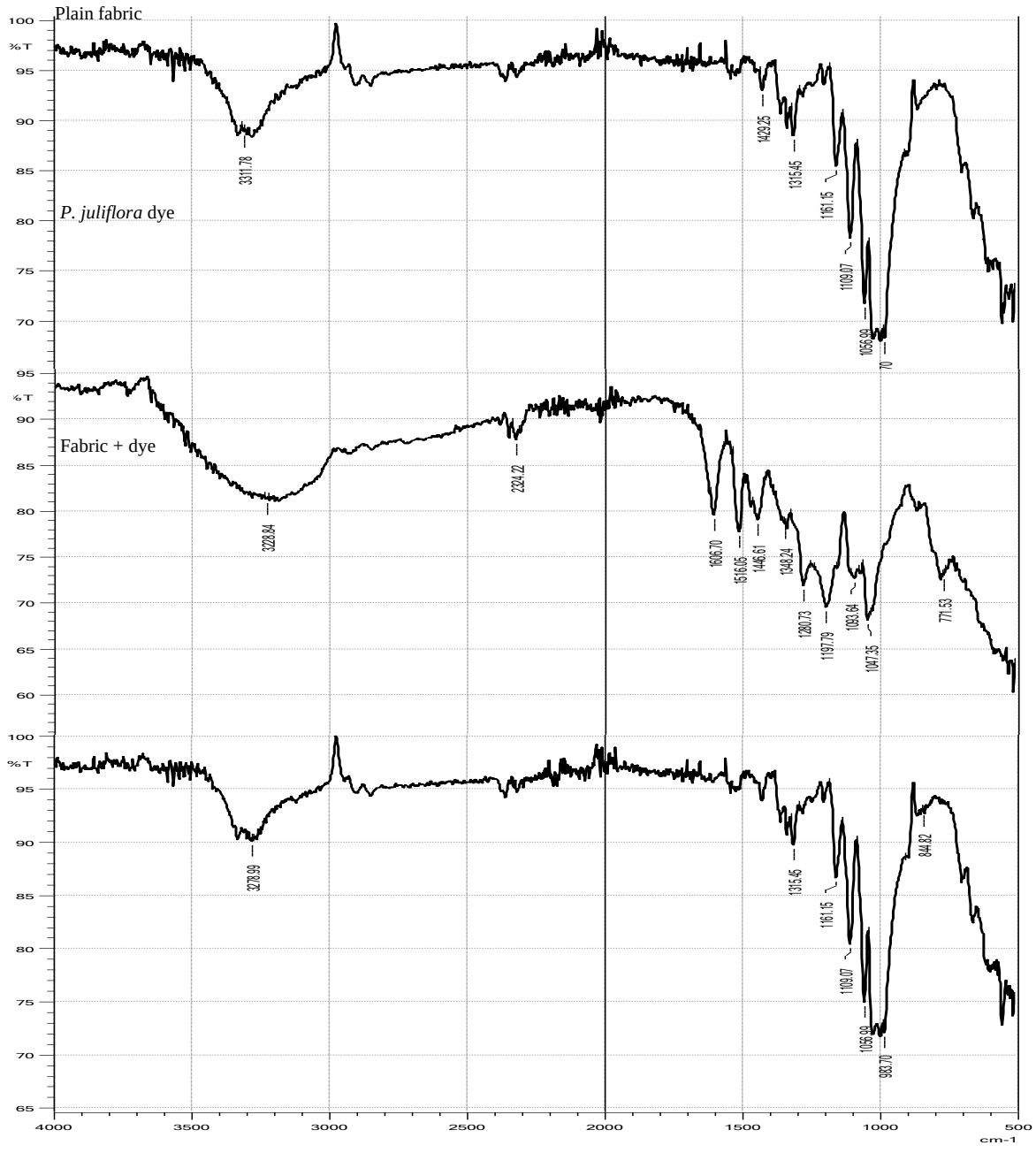

Figure 4.14: FTIR spectra of Fabric, dye and Fabric dyed with *P. juliflora*

FTIR, was used to analyse the dyeing properties of the dye imparted on to the fabric. A comparative analysis of the FTIR of the two pieces of fabric showed slight differences between the dye and the undyed fabric i.e. the presence of new peaks that were not present in the plain fabric such as the peak at 3278.99 for OH bond and 844.82 for =C-H aromatic ring. This showing that, the fabric was dyed.

4.4 Physicochemical Characterization of Biochar

Previous studies, suggest that the quality of biochar, is dependent on a number of factors such as the pyrolysis temperature, pyrolysis speed, plant being used as preparing material and time(Mary, Niveditha, & Mary, 2016). In this work, we studied the effect of pyrolysis temperature on the quality of biochar. The biochar, was characterized physically using Scanning Electron Microscope (SEM) for its surface properties and Transmission electron microscope (TEM) for its pore sizes. They were then characterized chemically using Fourier Transformed Infra-red spectroscopy (FTIR) for functional groups present , X-Ray Diffractometer (XRD) for its composition and crystalline properties, and Electron Dispersion X-Ray (EDX) for its elemental composition (J. Zhang *et al*., 2015).

4.4.1 Physical Characterization

Physical characterization of the different sets of biochar was done using microscopic techniques namely SEM and TEM.

4.4.1.1 SEM Analysis

4.4.1.1.1 SEM images of AS 300 ℃ and AS 500 ℃

Figure 4.15 below, shows SEM images for biochar samples of *Aloe succotrina* obtained at 300 ℃ and 500 ℃ labelled as A for AS300 and B for AS500 respectively.

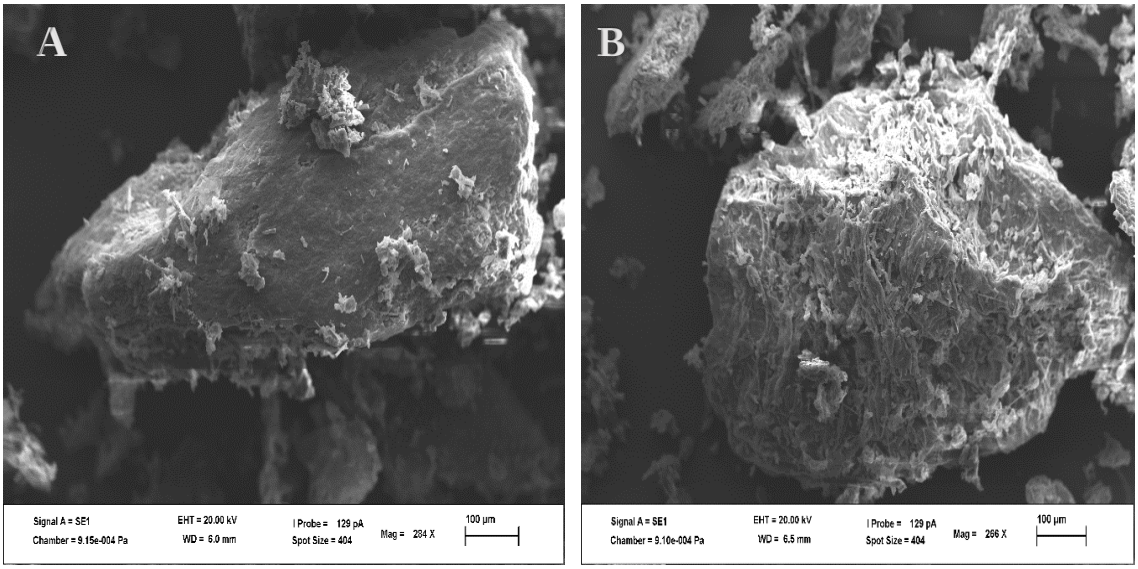

Figure 4.15: SEM images for *Aloe succotrina* 300 ℃ and 500 ℃

Image A for AS300 shows the biochar to have a less porous flat surface structure of the with islands of fibrous matter. Image B on the other hand, for AS500 has large channel-like structures proliferating the surface of the biochar, showing retention of fibrous morphology embedded in the channels. This porous structure, was created by the increased pyrolysis temperature which led to the increased decomposition of organic matter, giving the structure a larger surface area to volume ratio i.e. more binding sites as an adsorbent when compared with the biochar at 300 ℃ (Gopal *et al*., 2014; Jain, Garg, & Kadirvelu, 2011).

4.4.1.2.2 SEM images of PJ 300 and PJ 500

Figure 4.16 shows SEM images of biochar made from *Prosopis juliflora* at 300 ℃ and 500 ℃. These are labelled as PJ 300 (image C) and PJ 500 (image D) respectively.

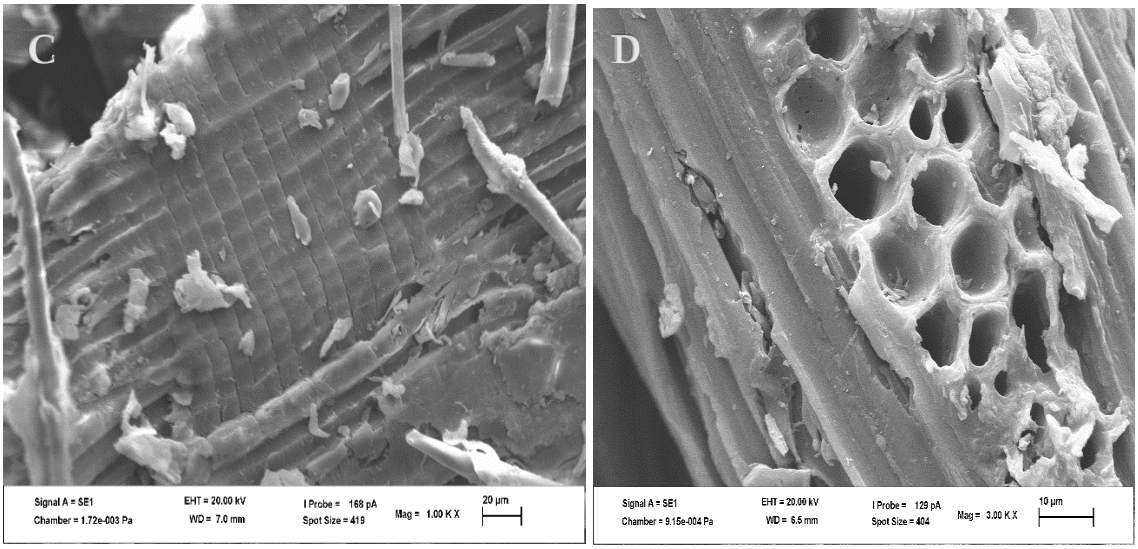

Figure 4.16: SEM images for *Prosopis juliflora* 300 ℃ and 500 ℃

The image of PJ 300 (Figure 4.16 C) shows a little cracked flat sheet of rod-like features with little porosity. A more porous structure of the biochar (Figure 4.16 D) was created as pyrolysis temperature increased to 500 ℃. In this case, as a result of the increase in pyrolysis temperature from 300℃ to 500℃ more organic matter was decomposed and the organic matter escaped to give a more porous structure. This pores, had larger cracks on the surface of the biochar to give a mesoporous structure of higher surface area to volume ratio (Jain *et al*., 2011; Liang, Chen, Liu, & Zheng, 2016).

4.4.1.2 Transmission Electron Microscope (TEM) analysis

4.4.1.2.1 TEM images for AS 300 and AS 500

Figure 4.17 below, shows TEM images for AS 300 labelled as image E and AS 500 labelled as F respectively.

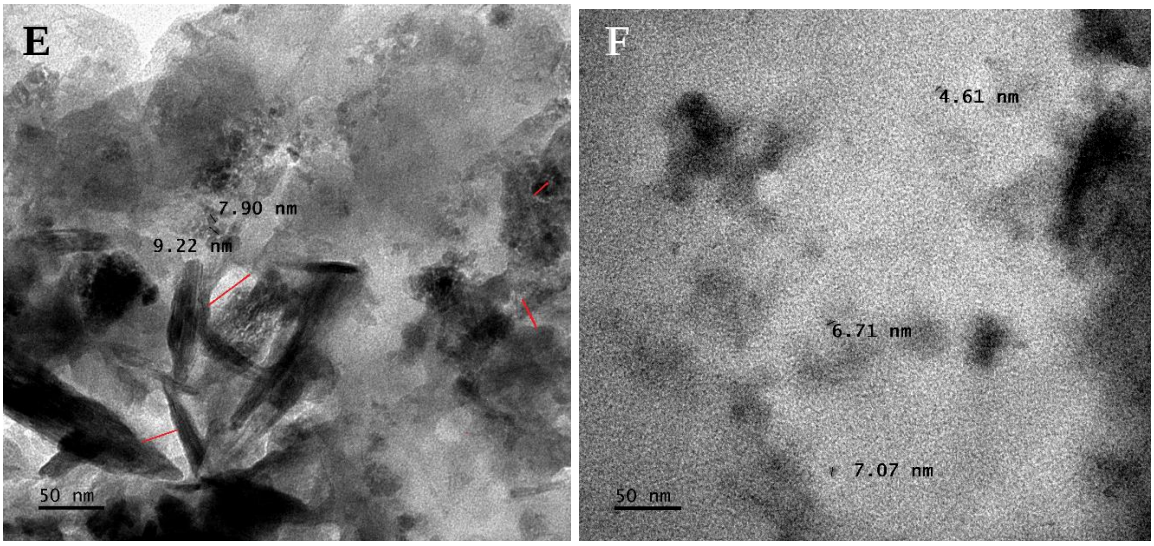

Figure 4.17: TEM images of AS 300 and AS 500

TEM images, were used to show the sizes of the different sets of biochar. From the images, it can be visualized that temperature had an effect on the particle sizes of the individual biochar, with the biochar prepared at 300 ℃, having larger sizes than the biochar prepared at 500 ℃. Hence implying that the biochar at 500 ℃, had a larger surface area to volume ratio when compared with the biochar prepared at 300 ℃.

4.4.1.3.2 TEM images for PJ300 and PJ500

Figure 4.18 below, shows TEM images for PJ 300 labelled as image G and PJ 500 labelled as H.

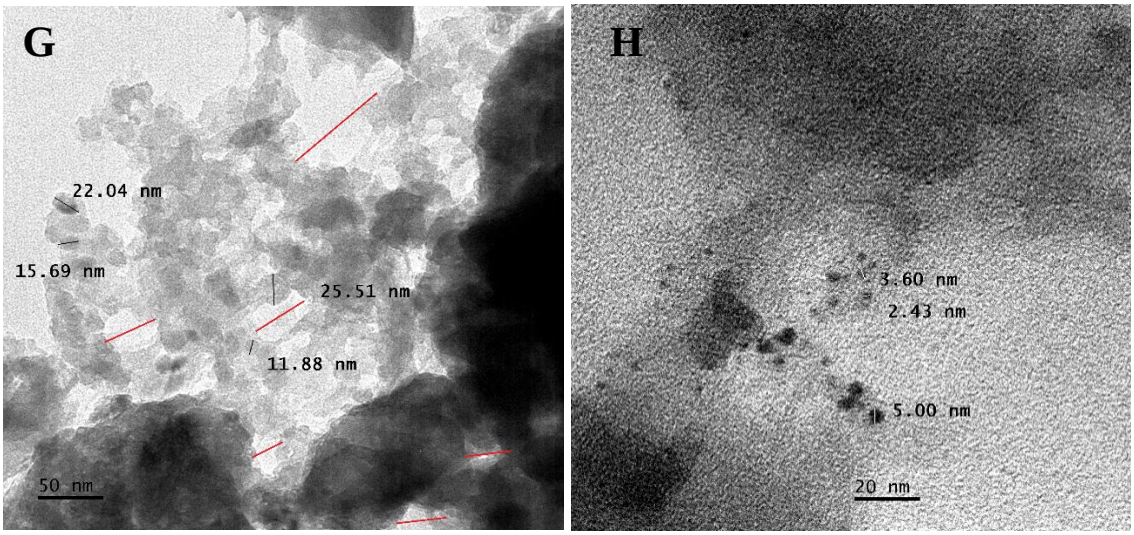

Figure 4.18: TEM images of PJ 300 and PJ 500

TEM images showed the particle sizes of the biochar prepared at 300℃ and 500℃ to be of different sizes. The biochar prepared at 300℃ had larger particle sizes ranging between 11-25 nm as depicted in image G above in figure 4.18. These, aggregated together to form nano cages of sizes between 25 nm and 100 nm. Thus, having a lower surface area to volume ratio than the biochar prepared at 500 ℃ which were smaller in size.

4.4.1.2 Chemical Characterization

Chemical characterization of the prepared biochar were characterised using FTIR, XRD and EDX

4.4.1.2.1 FTIR of Biochar derived from *Aloe succotrina* at 300℃ and 500 ℃

To compare the chemical properties of the two sets of biochar, an FTIR spectra for the two sets of biochar was run between the regions 4000-400 cm^{-1}. The FTIR spectrum of the two sets of biochar are shown in the figure 4.19 below.

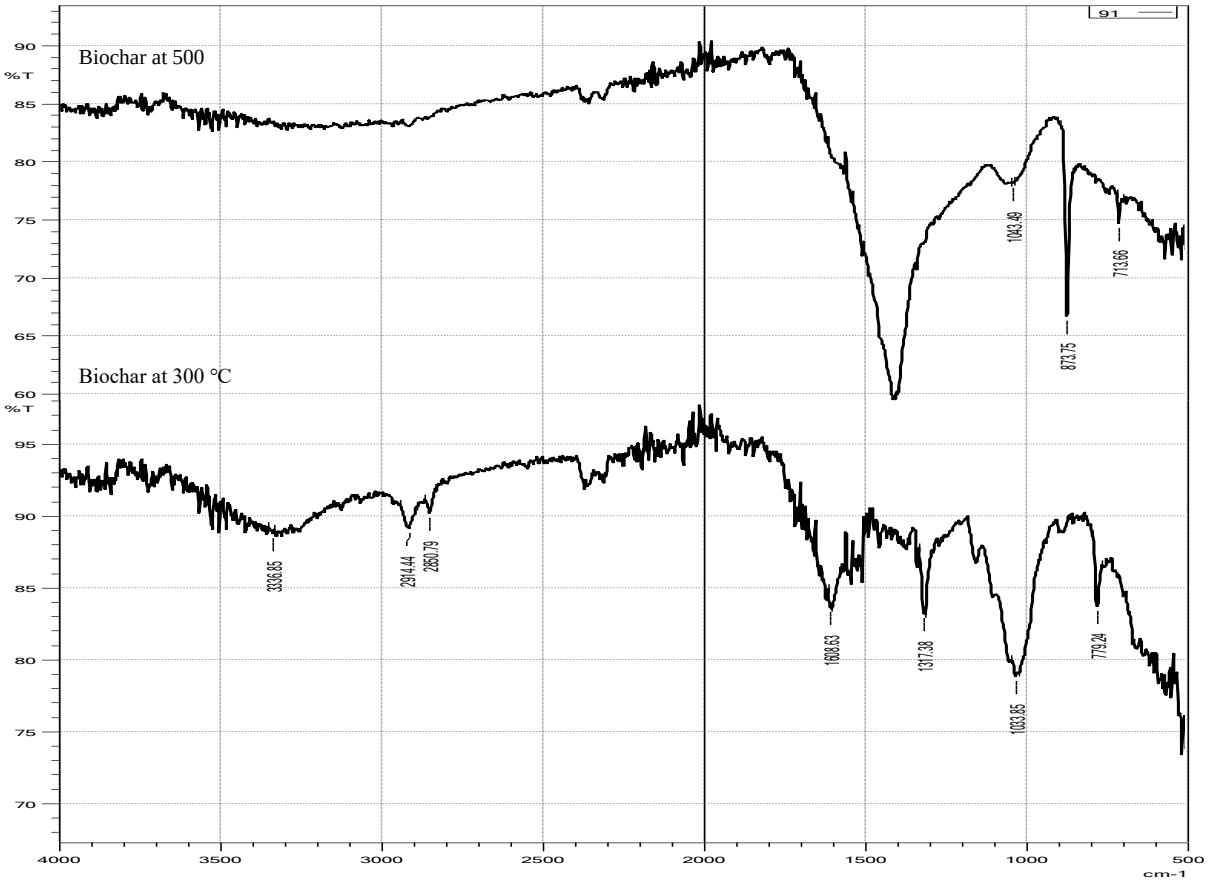

Figure 4.19: FTIR spectra of *Aloe succotrina* biochar prepared at 300℃ and 500 ℃

Studies have shown that changes in pyrolysis temperature leads to a variation in the chemical composition of biochar (Wang & Wang, 2019). This is depicted in Figure 4.19 above in which the FTIR of biochar prepared at 300 ℃ (AS 300) had more functional groups than the biochar prepared at 500 ℃ (X. Zhang, Zhang, Yuan, Li, & Han, 2019). In this case the biochar prepared at 300℃ had the absorption peaks of 3336.85 and 2914.44 for O-H groups 2850.79 for C-H_2, 1608.63 for amide, N-H_2 bending. Additional peaks were at 1317.38 for C-H wagging, 1033.85 for C-O stretching and 779.24 for aromatic C-H band thus making it more organic in nature (Çelekli, Ilgün, & Bozkurt, 2012; Z. Ding *et al*., 2016). The biochar at 500 ℃, on the other hand, had fewer functional groups with

absorption bands of 1406.11 for C-H bonds bending mode, 1043.49 stretching mode and 873.75 for =C-H aromatic ring and 713.66 for =C-H bending mode . These results are consistent with documented findings (Z. Ding *et al*., 2016) that showed that temperature increases enhances decomposition of organic matter thereby decreasing functional groups on biochar.

4.4.1.1.2 FTIR of Biochar derived from *Prosopis juliflora* at 300℃ and 500 ℃

Figure 4.20 below, shows and FTIR spectrum of biochar derived from *P. juliflora* at 300 ℃ (PJ 300) and 500 ℃ (PJ 500).

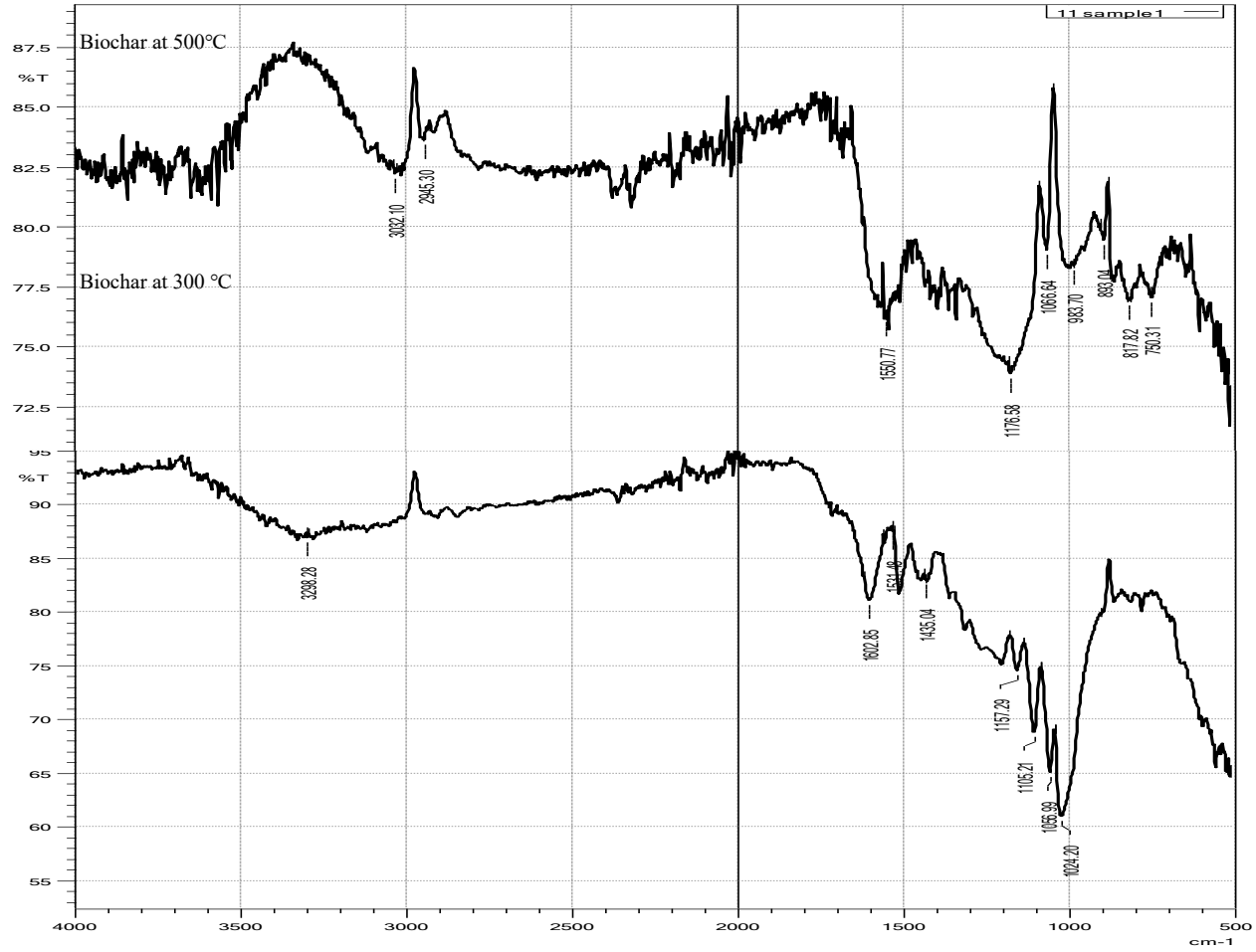

Figure 4.20: FTIR spectra of *Prosopis juliflora* biochar prepared at 300℃ and 500 ℃

Functional group characteristics of biochar derived from *Prosopis juliflora* at 300 ℃ and 500 ℃ mirrored the same results as the biochar derived from *A. succotrina* as described under Section 4.4.1.2.1 above. Briefly, the biochar prepared at 500 ℃ had lesser functional groups than the biochar prepared at 300 ℃. The biochar prepared at 500 ℃, had functional groups at 3032.10 and 2945.30 for O-H stretching mode attributed to carboxylic acid, 1550.77 for C=C and N-H, 1066.64- for C-O, 983.70 for =C-F and 817.82 for =C-H bending. The biochar at 300 had the functional groups 3298.28 for O-H carboxylic acid, 1602.85 for a primary amine and 1531.48 for C=C bond, 1435.04 for C-O-H, 1157 for C=O, 1106.21for C-O, 1056.99 and 1024.21 for C-O for ethers and alcohols.

4.4.1.2.3 EDX analysis for AS 300 ℃ and AS 500 ℃

EDX elemental analysis showed that as the temperature increased from 300 ℃ to 500 ℃, there was a subsequent increase in carbon content and a corresponding decrease in hydrogen and oxygen content. This is in agreement with FTIR in which a variation of heat from 300-500 ℃ led to an increased carbonization of biochar (K. Kim *et al*., 2012; Mary *et al*., 2016). Equally, the EDX elemental analysis showed an increase in percent atomic carbon from 63.14% to 75.16 %. Similarly, the amount of oxygen reduced from 32.08 to 17.69 as a result of removal of most organic bonds containing the oxygen bond, essentially showing that the two sets of biochar are different chemically.

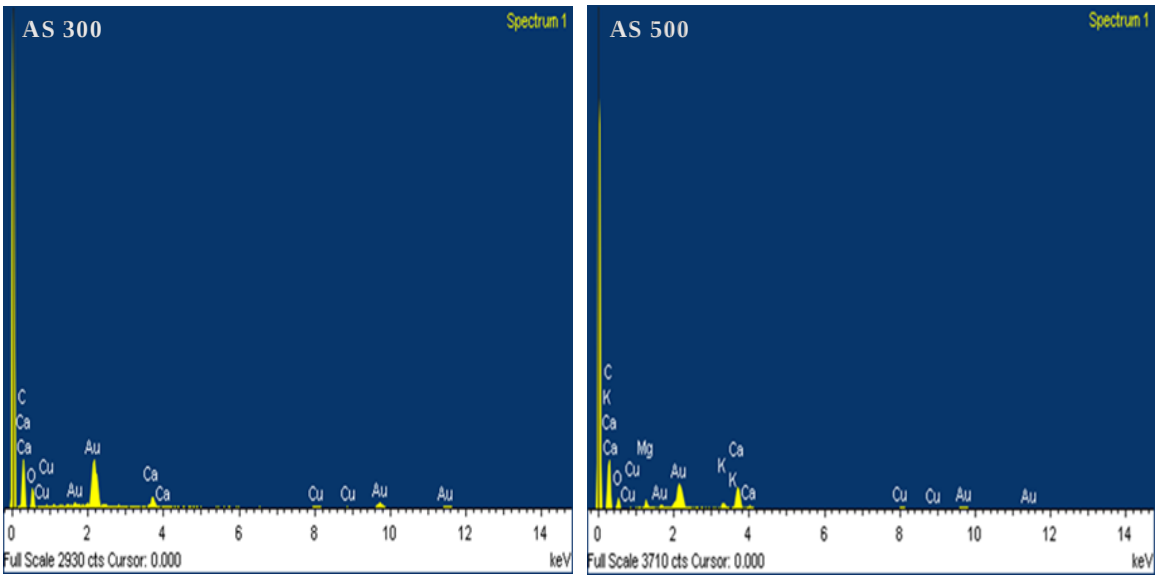

Element	Weight%	Atomic%
C K	44.34	63.14
O K	30.01	32.08
Al K	0.52	0.33
Si K	0.54	0.33
Ca K	3.87	1.65
Cu K	3.69	0.99
Au M	17.04	1.48
Totals	100.00	

Element	Weight%	Atomic%
C K	53.01	75.16
O K	16.62	17.69
Mg K	1.37	0.96
K K	1.39	0.60
Ca K	7.48	3.18
Cu K	3.70	0.99
Au M	16.43	1.42
Totals	100.00	

Figure 4.21: EDX for AS 300 ℃ and AS 500

4.4.1.2.1 EDX analysis for PJ 300 and PJ 500

EDX elemental analysis of PJ 300 and PJ 500 also showed that as the pyrolysis temperature increased, so did the increase in carbon content with the carbon content of PJ 300 being 48.69 and PJ 500 being 69.46 . %. Similarly, the amount of oxygen reduced from 29.88 to 8.32 as a result of removal of most organic bonds containing the oxygen bond, essentially

showing that the two sets of biochar are different chemically. The presence of, gold may have come from the silicon wafer used.

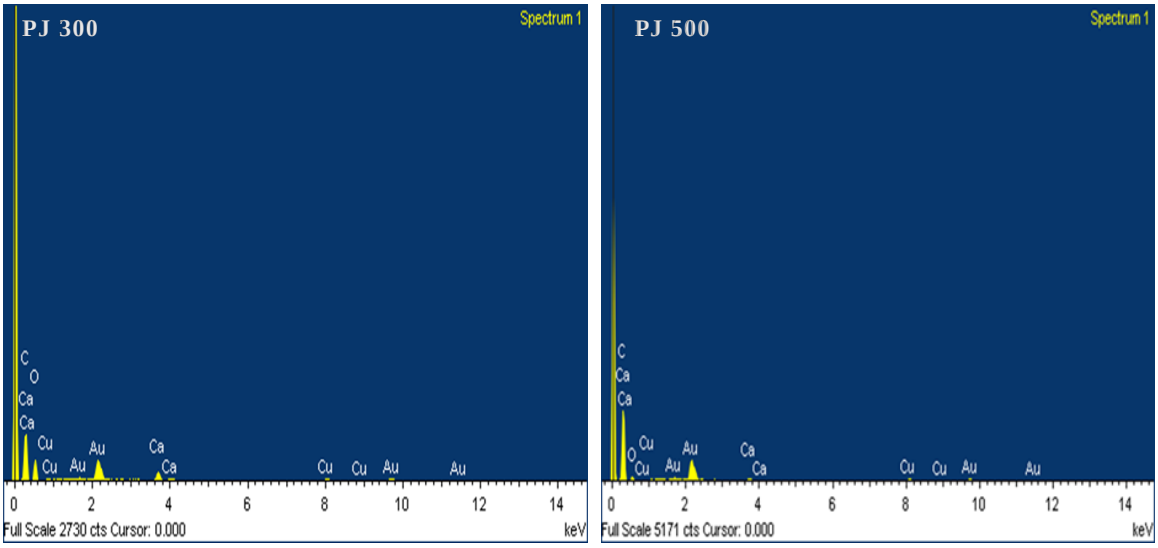

Element	Weight%	Atomic%
C K	48.69	66.76
O K	29.03	29.88
Ca K	2.82	1.16
Cu K	3.25	0.84
Au M	16.21	1.36
Totals	100.00	

Element	Weight%	Atomic%
C K	69.46	89.18
O K	8.63	8.32
Ca K	0.51	0.20
Cu K	3.79	0.92
Au M	17.61	1.38
Totals	100.00	

Figure 4.22: EDX images for *Prosopis juliflora* 300 ℃ and 500 ℃

4.4.1.4 XRD Analysis

4.4.1.4.1 XRD spectra of Biochar derived from *Aloe succotrina*

The XRD spectra captured in figure 4.23 below showed the biochar prepared at 300 ℃ to be amorphous. This, is because, it did not have well defined sharp peaks and instead had wide peaks. Equally, the spectra of the biochar prepared at 500℃ showed that it was amorphous although it had more ordered structures, shown by the slightly sharper peaks (

Wambu & Attahiru, 2018). This, showing that the pyrolysis temperature, can be effectively be used to change the internal structure of the biochar (C. Zhang *et al*., 2020).

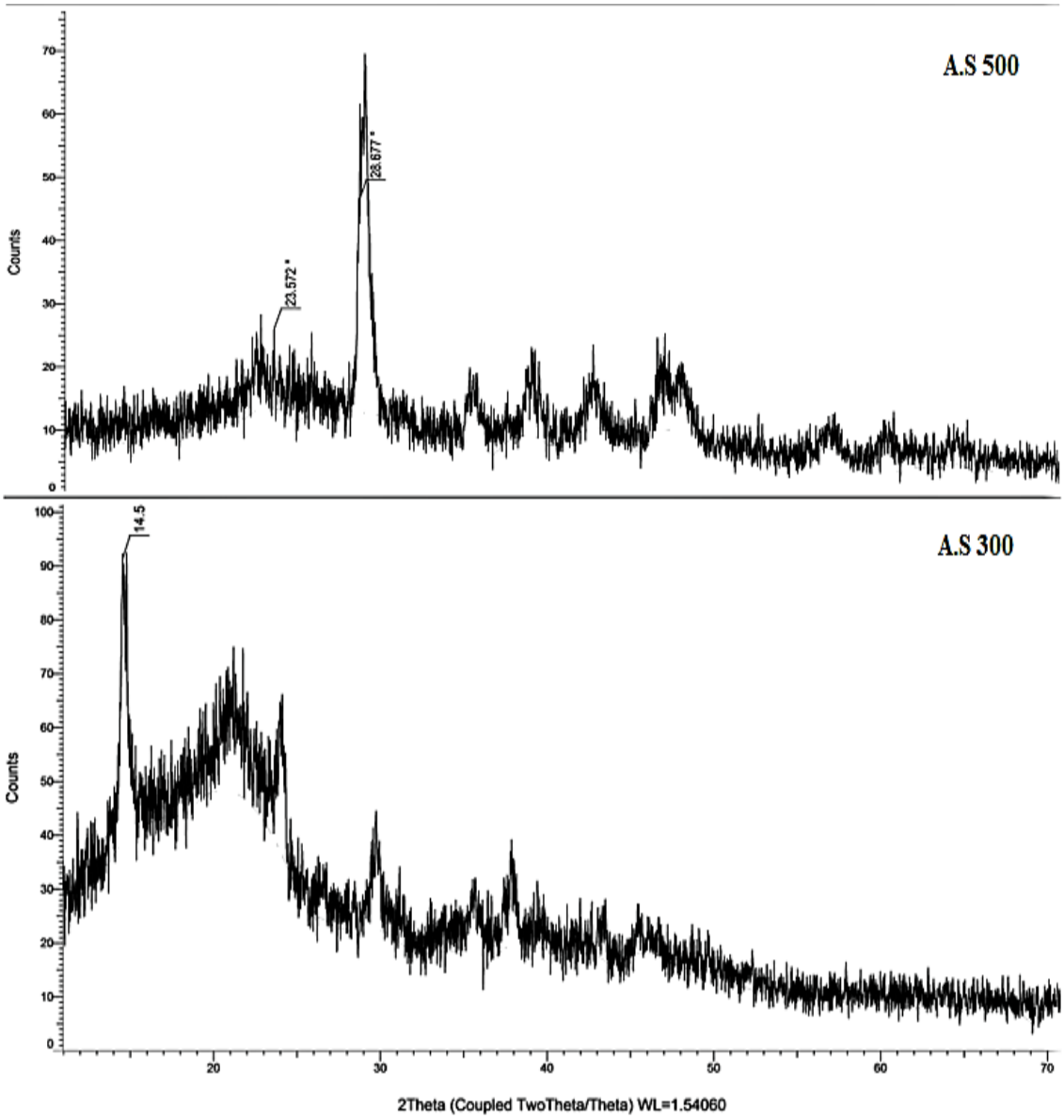

Figure 4.23: XRD spectra of Biochar derived from *Aloe succotrina*

Both the XRD spectra of the biochar prepared at 500℃ and 300℃ showed varied peaks. With the peaks at 14.4 and 23.572 and 28.677 showing that they both contained a certain portion of cellulose within their structure (X. Zhang *et al*., 2019). As the temperature increases, there is a loss of intensity of the peak around 14.5 and a gain of peaks at 23.572

and 28.677 a characteristic region of cellulose. The loss of intensity showed that the biochar prepared at 500 ℃ had a significant loss of cellulose, hence in comparison, the biochar at 300 ℃, is chemically more organic than that at 500 ℃ (K. Kim *et al*., 2012; C. Zhang *et al*., 2020; X. Zhang *et al*., 2019).

4.4.1.4.2 XRD spectra of biochar derived from *Prosopis juliflora*

The XRD spectra of PJ 500 and PJ 300 are captured in figure 4.24 below.

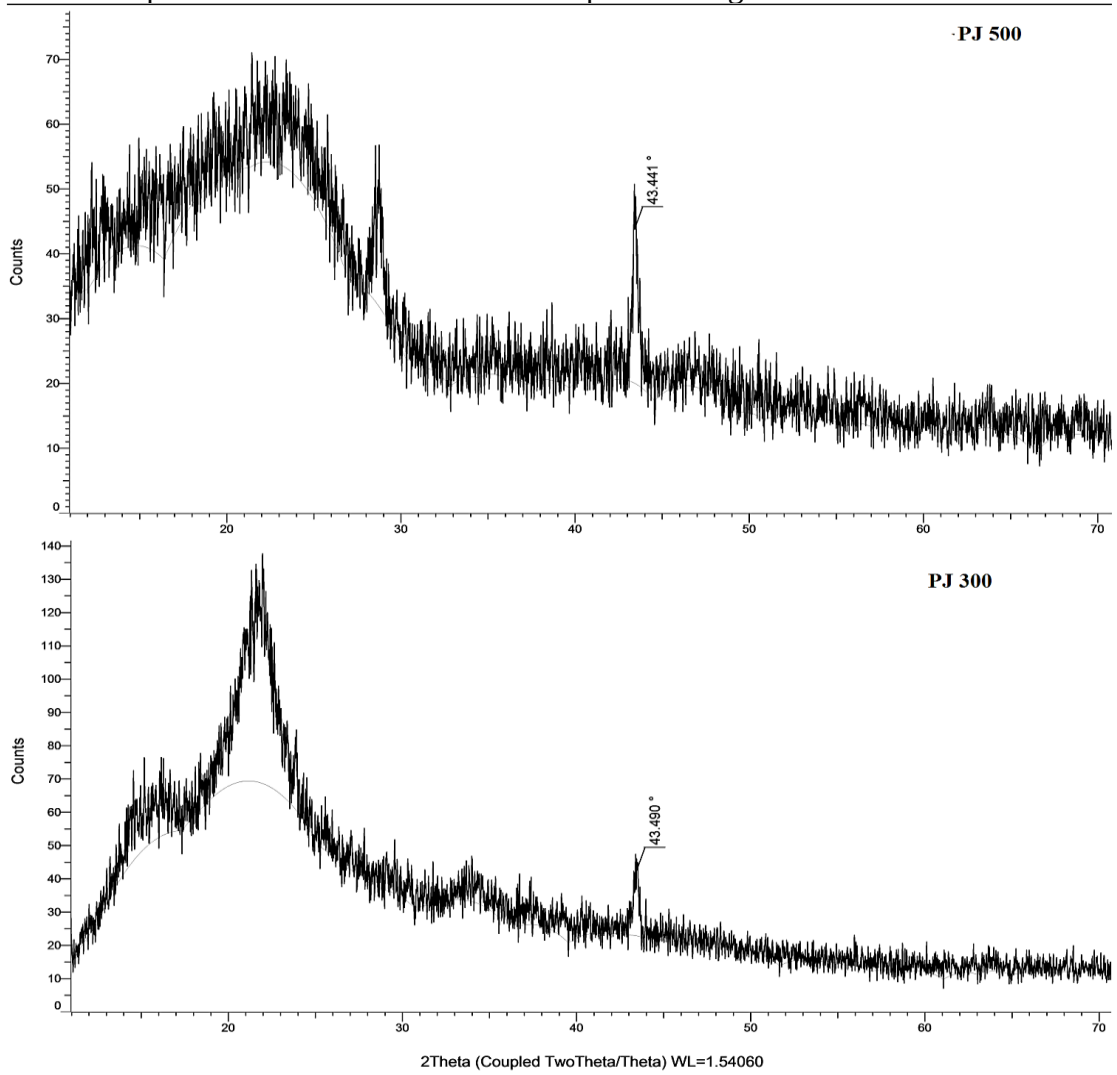

Figure 4.24: XRD spectra of Biochar derived from *Aloe succotrina*

The XRD patterns of the biochar from *Prosopis juliflora* also showed the biochar to be relatively amorphous. Equally, the two XRD spectra showed that the two sets of biochar

had different chemical properties. The spectrum of PJ 300 had a significantly higher peaks at 23.572 and 28.677, which is a characteristic region of cellulose. Showing that the higher the temperature the higher the loss of organic compounds such as cellulose, leading to an increased carbonization of the same (K. Kim *et al*., 2012; C. Zhang *et al*., 2020; X. Zhang *et al*., 2019).

4.5 Remediation studies

Remediation studies, were done for the removal of reactive red 120 (RR120) and methyl violet 2b using biochar derived from the waste biomass of *P. juliflora* and *A. succotrina* at pyrolysis temperatures of 300℃ and 500 ℃.

4.4.2.1 Removal of Reactive Red

4.4.2.1.1 Effect of pH on the adsorption of reactive red

The effect of the pH of the aqueous solution on the adsorption of reactive red is documented in figure 4.25 below. From the graph, it can be concluded that at low pH, the removal efficiencies hence adsorption capacities of the dye are highest. On the other hand, as pH increases towards basic, the removal efficiencies reduce. This is because, the pH of the solution affects two fundamental things in removal of dyes namely the degree of ionization of the dye and the surface charge of the biochar (Elkady, Ibrahim, & El-latif, 2011). This, has also been reported in other literature which suggest that anionic dyes such as reactive reds adsorption will increase as pH decreases and becomes more acidic and vice versa (Mubarak *et al*., 2017; Senthilkumaar, Kalaamani, & Porkodi, 2006). This is illustrated in figure 4.25 below.

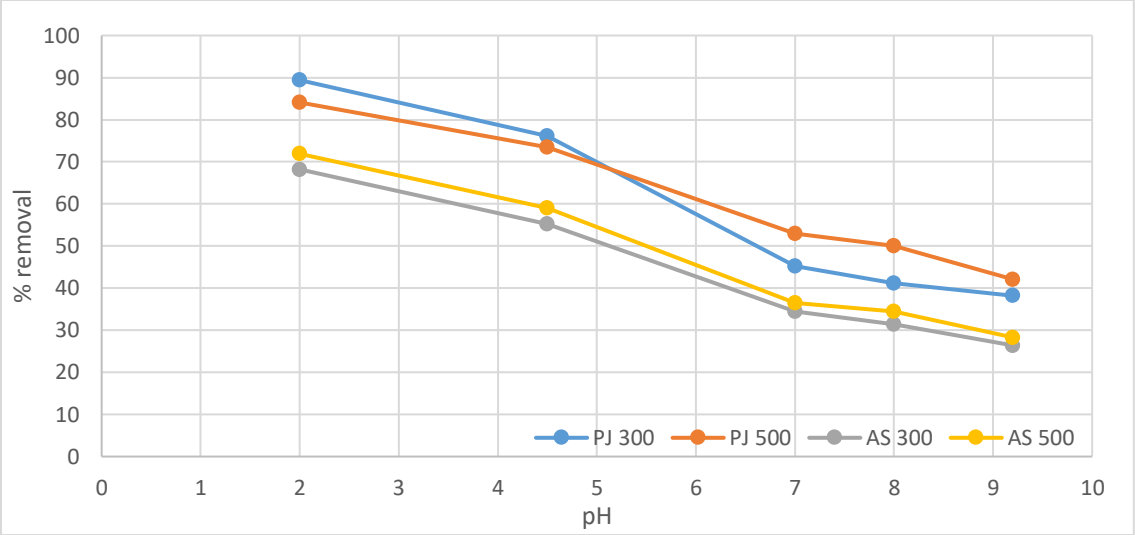

Figure 4.25: Effect of pH on the adsorption of R.R 120 dye at 300° and 500

Both sets of biochar's prepared at 300 °C and 500 °C were efficient with percentage removals of up-to 70.9 % and 68.2 %respectively for AS 500 and AS 300 while it was 90 and 84% effective for PJ 300 and PJ 500 respectively. With the graphs suggesting that for the case of prosopis juliflora biochar, the biochar prepared at 300° C was more efficient than that prepared at 500 °C under the given conditions from both *Prosopis juliflora* while for *Aloe succotrina* the biochar prepared at 500 was more effective.

4.4.2.1.2 Effect of initial concentration on the adsorption of reactive red

The effects of the initial concentration of the RR dye on the percentage removal of the dye in an aqueous solution is documented in figure 4.26 below.

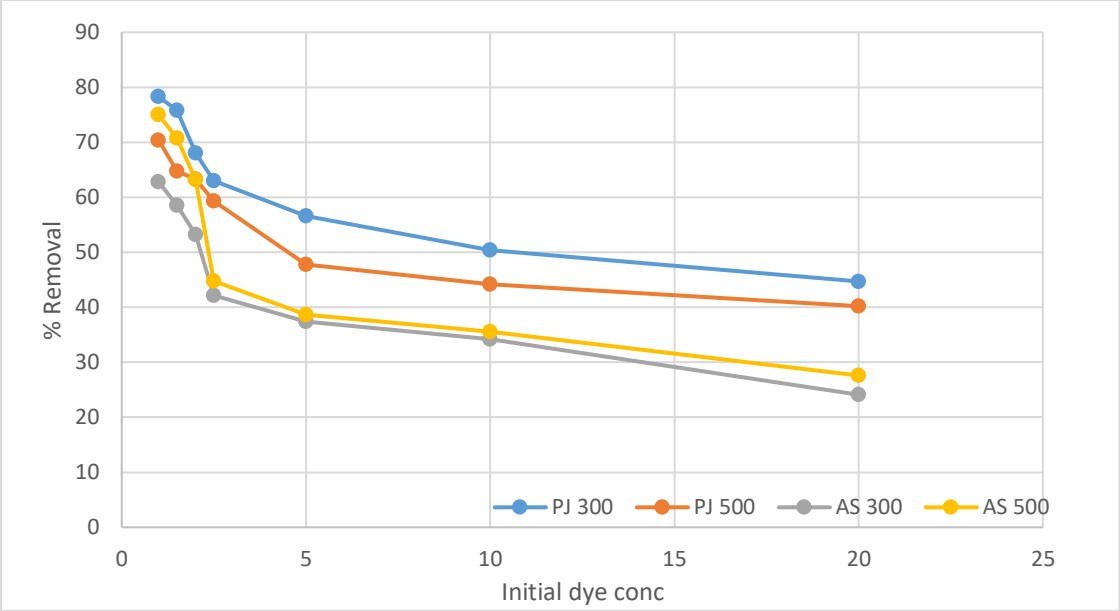

Figure 4.26: Effect of initial concentration on the adsorption of RR120

From the graph, it can be deduced that as the concentration of the dye increases, so does the percentage removal reduce. This, can be attributed by saying that with an increase in concentration, there is also an increase in the number of molecules that bind into the biochar binding sites, hence the lower percentage removals. This observations have also been made in other literature (Mohamed E. Mahmoud , Gehan M. Nabil , Nabila M. El-Mallah , Heba I. Bassiouny , Sandeep Kumar , 2016; Parvin, 2015; Vijayakumar *et al*., 2016).

4.4.2.1.3 Effect of temperature on the adsorption of reactive red

The effect of temperature on the adsorption of biochar is as documented in figure 4.27 below. As the temperature increases up-to 50 ℃, so does the percentage dye removal increase this suggesting that the adsorption process is endothermic in nature showing the potential of both chemisorption and physisorption processes being the reason of adsorption (Çelekli, Al-nuaimi, & Bozkurt, 2019; Munagapati *et al*., 2019; Oueslati, Lima, Ayachi, Cunha, & Ben Lamine, 2020). The effect of temperature has been studied in other studies with the conclusion that in endothermic processes an increase in temperature leads to an

increase in kinetic energy within the adsorbate which in turn increase the sorption process (Wekoye, Wanyonyi, Wangila, & Tonui, 2020).

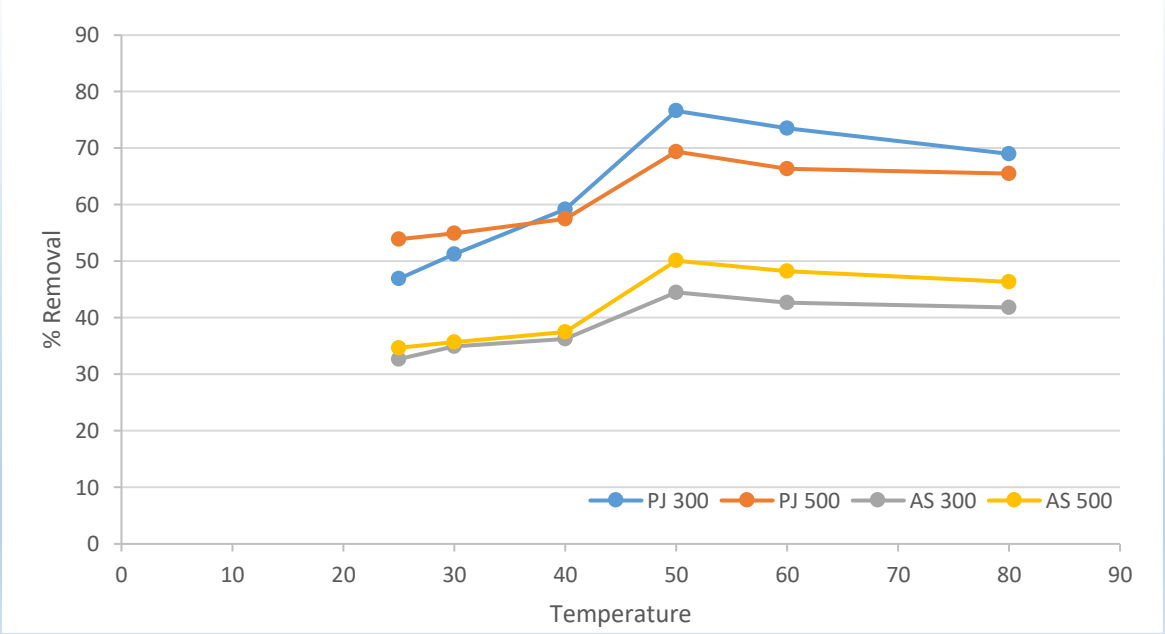

Figure 4.27: Effect of temperature on the adsorption of R.R 120

At temperatures above 50 ℃, there is a decrease in percentage removals this is possibly because at higher temperatures, there is an increase in molecular mobility making it counter-productive and in the process leading to a shift in equilibrium towards desorption (Shikuku *et al*., 2018).

4.4.2.1.4 Effect of agitation speed on the adsorption of reactive red

The effect of the agitation speed on the percentage removal of dyes was studied and the results documented below in figure 4.28.

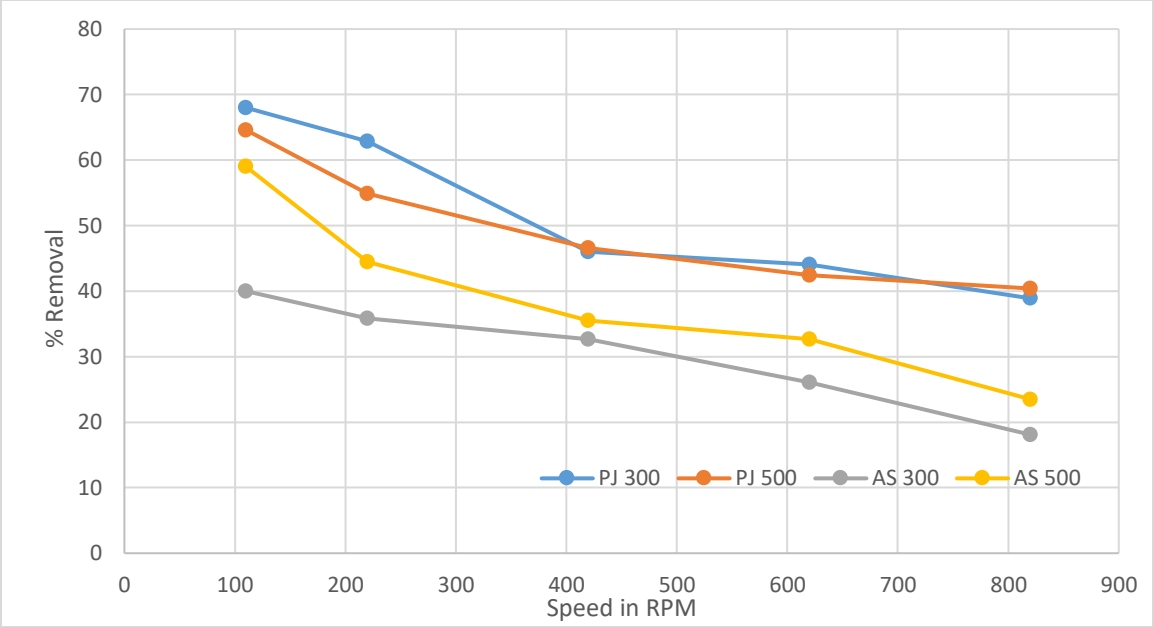

Figure 4.28: Effect of rotation speed on the removal of R.R 120

The agitation speed, is considered as an important parameter in optimization of adsorption. This is because it chiefly affects the movement of dye molecules from the aqueous solution into the adsorbent. At very slow speed, adsorption process is slow and takes a longer time while at high speeds beyond the optimum point, desorption begins to occur. This is because the high centrifugal force as a result of the speed of rotation is so high that it breaks the adsorbate-adsorbent bonds (Das, Banerjee, & Mondal, 2014).

4.4.2.1.5 Effect of contact time on the adsorption of reactive red

The effect of the contact on the percentage removal of dyes was studied and the results documented below in figure 4.29. For PJ 300, the adsorption of the dye increased rapidly upto about 60th Minutes where it reached an equilibrium, for PJ 500, adsorption also increased rapidly upto the 40th Minute then it slowed down. For AS 300 and AS 500, adsorption increased rapidly upto the 50th and 30th minute respectively where after that, it leveled. This results are also mirrored by (Celekli, Yavuzatmaca, & Bozkurt, 2010), whose

equilibrium time for the adsorption of RR120 on pistacio rice husks was 60 minutes and also with (Çelekli *et al*., 2012) who studied the adsorption of RR120 on *Chara contraria* and found the equilibrium to flatten after 30 minutes.

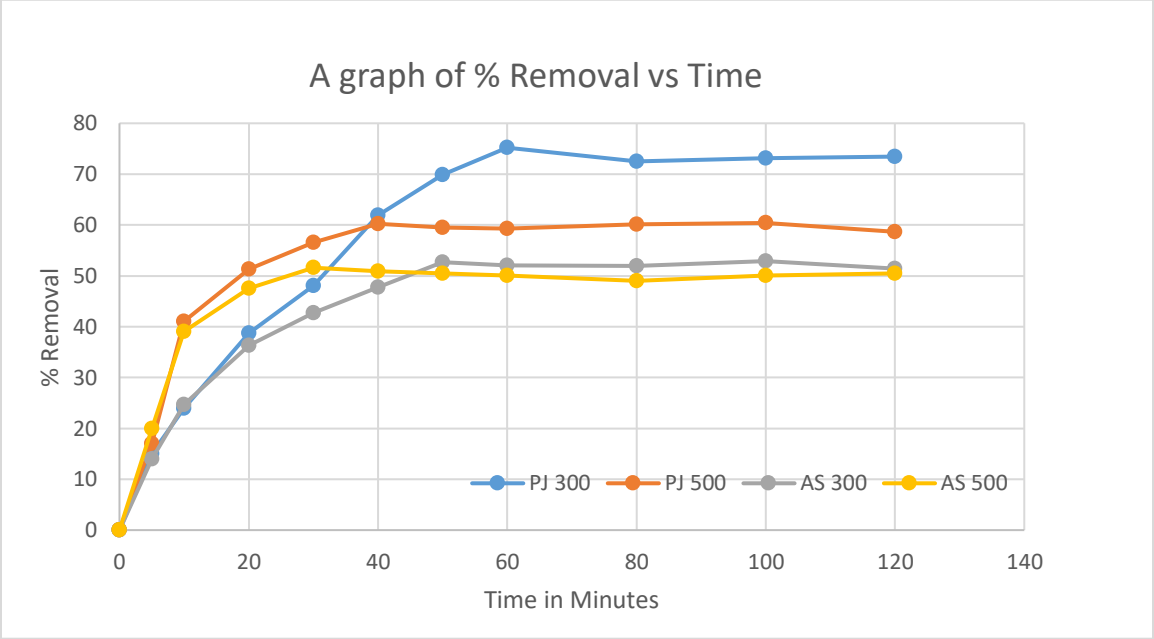

Figure 4.29: Effect of contact time on the adsorption of r. red dye at 300° and 500 °C

4.4.2.2 Adsorption Kinetics and Isotherms

Adsorption data for these experiments were analysed for their kinetics with non-linear pseudo 1st order, pseudo second order and elovich models. Isotherm studies, were analysed using langmuir, freundlich and jovanovic monolayer and the results tabulated. A combination of statistical tests such as $R_{Pearson}$, R^2, R^2_{adj}, chi-χ^2, RMSE and MSE were used to compare data between experimental data and calculated data. This, was done using CAVS adsorption software.

For non-linear kinetics fittings, a graph of (q_t vs t) was plotted and statistical data used to analyse the models that fit the kinetics the best (Markandeya, Shukla, & Kisku, 2015). Figure 4.30 below, represents the kinetic modelling for the removal of R.R 120 against

PJ300, PJ500, AS300 and AS500. For all the four sets of biochar, the best model that fits the adsorption kinetics was Pseudo 1st order > Pseudo second order> elovich model. This is because statistically, it has the highest values of $R_{pearson,}$ R^2, R^2_{adj} and the lowest values of χ^2 , RMSE and MSE (M. K. Dahri *et al*., 2013; Markandeya *et al*., 2015).

The closeness of values between the q_e in the pseudo second order kinetic model (19.66597) and in Langmuir isotherm model with (20.642784) suggest that for the case of PJ300, the adsorption process is not only a physisorption process, but also a chemisorption process that involves the exchange and/or sharing of electrons between the adsorbent and the adsorbate (M. K. Dahri *et al*., 2013). This maybe because as shown in the previous FTIR images in figure 4.16, the PJ 300 biochar was more organic in nature.

Table 4.15: Kinetic parameters and residual analysis for the removal of reactive red 120 using PJ300, PJ500, AS300 and AS 500.

	PJ 300	PJ 500	AS 300	AS 500
Pseudo 1st Order				
K_f (h^{-1})	0.037216	0.08384	0.060558	0.126703
q_e	15.69191	12.68151	10.53969	10.13888
$R_{Pearson}$	0.991125	0.987527	0.996412	0.984911
R^2	0.982318	0.974113	0.992788	0.965279
R^2_{adj}	0.977266	0.966717	0.990727	0.955359
χ	0.305680	0.361907	0.052290	0.193384
RMSE	0.577467	0.458972	0.218797	0.346407
MSE	0.333469	0.210655	0.047872	0.119998
Pseudo 2nd Order				
K_s (g mg^{-1} h)	0.001904	0.00746	0.005976	0.017141
qe	19.66597	14.4046	12.29509	11.04301
R Pearson	0.982211	0.974517	0.98508	0.933264
R^2	0.963888	0.945212	0.968619	0.865431
R^2_{adj}	0.95357	0.929559	0.959653	0.826982
χ	0.565416	0.706351	0.264163	0.650564
RMSE	0.825255	0.667713	0.456393	0.681969
MSE	0.681046	0.445841	0.208295	0.465082
Elovich				
α	1.042565	3.99269	1.763011	15.26618
β	0.193852	0.366775	0.379445	0.638071
$R_{Pearson}$	0.968343	0.921828	0.95246	0.822161
R^2	0.936607	0.849058	0.906238	0.67588
R^2_{adj}	0.918494	0.805932	0.879449	0.583274
χ	1.049509	1.564176	0.822253	1.46599
RMSE	1.0934113	1.108290	0.788895	1.05838
MSE	1.1955483	1.228308	0.622356	1.12018

PJ 300

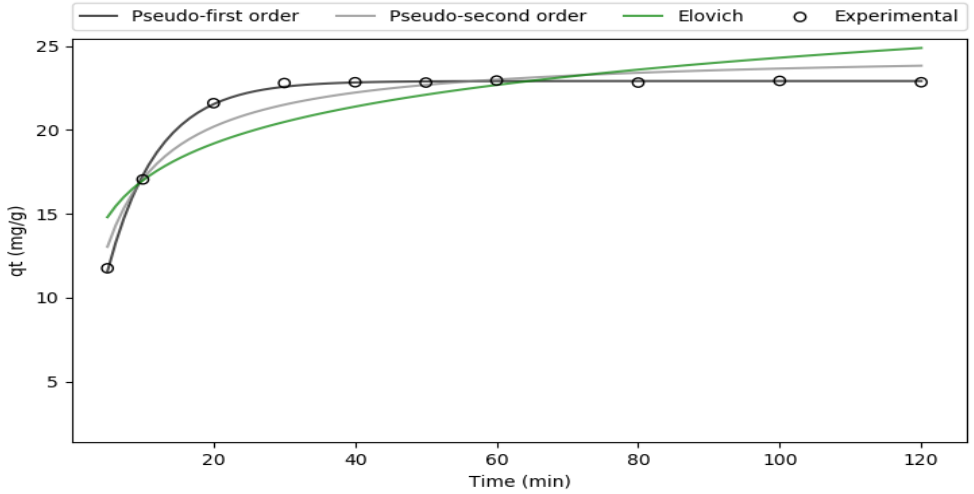

PJ 500

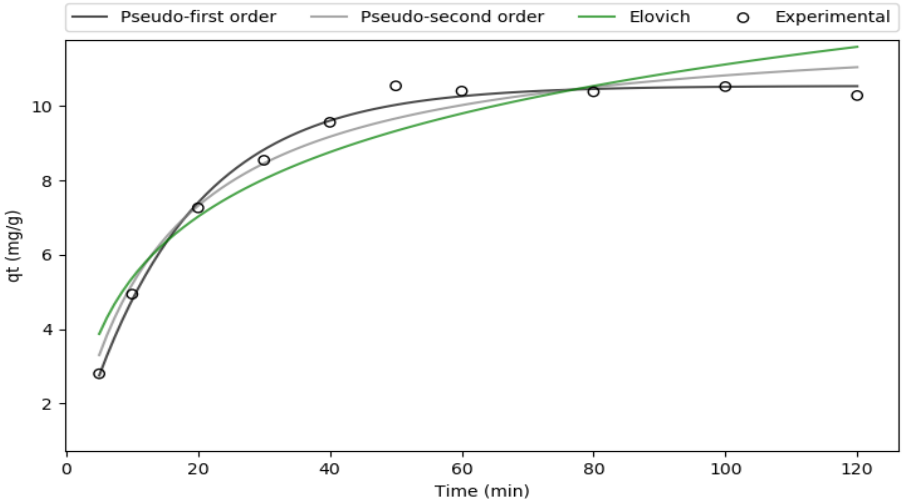

AS 300

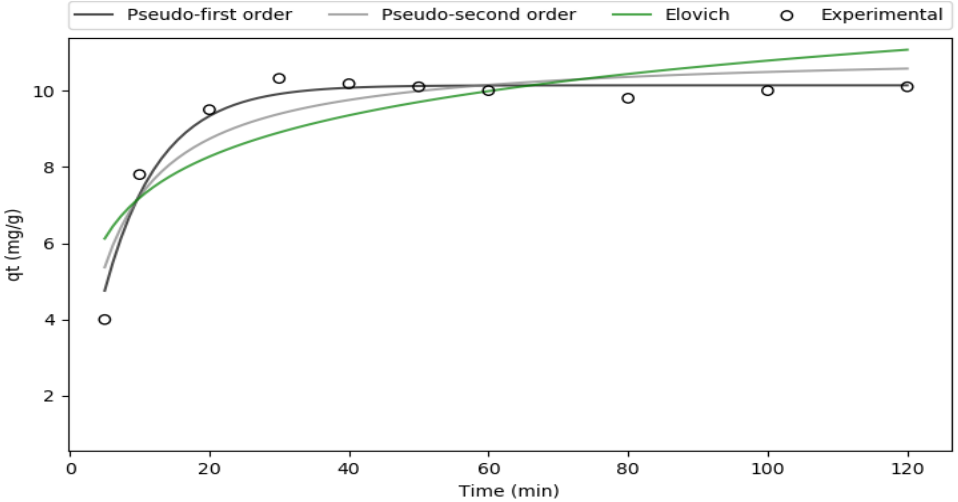

AS 500

Figure 4.30: Kinetic Modelling for the removal of R.R using Biochar derived from *P. juliflora* and *Aloe succotrina* at 300℃ and 500℃

Table 4.16: Isotherm parameters for the removal of Reactive Red using PJ300, PJ 500, AS 300 and AS 500

	PJ 300	**PJ 500**	**AS 300**	**AS 500**
Freundlich				
K_f (mg/g)	2.147719	2.109645	1.426097357	1.439832193
n_f	1.482846633	1.645554	1.634132721	1.410666538
$R_{Pearson}$	0.996030363	0.994363063	0.995608702	0.995195564
R^2	0.991026159	0.988534104	0.991235201	0.988562807
R^2_{adj}	0.986539238	0.982801155	0.986852802	0.98284421
χ	0.350264399	0.153450495	0.122880081	0.578224484
RMSE	0.296346541	0.292420669	0.19585697	0.271205196
MSE	0.087821272	0.085509848	0.03836	0.073552259
Jovanovic monolayer				
K_j (mg g^{-1})	0.129664034	0.212009172	0.156693822	0.090378
q_m	13.93333	9.656875929	7.748242607	12.66975036
$R_{Pearson}$	0.992171056	0.997399787	0.994709652	0.992842621
R^2	0.965637044	0.990867826	0.980100386	0.967211601
R^2_{adj}	0.948455566	0.98630174	0.970150579	0.950817401
χ	3.347625819	0.7427991	1.070538461	3.213995831
RMSE	0.579903762	0.260970332	0.295114386	0.459196307
MSE	0.336288373	0.068105514	0.087092501	0.210861249
Langmuir				
q_m	20.64278469	13.55755496	10.96842398	19.57544316
K_L	0.095194089	0.166556629	0.122257512	0.062039355
$R_{Pearson}$	0.991597774	0.9970516	0.994394938	0.99228498
R^2	0.968864437	0.991977789	0.982803801	0.969309529
R^2_{adj}	0.953296656	0.987966683	0.974205701	0.953964294
χ	2.772260147	0.55223699	0.8209201	2.855482399
RMSE	0.551999935	0.244596987	0.274336939	0.444262908
MSE	0.304703929	0.07807987	0.075260756	0.197369531

In the analysis of adsorption isotherms, of RR 120 against the prepared biochar, all the three models fitly described the adsorption process with the best for PJ 300 being Freundlich >Langmuir > Jovanovic monolayer model. This is because, statistically the best isotherm is the one that has the highest values of $R_{pearson,}$ R^2, R^2_{adj} and the lowest values of χ^2 , RMSE and MSE (M. K. Dahri *et al*., 2013; Markandeya *et al*., 2015). For PJ 500, the best isotherm models were Langmuir>Jovanovic monolayer>Freundlich. For AS 300, the best models were Freundlich >Langmuir > Jovanovic monolayer while for AS 500 it was Freundlich >Langmuir > Jovanovic monolayer.

Because the q_{max} for adsorption was highest for PJ 300 then it was considered the most effective biochar of the four for the removal of RR120 at 20.6427. Compared to commercially activated carbon which was used as standard for comparative studies, the biochar, was found to be effective although slightly lower in its adsorption capacity.

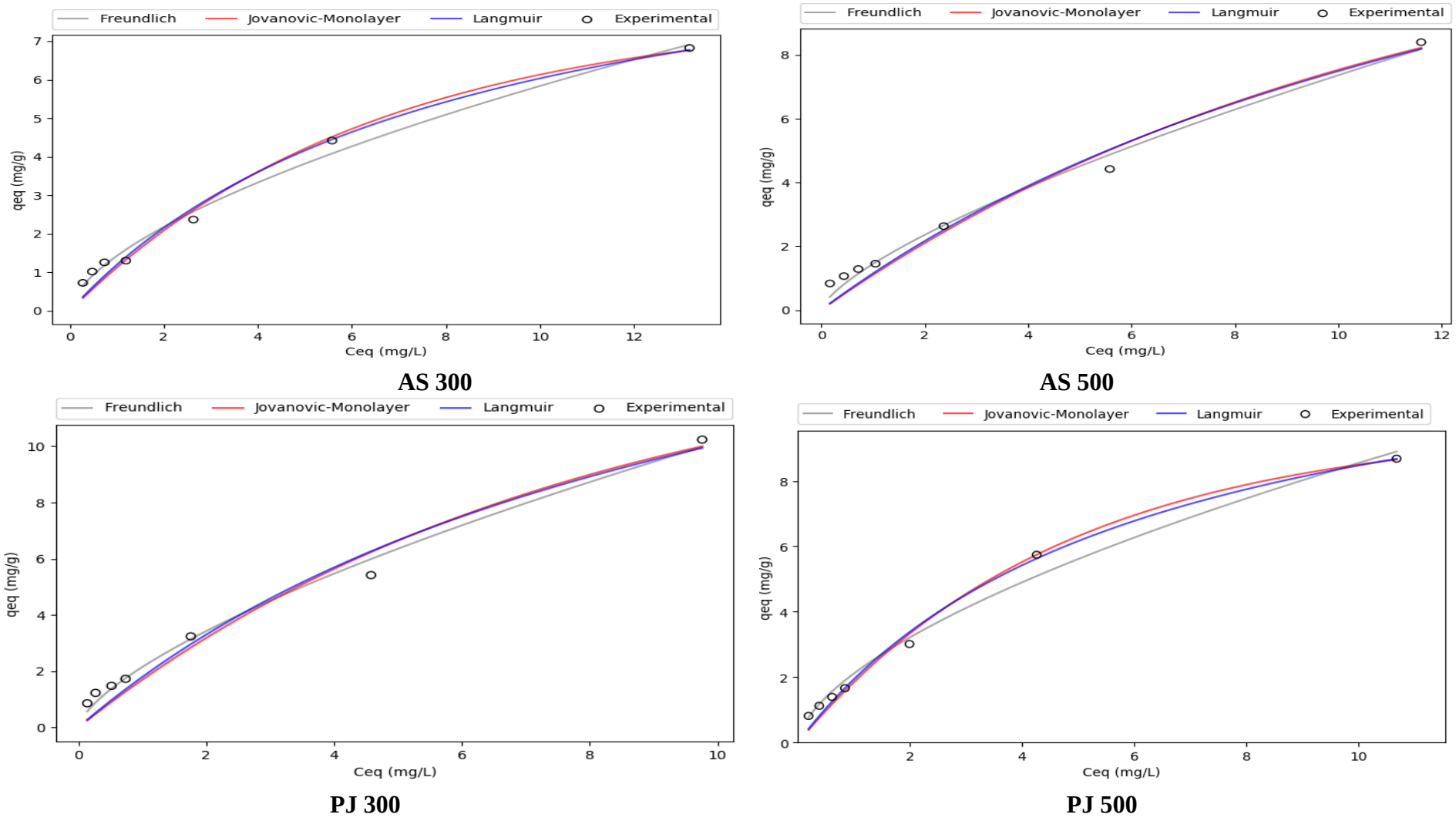

Figure 4. 31: Isotherms for the removal of R.R using Biochar derived from *P.juliflora* and *Aloe succotrina* at 300℃ and 500℃

Table 4.17: Comparative Analysis of adsorption capacities of reactive red 120 with other adsorbents

Biomass material	**Q_0 (mg/g)**	**Reference**
Coconut tree fibre	189	(Senthilkumaar *et al*., 2006)
Jute flower	125	(Senthilkumaar *et al*., 2006)
Pumpkin husk	98.1	(Çelekli, Çelekli, Çiçek, & Bozkurt, 2014)
Pumice stone	2.32	(Hossein & Behzad, 2012)
Chitosan/zeolite composite	43.79	(Dehghani, Dehghan, & Najafpoor, 2017)
Quaternary amine modified orange peel powder	344	(Munagapati *et al*., 2019)
Chitin	46.1	(Torun, Aracagök, & Kabalak, 2018)
Chitosan/modified montmorillonite beads	5.608	(Kittinaovarat, Kansomwan, & Jiratumnukul, 2010)
Hydrilla verticillata	120.85	(Naveen, Saravanan, Baskar, & Renganathan, 2011)
Chitosan/Zeolite composite	19.4	(Dehghani *et al*., 2017)
Agave sisalana	110	(Dev, Venugopal, Kumar, Miranda, & Ramakrishna, 2010)
Chitosan beads	129.9	(Mubarak *et al*., 2017)
Activated carbon from waste tea	250	(Auta, 2020)
Chara contraria	102.90	(Çelekli *et al*., 2012)
Activated carbon (Control)	243.5	This study
Prosopis juliflora @300℃	20.643	This study
Prosopis juliflora @500℃	13.558	This study
Aloe succotrina @300 ℃	10.968	This study
Aloe succotrina @500℃	19.575	This study

4.4.2.3 SEM Images before and after adsorption

SEM images before and after adsorption, showed a difference in surface morphology of the biochar before adsorption and after adsorption. With the images serving as proof of adsorption of dye onto the surface of the biochar.

4.4.2.3.1 SEM Images for AS 300 and AS 500 before and after Adsorption

SEM images for AS 300 before and after adsorption are captured as images I, J respectively and equally for AS 500 as K and L.

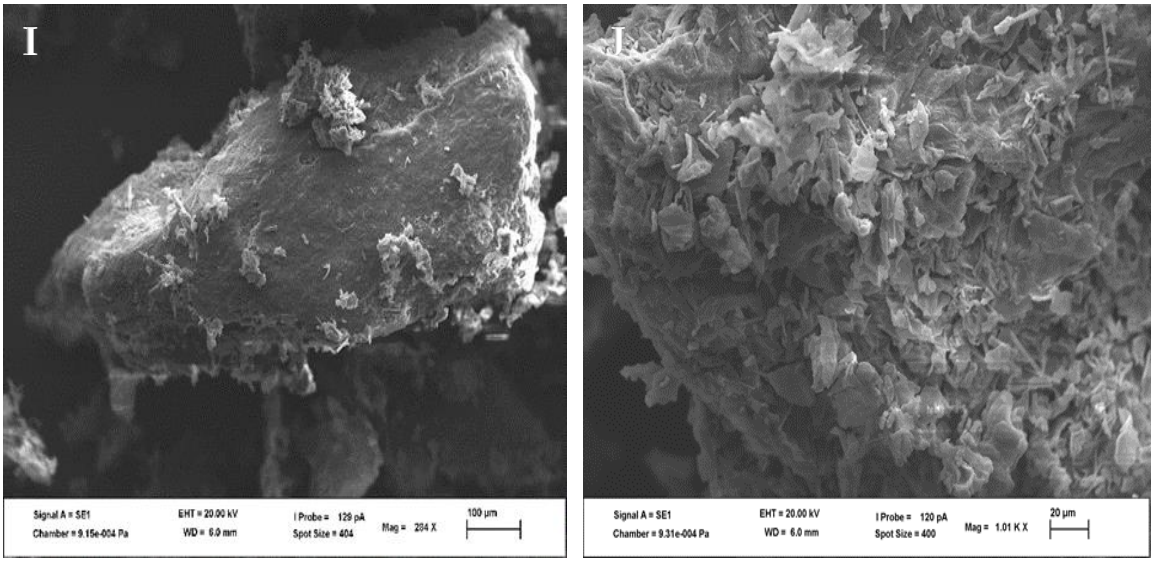

Figure 4.32: SEM Images for AS300 before and after Adsorption with RR120

Images I and J serve as evidence before and after adsorption. Before adsorption, the surface of the image I is smooth with flat surface structures with islands of fibrous matter. After adsorption, the image J, has matter that is embedded on the surface covering the previously soft surface thus serving as proof of adsorption (S. Ahmad, Wong, & Veloo, 2018).

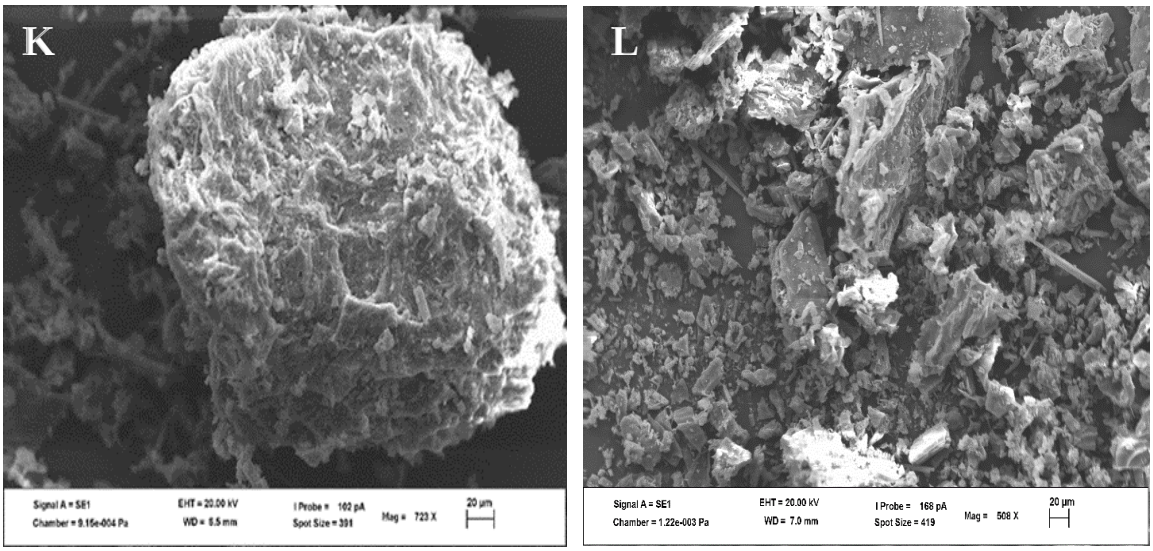

Figure 4.33: SEM images for *Aloe succotrina* at 500 before and after adsorption

Image K, which is for the image before adsorption, has a mesoporous structure before adsorption. The mesoporous structures, have pockets which serve as cavity sites for the adsorption of the dye. As a result, the dyes and adsorb on the surface an embed themselves into the cavities thereby shown by image L.

4.4.2.3.2 SEM Images for PJ 300 and PJ 500 before and after Adsorption

SEM images for PJ 300 before and after adsorption are captured as images M and N in figure 4.34 respectively and images O and P for PJ 500 in figure 4.35 below.

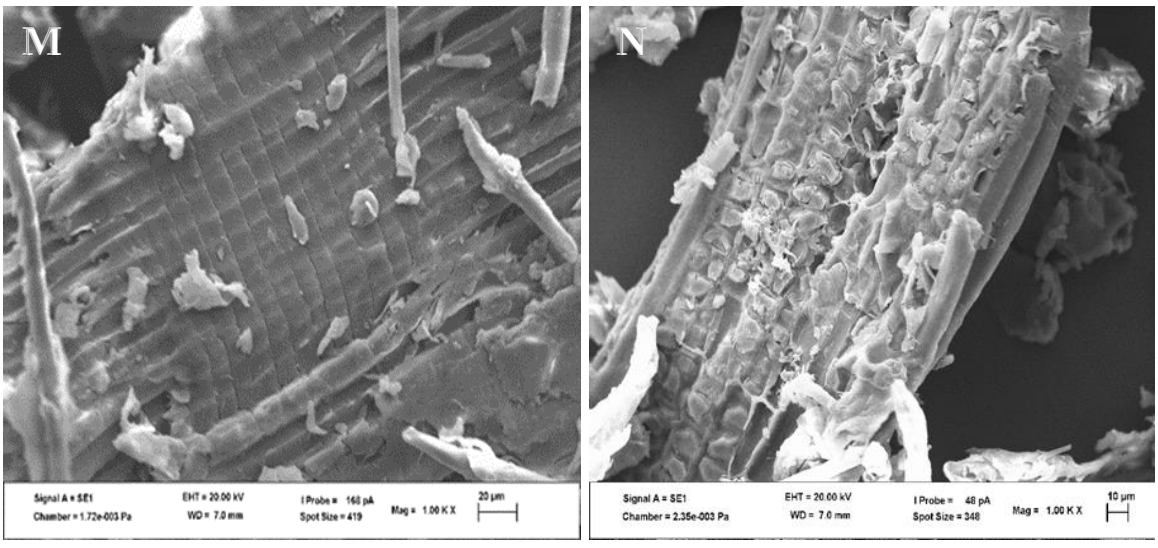

Figure 4.34: SEM Images for *P. juliflora* at 300 before and after Adsorption with RR120

SEM images for figure M and Figure N before and after adsorption, show a difference in surface structure before and after adsorption. The previous fibrous nature of the biochar in M, is covered by particles that are embedded on to it showing that adsorption has taken place (S. Ahmad *et al*., 2018).

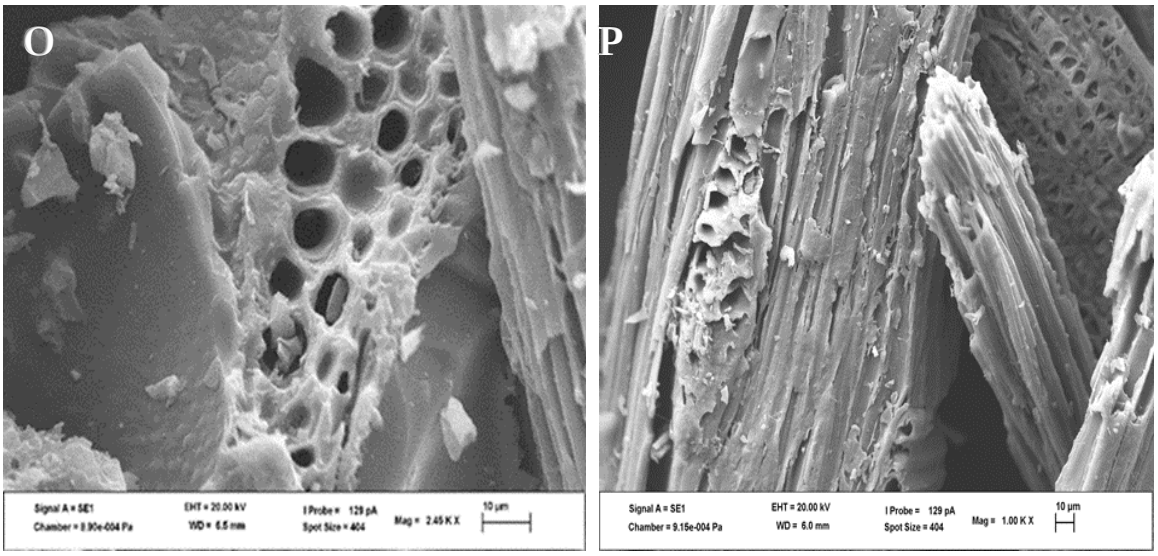

Figure 4.35: SEM Images for *Prosopis juliflora* at 500 before and after adsorption

The SEM images before and after adsorption showed are shown in figure 4.35 above. In this case, the grooves, the fibrous networks and pores that were present in the biochar, were filled with the dye particle after adsorption giving the SEM images in image P of figure 4.35 (S. Ahmad *et al*., 2018). This information can equally be confirmed by the use of Transmission electron microscope (TEM) images and FTIR plots, attached as appendix 9-12 and appendix 1-4 which show that the particle sizes of the biochar before adsorption and after adsorption being slightly larger than the same sizes before adsorption. Equally, the FTIR images show additional functional groups not present initially in the biochar being present after adsorption this, serving as proof of adsorption.

4.4.2.3 Removal of Methyl Violet 2b

4.4.2.1 Effect of pH on the adsorption of Methyl violet 2b

The effect of pH on adsorption of methyl violet 2b from an aqueous solution is shown in figure 4.36 below. From the trend of the graph below, it can be concluded that the adsorption of the dye, increases with an increase in pH up-to pH 8 where it begins to decrease again. This, can be accounted for by the fact that, the dye is cationic in nature and therefore in an acidic media, there is a large amount of hydrogen ions in the aqueous system which in-turn, competes for adsorption sites on the biochar with the cationic molecules of the MV2b dye (Lim *et al*., 2015).

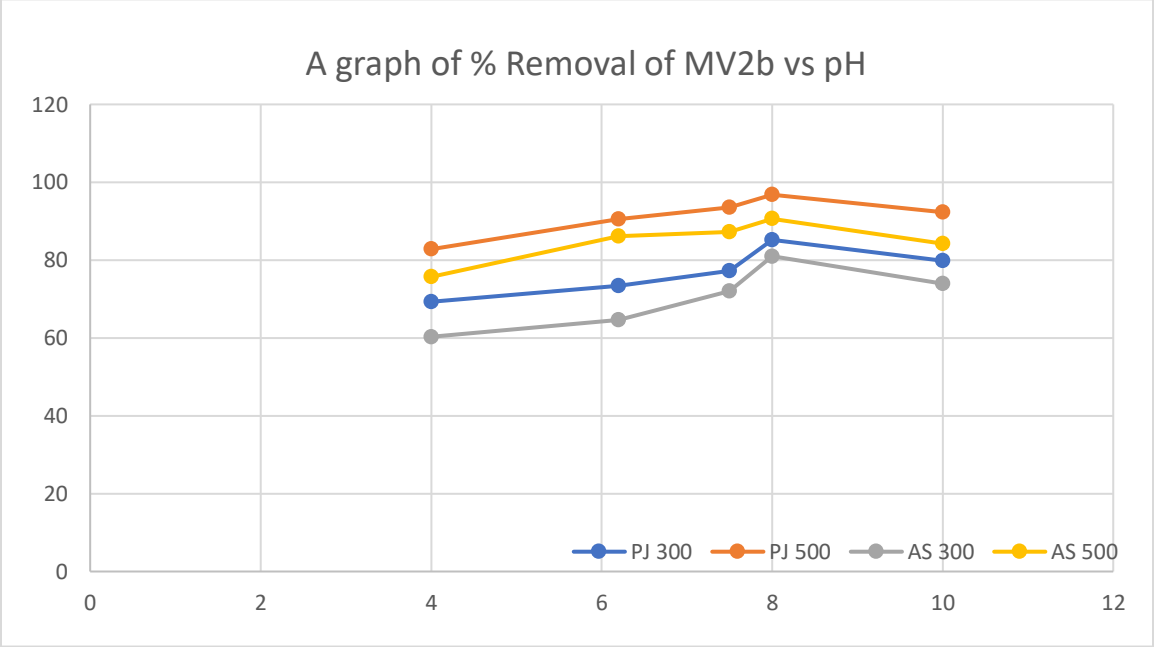

Figure 4.36: A graph of % removal vs pH

At pH of 2, the dye disintegrated in colour and nature and therefore the study did not cover this pH range. This was also observed by other based on literature which suggest that at very acidic pH levels the dye molecules break down hence the dye loses its characteristic colour (M. K. Dahri *et al*., 2013; Fahad, Ali, & Hameed, 2018).

4.4.2.2 Effect of initial concentration on the adsorption of Methyl violet 2b

The effects of the initial concentration of the Methyl violet dye on the percentage removal of the dye in an aqueous solution is documented in figure 4.37 below. From the graph, it can be concluded that the percentage removal decreases as the concentration increases. This is because, as the concentration increases, there is also an increase in the number of molecules that bind into the respective amount of binding sites, which in turn lowers the percentage removals, (Parvin, 2015; Vijayakumar *et al*., 2016).

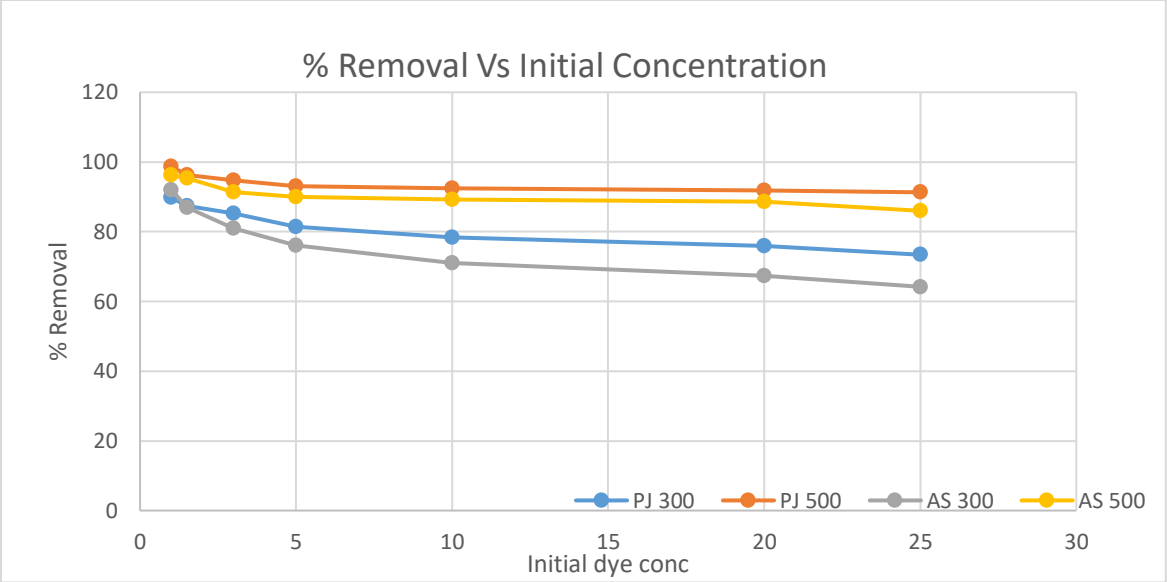

Figure 4.37: A Graph of % removal vs Initial Concentration

4.4.2.3 Effect of temperature on the adsorption of Methyl violet 2b

The effect of temperature on the adsorption of the biochar against methyl violet 2b, is as shown in the figure 4.38 below.

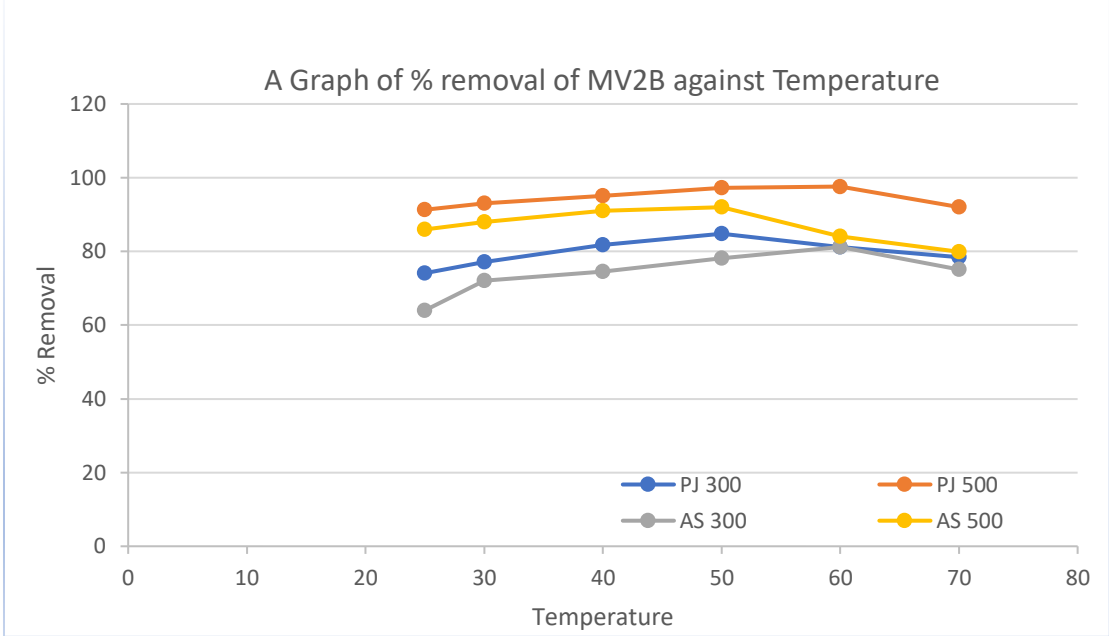

Figure 4.38 : A Graph of % removal against temperature

The results show that as the temperature increases, so does the adsorption process increase up to 60 ℃, for PJ 500 and up to 50 ℃ for the rest. This suggesting that the adsorption process is endothermic in nature. A further increase in temperature, doesn't change the percentage removal (Raziq *et al*., 2015). It has been noted that, increasing the temperature in adsorption processes, often increases the kinetic energy and mobility of the dyeing molecules (Wekoye *et al*., 2020)**.**

4.4.2.4 Effect of agitation speed on the adsorption of MV2b

The effect of the agitation speed on the percentage removal of dyes was studied and the results documented below in figure 4.39 below.

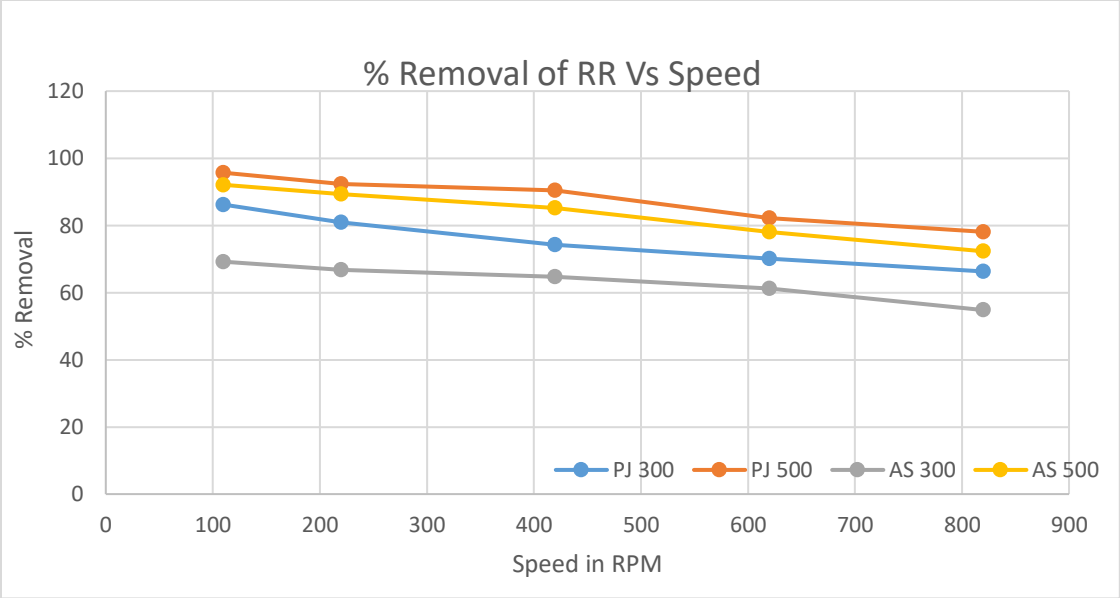

Figure 4.39: A graph of percentage removal vs agitation speed

For all the cases, adsorption decreased with an increase in the agitation speed suggesting that the speed of 120 was the best speed for adsorption of the range that was studied in these experiments.

4.4.2.5 Effect of contact time on the adsorption of methyl violet 2b

The effect of the contact time on the percentage removal of dyes was studied and the results documented below in figure 4.40 below. The results show that the adsorption process is rapid over the first 30 minutes and subsequently slows down till equilibration for the *P.juliflora* biochar and 20 minutes for the Aloe biochar then equally equilibrating. Similar results were also obtained by (Raziq, Kooh, Dahri, *et al*., 2017) whose adsorption process was very rapid at the initial 20 minutes equilibrated after 60 minutes. (Saffari & Shojaei, 2019) also whose process was very rapid for the first 30 minutes and (Nooraee Nia, Rahmani, Kaykhaii, & Sasani, 2017) whose process was very rapid over the first 10 minutes, (Lim *et al*., 2014). This is because initially, there are more available binding sites hence the process is rapid and thus after time the process is slower (Bonetto *et al*., 2015).

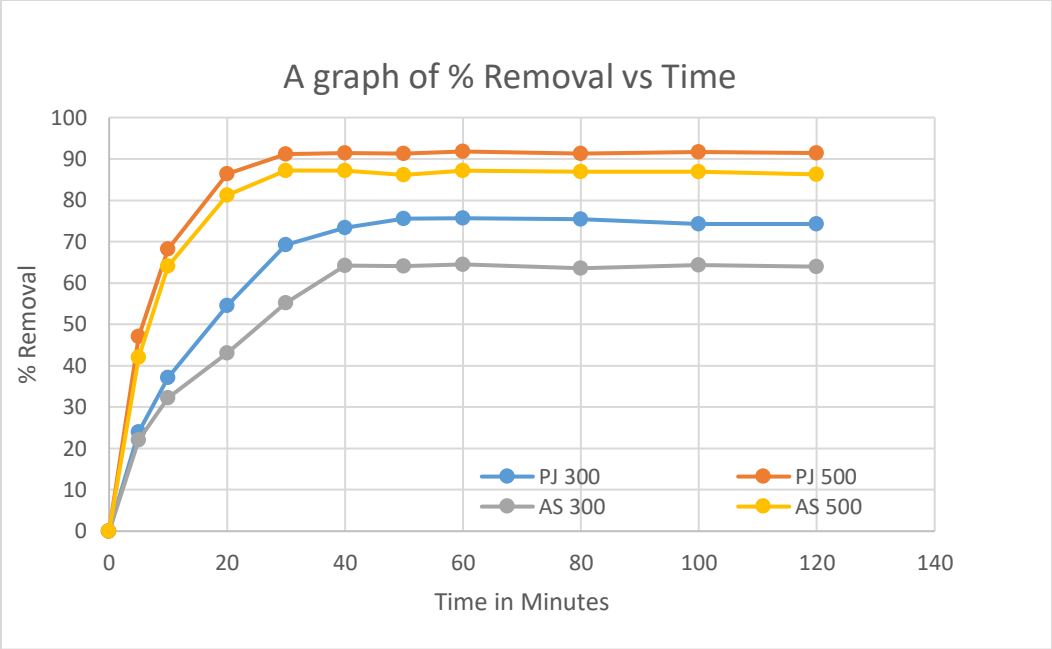

Figure 4.40: A graph of % removal vs Time

4.4.2.6 Kinetics and adsorption Isotherms

A graph of (q_t vs t) was plotted for plotted for all the sets of biochar for the removal of MV2b. For PJ300, PJ500 and AS 500 the best model that fits the adsorption kinetics was Pseudo 1st order > Pseudo second order> elovich model. This is because statistically, it has the highest values of $R_{pearson}$, R^2, R^2_{adj} and the lowest values of χ^2, RMSE and MSE (M. K. Dahri *et al*., 2013). For AS 300, it was Pseudo 1st order > elovich model>Pseudo second order. A detailed table of each of the parameters is in table 4.18 below.

Table 4.18: Kinetic parameters for the removal of Methyl Violet using PJ300, PJ 500, AS 300 and AS 500

	PJ 300	**PJ 500**	**AS 300**	**AS 500**
Pseudo 1st Order				
K_f (h^{-1})	0.07034	0.140555	0.066943	0.133404
q_e	19.05181	22.92011	16.21405	21.77772
$R_{Pearson}$	0.995322	0.999362	0.988578	0.998799
R^2	0.990664	0.99869	0.975425	0.997549
R^2_{adj}	0.987996	0.998315	0.968404	0.996848
χ	0.129911	0.009503	0.369526	0.014881
RMSE	0.428853727	0.128391	0.584053	0.176028
MSE	0.183916	0.016484	0.341118	0.030985
Pseudo 2nd Order				
K_s (g mg^{-1} h)	0.0041	0.009019	0.004623	0.008785
qe	21.84254	24.72591	18.60913	23.58647
$R_{Pearson}$	0.976017	0.9704	0.976306	0.965500
R^2	0.950573	0.940105	0.952715	0.930023
R^2_{adj}	0.936451	0.922992	0.939205	0.910030
χ	0.644630905	0.397600	0.468934	0.506815
RMSE	0.986755805	0.86809	0.810157	0.940475
MSE	0.973687	0.753579601	0.656354	0.884494
Elovich				
α	4.50717	75.54078495	3.66669	46.84694
β	0.230172	0.06326253	0.268538	0.31564
$R_{Pearson}$	0.930274	0.873291	0.941757	0.866996
R^2	0.864738	0.762624	0.886488	0.751657
R^2_{adj}	0.826092	0.694802	0.854056	0.680702
χ	1.833375	1.590234	1.196694	1.787489
RMSE	1.632355	1.728169	1.255246	1.771735
MSE	2.664583	2.986567	1.575643	3.139028

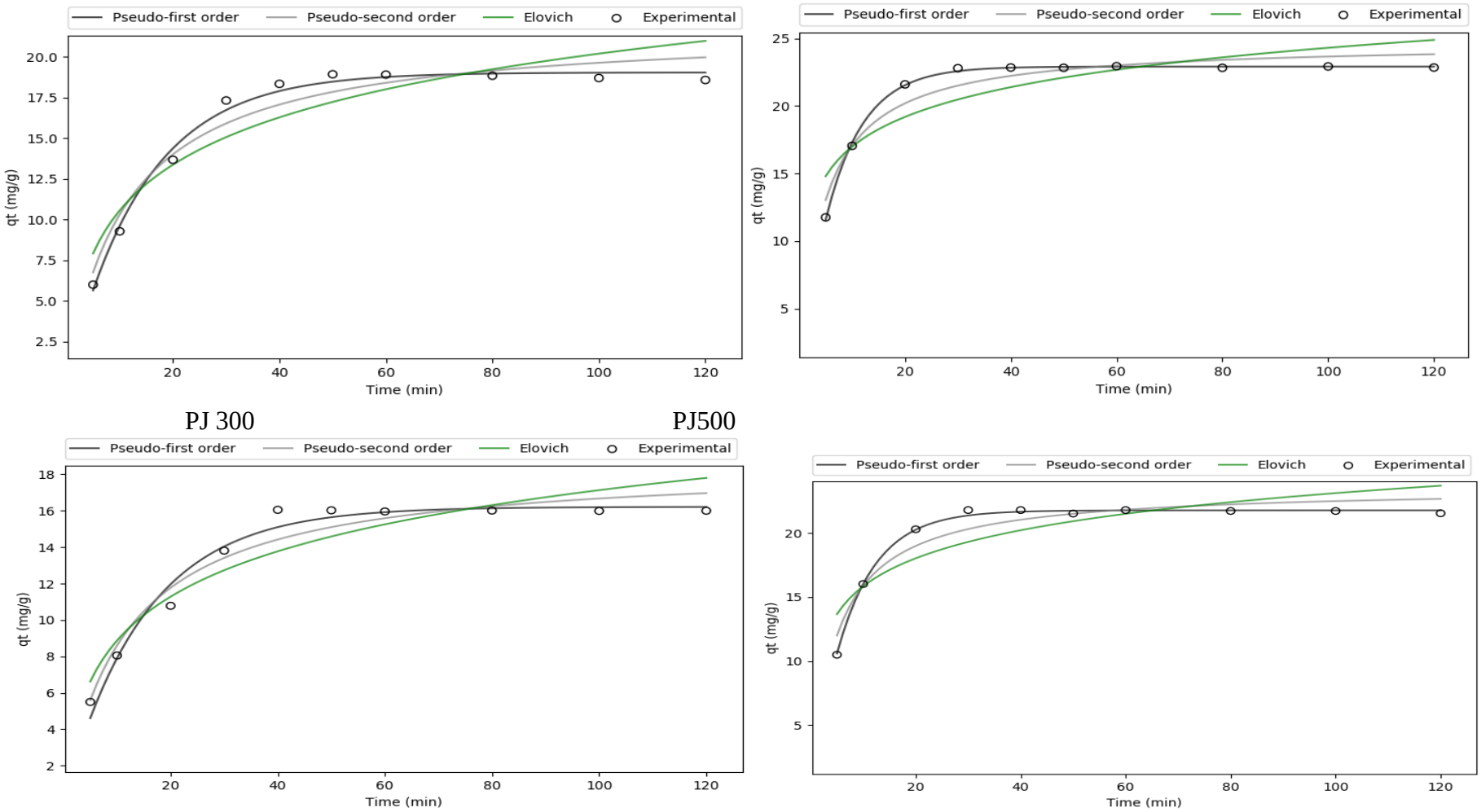

Figure 4.41: Kinetic modelling for the removal of MV2B using biochar derived from *P. juliflora* and *Aloe succotrina* at 300 ℃ and 500 ℃

Table 4.19: Isotherm parameters for the removal of Methyl Violet using PJ300, PJ 500, AS 300 and AS 500

	PJ 300	**PJ 500**	**AS 300**	**AS 500**
Freundlich				
K_f (mg/g)	4.513368	12.08277	3.5381	8.678119
n_f	1.335399	1.208913	1.437645	1.325512
$R_{Pearson}$	0.999216	0.999169	0.99913	0.995224
R^2	0.998432	0.99792	0.998139	0.990462
R^2_{adj}	0.997648	0.99688	0.997208	0.985693
χ	0.050307369	1.4385461	0.2148825	0.459404
RMSE	0.256671608	0.3682180	0.24295761	0.747185
MSE	0.06588	0.1355845	0.059028	0.558285
Jovanovic monolayer				
K_j (mg g^{-1})	0.167719975	0.3015	21.3504	31.97491
q_m	27.26342	47.42443	0.153429	0.32869
$R_{Pearson}$	0.999153	0.999246	0.998649	0.997585
R^2	0.996662	0.996465	0.992973	0.994569
R^2_{adj}	0.994993	0.994697	0.989459	0.991853
χ	0.871772062	4.177561	2.665421	1.636446
RMSE	0.374515994	0.480031	0.472096	0.563826
MSE	0.140262	0.230430	0.222875	0.317899
Langmuir				
q_m	43.96221058	82.53015	32.99466	52.36561
K_L	0.107852306	0.175746	0.104931	0.206024
$R_{Pearson}$	0.999113778	0.999213	0.998585	0.997235
R^2	0.996924607	0.996532	0.993704	0.993934
R^2_{adj}	0.99538691	0.994797	0.990556	0.990902
χ	0.75885513	4.070604	2.348628	1.558394
RMSE	0.359499024	0.475488	0.4468676	0.595853
MSE	0.129239548	0.226089	0.1996906	0.355041

In the analysis of adsorption isotherms, of RR 120 against the prepared biochar, all the three models fitly described the adsorption process with the best for PJ500 being freundlich >Langmuir > jovanovic monolayer. This is because statistically, the best isotherm is the one that has the highest values of R pearson, R^2, R^{2adj} and the lowest values of $\chi 2$, RMSE and MSE (M. K. Dahri *et al*., 2013; Markandeya *et al*., 2015). For PJ 500, PJ300 and AS300 the best isotherms were in the order Langmuir>Jovanovic monolayer>Freundlich while for AS 500 it was jovanovic monolayer>freundlich >Langmuir .

The highest q_{max} amount, for the adsorption of MB2B was 82.43 mg/g making it the most efficient biochar of the four for the removal MB2b. This was compared against commercially activated carbon which had an adsorption capacity of 504.9 mg/g and other adsorbents in literature and the results tabulated in table 4.20 below. Compared to other adsorbents in literature, it can be concluded that for the removal of MV2B, PJ 500 can used as a low cost adsorbent.

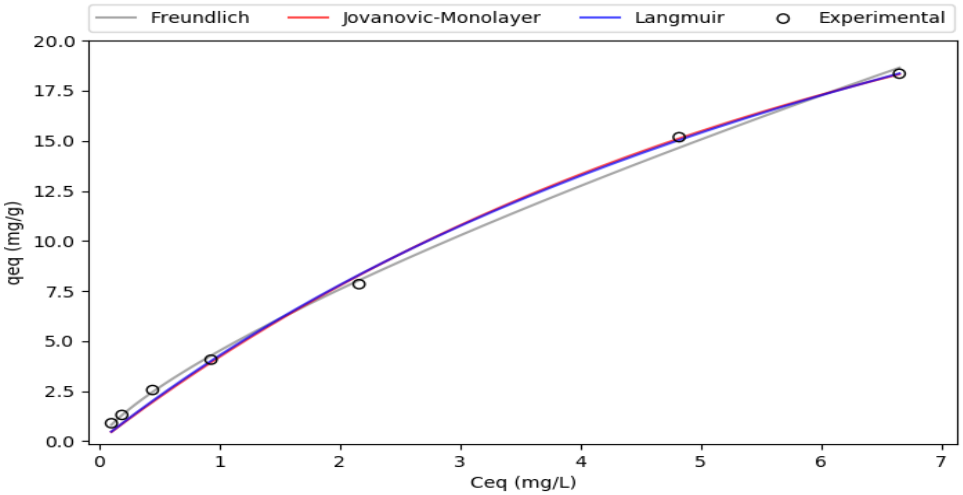

PJ 300

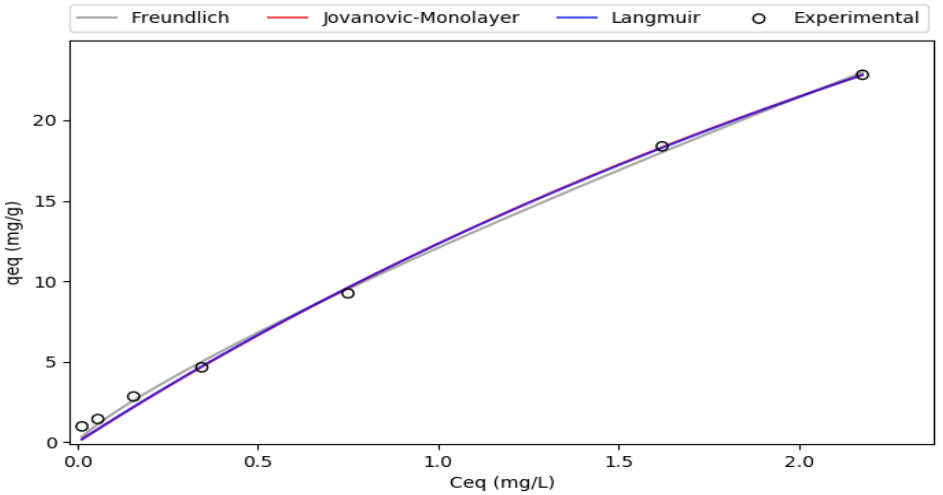

PJ 500

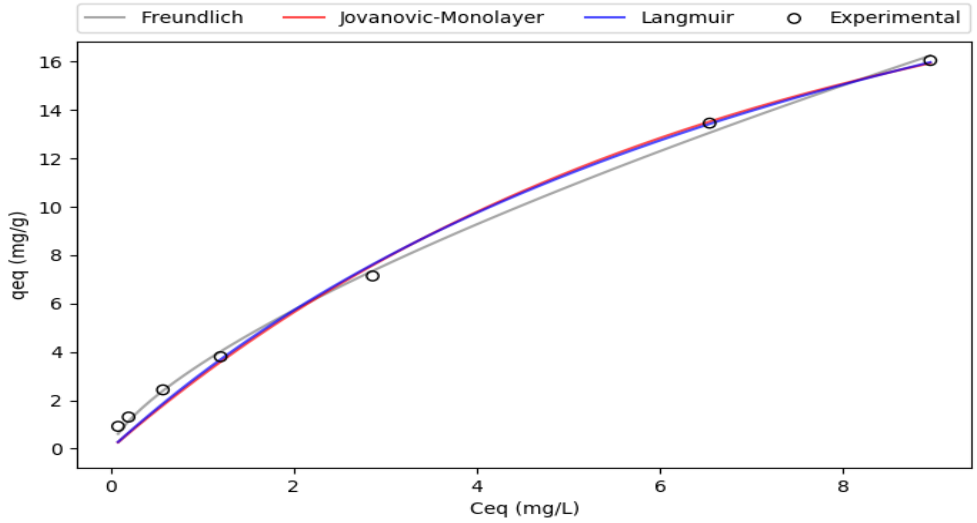

AS 300

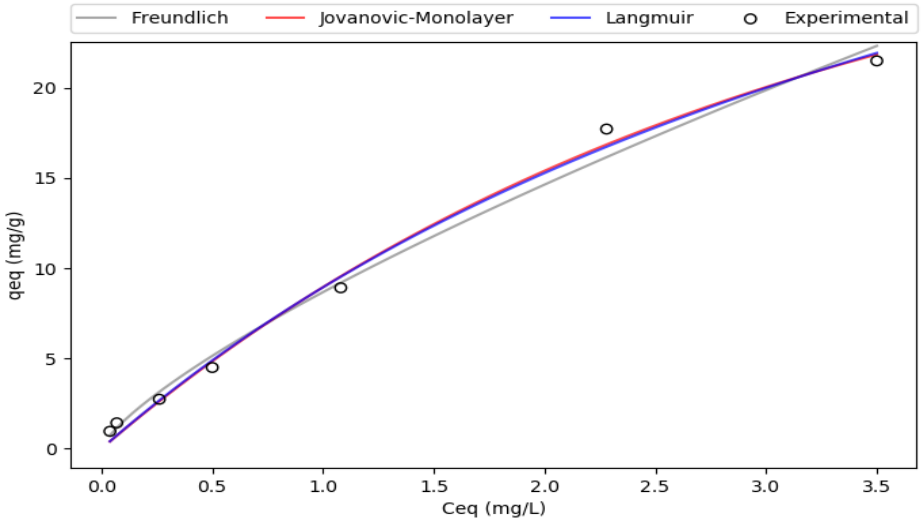

AS 500

Figure 4.42: Isotherm studies for the removal of MV2B from biochar derived from *P.juliflora* and *A. succotrina* at 300 ℃ and 500 ℃

Table 4.20: Comparative Analysis of adsorption capacities of Methyl violet 2b with other biomass

Biomass material	Q_o (mg/g)	Reference
Casuarina equisetifolia	164.99	(M. K. Dahri *et al*., 2013)
Casuarina equisetifolia	63.12	(M. K. Dahri, Raziq, Kooh, & Lim, 2017)
Waste Paper	97.63	(Fahad *et al*., 2018)
Artocarpus heterophyllus	126.7	(M. Dahri, Kooh, & Lim, 2016)
Soya beans waste	180.7	(Kooh, Dahri, Lim, Lim, & Malik, 2016)
Azolla pinnata	323.4	(Raziq *et al*., 2015)
Lemna minor-Duckweed	332.5	(Lim *et al*., 2014)
Ipomoea aquatica	267.9	(Ling *et al*., 2020)
Palm kernel activated carbon	151.22	(Saffari & Shojaei, 2019)
Artocarpus odoratissimus	263.7	(Raziq, Kooh, & Lim, 2017)
Nepenthes rafflesian	288.7	(Raziq, Kooh, Dahri, *et al*., 2017)
Banana peel	37.41	(Abbas, Kamar, & Hossien, 2018)
Activated carbon (Control)	504.9	This study
Prosopis juliflora @300℃	43.962	This study
Prosopis juliflora @500℃	82.530	This study
Aloe succotrina @300 ℃	32.995	This study
Aloe succotrina @500℃	52.366	This study

4.4.2.7 SEM Images before and after adsorption

SEM images for AS 300 before and after adsorption are captured as images Q, R respectively and equally for AS 500 as S and T.

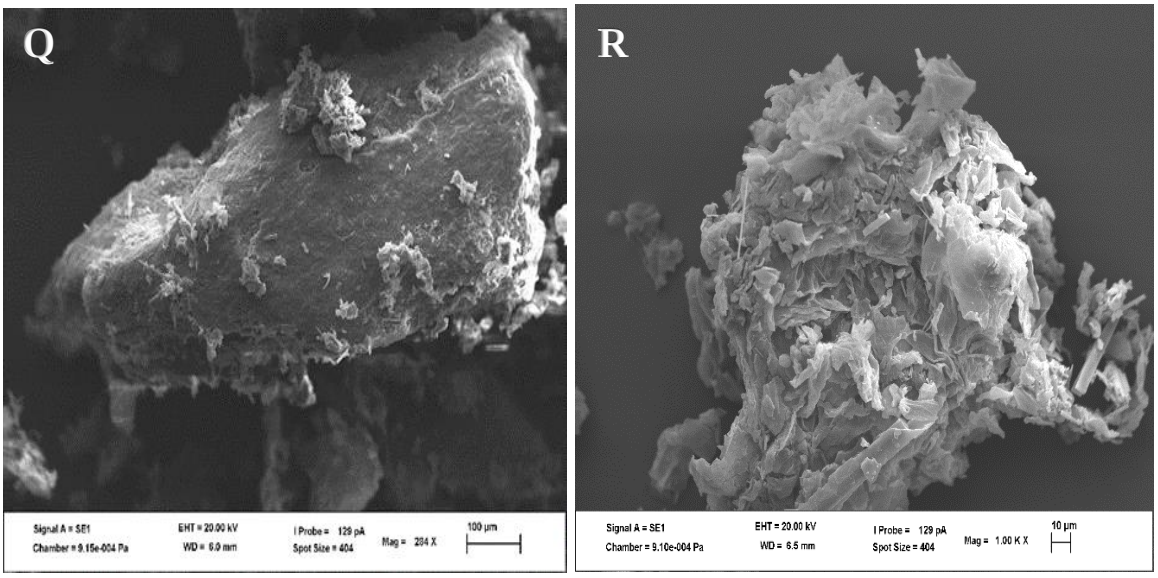

Figure 4.43: SEM Images for *Aloe Succotrina* at 300 before and after Adsorption with MB-2b

The images Q and R, show a difference in surface before and after adsorption. With the images before adsorption (Q) showing a flat surface with little islands of fibrous matter whereas image R, shows that this surface, after adsorption had additional particles loaded on this surface,

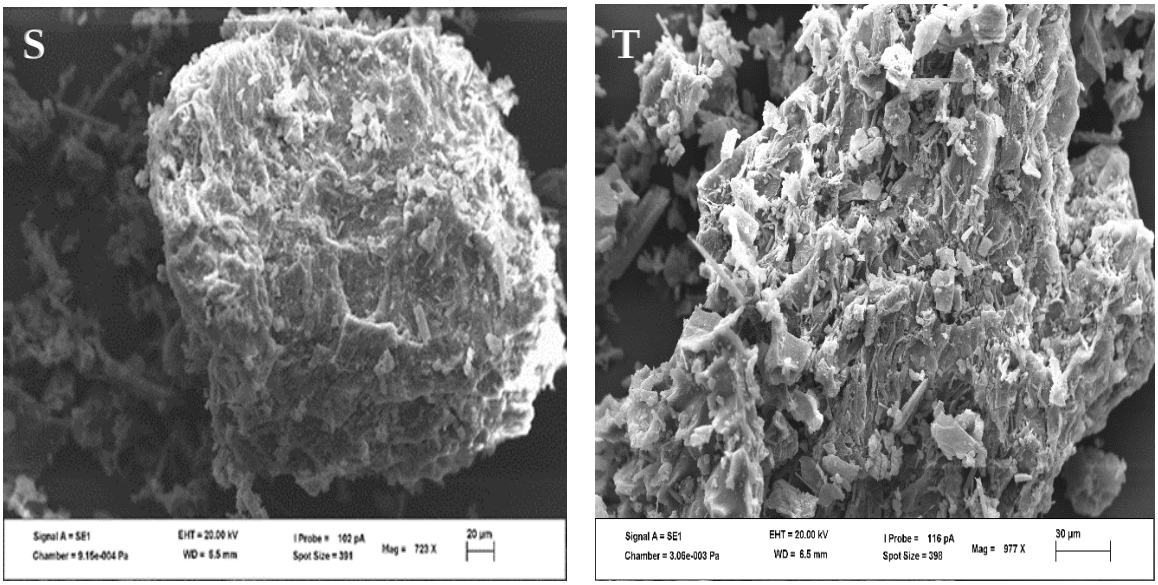

Figure 4.44: SEM Images for *Aloe Succotrina* at 300 before and after Adsorption with MB-2b

Image S, which is for the image before adsorption, has a mesoporous structure before adsorption. After adsorption, the image T, shows that the mesoporous structures serve as sites for the adsorption of the dye. As a result, the dyes, adsorb on the surface an embedd themselves into the surface this serving as proof of adsorption.

4.4.2.7 SEM Images for PJ 300 and PJ 500 before and after Adsorption

SEM images for PJ 300 before and after adsorption are captured as images M and N in figure 4.45 respectively and images O and P for PJ 500 before and after adsorption in figure 4.46 below.

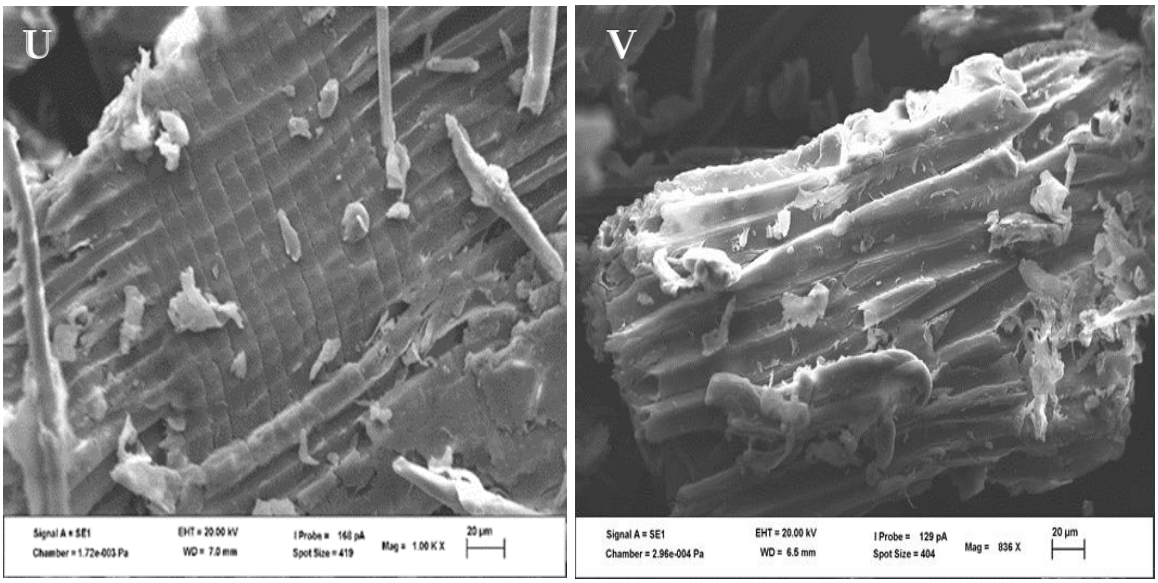

Figure 4.45: SEM Images for *Prosopis juliflora* at 500 before and after adsorption

SEM images for figure U and Figure V, before and after adsorption, show a difference in surface structure before and after adsorption. The previous fibrous nature of the biochar in M, is covered by particles that are embedded on to the fibres showing that adsorption has taken place (S. Ahmad *et al*., 2018).

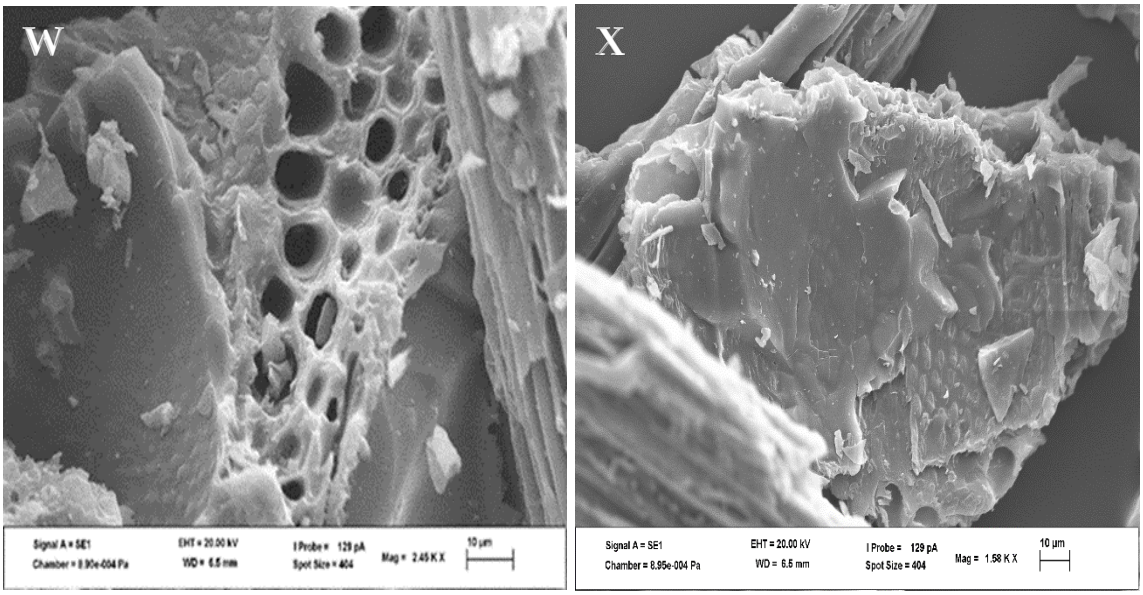

Figure 4.46: SEM Images for *Prosopis juliflora* at 500 before and after adsorption

The SEM images before and after adsorption showed that adsorption took place, with the fibrous networks and pores that were present in the biochar, serving as cavities and sites for embedding of dye onto it. (S. Ahmad *et al*., 2018). From the images, it can be visualized that the grooves and fibrous networks, provided for a better surface for adsorption than the flat surfaces, with the mesoporous pores equally providing for a larger surface area for adsorption.

CHAPTER FIVE

CONCLUSION AND RECOMMENDATIONS

5.1 CONCLUSION

The present study, shows that it is possible to produce natural dyes from acetonic extracts of the heartwood of *Prosopis juliflora* with reliable fastness with respect to colour, light and wash fastness. The use of mordants in the dyeing process first produced shades that varied from jungle green to brown and khaki depending on the mordant used and the mordanting technique. Also, the addition of mordants improved the fastness properties of the dyes.

Extracts of the *Aloe succotrina* leaves, showed reliable light and colourfastness with poor wash fastness with the addition of mordants also changing the colour depending on the mordant and mordanting type but failing to improve the wash fastness significantly. GC-MS evaluation of the plant extracts yielded significant dyeing compounds for each of the plants such as orcinol which has been identified previously in purple-coloured lichens (*Roccella tinctoria*) and catechol which is a benzadiol that occurs naturally in plants and can result from the pyrolysis of catechin, a known flavonoid responsible for yellow-brownish dyes.

Biochar derived from *Prosopis juliflora* and *Aloe succotrina* proved to be potential low-cost adsorbents for the removal of both RR120 and MV2b. For RR120, adsorption relied heavily on the pH of the solution, with lower pH increasing the rate and amount of adsorption with the optimum conditions being pH 2. Adsorption process favoured pseudo first order and Freundlich models signifying that the adsorption was heterogenous.

For MV2b, the adsorption process was best described by pseudo first order and Langmuir with the adsorption process being heavily on pH of above 7.

5.2 RECOMMENDATIONS

i) Assessment of the dyeing properties of the dyes using varying natural mordants and a combination of both natural and synthetic mordants

ii) Improving of the dyeing properties of the *Aloe succotrina* by functionalization of the dye.

iii) Testing of antimicrobial potentials of the finished fabrics against common microbes.

iv) Improving the remediation properties of both biochar's by functionalization, either by alkaline or acid treatment.

REFERENCE

Abbas, S. H., Kamar, F. H., & Hossien, Y. K. (2018). Adsorption Of Methyl Violet 2b Dye From Aqueous Solutions Onto Waste Of Banana Peel Using Fixed-Bed. *International Journal of Civil Engineering and Technology*, *9*(9), 2094–2109.

Abd Mutali, M., Rahman, M.A., Othman, M.H.D., Ismail, A.F., & Jaafar, J. (2017). Scanning Electron Microscopy (SEM) and Energy-Dispersive X-Ray (EDX) Spectroscopy. *Membrane Characterization* 9, 161-179. https://doi.org/10.1016 /B978- 0-444-63776-5.00009-7.

Abdelwahab, O., Fouad, Y.O., Amin, N.K., Mandor, H. (2015).Kinetic and Thermodynamic aspects of cadmium adsorption onto raw and activated guava (Psidium guajava) leaves *Environmental Progress and Sustainable Energy* 34, 351-358. https://doi.org/10.1002/ ep.11991.

Abid, M.F., Zablouk, M.A., Abid-Alameer, A.M. (2012). Experimental study of dye removal from industrial wastewater by membrane technologies of reverse osmosis and nano filtration. *J Environ Health Sci Engineer* 9, 17 https://doi.org/10.1186/ 1735-2746-9-17

Abuamer, K. M., Maihub, A. A., & El-ajaily, M. M. (2014). The Role of Aromatic Schiff Bases in the Dyes Techniques. *International Journal of Organic Chemistry*, *4*(March), 7–15.

Abubacker, M. N., & Deepalakshmi, T. (2013). In vitro Antifungal Potentials of Bioactive Compound Methyl Ester of Hexadecanoic Acid Isolated from Annona muricata Linn . (Annonaceae) Leaves. *Biosciences Biotechnology Research Asia*, *10*(December), 879–884.

Adib, M., Razi, M., Nur, M., & Mohd, A. (2017). Factor Affecting Textile Dye Removal Using Adsorbent From Activated Carbon : A Review. *ISCEE*, *06015*, 1–17.

Affat, S.S. (2021) Classifications, Advantages, Disadvantages, Toxicity Effects of Natural and Synthetic Dyes: A review. *University of Thi-Qar Journal of Science*, 8 (1), 130-135.

Ahmad, M., Megat, K., Zubaidah, S., Jamaludin, M., & Khalid, K. (2018). Methylene Blue Adsorption on Aloe vera Rind Powder : Kinetics , Isotherm and Mechanisms. *Nature Environment and Pollution Technology*, *17*(4), 1055–1064.

Ahmad, S., Wong, Y. C., & Veloo, K. V. (2018). Sugarcane bagasse powder as biosorbent for reactive red 120 removals from aqueous solution. *IOP Conference Series: Earth and Environmental Science*, *140*(1).https://doi.org/10.1088/1755-1315/140/1/012027.

Ahmad, V, Basha A, Haque W (1978) New alkaloids from Prosopis juliflora DC. Z Naturforschung 33:347–348. https://doi.org/10.1515/znb-1978-0322.

Albroomi, H. I., Elsayed, M. A., Baraka, A., Kazem, M., & Forces, O. A. (2015). Factors Affecting The Removal Of A Basic And An Azo Dye From Artificial Solutions By Adsorption. *Journal of the Turkish Chemical Society*, *2*(1), 17–33.

Al-Ghouti, M.A., Al-Absi, R.S. (2020) Mechanistic understanding of the adsorption and thermodynamic aspects of cationic methylene blue dye onto cellulosic olive stones biomass from wastewater. Sci Rep 10, 15928. https://doi.org/10.1038/s41598-020-72996-3.

Al-Ghouti, M.A., Da'ana, D.A. (2020) Guidelines for the use and interpretation of adsorption isotherm models: A review. *Journal of Hazardous Materials* 393, 1223 83. https://doi. org / 10.1016/j.jhazmat.2020.122383.

Ali, N. F., & El-Mohamedy, R. S. R. (2011). Eco-friendly and protective natural dye from red prickly pear (Opuntia Lasiacantha Pfeiffer) plant. *Journal of Saudi Chemical Society*, *15*(3), 257–261. https://doi.org/10.1016/j.jscs.2010.10.001.

Ali, S., Hussain, T., & Nawaz, R. (2009). Optimization of alkaline extraction of natural dye from Henna leaves and its dyeing on cotton by exhaust method. *Journal of Cleaner Production*, *17*(1), 61–66. https://doi.org/10.1016/j.jclepro.2008.03.002.

Aljeboree, A. M., Alshirifi, A. N., & Alkaim, A. F. (2017). Kinetics and equilibrium study for the adsorption of textile dyes on coconut shell activated carbon. *Arabian Journal of Chemistry*, *10*, S3381–S3393. https://doi.org/10.1016/j.arabjc.2014.01.020.

Almeida, J. de D., Bennemann, G. D., Bianchi, C. C., & Freitas, G. B. L. de. (2014). Colorful, Cute, Attractive and Carcinogenic: The Dangers of Dyes. *Cancer Research Journal*, *2*(6), 42. https://doi.org/10.11648/j.crj.s.2014020601.15

Almeida, M., Erthal, R., Padua, E., Silveira, L., Am, L. (2008). Response surface Methodology (RSM) as a tool for optimization in analytical chemistry. *Talanta*, *76*, 965–977. https://doi.org/10.1016/j.talanta.2008.05.019

Al-rubaye, A. F., Hameed, I. H.,Kadhim, M. J.(2017). A Review:Uses of Gas Chromatography -Mass Spectrometry (GC-MS) Technique for Analysis of Bioactive Natural Compounds of Some Plants A Review : *International Journal of Toxicological and Pharmacological Research*, (March). https://doi.org/10.25258/ijtpr.v9i01.9042

Altemimi, A., Lakhssassi, N., Baharlouei, A., Watson, D. G., & Lightfoot, D. A. (2017). Phytochemicals: Extraction, Isolation, and Identification of Bioactive Compounds from Plant Extracts. *Plants*, *6*, 42. https://dx.doi.org/10.3390%2Fplants6040042

Añibarro-Ortega, M., Pinela, J., Barros, L., Ćirić, A., Silva, S. P., Coelho, E., … Ferreira, I. C. F. R. (2019). Compositional features and bioactive properties of aloe vera leaf (Fillet, mucilage, and rind) and flower. *Antioxidants*, *8*(10), 1–21. https://doi.org/10.3390/ antiox8100444

Annapoorani, G., & Divya, S. (2015). Extraction of Eco-Friendly Natural Dyes Obtained From Aloe Vera, Green Chirayta and Indian Whitehead Leaves and Their Application on Cotton Fabric. *ISSN International Journal of Interdisciplinary Research and Innovations ISSN*, *3*(3), 2348–1218.

Ansari, V. A., Sirbaiya, A. K., Kumar, R., & Usmani, A. (2016). An insight of pharmacognostic and phytopharmacology study of Adenanthera pavonina. *Journal of Chemical and Pharmaceutical Research*, *8*(2), 586–596.

Anyalogbu, E. A., Ezeji, E. U., & Nwalozie, C. J. (2013). Phytochemical Screening and Anti- malaria / Typhoid Fever Activities of Alstonia boonei (De Wild) Stem Bark Powder. *Medicinal and Aromatic Plant Science and Biotechnology*, (1989), 1–3.

Aqeel, A., Khursheed, A.K., Viqaruddin, A., & Sabiha, Q. (1989). Antimicrobial activity of Ardila-Leal, L.D.; Poutou-Piñales, R.A.; Pedroza-Rodríguez, A.M.; Quevedo-Hidalgo, B.E. A Brief History of Colour, the Environmental Impact of Synthetic Dyes and Removal by Using Laccases. *Molecules* 2021, 26, 3813. https://doi.org/10. 3390/molecules26133813

Aruna, Bagotia, N., Sharma, A.K., & Kumar, S. (2021). A review on modified sugarcane bagasse biosorbent for removal of dyes. *Chemosphere* 268, 129309**.** https://doi.org/10.1016/j.chemosphere.2020.129309

Auta, M. (2020). Batch Adsorption Of Reactive Red 120 From Waste Waters Using Activated Carbon. *International Journal of Advanced Engineering Technology*, *III* (III Sept), 24– 28.

Ayawei, N., Ebelegi, A. N., & Wankasi, D. (2017). Modelling and Interpretation of Adsorption Isotherms. *Journal of Chemistry*. https://doi.org/10.1155/2017/ 3039817

Azahar, F., Mitra S., A. Yabushita, A. Harata, B. Saha, K. Thu (2018) Improved model for the isosteric heat of adsorption and impacts on the performance of heat pump cycles. *Appl. Therm. Eng*., 143, 688-700.

Azam MM, Tewari JC, Singh Y, Roy MM (2011) *Prosopis juliflora*, a rich source of antioxidant product. Central Arid Zone Research Institute, Jodhpur

Banerjee, S., & Chattopadhyay, M.C. (2017) Adsorption characteristics for the removal of a toxic dye, tartrazine from aqueous solutions by a low cost agricultural by-product. *Arabian Journal of Chemistry* 10, S1629-S1638. https://doi.org/10.1016/j.arabjc.2013. 06.005

Bani, P., Grossi, P., Lucini, L., Pellizzoni, M., & Minuti, A. (2016). Administration of Aloe arborescens homogenate to cattle : interaction with rumen fermentation and gut absorption of aloin. *Italian Journal of Animal Science*. https://doi.org/10.1080/1828051X .2016.1157007

Bartošová, A., Blinová, L., Sirotiak, M., & Michalíková, A. (2017). Usage of Ftir-Atr As Non- Destructive Analysis of Selected Toxic Dyes. *RPUT*, *25*(40), 103–111.

Bazrafshan, E., Mostafapour, F.K., Hosseini, A.R., Khorshid, & Mahvi, A.H. (2013) Decolorisation of Reactive Red 120 Dye by Using Single-Walled Carbon Nanotubes in Aqueous Solutions. *Journal of Chemistry*, 2013, 938374, 8 pages. https://doi.org/10.1155/2013/938374.

Beaver, J. (2018) The physical basis of color. In: The Physics and Art of Photography, Morgan & Claypool Publishers, vol. 2, pp 8-23.

Benkhaya S., Achiou B., Ouammou M., Bennazha J., Younssi S.A., M'rabet S., El Harfi A. (2019).Preparation of low-cost composite membrane made of polysulfone /polyetherimide ultrafiltration layer and ceramic pozzolan support for dyes removal. *Materials Today Communication 19*, 212–219. https://doi.org/10.1016/j.mtcomm. 2019.02.002.

Benkhaya, S., El Harfi, S, & El Harfi, A. (2017) Classifications, properties and applications of textile dyes: A review. *Appl. J. Envir. Eng. Sci.* 3 (3), 311-320.

Benkhaya, S., M'rabet, S., & El Harfi, A. (2020). Classifications, properties, recent synthesis and applications of azo dyes. *Heliyon*, 6(1), e03271. https://doi.org/10.1016/ j.heliyon.2020.e03271.

Berradi, M., Hsissou, R., Khudhair, M., Assouag, M., Cherkaoui, O., El Bachiri, A., & El Harfi, A. (2019). Textile finishing dyes and their impact on aquatic environs. *Heliyon*, 5(11),e 02711. https://doi.org/10.1016/j.heliyon.2019.e02711

Bhatia, D., Sharma, D.R., Singh, J. & Kanwar, R.S. (2017) Biological methods for textile

Dye removal from wastewater: A review, Critical Reviews in *Environmental Science and Technology*, 47:19, 1836-1876. DOI: 10.1080/10643389.2017.1393263

Biesaga, M. (2011). Influence of extraction methods on stability of flavonoids. *Journal of Chromatography A*, *1218*(18), 2505–2512. https://doi.org/10.1016/j.chroma.2011.02. 059

Bjorå, C. S., Wabuyele, E., Grace, O. M., Nordal, I., & Newton, L. E. (2015). The uses of Kenyan aloes: An analysis of implications for names, distribution and conservation. *Journal of Ethnobiology and Ethnomedicine*, *11*(1). https://doi.org/10.1186/s13002-015-0060-0

Bonetto, L.R., Ferrarini, F., de Marco, C., Crespo, J.S., Guégan, R., & Giovanel, M. (2015) Removal of methyl violet 2B dye from aqueous solution using a magnetic composite as an adsorbent. *Journal of Water Process Engineering* 6, 11-20. https://doi.org/10.1016/j.jwpe.2015.02.006.

Botes, L., Westhuizen, F. H. Van Der, & Loots, D. T. (2008). Phytochemical Contents and Antioxidant Capacities of Two Aloe greatheadii var. davyana Extracts. *Molecules*, 2169–2180. https://doi.org/10.3390/molecules13092169

Bouslimani, A., Sanchez, L. M., Garg, N., & Dorrestein, P. C. (2014). Mass spectrometry of natural products: Current, emerging and future technologies. *Natural Product Reports*, *31*(6), 718–729. https://doi.org/10.1039/c4np00044g

Bunaciu, A. A., Udriştioiu, E. gabriela, & Aboul-enein, H. Y. (2015). X-Ray Diffraction : Instrumentation and Applications. *Critical Reviews in AnalyticalChemistry*.https://doi. org/10.1080/10408347.2014.949616

Burhan, M., Shahzad, M.W, & Ng, K.C. (2018) Energy distribution function based Universal adsorption isotherm model for all types of isotherm. *International Journal of Low-Carbon Technologies* 13(3), 292–297. https://doi.org/10.1093/ijlct/cty031

Busi, S., Chatterjee, R., Rajkumari, J., & Hnamte, S. (2016). Ecofriendly biosorption of dyes and metals by bacterial biomass of Aeromonas hydrophila RC1. *Journal of environmental biology*, 37(2), 267–274.

Butnariu, M. (2016). Methods of Analysis (Extraction, Separation, Identification and Quantification) of Carotenoids from Natural Products. *Journal of Ecosystem & Ecography*, *6*(2). https://doi.org/10.4172/2157-7625.1000193.

Calà, E., Benzi, M., Gosetti, F., Zanin, A., Gulmini, M., Idone, A., … Aceto, M. (2019).

Towards the identification of the lichen species in historical orchil dyes by HPLC-MS / MS. *Microchemical Journal*, *150*(June), 104140. https://doi.org/10.1016/zj.microc. 2019.104140.

Carmen, Z., & Daniela, S. (2012). Textile Organic Dyes – Characteristics , Polluting Effects and Separation / Elimination Procedures from Industrial Effluents- A Critical Overview. In *InTech*,.

Casselman, K. L. (1994). Lichen Dyes : Preparation and Dyeing. *Maine Naturalist*, *2*(2), 105–110.

Çelekli, A., Al-nuaimi, A. I., & Bozkurt, H. (2019). Adsorption kinetic and isotherms of Reactive Red 120 on Moringa oleifera seed as an eco-friendly process. *Journal of Molecular Structure*, *1195*, 168–178. https://doi.org/10.1016/j.molstruc.2019.05.106.

Çelekli, A., Çelekli, F., Çiçek, E., & Bozkurt, H. (2014). Predictive modeling of sorption and desorption of a reactive azo dye by pumpkin husk. *Environmenmental Science Pollution Research*, 5086–5097. https://doi.org/10.1007/s11356-013-2452-9.

Çelekli, A., Ilgün, G., & Bozkurt, H. (2012). Sorption equilibrium, kinetic, thermodynamic, and desorption studies of Reactive Red 120 on Chara contraria. *Chemical Engineering Journal*, *191*, 228–235. https://doi.org/10.1016/j.cej.2012.03.007.

Celekli, A., Yavuzatmaca, M., & Bozkurt, H. (2010). Modeling the removal of reactive red 120 on pistachio husk. *Clean - Soil, Air, Water*, *38*(2), 173–180. https://doi.org/10.1002/clen.200900197.

Chakraborty, J.N. (2014). Colouring materials. Fundamentals and Practices in Colouration of Textiles, pp. 12-21. https://doi.org/10.1016/B978-93-80308-46-3.50002-9.

Chali Yadeta, N. (2019). Phytochemical Investigation and Antioxidant Activity of Root Extract of Aloe gilbertii Reynoldsfrom Konso, Southern Ethiopia. *American Journal of Applied Chemistry*, *7*(5), 130. https://doi.org/10.11648/j.ajac.20190705.11.

Chao, Y., Ho, T., Cheng, Z., Kao, L., & Tsai, P. (2017). A Study on Combining Natural Dyes and Environmentally-friendly Mordant to Improve Color Strength and Ultraviolet Protection of Textiles. *Fibers and Polymers*, *18*(8), 1523–1524. https://doi.org/10.1007 /s12221-017-6964-7.

Chavan, R. B. (2011). Environmentally friendly dyes. In *Handbook of Textile and Industrial Dyeing: Principles, Processes and Types of Dyes* (Vol. 1). Woodhead

Publishing Limited. https://doi.org/10.1533/9780857093974.2.515.

Chemat, F., Abert Vian, M., Ravi, H. K., Khadhraoui, B., Hilali, S., Perino, S., & Tixier, A. F. (2019). Review of Alternative Solvents for Green Extraction of Food and Natural Products: Panorama, Principles, Applications and Prospects. *Molecules*, *24*, 3007. https://doi.org/10.3390/molecules24163007.

Chengaiah, B., Rao, K. M., Kumar, K. M., Alagusundaram, M., & Chetty, C. M. (2010). Medicinal importance of natural dyes-a review. *International Journal of PharmTech Research*, *2*(1), 144–154.

Chiocchio, I., Mandrone, M., Tomasi, P., Marincich, L., & Poli, F. (2021). Plant Secondary Metabolites: An Opportunity for Circular Economy. *Molecules* (Basel, Switzerland), 26(2), 495. https://doi.org/10.3390/molecules26020495.

Chung, C., Lee, M., & Choe, E. K. (2004). Characterization of cotton fabric scouring by FTIR ATR spectroscopy. *Carbohydrate Polymers*, *58*(4), 417–420. https://doi.org/10.1016/j.carbpol.2004.08.005.

Cuixia, Y., Yingming, X., Lin, W., Xuefeng, L., Yuebing, S., & Hongtao, J. (2020). Effect of different pyrolysis temperatures on physico-chemical characteristics and lead(II) removal of biochar derived from chicken manure. *RSC Advances*, *10*(7), 3667–3674. https://doi.org/10.1039/c9ra08199b

Dahri, M. K., Raziq, M., Kooh, R., & Lim, L. B. L. (2013). Removal of Methyl Violet 2B from Aqueous Solution Using Casuarina equisetifolia Needle. *Environmental Chemistry:Hindawi Publishing Corporation*, 8.

Dahri, M. K., Raziq, M., Kooh, R., & Lim, L. B. L. (2017). Water remediation using *Casuarina equisetifolia* cone as adsorbent for the removal of methyl violet 2B dye using batch experiment method. *Journal of Environment and Biotechnology*, *6*(1), 34–42.

Dahri, M., Kooh, M., & Lim, L. (2016). Adsorption of Toxic Methyl Violet 2B Dye from Aqueous Solution Using *Artocarpus heterophyllus* (Jackfruit) Seed as an Adsorbent. *American Chemical Science Journal*, *15*(2), 1–12. https: //doi.org/10.9734/acsj/ 2016/27127

Dan, T. V. (2001). Phytoremediation of metal contaminated soils: Metal tolerance and metal accumulation in *Pelargonium sp.* University of Guelph.

Das, P., Banerjee, P., & Mondal, S. (2014). Mathematical modelling and optimization of synthetic textile dye removal using soil composites as highly competent liner material. *Environmental Science Pollution Research*.

https://doi.org/10.1007/s11356-014-3419-1

Dassanayake, R.S.; Acharya, S.; Abidi, N. Recent Advances in Biopolymer-Based Dye Removal Technologies. Molecules 2021, 26, 4697. https://doi.org/10.3390/molecules 26154697

Dassanayake, R.S.; Acharya, S.; Abidi, N. Recent Advances in Biopolymer-Based Dye Removal Technologies. Molecules 2021, 26, 4697. https://doi.org/10.3390/ molecules 26154697

De Brito Damasceno G.A., Souto A.L., da Silva I.B., Roque A.., Ferrari M., Giordani R.B. (2018) *Prosopis juliflora*: Phytochemical, Toxicological, and Allelochemicals. In: Merillon JM., Ramawat K. (eds) Co-Evolution of Secondary Metabolites. *Series in Phytochemistry*. Springer, Cham. https://doi.org/10.1007/978-3-319-76887-8_151.

De Farias Silva et al. (2020) Basic-dye adsorption in albedo residue: Effect of pH, contact time, temperature, dye concentration, biomass dosage, rotation and ionic strength. *Journal of King Saud University - Engineering Sciences*, 32(6), 351-359. https://doi.org/10. 1016/j.jksues.2019.04.006.

De Keijzer, M, van Bommel, M.R., Hofmann-de Keijzer, R., Knaller, R., & Oberhumer, E. (2012) Indigo carmine: Understanding a problematic blue dye. *Studies in Conservation* 57, S87-S95. https://doi.org/10.1179/2047058412Y.0000000058.

Deena, T., Jebaseelan, E. J. S., & Roopan, S. M. (2019). Green Synthesis, Characterization and Applications of Nanoparticles. *Micro and Nano Technologies*, *12*, 303-319.

Dehghani, M. H., Dehghan, A., & Najafpoor, A. (2017). Removing Reactive Red 120 and 196 using chitosan/zeolite composite from aqueous solutions: Kinetics, isotherms, and process optimization. *Journal of Industrial and Engineering Chemistry*, *51*, 185–195. kitti

Dev, V. R. G., Venugopal, J. R., Kumar, T. S., Miranda, L. R., & Ramakrishna, S. (2010). Agave sisalana, a biosorbent for the adsorption of Reactive Red 120 from aqueous solution. *Journal of the Textile Institute*, *101*(5), 414–422. https://doi.org/10.1080/00405000802445289

Dharajiya,D., Pagi, N., Jasani, H., & Patel, P.(2017).Antimicrobial Activity and Phytochemical Screening of Aloe vera *(Aloe barbadensis Miller)*. *6*(3), 2152–2162.

Ding, Y., & Freeman, H. S. (2017). Mordant dye application on cotton: optimisation and combination with natural dyes. *Coloration Technology*, *133*(5), 369–375. https://doi.org/10.1111/cote.12288.

Ding, Z., Wan, Y., Hu, X., Wang, S., Zimmerman, A. R., & Gao, B. (2016). Sorption of Lead and methylene blue onto hickory biochars from different pyrolysis temperatures: Importance of physicochemical properties. *Journal of Industrial and Engineering Chemistry*. https://doi.org/10.1016/j.jiec.2016.03.035.

Dos Santos Silva, L.; De Oliveira Carvalho, J.; De Sousa Bezerra, R.D.; Da Silva, M.S.; Ferreira, F.J.L.; Osajima, J.A.; Da Silva Filho, E.C. (2018). Potential of Cellulose Functionalized with Carboxylic Acid as Biosorbent for the Removal of Cationic Dyes in Aqueous Solution. *Molecules* , 23, 743. https://doi.org/10.3390/molecules23040743

Dutta et al. (2021) Recent advances on the removal of dyes from wastewater using various adsorbents: a critical review. *Mater. Adv.*, 2021, 2, 4497-4531. https://doi.org/10.1039/D1MA00354B

Dwivedi, P., & Tomar, S. T. (2018). Bioremediation Of Textile Effluent For Degradation And Decolourization Of Synthetic Dyes : A Review. *International Journal of Current Research in Life Sciences* Vol. 07, No. 04, Pp.1948-1951, April, 2018, *07*(04), 1948–195.1

Elango, G., Rathika, G., & Elango, S. (2017). Physico-Chemical Parameters of Textile Dyeing Effluent and Its Impacts with Casestudy. *International Journal of Research in Chemistry and Environment*, *7*(1), 17–24.

Elkady, M. F., Ibrahim, A. M., & El-latif, M. M. A. (2011). Assessment of the adsorption kinetics , equilibrium and thermodynamic for the potential removal of reactive red dye using eggshell biocomposite beads. *Desalinatiom*, *278*(1–3), 412–423. https://doi.org/10.1016/j.desal.2011.05.063.

Elshaarawy R.F., Sayed T.M., Khalifa H.M., El-Sawi E.A. (2017). A mild and convenient protocol for the conversion of toxic acid red 37 into pharmacological (antibiotic and anticancer) nominees: organopalladium architectures. *Compt. Rendus Chem*. 2017;20: 934–941.

Eschen, R., Bekele, K., Mbaabu, P.R., Kilawe, C.J., Eckert, S. (2021) *Prosopis juliflora* management and grassland restoration in Baringo County, Kenya: Opportunities for soil carbon sequestration and local livelihoods. *Journal of Applied Ecology*. 58(6), pp. 1302-1313.

Espinosa-Morales, Reyes, J., Hermosín, B., & Azamar-Barrios, J. A. (2012). Characterization of a Natural Dye by Spectroscopic and Chromatographic Techniques. *Materials Research Society Symposium Proceedings*, *1477*, 61–66. https://doi. org/10.1557/opl.2012

Eugin Amala, V., & Jeyaraj, M. (2014). Determination of antibacterial, Antifungal, Bioactive constituents of triphala by FT-IR and GC-MS analysis. *International Journal of Pharmacy and Pharmaceutical Sciences*, *6*(8), 123–126.

Ezyanie Safie, N., Ahmad Ludin, N., Sukor Su, M., Hisham Hamid, N., Sepeai, S., Adib Ibrahim, M., & Asri Mat Teridi, M. (2015). Preliminary Study Of Natural Pigments Photochemical Properties Of Curcuma Longa L. And Lawsonia Inermis L. As TiO_2 Photoelectrode Sensitizer. *Malaysian Journal of Analytical Sciences*, *19*(6), 1243–1249.

Fahad, B. M., Ali, N. S., & Hameed, T. T. (2018). Using Paper Waste as Adsorbent for Methyl Violet dye removal from waste water. *Journal of Engineering and Sustainable Development*, *2*(01), 1–11.

Fathey, R., & Kamel. (2011). Degradation of Some Textile Dyes using Biological and Physical Treatments. *Bachelor Of Science Microbiology-Chemistry (2003) Faculty of Science Ain-Shams University*, (2003).

Ferreira, E. S. B., Hulme, A. N., Quye, A., & Ferreira, E. (2004). The natural constituents of historical textile dyes. *Chem. Soc. Rev*, 329–336.

Fisch, M. H., Flick, B. H., & Ardrttit, J. (1973). Structure And Antifungal Activity Of Hircinol ,Loroglossol And Orchinol ". *Phytochemistry*, *12*(1963), 437–441.

Flowers, R. M. S., Susanti, D., Awang, N. A., Qaralleh, H., & Ibrahim, H. (2013). Antimicrobial Activity and Chemical Composition of Essential Oil of Malaysian Etlingera elatior (Jack). *Journal of Essential Oil Bearing Plants*, *5026*(16), 294–299. https://doi.org/10.1080/0972060X.2013.793968

Fomenko, E.V., Yumashev, V.V., Kukhtetskiy, S.V., Zhizhaev, A.M., & Anshits, A.G. (2020). *Energy & Fuels* 2020 34 (7), 8848-8856. https://doi.org/10.1021/acs.energyfuels. 0c01345.

Foo, K., & Hameed, B. (2010) Insights into the modeling of adsorption isotherm systems. *Chem. Eng. J*., 156 (1), 2-10.

Ford, L. L. (2017). Chemical Analysis and Elucidation of Anthraquinone and Flavonoid Type Compounds with Applications to Historical Artefacts and Sustainability. *Phd Thesis University of Leeds*, (April).

Fouad, Z., & Lahcen, Z. (2020) Anti diabetic medicinal plants in Morocco: Ethnobotanical survey of the population of Béni mellal. Plant Archives, 20(1), pp. 337-343.

Fouad, Z., Fatiha, E.A., Larbi, E.G., Lahcen, Z. (2019) Ethnobotanical survey of medicinal plants used in the traditional treatment of diabetes and gout in the north of Morocco (Tangier, Tetouan and Chefchaouen cities). *Plant Archives*, 19(2), pp. 2731-2737

Freeman, H. S. (2017). *Mordant dye application on cotton : optimisation and combination with natural Coloration Technology*. https://doi.org/10.1111/ cote.12288

Fujiki, J., Kawakita, T., Teshima, K., & Furuya, E. (2017). A Simple Method for the Determination of Adsorption Kinetic Parameters Using Recycle Fixed-Bed Adsorber. Transport in Porous Media, 120(2), 359–372. doi:10.1007/s11242-017-0925-x

Gao, Y., & Cranston, R. (2008). Recent Advances in Antimicrobial Treatments of Textiles. *Textile Research Journal*, *78*(1), 60–72. https://doi.org/10.1177/0040517507082332

Garg, S. (2018). A Study on Elimination of heavy metals by using various types of Adsorbent with Optimized Cost. *Interntional Journal of Scientific Research and Review*, *7*(4), 89–94.

Giannakoudakis, D. A., Hosseini-bandegharaei, A., Tsafrakidou, P., Triantafyllidis, K. S., Kornaros, M., & Anastopoulos, I. (2018). Aloe vera waste biomass-based adsorbents for the removal of aquatic pollutants : A review. *Journal of Environmental Management*, *227*(July), 354–364. https://doi.org/10.1016/j.jenvman.2018.08.064

Gokhale, S. B., Tatiya, A. U., Bakliwal, S. R., & Fursule, R. A. (2004). Natural dye yielding plants in India. *Natural Product Radiance*, *3*(August), 228–234. Retrieved from http://indianmedicine.eldoc.ub.rug.nl/root/G3/187g/

Gooby, B. (2020) The Development of Methodologies for Color Printing in Digital Inkjet Textile Printing and the Application of Color Knowledge in the Ways of Making Project, *Journal of Textile Design Research and Practice 8(3)*, 358-383. https://doi.org/10.1080/20511787.2020.1827802

Gopal, N., Asaithambi, M., Sivakumar, P., & Sivakumar, V. (2014). Adsorption studies of a direct dye using polyaniline coated activated carbon prepared from *Prosopis juliflora*. *Journal of Water Process Engineering*. https://doi.org/10.1016/j.jwpe.2014.05.008.

Grace, O. M., Simmonds, M. S., Smith, G. F., & van Wyk, A. E. (2008). Therapeutic uses of Aloe L. (Asphodelaceae) in southern Africa. Journal of ethnopharmacology, 119(3), 604–614. https://doi.org/10.1016/j.jep.2008.07.002.

Grace, O., Simmonds, M., Smith, G., & Van Wyk, A. (2009). Documented utility and biocultural value of Aloe L. (Asphodelaceae): a review. *Economic Botany, 63*, 167–178. https://doi.org/10.1007/s12231-009-9082-7.

Guha, A. K. (2019). A Review on Sources and Application of Natural Dyes in Textiles. *International Journal of Textile Science*, *8*(2), 38–40. https://doi.org/10.5923/j.textile.20190802.02.

Gupta, V.K. (2019) Fundamentals of Natural Dyes and Its Application on Textile Substrates. In: Chemistry and Technology of Natural and Synthetic Dyes and Pigments, Intech Open, pp. 1-32.

Hagan, E., & Poulin, J. (2021) Statistics of the early synthetic dye industry. *Heritage Science 9*, 33. https://doi.org/10.1186/s40494-021-00493-5

Hamzezadeh, A., Rashtbari, Y., Afshin, S., Morovati, M., & Vosoughi, M. (2020) Application of low-cost material for adsorption of dye from aqueous solution. International Journal of *Environmental Analytical Chemistry*. https://doi.org/10.1080/03067319.2020. 1720011.

Harrache, Z., Abbas, M., Aksil, T., & Trari, M. (2019). Thermodynamic and kinetics studies on adsorption of Indigo Carmine from aqueous solution by activated carbon. *Microchemical Journal*, *144* (July 2018), 180–189. https://doi.org/10.1016/j.microc.2018.09.004.

Harris, P.J.F. Transmission Electron Microscopy of Carbon: A Brief History. *C* 2018, 4, 4. https://doi.org/10.3390/c4010004.

Hassaan, M. A., & Nemr, A. El. (2017). To cite this article: Mohamed A. Hassaan, Ahmed El Nemr. Health and Environmental Impacts of Dyes: Mini Review. *American Journal of Environmental Science and Engineering*, *1*(3), 64–67. https://doi.org/10.11648/j.ajese.20170103.11.

Haule, L., Nambela, L., & Samwel, J. (2017). *Ftir Analysis of Cotton Fabric Dyed With Natural Dyes*. Retrieved from http://repository.costech.or.tz//handle /20.500.11810 /4526

He, X., Liu, Z., Niu, W., Yang, L., Zhou, T., Qin, D., … Yuan, Q. (2017). Effects of pyrolysis temperature on the physicochemical properties of gas and biochar obtained from pyrolysis of crop residues. *Energy*.

https://doi.org/10.1016/j.energy.2017.11.062.

Hernández-Zamora, M., Cristiani-Urbina, E., Martínez-Jerónimo, F., Perales-Vela, H. V., Ponce-Noyola, T., Montes-Horcasitas, M., & Cañizares-Villanueva, R. O. (2015). Bioremoval of the azo dye Congo Red by the microalga Chlorella vulgaris. Environmental science and pollution research international, 22(14), 10811–10823. https://doi.org/10.1007/s11356-015-4277-1.

Holder, C.F., & Schaak, R.E. (2019) Tutorial on Powder X-ray Diffraction for Characterizing Nanoscale Materials. *ACS Nano* 13, 7, 7359–7365. https://doi.org/10.1021/acsnano.9b05157.

Hossain, M., Ngo, H., & Guo, W. (2013). Introductory of Microsoft Excel SOLVER function- Spreadsheet method for isotherm and kinetics modelling of metals biosorption in water and wastewater. *Journal of Water Sustainability*, *3*(4), 223–237.

Hossain, R., Rahman, M. A., Ara, N. J., & Alam, A. S. (2016). Removal of Levafix Red from Aqueous Solution with Treated Jute Stick and its Relevance to Pharmaceutical Field. *Bangladesh Pharmaceutical Journal*, 19(1), 75–84. https://doi.org/10.3329/bpj.v19i1. 29242.

Hossein, M. A., & Behzad, H. (2012). Removal of Reactive Red 120 and Direct Red 81 dyes from aqueous solutions by Pumice. *Research Journal of Chemistry and Environment*, *16*(1).

Hunger K. (2007) Important chemical chromophores of dye classes. In: Industrial dyes: chemistry, properties, applications. Weinheim, Germany: Wiley-VCH Verlag GmbH & Co. KGaA; 2003. p. 13-4.91.

Hussein, H. J., Hadi, M. Y., & Hameed, I. H. (2016). Study of chemical composition of *Foeniculum vulgare* using Fourier transform infrared spectrophotometer and gas chromatography - mass spectrometry. *Journal of Pharmacognosy and Phytotherapy*, *8*(3), 60–89. https://doi.org/10.5897/JPP2015.0372.

Ibrahim, M,, Nadir, M., Ali, A., Ahmad, V.U., & Rasheed, M. (2013) Phytochemical analyses of *Prosopis juliflora* Swartz DC. *Pakistan Journal of Botany 45*, 2101–2104. https://www.pakbs.org/pjbot/PDFs/45(6)/38.pdf.

Ibrahim, S.A., Rizk, H.F., Aboul-Magd, D.S., &, Ragab, A. (2021) . Design, synthesis of new magenta dyestuffs based on thiazole azomethine disperse reactive dyes with antibacterial potential on both dyes and gamma-irradiated dyed fabric. *Dyes and Pigments*, 193,109504. https://doi.org/10.1016/j.dyepig.2021.109504.

Iftekhar, S., Lakshmi, D., Srivastava, V., Bilal, M., & Sillanp, M. (2018). Understanding the factors affecting the adsorption of Lanthanum using different adsorbents : A critical review. *Chemosphere*, *204*, 413–430. https://doi.org/10.1016.

Igwe, O. U., & Mgbemena, M.-A. N. (2015). Chemical Profiling And Antibacterial Activity Screening Of The Medicinal Chemistry & Analysis Chemical Profiling And Antibacterial Activity. *International Journal of Medicinal Chemistry & Analysis Www.Ijmca.Com*, *4*(3), 155–161.

Ilukor, J., Rettberg, S., Treydte, A., & Birner, R. (2016) To eradicate or not to eradicate? Recommendations on *Prosopis juliflora* management in Afar, Ethiopia, from an interdisciplinary perspective. Pastoralism 6, 14. https://doi.org/10.1186/s13570-016-0061-1.

Inglezakis, V., Poulopoulos, S., & Kazemian, H. (2018) Insights into the S-shaped sorption isotherms and their dimensionless forms. Microporous Mesoporous Mater., 272 pp. 166-176.

Islam, M., Hasan, K. M. F., & Deb, H. (2016). Improving the Fastness Properties of Cotton Fabric through the Implementation of Different Mordanting Agents Dyed with Natural Dye Extracted from Marigold. *American Journal of Polymer Science and Engineering*, *4*(2018), 1–17.

İşmal, Ö. E., & Yildirim, L. (2018). Metal mordants and biomordants.*The Impact and Prospects of Green Chemistry for Textile Technology*, 57–82. https://doi.org/10.1016 /B978-0-08-102491-1.00003-4.

Jadhav, A.C., & Jadhav, N.C. (2021) Treatment of textile wastewater using adsorption and adsorbents. In: Sustainable Technologies for Textile Wastewater Treatments, The Textile Institute Book Series, pp. 235-273. https://doi.org/10.1016/B978-0-323-85829-8.00008-0.

Jain, M., Garg, V. K., & Kadirvelu, K. (2011). Investigation of Cr (VI) adsorption onto chemically treated Helianthus annuus : Optimization using Response Surface Methodology. *Bioresource Technology*, *102*(2), 600–605. https://doi.org/10.1016/j.biortech.2010.08.001

Jamadar, D., & Sannapapamma, K. (2018). GC-MS analysis and colour fastness properties of silk yarn dyed with *Acacia nilotica* pods. *The Pharma Innovation Journal 2018;*, *7*(8), 474–479.

Janani, L., Hillary, L., & Phillips, K. (2014). Mordanting Methods for Dyeing Cotton Fabrics with Dye from *Albizia Coriaria* Plant Species. *International Journal of Scientific and Research Publications*, *4*(10), 1–6.

Jayakumari, S., Ram, M., Rao, K., Kumaran, D., & Ramesh, A. (2017). The GC MS Analysis of a Rare Medicinal Plant *Aloe barbadensis*. *9*(7), 1035–1037.

Ji, B., Wang, J., Song, H., & Chen, W. (2019). Journal of Environmental Chemical Engineering Removal of methylene blue from aqueous solutions using biochar derived from a fallen leaf by slow pyrolysis : Behavior and mechanism. *Journal of Environmental Chemical Engineering*, *7*(3), 103036. https://doi.org/10.1016/j.jece.2019.103036

Jihad, R. (2014). Dyeing of Silk Using Natural Dyes Extracted From Local Plants. *International Journal of Scientific & Engineering Research*, *5*(11).

Joshi, M., Ali, S. W., Purwar, R., & Rajendran, S. (2009). Ecofriendly antimicrobial finishing of textiles using bioactive agents based on natural products. *Indian Journal of Fibre and Textile Research*, *34*(3), 295–304.

Jothi, D. (2008). Extraction of natural dyes from African marigold flower (Tagetes ereectal) for textile coloration. *Autex Research Journal*, *8*(2), 49–53.

Jyoti, V. V., Giridhar, G., Shameembanu, A. B., Rajkumari, D. D., & Rajashri, K. (2015). Identification of bio-active components in leaf extracts of Aloe vera, Ocimum tenuiflorum (Tulasi) and Tinospora cordifolia (Amrutballi). *Journal of Medicinal Plants Research*, *9*(28), 764–770. https://doi.org/10.5897/jmpr2013.5197

Kajjumba, G. W., Emik, S., Öngen, A., Özcan, H. K., & Aydın, S. (2018). Modelling of Adsorption Kinetic Processes—Errors, Theory and Application. In *Advanced Sorption Process Applications* (pp. 0–19). Intech Open. https://doi.org/http://dx.doi.org /10.5772/intechopen.80495

Kalaichelvi, K., & Dhivya, S. M. (2017). Screening of phytoconstituents, UV-VIS Spectrum and FTIR analysis of *Micrococca mercurialis* (L.) Benth. *International Journal of Herbal Medicine*, *5*, 40-44.

Kamatou, G. P. P., & Viljoen, A. M. (2017). Comparison of fatty acid methyl esters of palm and palmist oils determined by GCxGC–ToF–MS and GC–MS/FID. *South African Journal of Botany*, *112*, 483–488. https://doi.org/10.1016/j.sajb.2017.06.032.

Kannan, T. V. K. (2014). An innovative and novel method of removal of Rhodamine- B dye by Activated carbon prepared from Seeds of *Prosopis juliflora*. *EnviroGeoChemica Acta*, *1*, 140–146.

Kant, R. (2012). Textile dyeing industry an environmental hazard. *Natural Science*, *04*(01), 22–26. https://doi.org/10.4236/ns.2012.41004.

Kasiri, M. B.,Safapour, S.(2014). Natural dyes and antimicrobials for green treatment of textiles. *Environmental Chemistry Letters*, *12*(1), 1–13. https://doi.org/10.1007/s10311-013-0426-2.

Katheresan, V.; Kansedo, J.; Lau, S.Y. Efficiency of various recent wastewater dye removal methods: A review. J. Environ. Chem. Eng. 2018, 6, 4676–4697. https://doi.org/10.1016/j.jece.2018.06.060

Ketema, A., & Worku, A. (2020). Antibacterial Finishing of Cotton Fabric Using Stinging Nettle (Urtica dioica L.) Plant Leaf Extract. *Journal of Chemistry*, *2020*. https://doi.org /10.1155/2020/4049273.

Key Colour (2016). The Evolution Of Textile Dyes: History And Development. Retrieved From https://www.keycolour.net/blog/the-evolution-of-textile-dyes-history-and-development/.

Khaing, T. (2011). Evaluation of the Antifungal and Antioxidant Activities of the Leaf Extract of Aloe vera. *World Academy of Science, …*, 2009–2011. Retrieved from http://www.waset.org/publications/2624

Khalfaoui, M., Knani, S., Hachicha, M., & Lamine, A. (2003) New theoretical expressions for the five adsorption type isotherms classified by BET based on statistical physics treatment. *J. Colloid Interface Sci*., 263 (2) pp. 350-356.

Khan, M. N., Parmar, D. K., & Das, D. (2021). Recent Applications of Azo Dyes: A Paradigm Shift from Medicinal Chemistry to Biomedical Sciences. *Mini reviews in medicinal chemistr*y, 21(9), 1071–1084. https://doi.org/10.2174/1389557520999201123210025

Khandelwal, P., Sharma, R. A., & Agarwal, M. (2016). Phytochemical analyses of various parts of *Prosopis juliflora*. *Mintage Journal of Pharmaceutical & Medical Sciences*, *5*(1), 16–18. https://doi.org/10.11648/j.ijpc.20160201.12.

Khaniabadi, Y. O., Mohammadi, M. J., Shegerd, M., Sadeghi, S., & Saeedi, S. (2017). Removal of Congo red dye from aqueous solutions by a low-cost adsorbent : activated carbon prepared from Aloe vera leaves shell. *Kerman University of Medical Sciences*, *4*(1), 29–35. https://doi.org/10.15171/EHEM.2017.05.

Khurshid, M., Muhammad, M. F., Asad, M., & Shah, S. N. H. (2015). Assessment of eco-friendly natural antimicrobial textile finish extracted from aloe vera and neem plants. *Fibres and Textiles in Eastern Europe*, *23*(6), 120–123.

https://doi.org/10.5604/ 12303666.1172176.

Kim, K., Jae, K., Cho, T. S., & Choi, J. W. (2012). Influence of pyrolysis temperature on physicochemical properties of biochar obtained from the fast pyrolysis of pitch pine (Pinus rigida). *Bioresource Technology*, *118*, 158–162. https://doi.org/10.1016/j.biortech.2012.04.094.

Kim, Y. W., Kim, J. H., Moon, D. H., Shin, H. J. (2019). Adsorption and precipitation of anionic dye Reactive Red 120 from aqueous solution by aminopropyl functionalized magnesium phyllosilicate. *Korean Journal of Chemical Engineering*, *36*(1), 101–108. https://doi.org/10.1007/s11814-018-0168-8.

Kittinaovarat, S., Kansomwan, P., & Jiratumnukul, N. (2010). Applied Clay Science Chitosan/modi fi ed montmorillonite beads and adsorption Reactive Red 120. *Applied Clay Science*, *48*(1–2), 87–91. https://doi.org/10.1016/j.clay.2009.12.017.

Kooh, M. R. R., Dahri, M. K., Lim, L. B. L., Lim, L. H., & Malik, O. A. (2016). Batch adsorption studies of the removal of methyl violet 2B by soya bean waste: isotherm, kinetics and artificial neural network modelling. *Environmental Earth Sciences*, *75*(9). https://doi.org/10.1007/s12665-016-5582-9.

Koseoglu, A.U. (2019) Innovations and Analysis of Textile Digital Printing Technology. *International Journal of Science, Technology and Society* 7(2), 38-43. https://doi.org/10.11648/j.ijsts.20190702.12

Kowsalya, E., Sharmila, S., & Rebecca, L. J. (2020). Effect Of Dye Concentration On Adsorption Efficiency. Plant Cell Biotechnology And Molecular Biology, 20(23-24), 1350-1353. Retrieved from https://www.ikprress.org/index.php/PCBMB/article/ view/ 4890.

Kudzinski, V., & Wojciechowski, B. W. (1977). On the Jovanovic model of adsorption I. An extension for mobile adsorbed layers. *Colloid and Polymer Science Kolloid-Zeitschrift & Zeitschrift Für Polymere*, *255*(9), 869–880. https://doi.org/10.1007/BF01617094.

Kumar, A., & Konar, A. (2011). Dyeing of Textiles with Natural Dyes. *Natural Dyes*, (November 2011). https://doi.org/10.5772/2134.

Kumar, A., Dixit, U., Singh,K., Gupta, S.P., & Beg, M.S.J. (2021) Structure and Properties of Dyes and Pigments. In: Dyes and Pigments - Novel Applications and Waste Treatment, *IntechOpen*, pp. 1-19. DOI: 10.5772/intechopen.97104.

Kumar, M., & Tamilarasan, R. (2013). Kinetics and Equilibrium Studies on the Removal of Victoria Blue Using *Prosopis juliflora*-Modified Carbon/Zn/Alginate Polymer Composite Beads. *Journal of Chemical & Engineering Data*, 58(3), 517–527. doi:10.1021/je3012309.

Kumar, M., & Tamilarasan, R. (2013). Modeling of experimental data for the adsorption of methyl orange from aqueous solution using a low cost activated carbon prepared from *Prosopis juliflora*. *Polish Journal of Chemical Technology*, *15*(2), 29–39. https://doi.org/10.2478/pjct-2013-0021

Kumar, M., Tamilarasan, R., 2014. Removal of Victoria Blue using *Prosopis juliflora* bark carbon: kinetics and thermodynamic modeling studies. J. Mater. Environ. Sci. 5, 510–519.https://www.jmaterenvironsci.com/Document/vol5/vol5_N2/62-JMES-602-2014-KumarTamilarasan.pdf.

Kumaresan, M., Palanisamy, P. N., & Kumar, P. E. (2011). Application of eco-friendly natural dye on silk using combination of motdants. *International Journal of Chemistry Research*, *2*(1), 11–14.

Kumbhar, S., Hankare, P., Sabale, S., & Kumbhar, R. (2019). Eco - friendly dyeing of cotton with brown natural dye extracted from Ficus amplissima Smith leaves. *Environmental Chemistry Letters*, (0123456789), 1–6. https://doi.org/ 10.1007/s10311-018-00854-w

Kundal, J., Singh, S. V., & Mc, P. (2016). Extraction of Natural Dye from Ficus cunia and Dyeing of Polyester Cotton and Wool Fabric Using Different Mordants , with Evaluation of Colour Fastness Properties. *Natural Products Chemistry & Research*, *4*(3). https://doi.org/10.4172/2329-6836.1000214.

Kundu, S., & Gupta, A. (2006) Arsenic adsorption onto iron oxide-coated cement (IOCC): regression analysis of equilibrium data with several isotherm models and their optimization. Chem. Eng. J., 122 (1-2), 93-106.

Kurniawati, D., Bahrizal, T.K., Sari, F., Adella, & Salmariza, S. (2021) Effect of Contact Time Adsorption of Rhodamine B, Methyl Orange and Methylene Blue Colours on Langsat Shell with Batch Methods. *Journal of Physics: Conference Series*, 1788 012008. https://doi.org/10.1088/1742-6596/1788/1/012008.

Kuśmierek, K., & Świątkowski, A. (2015) The influence of different agitation techniques on the adsorption kinetics of 4-chlorophenol on granular activated carbon. *Reaction Kinetics, Mechanisms and Catalysis* 116, 261–271. https://doi.org/10.1007/s11144-015-0889-1.

Kyi, P. P., Quansah, J. O., Lee, C., & Moon, J. (2020). The Removal of Crystal Violet from Textile water using Palm Kernel shell-Derived biochar. *Applied Sciences*, *10*.

Lakshmibai, R, & Amirtham, D. (2018) Phytochemical analysis and antioxidant activity of *Prosopis juliflora* thorn extract. *Malaya Journal of Biosciences 5(1)*, 21-27.

Lakshmibai, R. (2015). Preliminary Phytochemical Analysis and Antioxidant Activities of *Prosopis Juliflora* and *Mimosa Pudica* Leaves. *International Journal of Scientific Engineering and Technlogy Research*, *4*(30), 5766–5770.

Ledakowicz, S., & Paździor, K. (2021). Recent Achievements in Dyes Removal Focused on Advanced Oxidation Processes Integrated with Biological Methods. Molecules (Basel, Switzerland), 26(4), 870. https://doi.org/10.3390/molecules26040870 .

Lee, J.; Kang, M.H.; Lee, K.-B.; Lee, Y. (2013) Characterization of Natural Dyes and Traditional Korean Silk Fabric by Surface Analytical Techniques. *Materials* 6, 2007-2025. https://doi.org/10.3390/ma6052007.

Lee, Y. H., & Kim, H. Do. (2004). Dyeing properties and colour fastness of cotton and silk fabrics dyed with Cassia tora L. extract. *Fibers and Polymers*, *5*(4), 303–308. https://doi.org/10.1007/BF02875529

Leech, K (2020) Universal analytical method for characterization of yellow and related natural dyes in liturgical vestments from Krakow. Journal of Cultural Heritage *46*, 108-118. https://doi.org/10.1016/j.culher.2020.04.011

Leech, K (2020) Universal analytical method for characterization of yellow and related natural dyes in liturgical vestments from Krakow. Journal of Cultural Heritage *46*, 108-118. https://doi.org/10.1016/j.culher.2020.04.011

Lellis, B., Fávaro-Polonio, C.Z., Pamphile, J.A., & Polonio, J.C. (2019) Effects of textile dyes on health and the environment and bioremediation potential of living organisms. *Biotechnology Research and Innovation*, 3(2), 275-290. https://doi.org/10.1016/j.biori. 2019.09.001.

Lellis, B., Fávaro-Polonio, C.Z., Pamphile, J.A., & Polonio, J.C. (2019) Effects of textile dyes on health and the environment and bioremediation potential of living organisms. *Biotechnology Research and Innovation* 3(2), 275-290. https://doi.org/10.1016/j.biori.2019.09.001.

Liang, H., Chen, L., Liu, G., & Zheng, H. (2016). Surface morphology properties of biochars produced from different feedstocks. *International Conference on Civil, Transportation and Environment*, 1205–1208.

Lim, L. B. L., Priyantha, N., Chan, C. M., Matassan, D., Chieng, H. I., & Kooh, M. R. R. (2014). Adsorption Behavior of Methyl Violet 2B Using Duckweed: Equilibrium and Kinetics Studies. *Arabian Journal for Science and Engineering*, *39*(9), 6757–6765. https://doi.org/10.1007/s13369-014-1224-2.

Lim, L. B. L., Priyantha, N., Chan, C. M., Matassan, D., Chieng, H. I., & Kooh, M. R. R. (2015). Investigation of the sorption characteristics of water lettuce (WL) as a potential low-cost biosorbent for the removal of methyl violet 2B. *Desalination and Water Treatment*, (April), 37–41. https://doi.org/10.1080/19443994.2015.1017740.

Ling, T., Muhammad, K., Rahimi, R., Muhammad, K., Dahri, K., Afiqah, N., … Lim, L. (2020). Aquatic plant , Ipomoea aquatica , as a potential low-cost adsorbent for the effective removal of toxic methyl violet 2B dye. *Applied Water Science*, *10*(12), 1–13. https://doi.org/10.1007/s13201-020-01326-9.

Liu, P., Chen, D., & Shi, J. (2013). Chemical Constituents,Biological Activity and Agricultural Cultivation of Aloe vera. *Asian Journal of Chemistry*, *25*(12), 6477–6485.

Ma, L., Han, T., Jia, J., & Wu, H. (2020) Cooperative physisorption and chemisorption of hydrogen on vanadium-decorated benzene. *RSC Advances* 10, 37770-37778. https://doi.org/10.1039/D0RA06057G.

Malik, R., Lata, S., & Singhal, S. (2015). Removal of Heavy Metal From Waste Water By the Use of Modified Aloe Vera Leaf Powder. *International Journal of Basic and Applied Chemical Sciences*, *5*(2), 2277–20736.

Maltanava,H.M.,Poznyak,S.K.,Belko,N.V., Samtsov, M.P.(2021). Optical and Electrochemical properties of Indotricarbocyanine Dyes for Photodynamic Therapy. *Journal of Applied Spectroscopy 88(3),* 489-495. https://doi.org/10.1007/s10812-021-01198-0.

Manhita, A., Ferreira, T., Candeias, A., & Barrocas Dias, C. (2011). Extracting natural dyes from wool-an evaluation of extraction methods. *Analytical and Bioanalytical Chemistry*, *400*(5), 1501–1514. https://doi.org/10.1007/s00216-011-4858-x.

Mani, P. (2017). Phytochemical and Pharmacological Analysis of Ethanolic Extracts of *Prosopis Juliflora* (Sw.). *World Journal of Pharmacy and Pharmaceutical Sciences*, *6*(9), 2059–2069. https://doi.org/10.20959/wjpps20179-10109.

Mariajancyrani, J., Chandramohan, G., Brindha, P., & Saravanan, P. (2014). GC-MS Analysis of Terpenes from Hexane Extract of *Lantana camara* Leaves. *International Journal Of Advances In Pharmacy, Biology And Chemistry*, *3*(1), 37–

41.

Markandeya, S., Shukla, S. P., & Kisku, G. C. (2015). Linear and Non-Linear Kinetic Modeling for Adsorption of Disperse Dye in Batch Process. *Research Journal of Environmental Toxicology*, *9*(6), 320–331. https://doi.org/10.3923/rjet.2015.320.331.

Mary, G. S., Niveditha, P. S. S., & Mary, G. S. (2016). Production , characterization and evaluation of biochar from pod (Pisum sativum) , leaf (Brassica oleracea) and peel (Citrus sinensis) wastes. *International Journal of Recycling of Organic Waste in Agriculture*, *5*(1), 43–53. https://doi.org/10.1007/s40093-016-0116-8.

Maundu, P., Kibet, S., Morimoto, Y., Imbumi, M., & Adeka, R. (2009). Impact of *Prosopis juliflora* on Kenya ' s semi-arid and arid ecosystems and local livelihoods. *Biodiversity*, 37–41. https://doi.org/10.1080/14888386.2009.9712842

Mehdinejadiani, B., Amininasa, S. M., & Manhooei, L. (2018). Linear and Non-Linear Methods for Estimating the Isotherm Parameters of Nitrate Adsorption Onto Modified. In P. Gastescu & P. Bretcan (Eds.), *4th International Conference Water resources and wetlands, 5-9 September 2018, Tulcea (Romania) LINEAR* (pp. 64–70). Tulcea (Romania): Water resources and wetlands.

Melese, T., Chala, K., Ayele, Y., & Abdisa, M. (2020). Preparation , characterization of raw corncob adsorbent for removal of heavy metal ions from aqueous solution using batch method. 14(December), 81–90. https://doi.org/10.5897/AJPAC2019.0817

Mohamed E. Mahmoud , Gehan M. Nabil, Nabila M. El-Mallah, Heba I. Bassiouny, Sandeep Kumar, T. M. A.-F. (2016). Kinetics , isotherm , and thermodynamic studies of the adsorption of reactive red 195 A dye from water by modified Switchgrass Biochar adsorbent. *Journal of Industrial and Engineering Chemistry*. https://doi.org/10.1016/j.jiec.2016.03.020

Mościpan, M., Zarębska, M., & Kulesza, R. (2016). Application of chromatographic techniques for determination of azo dyes and theirs degradation products in consumer goods. *Chemik*, *70*(3), 135–143.

Mourabet, M., Rhilassi, A. El, Boujaady, H. El, & Taitai, A. (2017). Use of response surface methodology for optimization of fluoride adsorption in an aqueous solution by Brushite. *Arabian Journal of Chemistry*, *10*, S3292–S3302. https://doi.org/10.1016/j.arabjc.2013.12.028.

MSK (2021) A Brief History Of Dyeing Fabric. Retrieved from https://so-sew- easy.com /history -of- dyeing -fabric/

Mubarak, N. S. A., Jawad, A. H., & Nawawi, W. I. (2017). Equilibrium, kinetic and thermodynamic studies of Reactive Red 120 dye adsorption by chitosan beads from aqueous solution. *Energy, Ecology and Environment*, *2*(1), 85–93. https://doi.org/10.1007/s40974-016-0027-6.

Muller, G. C., Junnila, A., Traore, M. M., Traore, S. F., Doumbia, S., Sissoko, F., Dembele, S. M., Schlein, Y., Arheart, K. L., Revay, E. E., Kravchenko, V. D., Witt, A., & Beier, J. C. (2017). The invasive shrub *Prosopis juliflora* enhances the malaria parasite transmission capacity of Anopheles mosquitoes: a habitat manipulation experiment. Malaria journal, 16(1), 237. https://doi.org/10.1186/s12936-017-1878-9.

Munagapati, V. S., Wen, J., Pan, C., Gutha, Y., & Wen, J. (2019). Enhanced adsorption performance of Reactive Red 120 azo dye from aqueous solution using quaternary amine modi fi ed orange peel powder. *Journal of Molecular Liquids*, *285*, 375–385. https://doi.org/10.1016/j.molliq.2019.04.08.

Mustroph,H. (2014).Dyes,General Survey. In:Ullmann's Encyclopedia of Industrial Chemistry.Wiley-VCH.https://onlinelibrary.wiley.com/doi/10.1002/14356007.a09_073.pub 2

Mutavi, S.K. (2021) Effects of *Prosopis juliflora* pod and leaf meal on physicalcharacteristics of teeth and bones of goats in Kitui County, Kenya. Livestock Research for Rural Development 32(10). https://lrrd.cipav.org.co/lrrd32/10/skmut32163.html.

Nakano H, Fujii Y, Yamada K, Kosemura S, Yamamura S, Hasegawa K, Suzuki T (2002) Isolation and identification of plant growth inhibitors as candidate(s) for allelopathic substance(s), from aqueous leachate from mesquite (*Prosopis juliflora* (Sw.) DC.) leaves. Plant Growth Regulation 37:113–117. https://doi.org/10.1023/A:1020579101938.

Nakano, H., Nakajima, E., Hiradate, S., Fujii, Y., Yamada, K., Shigemori, H., & Hasegawa, K. (2004). Growth inhibitory alkaloids from mesquite (*Prosopis juliflora* (Sw.) DC.) leaves. *Phytochemistry* 65(5), 587–591. https://doi.org/10.1016/j.phytochem.2004.01. 006.

Nalimu, F., Oloro, J., Kahwa, I., & Ogwang, P. E. (2021). Review on the phytochemistry and toxicological profiles of *Aloe vera* and *Aloe ferox*. *Future Journal of Pharmaceutical Sciences, 7*, 145. https://doi.org/10.1186/s43094-021-00296-2.

Naveen, N., Saravanan, P., Baskar, G., & Renganathan, S. (2011). Equilibrium and kinetic modeling on the removal of Reactive Red 120 using positively charged *Hydrilla verticillata*. *Journal of the Taiwan Institute of Chemical Engineers*, *42*(3), 463–

469. https://doi.org/10.1016/j.jtice.2010.08.007.

Nawaz, H., Shad, M. A., Rehman, N., Andaleeb, H., & Ullah, N. (2020). Effect of solvent polarity on extraction yield and antioxidant properties of phytochemicals from bean (*Phaseolus vulgaris*) seeds. *Brazilian Journal of Pharmaceutical Sciences, 56*, e17129. https://doi.org/10.1590/s2175-97902019000417129.

Nejatzadeh-barandozi, F. (2013). Antibacterial activities and antioxidant capacity of *Aloe vera*. 1–8.

Nema, R., Khare, S., Pradhan, A., & Gupta, A. (2012). Antibacterial and antifungal activity of *Terminalia Arjuna* leaves extract with special reference to flavanoids. *Basic Research Journal of Medicine and Clinical Sciences ISSN 2315-6864*, *1*(November), 63–65.

Ng, K.C., Burhan, M., Shahzad, M.W. & Ismail, A.B. (2017) A Universal Isotherm Model to Capture Adsorption Uptake and Energy Distribution of Porous Heterogeneous Surface. *Scientific Reports* 7, 10634. https://www.nature.com/articles/s41598-017-11156-6

Ngeno, E. C., Orata, F., Baraza, D. L., & Shikuku, V. (2016). Adsorption of Caffeine and Ciprofloxacin onto Pyrolitically Derived Water Hyacinth Biochar: Isothermal, Kinetic and Thermodynamic Studies. https://doi.org/10.17265/1934-7375/2016.04.006.

Nidheesh, P.V. , Gandhimathi, R. , & Ramesh, S.T. (2013) Degradation of dyes from aqueous solution by Fenton processes: a review Environ. Sci. Pollut. Res., 20, 2099-2132. https://doi.org/10.1007/s11356-012-1385-z.

Nidhi, G. (2020) Colour and Constitutions: Synthesis of malachite green, fluorescein, synthesis and structure of Indigotin. Lecture Notes. https://new.bhu.ac.in/Content/Syllabus /Syllabus_ 3006312720200419082120.pdf

Niran, O. B., Olawale, S. A., & Ushie, U. J. (2018). *Isotherm Studies of Adsorption of Methylene Blue by Palm Kernel Shell*. *1*(1), 1–9. https://doi.org/10.9734/AJACR/2018/41300.

Nooraee Nia, N., Rahmani, M., Kaykhaii, M., & Sasani, M. (2017). Evaluation of Eucalyptus leaves as an adsorbent for decolorization of Methyl Violet (2B) dye in contaminated waters: Thermodynamic and Kinetics model. *Modeling Earth Systems and Environment*, *3*(2), 825–829. https://doi.org/10.1007/s40808-017-0338-4.

Odero, M. P., Munyendo, W. L., & Kiprop, A. K. (2017). Quantitative Analysis of the

Flavonoid Mesquitol in the Medicinal Plant *Prosopis juliflora* with Seasonal Variations in Marigat , Baringo County-Kenya. *5*(6), 107–112. https://doi.org/10.11648/j.sjac. 20170506.16

Odion, E. E., Ogboru, R. O., & Ighene, M. O. (2020). Identification of Compounds in *Elaeis guineensis* Fruits using GC-MS. *Dhaka University Journal of Pharmaceutical Sciences*, *19*(2), 153–159. https://doi.org/10.3329/dujps.v19i2.50631.

Ofomaja, A.E., Ukpebor, E.E., & Uzoekwe, S.A. (2011) Biosorption of methyl violet onto palm kernel fiber: diffusion studies and multistage process design to minimize biosorbent mass and contact time. *Biomass Bioenergy*, 35, 4112-4123. https://doi.org/10.1016/j.biombioe.2011.05.024.

Osmari, T. A., Gallon, R., Schwaab, M., Barbosa-Coutinho, E., Severo, J. B., & Pinto, J.C. (2013). Statistical analysis of linear and non-linear regression for the estimation of adsorption isotherm parameters. *Adsorption Science and Technology*, *31*(5), 433–458. https://doi.org/10.1260/0263-6174.31.5.433.

Oueslati, K., Lima, E. C., Ayachi, F., Cunha, M. R., & Ben Lamine, A. (2020). Modeling the removal of Reactive Red 120 dye from aqueous effluents by activated carbon. *Water Science and Technology :A Journal of the International Association on Water Pollution Research*, *82*(4), 651–662. https://doi.org/10.2166/wst.2020.347.

Oueslati, K., Lima, E.C., Ayachi, F., Cunha, M.R., & Lamine, A.B. (2020) Modeling the removal of Reactive Red 120 dye from aqueous effluents by activated carbon. *Water Sci Technology* 15 August 2020; 82 (4): 651–662. https://doi.org/10.2166/wst.2020.347.

Pakkirisamy, M., Kalakandan, S. K., Ravichandran, K. (2014). Phytochemicalscreening, GC-MS, FT-IR analysis of methanolic extract of Curcuma caesia roxb (black turmeric). *Pharmacognosy Journal*, *9*(6), 952–956. https://doi.org/10.5530/pj.2017.6.149.

Parvin, M. (2015). Adsorption Of Dyes On Activated Carbon From Agricultural Wastes (United Arab Emirates University). United Arab Emirates University. https://doi.org/10.1260/0263617011494150.

Patnaik, P., Abbasi, T, Abbasi SA (2017) *Prosopis (Prosopis juliflora*): blessing and bane *Tropical Ecology* 58(3): 455–483, 2017.

Paul, D., Das, S. C., Islam, T., & Siddiquee, A. B. (2017). Effect of Temperature on Dyeing Cotton Knitted Fabrics with Reactive Dyes *Available online www.jsaer.com Journal of Scientific and Engineering Research , 2017 , 4 (12): 388-39.*

Pervaiz, S., Mughal, T. A., & Khan, F. Z. (2016). Leather Dyeing with Plants Dyes : A Review. *Journal of Biodiversity and Environmental Sciences*, *9*(1), 455–464.

Piaskowski, K., Świderska-Dąbrowska, R., & Zarzycki, P. K. (2018). Dye Removal from Water and Wastewater Using Various Physical, Chemical, and Biological Processes. Journal of AOAC International, 101(5), 1371–1384. https://doi.org/10.5740/jaoacint.18-0051.

Pittis, L.; Rodrigues de Oliveira, D.; Vega Gutierrez, S.M.; Robinson, S.C. Alternative Carrier Solvents for Pigments Extracted from Spalting Fungi. Materials 2018, 11, 897. https://doi.org/10.3390/ma11060897.

Polston, K., Parrillo-Chapman, L. and Moore, M. (2015) Print-on-Demand Inkjet Digital Textile Printing Technology: An Initial Understanding of User Types and Skill Levels. *International Journal of Fashion Design, Technology and Education 8(2)*, 87–96. https://doi.org/10.1080/17543266.2014.992050.

Poulin, J. (2018). A New Methodology for the Characterisation of Natural Dyes on Museum Objects Using Gas Chromatography–Mass Spectrometry. *Studies in Conservation*, *63*(1), 36–61. https://doi.org/10.1080/00393630.2016.1271097.

Prasad, M.N.V., & Tewari, J.C. (2016) *Prosopis Juliflora* (SW) DC: Potential for Bioremediation and Bioeconomy. In: Prasad, M.N.V. (Eds), Bioremediation and Bioeconomy, Amsterdam: Elsevier, pp. 49-76. http://dx.doi.org/10.1016/B978-0-12-802830-8.00003-4

Preeti, K., Ram Avatar, S., & Mala, A. (2015). Pharmacology and Therapeutic Application of *Prosopis juliflora*: A. *Review*. *Journal of Plant Sciences*, *3*(4), 234–240. https://doi.org/10.11648/j.jps.20150304.20.

Punrattanasin, N., Nakpathom, M., Somboon, B., & Narumol, N. (2013). Silk fabric dyeing with natural dye from mangrove bark (*Rhizophora apiculata* Blume) extract. *Industrial Crops & Products*, *49*, 122–129. https://doi.org/10.1016/j.indcrop.2013.04.041

Punzi et al. (2015) Combined anaerobic – ozonation process for treatment of textile wastewater: Removal of acute toxicity and mutagenicity. Journal of Hazardous Materials 292, 52-60. https://doi.org/10.1016/j.jhazmat.2015.03.018

Qi, Y., Zhu, J., Fu, Q., Hu, H. , & Huang, Q. (2017) Sorption of Cu by humic acid from the decomposition of rice straw in the absence and presence of clay minerals. J. Environ. Manage., 200 (2017), pp. 304-311. https://doi.org/10.1016/j.jenvman.2017.05.087

Radhi, I. K., Hussein, M. A., & Kadhim, Z. N. (2019). Factors Affecting the Adsorption of Some Ionic Dyes on the Surface of Modify CaO from Eggshell. Asian Journal of Applied Sciences, 7(1). https://doi.org/10.24203/ajas.v7i1.5690.

Ram Krishna Rao, M. (2018). Preliminary Phytochemical and Gc Ms Analysis of Different Extracts of Sphaeranthus Indicus Leaves. *Indo American Journal of Pharmaceutical Research*, *8*(April).

Ram, L. S., & Sonia, M. T. T. (2017). Treatment Of Textile Dyeing Effluent By Natural Adsorbents Using *Prosopis juliflora*. *SSRG International Journal of Civil Engineering*, (April), 194–198.

Rani, B., Kumar, V., Singh, J., Bisht, S., Teotia, P., Sharma, S., & Kela, R. (2014). Bioremediation of dyes by fungi isolated from contaminated dye effluent sites for bio-usability. Brazilian journal of microbiology : [publication of the Brazilian Society for Microbiology], 45(3), 1055–1063. https://doi.org/10.1590/s1517-83822014000300039.

Rápó, E.; Tonk, S. Factors Affecting Synthetic Dye Adsorption; Desorption Studies: A Review of Results from the Last Five Years (2017–2021). Molecules 2021, 26, 5419. https://doi.org/10.3390/molecules26175419.

Raskin, I., & Ensley, B. D. (Burt D. (1999). Phytoremediation of Toxic Metals: Using Plants to Clean the Environment. *Journal of Plant Biotechnology*, *1*(1), 304. https://doi.org/10.1016/S0958-1669(97)80106-1.

Rathore, A., Dadhich, R., Purohit, K., Sharma, S. K., Vaishnava, C. S., Joseph, B., & Khatri, A. (2019). Phytochemical screening and total phenolic and flavonoid content in leaves of *Prosopis cineraria (L .) Druce*. *7*(3), 1853–1855.

Raziq, M., Kooh, R., & Lim, L. B. L. (2017). Removal of the methyl violet 2B dye from aqueous solution using sustainable adsorbent Artocarpus odoratissimus stem axis. *Applied Water Science*, *7*(7), 3573–3581. https://doi.org/10.1007/s13201-016-0496-y

Raziq, M., Kooh, R., Dahri, M. K., & Lim, L. B. L. (2017). Removal of methyl violet 2B dye from aqueous solution using Nepenthes rafflesiana pitcher and leaves Removal of methyl violet 2B dye from aqueous solution using Nepenthes rafflesiana pitcher and leaves. *Applied Water Science*. https://doi.org/10.1007/s13201-017-0537-1

Raziq, M., Kooh, R., Lim, L. B. L., Khairud, M., Hoon, L., & Sarath, L. J. M. R. (2015). Azolla pinnata : An Efficient Low Cost Material for Removal of Methyl Violet 2B

by Using Adsorption Method. *Waste Biomass Valor*. https://doi.org/10.1007/s12649-015-9369-0

Rehman, F., Adeel, S., Ahmad, T., Mateen, A. & Amin, N. (2021) Statistical Optimization of Parameters for Eco-Friendly Dyeing of Cotton Using Direct Red 31 Dye, Journal of Natural Fibers, DOI: 10.1080/15440478.2021.1951420.

Robinson, T., Chandran, B., & Nigam, P. (2002). Removal of dyes from an artificial textile dye effluent by two agricultural waste residues, corncob and barley husk. *Environment International*, *28*(1–2), 29–33. https://doi.org/10.1016/S0160-4120(01)00131-3.

Robinson, Tim, McMullan, G., Marchant, R., & Nigam, P. (2001). Remediation of dyes in textile effluent: A critical review on current treatment technologies with a proposed alternative. *Bioresource Technology*, *77*(3), 247–255. https://doi.org/10.1016/S0960-8524(00)00080-8.

Rossi, T., Araújo, M. C., Brito, J. O., & Freeman, H. S. (2015). Wash F astness of Textile Fibers Dyed with Natural Dye from Eucalyptus Wood Steaming Waste. *International Journal of Materials and Textile Engineering*, *9*(7), 871–874.

Saadi, R., Saadi, Z., & Fazaeli, R. (2013) Determination of axial dispersion and overall mass transfer coefficients for Ni (II) adsorption on nanostructured γ-alumina in a fixed bed column: experimental and modeling studies. Desalin. Water Treat., 53 (8), 2193-2203.

Saffari, H. V. M. J., & Shojaei, S. Z. M. S. (2019). The removal of methyl violet 2B dye Using palm kernel activated carbon : thermodynamic and kinetics model. *International Journal of Environmental Science and Technology*, (0123456789). https://doi.org/10.1007/s13762-019-02271-0.

Saharan, P., Sharma, A.K. , Kumar, V., & Kaushal, I. (2019) Multifunctional CNT supported metal doped MnO_2 composite for adsorptive removal of anionic dye and thiourea sensingMater. Chem. Phys. 221, 239-249. https://doi.org/10.1016/j.matchemphys. 2018.09.001.

Sahithya, S., & Krishnaveni, C. (2021) Potential Utilization of a Weed *Prosopis juliflora* Leaf Extract Nanoparticle for Dye Degradation and Antibacterial Activity. In: Bioremediation and Green Technologies, Springer International Publishing. https://doi.org/10.1007/978-3-030-64122-1_12.

Salehi, B., Albayrak, S., Antolak, H., Kręgiel, D., Pawlikowska, E., Sharifi-Rad, M., . . . Sharifi-Rad, J. (2018). *Aloe* Genus Plants: From Farm to Food Applications and

Phytopharmacotherapy. *International Journal of Molecular Sciences, 19*(9), 2843. https://doi.org/10.3390/ijms19092843

Samanta, A. K., & Agarwal, P. (2009). Application of natural dyes on textiles. *Indian Journal of Fibre & Textile Research*, *34*(December), 384–399.

Sánchez, M., González-Burgos, E., Iglesias, I., & Gómez-Serranillos, M. P. (2020). Pharmacological Update Properties of Aloe Vera and its Major Active Constituents. *Molecules (Basel, Switzerland), 25*(6), 1324. https://doi.org/10.3390/molecules25061324

Sanghavi, L. K., & Ranga, S. V. (2017). A study of removal of basic violet 14 dye using *Prosopis juliflora* bark. *Bulletin of Environmental and Scientific Research*,*7*(1),1–6.

Sarkar, A. K. (2004). An evaluation of UV protection imparted by cotton fabrics dyed with natural colorants. *BMC Dermatology*, *4*, 1–8. https://doi.org/10.1186/1471-5945-4-15.

Sathiya, M. & Muthuchelian, K. (2008). Investigation of phytochemical profile and antibacterial potential of ethanolic leaf extract of *Prosopis juliflora* DC. Ethnobotanical leaflets 12, 1240-45. https://core.ac.uk/download/pdf/60544207.pdf.

Scimeca, M., Bischetti, S., Lamsira, H. K., Bonfiglio, R., & Bonanno, E. (2018). Energy Dispersive X-ray (EDX) microanalysis : A powerful tool in biomedical research and diagnosis. *European Journal of Histochemistry 2018;*, *62*. https://doi.org/10.4081/ejh.2018.284.

Scuderi, M., Pallecchi, I., Leo, A. et al. (2021) Nanoscale analysis of superconducting Fe(Se,Te) epitaxial thin films and relationship with pinning properties. Sci Rep 11, 20100. https://doi.org/10.1038/s41598-021-99574-5.

Selim, Y. & Mohamed, A.A. (2017) Role of Dyestuff in Improving Dye-Sensitized Solar Cell Performance. *Renewable Energy and Sustainable Development 3(1)*, 79-82. http://dx.doi.org/10.21622/RESD.2017.03.1.079.

Selvam, R. M., Athinarayanan, G., Raja, A. U., Singh, A. J. A. R., Kalirajan, K., & Selvakumar, P. M. (2015). Extraction of natural dyes from *Curcuma longa* , *Trigonella foenum graecum* and *Nerium oleander* , plants and their application in antimicrobial fabric. *Industrial Crops & Products*, *70*, 84–90. https://doi.org/10.1016/j.indcrop.2015.03.008

Senthilkumaar, S., Kalaamani, P., Porkodi, K., Varadarajan, P. R., & Subburaam, C. V. (2006). Adsorption of dissolved Reactive red dye from aqueous phase onto activated carbon prepared from agricultural waste. *Bioresource Technology*, *97*(14), 1618–1625. https://doi.org/10.1016/j.biortech.2005.08.001

Shaaban, A., Se, S. M., Mitan, N. M. M., & Dimin, M. F. (2013). Characterization of biochar derived from rubber wood sawdust through slow pyrolysis on surface porosities and functional groups. *Procedia Engineering*, *68*, 365–371. https://doi.org/10.1016/j.proeng.2013.12.193.

Shahid, A., Hossain, I., Hossain, D., & Ali, A. (2016). Effect of Different Dyeing Parameters on Color Strength & Fastness Properties of Cotton-Elastane (CE) and Lyocell-Elastane (LE) Knit Fabric. *International Journal of Textile Science*, *5*(1), 1–7. https://doi.org/10.5923/j.textile.20160501.01.

Sharma, A., Singh, A., Khosla, A., & Arya, S. (2021) Preparation of cotton fabric based non- invasive colorimetric sensor for instant detection of ketones. *Journal of Saudi Chemical Society 25*, *10*, 101340. https://doi.org/10.1016/j.jscs.2021.101340.

Shikuku, V. O., Zanella, R., Kowenje, C. O., Donato, F. F., Bandeira, N. M. G., & Prestes, O. D. (2018). Single and binary adsorption of sulfonamide antibiotics onto iron - modified clay : linear and nonlinear isotherms , kinetics , thermodynamics , and mechanistic studies. *Applied Water Science*, *8*(175). https://doi.org/10.1007/s13201-018-0825-4

Shindhal, T.; Rakholiya, P.; Varjani, S.; Pandey, A.; Ngo, H.H.; Guo, W.; Ng, H.Y.; Taherzadeh, M.J. A Critical Review on Advances in the Practices and Perspectives for the Treatment of Dye Industry Wastewater. Bioengineered 2021, 12, 70–87. https://doi.org/10.1080/21655979.2020.1863034.

Siddiqua, U. H., Ali, S., Muzaffar, S., Subhani, Z., Iqbal, M., Daud, H., Iqbal, D. N., & Nazir, A. (2021). Hetero-functional azo reactive dyes applied on cellulosic fabric and dyeing conditions optimization to enhance the dyeing properties. Journal of Engineered Fibers and Fabrics. https://doi.org/10.1177/1558925021996710.

Sims, R.A.; Harmer, S.L.; Quinton, J.S. (2019) The Role of Physisorption and Chemisorption in the Oscillatory Adsorption of Organosilanes on Aluminium Oxide. *Polymers* 11, 410. https://doi.org/10.3390/polym11030410.

Singh, R., Jain, A., Panwar, S., Gupta, D., & Khare, S. K. (2005). Antimicrobial activity of some natural dyes. *Dyes and Pigments*, *66*(2), 99–102. https://doi.org/10.1016/j.dyepig.2004.09.005.

Singh, S. (2012). Phytochemical analysis of different parts of *Prosopis juliflora*, *International Journal of Current Pharmaceutical Research 4(3),* 59-61. https://innovareacademics.in/journal/ijcpr/Issues/Vol4Issue3/532.pdf

Singh, S., & Kaushal, A. (2017) Adsorption phenomenon and its application in removal of lead from waste water: a review. *Int. J. Hydrol*., 1, 2.

Singh, Shachi, & Verma, S. (2011). Antibacterial properties of Alkaloid rich fractions obtained from various parts of *Prosopis juliflora*. *International Journal of Pharma Sciences and Research (IJPSR*, *2*(3), 114–120.

Singh, Shweta, & Singh, D. R. (2018). Application of natural mordants on textile. *International Journal of Applied Home Science*, *5*(1), 252–260.

Singleton, V. L., Orthofer, R., & Lamuela-Ravent, R. M. (1999). Analysis of Total Phenols and Other Oxidation Substrates and Antioxidants by Means of Folin-Ciocalteu Reagent. *Methods in Enzymology*, *299*(1974), 152–178.

Sirmah, P. K. (2018). Ability of (-) -Mesquitol Isolated from *Prosopis juliflora* Heartwood to Inhibit Fungal and Bacterial Growth in a Laboratory Test. *International Journal of Microbiology and Application A*, *5*(4), 93–98.

Sirmah, P., Mburu, F., Iaych, K., Dumarçay, S., & Gérardin, P. (2011). Potential antioxidant compounds from different parts of *Prosopis juliflora*. *Journal of Tropical Forest Science*, *23*(2), 187–195. https://doi.org/10.2307/23616919

Sivanandham, V. (2015). Phytochemical techniques - a review. *World Journal of Science and Research*, *1*(2), 80–91.

Slama, H.B.; Chenari Bouket, A.; Pourhassan, Z.; Alenezi, F.N.; Silini, A.; Cherif-Silini, H.; Oszako, T.; Luptakova, L.; Golińska, P.; Belbahri, L. Diversity of Synthetic Dyes from Textile Industries, Discharge Impacts and Treatment Methods. Appl. Sci. 2021, 11, 6255. https://doi.org/10.3390/app11146255.

Smoczyński, L.; Pierożyński, B.; Mikołajczyk, T. (2020) The Effect of Temperature on the Biosorption of Dyes from Aqueous Solutions. Processes 8, 636. https://doi.org/10.3390/pr8060636.

Song, Y., Wang, F., Bian, Y., Orori, F., Jia, M., & Xie, Z. (2012). Bioavailability assessment of hexachlorobenzene in soil as affected by wheat straw biochar. *Journal of Hazardous Materials*, *217–218*, 391–397. https://doi.org/10.1016/j.jhazmat. 2012.03.055.

Souissi, M., Guesmi, A., & Moussa, A. (2018). Valorization of natural dye extracted from date palm pits (*Phoenix dactylifera*) for dyeing of cotton fabric. Part 1:

Optimization of extraction process using Taguchi design. *Journal of Cleaner Production*. https://doi.org/10.1016/j.jclepro.2018.08.115.

Srivastava, A., & Singh, T. G. (2011). Utilization of aloe vera for dyeing natural fabrics. *Asian Journal of Home Science, 6*(1), 1–4.

Sukirtha, K., & Gowther, L. (2012). Antibacterial,antifungal and phytochemical analysis of selected medicinal plants. Journal of Natural product and Plant Resource; 2(6): 644-648.

Suleiman, M. H. A., & Ateeg, A. A. (2020). Antimicrobial and Antioxidant Activities of Different Extracts from Different Parts of *Zilla spinosa* (L.) Prantl. *Evidence-Based Complementary and Alternative Medicine, 2020*, 6690433. https://doi.org/10.1155/2020/6690433.

Sultan, M., Miyazaki, T., & Koyama, S (2018) Optimization of adsorption isotherm types for desiccant air-conditioning applications *Renew. Energy*, 121 pp. 441-450.

Surjushe, A., Vasani, R., & Saple, D. G. (2008). *Aloe vera*: a short review. *Indian Journal of Dermatology, 53*(4), 163–166.

Swenson, H., & Stadie, N. (2019) Langmuir's theory of adsorption: a centennial review. *Langmuir*, 35 (16), 5409-5426.

Tanaka, H., Oda, S., Ricci, G., Gotoh, H., Tabata, K., Kawasumi, R., Beljonne, D., Olivier, Y., & Hatakeyama, T. (2021) Hypsochromic Shift of Multiple-Resonance-Induced Thermally Activated Delayed Fluorescence by Oxygen Atom Incorporation. *Angewandte Chemie - International Edition, 60(33),* 17910-17914. https://doi.org/10.1002/anie. 202105032.

Tang, C. Y., & Yang, Z. (2017). Transmission Electron Microscopy (TEM). In *Membrane Characterization*. Elsevier B.V. https://doi.org/10.1016/B978-0-444-63776-5.00008-5.

Teli, M. D., Sheikh, J., & Shastrakar, P. (2013). Exploratory Investigation of Chitosan as Mordant for Eco-Friendly Antibacterial Printing of Cotton with Natural Dyes. *2013*.

Thommes, M., Kaneko, K., Neimark, A., Olivier, J., Rodriguez-Reinoso, F., Rouquerol, J. & Sing, K. (2015). Physisorption of gases, with special reference to the evaluation of surface area and pore size distribution (IUPAC Technical Report). *Pure and Applied Chemistry*, 87(9-10), 1051-1069. https://doi.org/10.1515/pac-2014-1117.

Torun, M., Aracagök, Y. D., & Kabalak, M. (2018). Kinetic and Equilibrium Studies of

Adsorption of Reactive Red 120 on Chitin. *Hittite Journal of Science and Engineering*, *5*(4), 307–311. https://doi.org/0.17350/HJSE19030000

Toso, S., Baranov, D., Altamura, D., Scattarella,F., Dahl, J., Wang, X., Marras, S.,… Manna, L (2021). Multilayer Diffraction Reveals That Colloidal Superlattices Approach the Structural Perfection of Single Crystals. *ACS Nano* 15(4), 6243-6256. https://doi.org/10.1021/ acsnano.0c08929.

Tyler, D.J. (2005) Textile Digital Printing Technologies. *Textile Progress 37*(4), 1-65. https://doi.org/10.1533/tepr.2005.0004.

Ugya, A. Y., & Priatamby, A. (2016). Phytoremediation of Landfill Leachates Using Pistia Stratiotes: A Case Study of Kinkinau U/Ma'azu Kaduna, Nigeria. *Journal of Chemical, Environmental and Biological Engineering*, *1*(1), 7–10. https://doi.org/ 10.11648/j.jcebe.20160101.12.

Ukiwe, L.N., S.I. Ibeneme, C.E. Duru, B.N. Okolue, G.O. Onyedika, C.A. Nweze (2013) Chemical and electro-coagulation techniques in coagulation-floccculation in water and wastewater treatment- A review. J. Adv. Chem., 9, 1988–1999. https://doi.org/10.24297/jac.v9i3.1006.

Van der Kooi, C. J., Elzenga, J. T., Staal, M., & Stavenga, D. G. (2016). How to colour a flower: on the optical principles of flower coloration. Proceedings. Biological sciences, 283(1830), 20160429. https://doi.org/10.1098/rspb.2016.0429.

Van Wyk, B.-E. (2013). Uses of aloe in traditional and modern medicine. *Aloe*, *50*, 53–57. Retrieved from http://search.ebscohost.com/login.aspx?direct=true&db=awn& AN= 709444& site=ehost-live

Vani, M., & Manikandan, T. (2018). Phytochemical Analysis and Antioxidant Activity of Acanthus ilicifolius. *International Journal of Current Research*, *10*(12), 76891–76896.

Venkatesh, S., Venkatesh, & Quaff, A.R. (2017) Dye decomposition by combined ozonation and anaerobic treatment: Cost effective technology. Journal of Applied Research and Technology 15, 340-345. https://doi.org/10.1016/j.jart.2017.02.006.

Verma, V. K., & Mishra, A. K. (2010). Kinetic and Isotherm Modeling of Adsorption of Dyes Onto Rice Husk Carbon. *Global NEST Journal*, *12*(2), 190–196. Retrieved from https://journal.gnest.org/sites/default/files/JournalPapers/190196_638_ VERM A _12-2. Pdf.

Vijayakumar, L., Pavithra, S., Satheshkumar, M., Balasubramaniam, L., Prakaash, S., Sriram, K., … Nadu, T. (2016). A Novel And Cost Effective Method For Textile

Dye Degradation Using Sawdust Of Prosopis. *International Journal of Advanced Engineering Technology*, *VII*(II), 166–169.

Vijayarachavan, K., Padmesh, T., Palanivelu, K., & Velan, M. (2006) Biosorption of nickel(II) ions onto Sargassum wightii: application of two-parameter and three-parameter isotherm models. J. Hazard. Mater., 133 (1-3), 304-308.

Vital, R.K., Saibaba, K.V.N., & Shaik, K.B. (2016) Dye Removal by Adsorption: A Review. *Journal of Bioremediation & Biodegradation 7, 371.* https://doi.org/10.4172/2155-6199.1000371

Wabuyele, E., Bjorå, C., Nordal, I., & Newton, L. (2006). Distribution, diversity and conservation of the genus Aloe in Kenya. *Journal of East African Natural History*, *95*, 213–225. https://doi.org/10.2982/0012-8317(2006)95[213:DDACOT]2.0.CO;2

Waihenya, R.K., Mtambo, M.A., Nkwenguila, G., Minga, U.M., (2002).Efficacy of crude extract of Aloe secundiflora against Salmonella gallinarum in experimentally infected free-range chickens in Tanzania. *J Ethnopharmacol.* 79:317–23.

Wang, J., & Wang, S. (2019). Preparation, modification and environmental application of biochar: a review. *Journal of Cleaner Production*. https://doi.org/10.1016/j.jclepro.2019.04.282

Wanyama, P. A. G., Kiremire, B. T., Ogwok, P., & Murumu, J. S. (2010). The effect of different mordants on strength and stability of colour produced from selected dye-yielding plants in Uganda. *International Archive of Applied Sciences and Technology*, *1*(2), 81–92.

Weber, K., & Quicker, P. (2018). Properties of biochar. *Fuel*, *217*(January), 240–261. https://doi.org/10.1016/j.fuel.2017.12.054

Wei, Q., & Guo, W. (2020). Chemical Components of Volatile Oil from Leaves and Stems of *Celtis sinensis* Pers. *Journal of Essential Oil Bearing Plants ISSN:*, *23*(4), 772–778. https://doi.org/10.1080/0972060X.2020.1794984.

Wekoye, J. N., Wanyonyi, W. C., Wangila, P. T., & Tonui, M. K. (2020). Environmental Chemistry and Ecotoxicology Kinetic and equilibrium studies of Congo red dye adsorption on cabbage waste powder. *Environmental Chemistry and Ecotoxicology*, *2*, 24–31. https://doi.org/10.1016/j.enceco.2020.01.004.

Wijekoon, M. M. J. O., Bhat, R., Karim, A. A., & Fazilah, A. (2013). Chemical composition and antimicrobial activity of essential oil and solvent extracts of torch ginger inflorescence (Etlingera elatior Jack.). *International Journal of Food*

Properties, *16*(6), 1200–1210. https://doi.org/10.1080/10942912.2011.579674.

World Health Organization (2002) Environment Protection Act. Standards for effluent discharge regulations. General Notice No 44, Geneva, Switzerland

Xu, Z., Cai, Jg. & Pan, Bc. (2013) Mathematically modeling fixed-bed adsorption in aqueous systems. J. Zhejiang Univ. Sci. A 14, 155–176. https://doi.org /10.1631/jzus.A1300029.

Yagub, M. T., Sen, T. K., Afroze, S., & Ang, H. M. (2014). Dye and its removal from aqueous solution by adsorption : A review. *Advances in Colloid and Interface Science*, *209*, 172–184. https://doi.org/10.1016/j.cis.2014.04.002.

Yan, X., Fan, X., Wang, Q., & Shen, Y. (2017) An adsorption isotherm model for adsorption performance of silver-loaded activated carbon Therm. Sci., 21 pp. 48-48.

Yang, D. M., & Yuan, J. M. (2016). COD and Color Removal from Real Dyeing Waste water by Ozonation. Water environment research : a research publication of the Water Environment Federation, 88(5), 403–407. https://doi.org/10.2175/ 106143016X 14504669768697

Yang, X., Zhang, S., Ju, M., & Liu, L. (2019). Preparation and modification of biochar materials and their application in soil remediation. *Applied Sciences (Switzerland)*, *9*(7). https://doi.org/10.3390/app9071365

Yaseen, D.A., Scholz, M. (2018) Treatment of synthetic textile wastewater containing dye mixtures with microcosms. *Environmental Science and Pollution Research* 25, 1980–1997. https://doi.org/10.1007/s11356-017-0633-7.

You, X. Y., Chen,J.G., Hu,Y.N., (1990). Studies on the relation between bladder cancer and benzidine or its derived dyes in Shanghai. *Br J Ind Med*. 47(8), 544.

Yu, L., & Luo, Y. (2014) The adsorption mechanism of anionic and cationic dyes by Jerusalem artichoke stalk-based mesoporous activated carbon. *Journal of Environmental Chemical Engineering* 2, 220-229. https://doi.org/10.1016/j.jece.2013.12.016.

Yu, Q., Wang, Q., Li, B., Lin, Q., & Duan, Y. (2015). Technological Development of Antibody Immobilization for Optical Immunoassays : Progress and Prospects Critical Reviews in Analytical Chemistry Technological Development of Antibody Immobilization for Optical Immunoassays : *Progress and Prospects*. (June 2016). https://doi.org/10.1080/ 10408347.2014.881249.

Yunus, W., Ahmad, W., Rahim, R., Ahmad, M. R., Ismail, M., Kadir, A., & Misnon, M. I. (2011). *The Application of Gluta Aptera Wood (Rengas) as Natural Dye on Silk and Cotton Fabrics*. *1*(4), 545–551.

Yusuf, M., Mohammad, F., & Shabbir, M. (2016). Eco-friendly and effective dyeing of wool with anthraquinone colorants extracted from Rubia cordifolia roots : Optimization , colorimetric and fastness assay. *Journal of King Saud University - Science*, 4–11. https://doi.org/10.1016/j.jksus.2016.06.005.

Yusuf, M., Shahid, M., Ibrahim, M., Ahmad, S., Ali, M., & Mohammad, F. (2015). Dyeing studies with henna and madder : A research on effect of tin (II) chloride mordant. *Journal of Saudi Chemical Society*, *19*(1), 64–72. https://doi.org/10.1016/j.jscs.2011.12.020.

Zhang, C., Zhang, Z., Zhang, L., Li, Q., Li, C., Chen, G., … Hu, X. (2020). Evolution of the functionalities and structures of biochar in pyrolysis of poplar in a wide temperature range. *Bioresource Technology*, *304*(December 2019), 123002. https://doi.org/10.1016/j.biortech.2020.123002.

Zhang, J., Lü, F., Zhang, H., Shao, L., Chen, D., & He, P. (2015). Multiscale visualization of the structural and characteristic changes of sewage sludge biochar oriented towards potential agronomic and environmental implication. *Scientific Reports*, *5*, 1–8. https://doi.org/10.1038/srep09406.

Zhang, X., Zhang, P., Yuan, X., Li, Y., & Han, L. (2019). Effect of pyrolysis temperature and correlation analysis on the yield and physicochemical properties of crop residue biochar. *Bioresource Technology*, 122318.https://doi.org/10.1016/j.biortech.2019.122318.

Zhao, F., Wang, P., Lucardi, R. D., Su, Z., & Li, S. (2020). Natural Sources and Bioactivities of 2,4-Di-Tert-Butylphenol and Its Analogs. *Toxins*, *12*(35), 1–26. https://doi.org/doi:10.3390/toxins12010035.

Ziarani, G.M., Moradi, R., Lashgari, N., & Kruger, H.G. (2018) Introduction and Importance of Synthetic Organic Dyes. In: *Metal-Free Synthetic Organic Dyes*, pp. 1-7. https://doi.org/10.1016/B978-0-12-815647-6.00001-7.

Zubairu, A., & Mshelia, Y. M. (2015). Effects of Selected Mordants on the Application of Natural Dye from Onion Skin (Allium cepa). *Science and Technology*, *5*(2), 26–32. https://doi.org/10.5923/j.scit.20150502.02

APPENDICES

APPENDIX 1: FTIR OF PJ 300: PJ 300RR: PJ 300MB

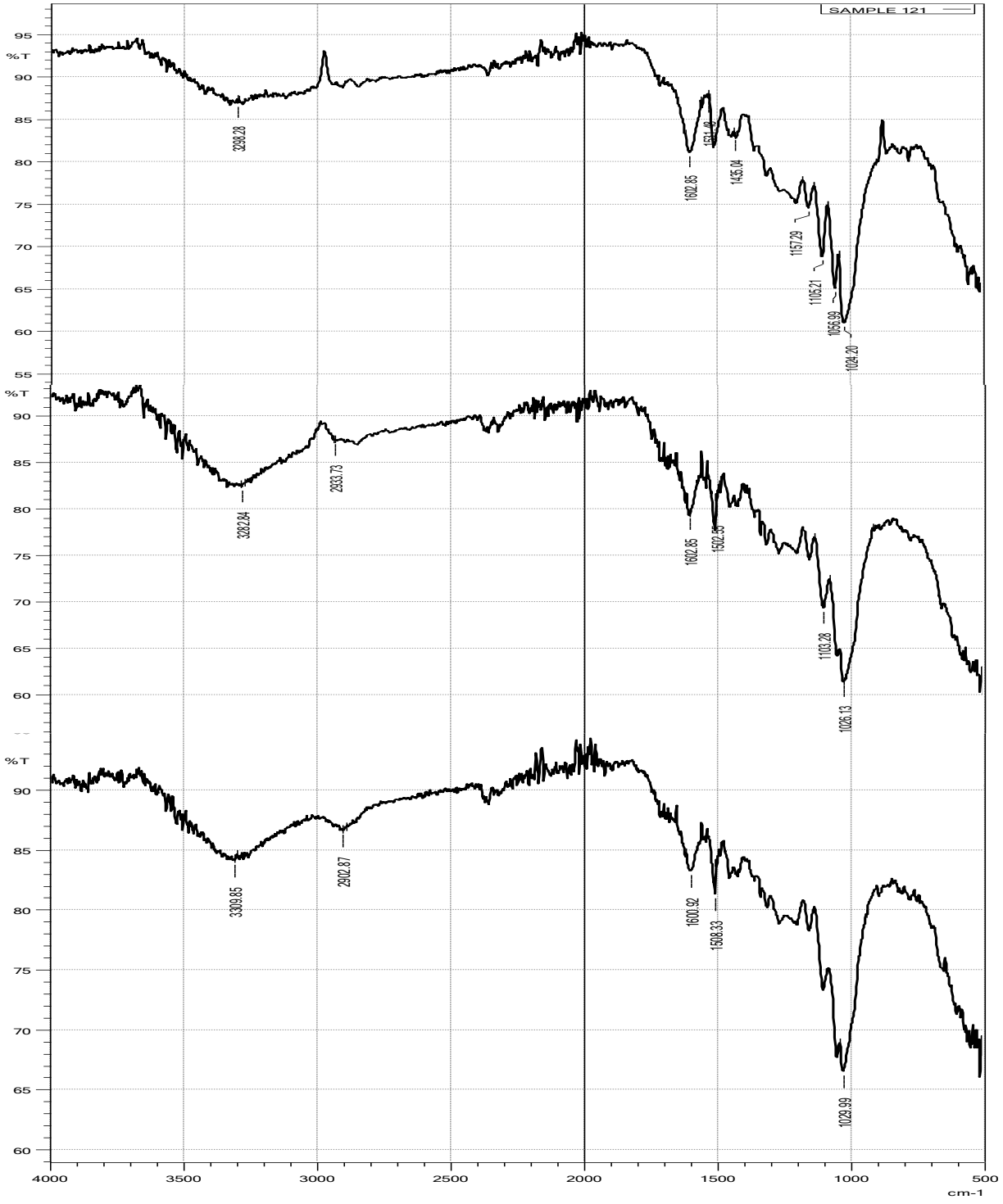

APPENDIX 2: FTIR OF PJ 500: PJ 500RR: PJ 500MB

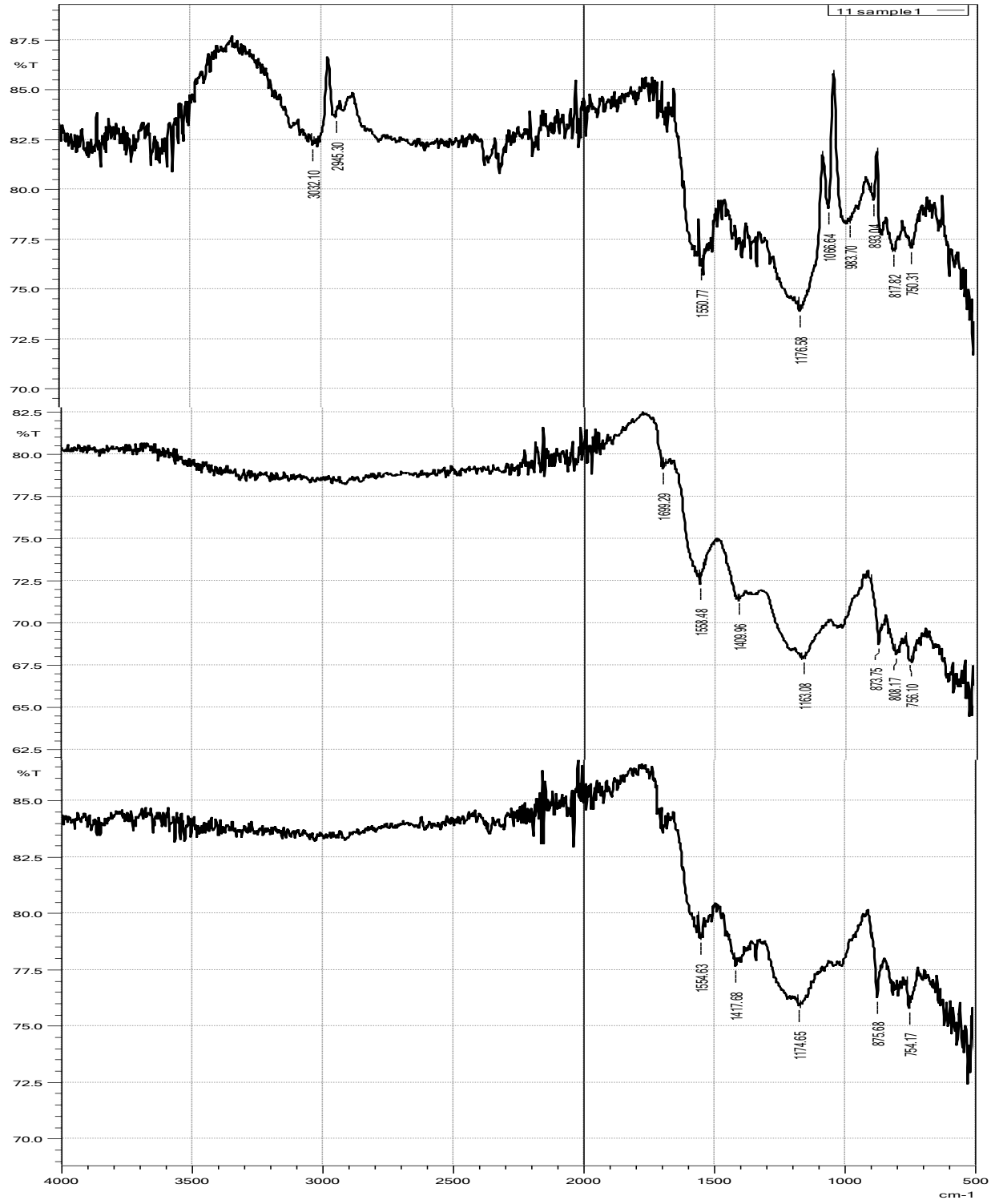

APPENDIX 3: FTIR OF AS 300: AS 300RR: AS 300MB

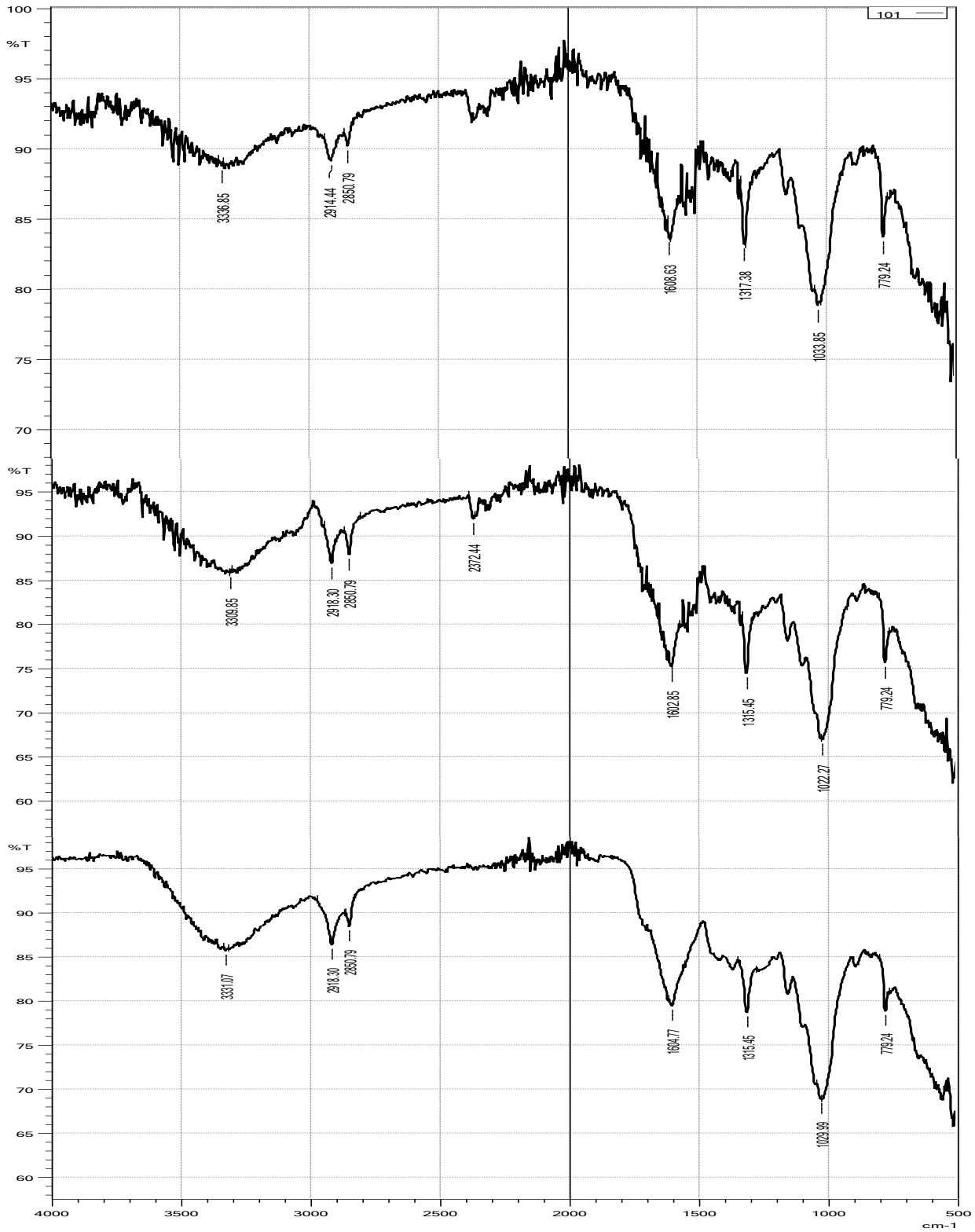

APPENDIX 4: FTIR OF AS 500: AS 500RR: AS 500MB

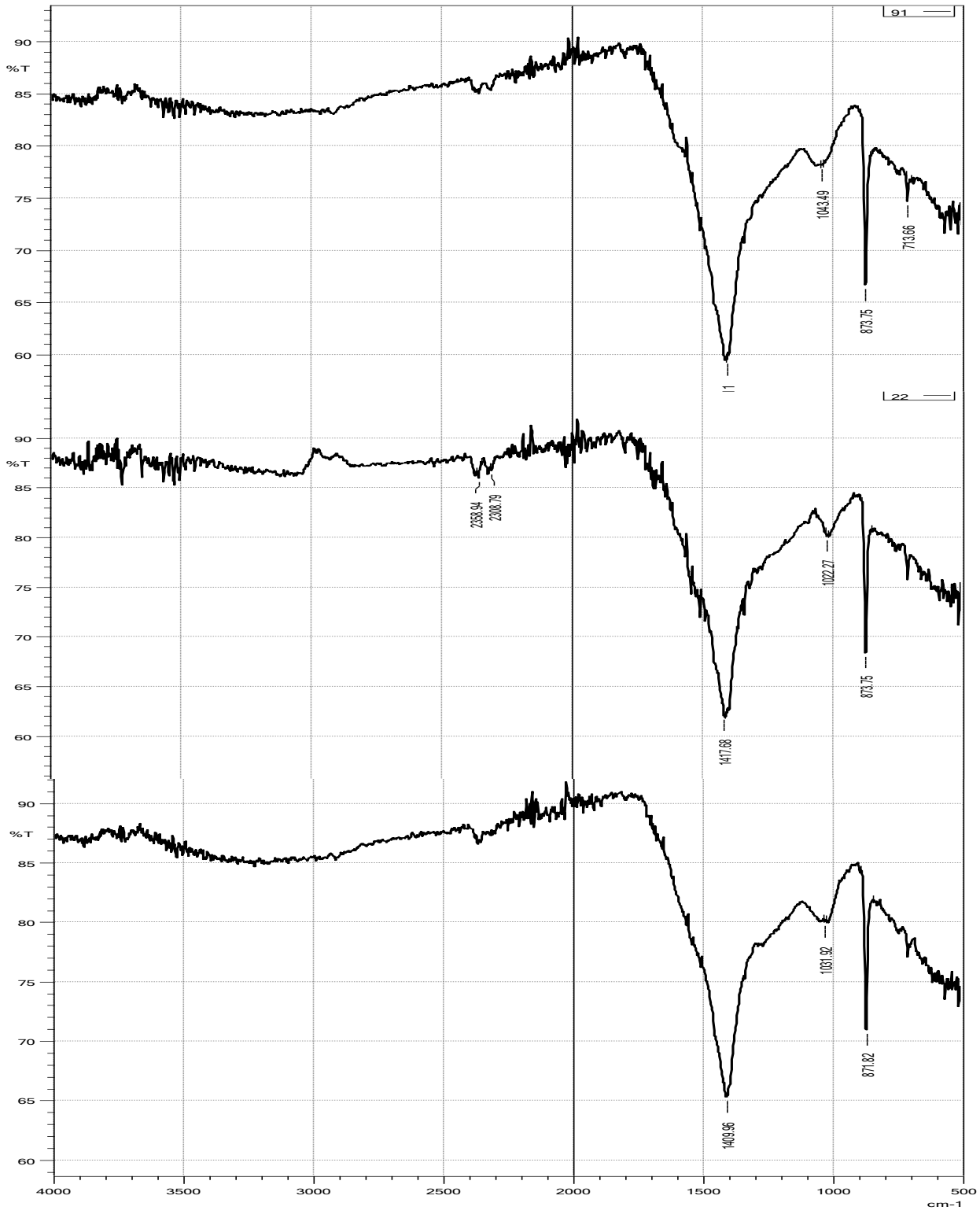

APPENDIX 5: XRD SPECTRUM OF PJ300

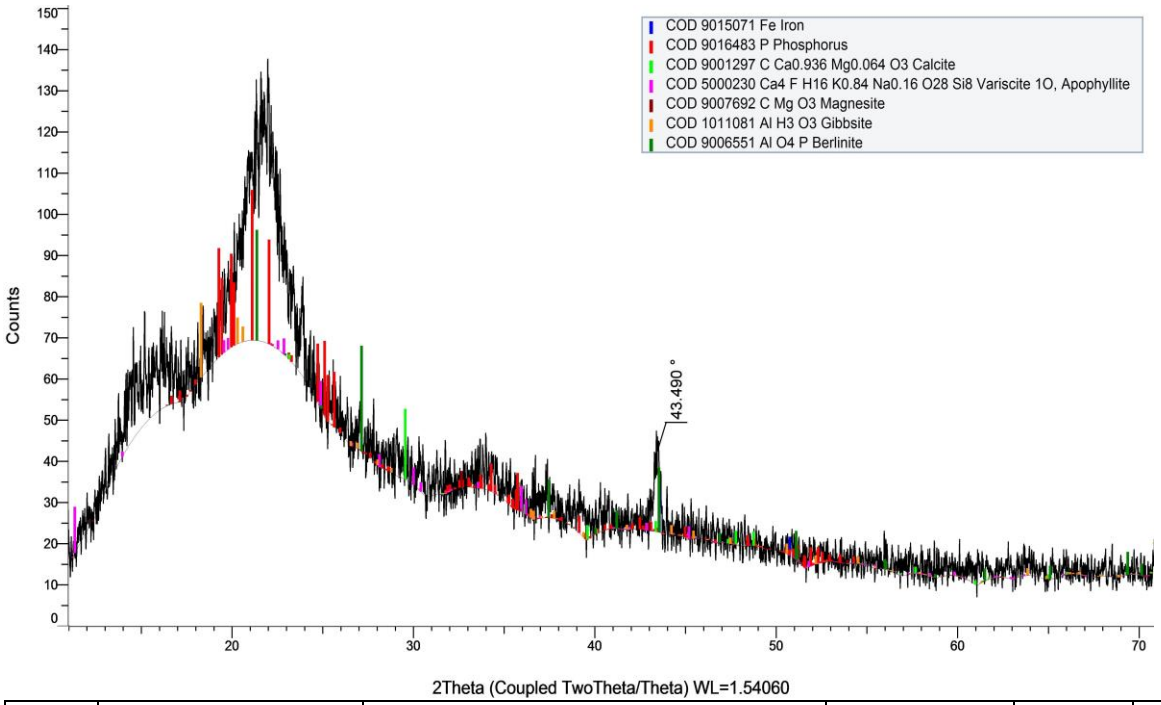

Index	Compound Name	Formula	Pattern #	I/Ic DB	S-Q
2	Phosphorus	P	COD 9016483	0.810	56.1 %
7	Berlinite	$Al\ O_4\ P$	COD 9006551	2.580	13.0 %
6	Gibbsite	$Al\ H_3\ O_3$	COD 1011081	2.060	10.9 %
4	Variscite 1O, Apophyllite	$Ca_4\ F\ H_{16}\ K_{0.84}\ Na_{0.16}\ O_{28}\ Si_8$	COD 5000230	1.420	9.8 %
3	Calcite	$C\ Ca_{0.936}\ Mg_{0.064}\ O_3$	COD 9001297	3.410	6.2 %
5	Magnesite	$C\ Mg\ O_3$	COD 9007692	1.910	2.6 %
1	Iron	Fe	COD 9015071	9.740	1.3 %

APPENDIX 6: XRD SPECTRUM OF PJ 500

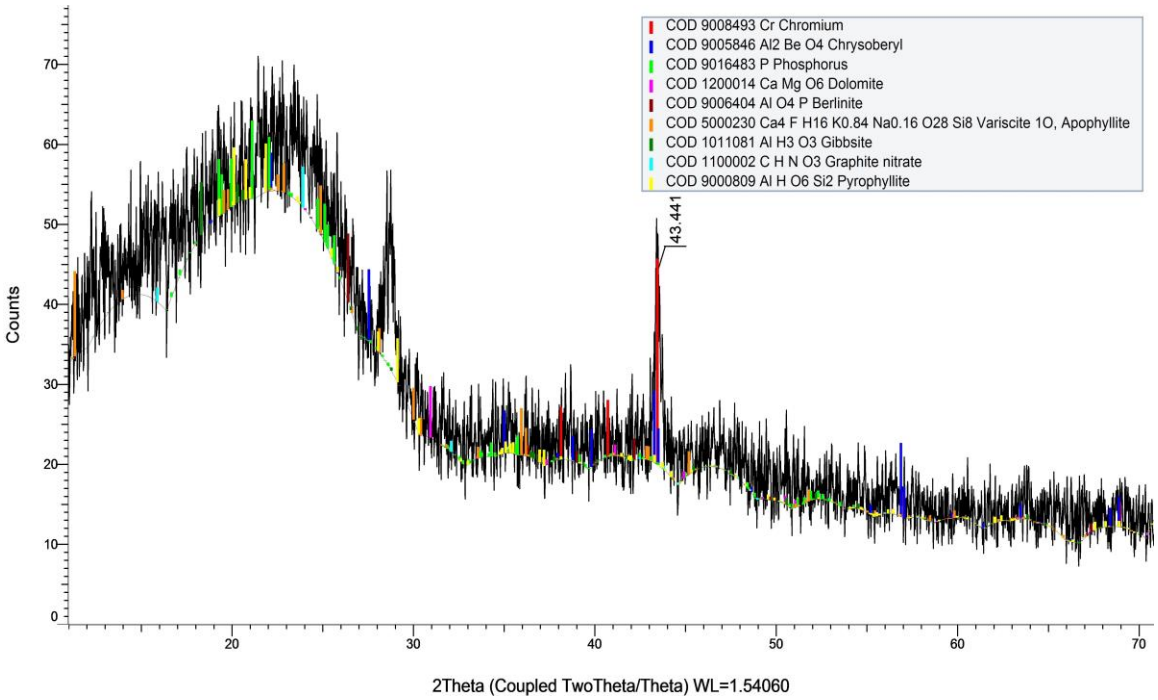

Index	Compound Name	Formula	Pattern #	I/Ic DB	S-Q
2	Chrysoberyl	Al_2 Be O_4	COD 9005846	0.700	24.2 %
3	Phosphorus	P	COD 9016483	0.810	22.2 %
9	Pyrophyllite	Al H O_6 Si_2	COD 9000809	0.820	16.2 %
6	Variscite 1O, Apophyllite	$Ca_4FH_{16}K_{0.84}Na_{0.16}O_{28}$ Si_8	COD 5000230	1.420	13.8 %
1	Chromium	Cr	COD 9008493	7.930	6.0 %
7	Gibbsite	Al H_3 O_3	COD 1011081	2.060	5.9 %
8	Graphite nitrate	C H N O_3	COD 1100002	11.610	4.9 %
4	Dolomite	Ca Mg O_6	COD 1200014	2.690	4.4 %
5	Berlinite	Al O_4 P	COD 9006404	6.390	2.5 %

APPENDIX 7: XRD SPECTRUM OF AS 300

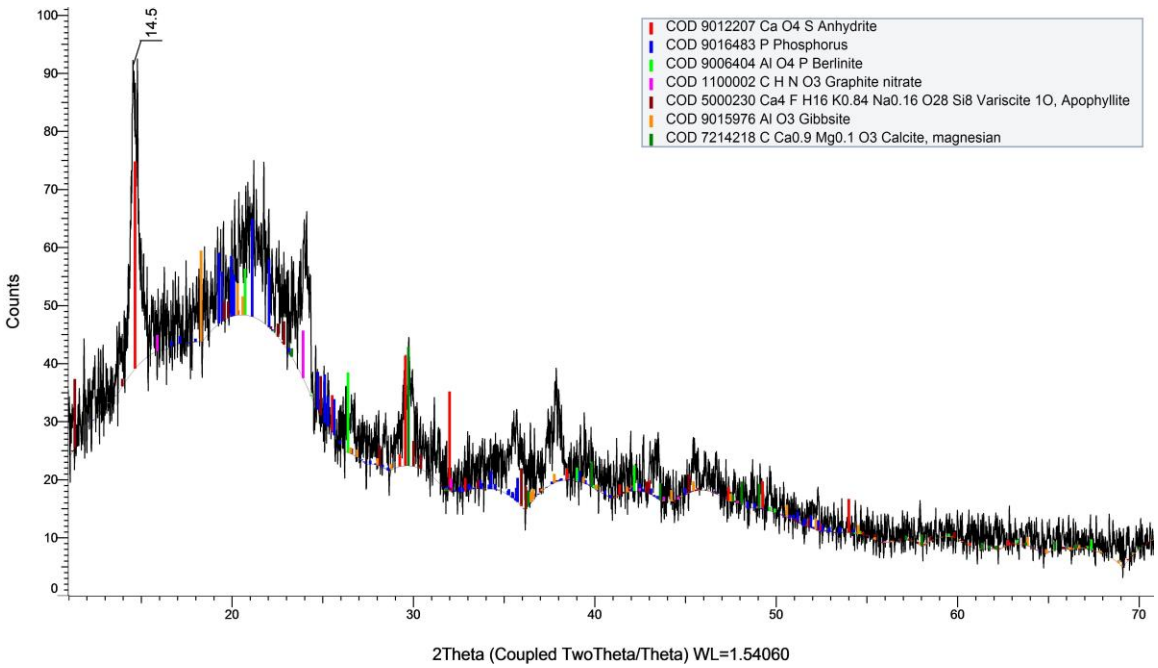

Index	Compound Name	Formula	Pattern #	I/Ic DB	S-Q
2	Phosphorus	P	COD 9016483	0.810	32.8 %
1	Anhydrite	CaO_4S	COD 9012207	2.490	22.6 %
5	Variscite1O, Apophyllite	$Ca_4FH_{16}K_{0.84}Na_{0.16}O_{28}Si_8$	COD 5000230	1.420	13.0 %
6	Gibbsite	AlO_3	COD 9015976	2.060	12.0 %
7	Calcite, magnesian	$C\ Ca_{0.9}Mg_{0.1}O_3$	COD 7214218	3.350	9.6 %
4	Graphite nitrate	$CHNO_3$	COD 1100002	11.610	6.6 %
3	Berlinite	AlO_4P	COD 9006404	6.390	3.4 %

APPENDIX 8: XRD SPECTRUM OF AS 500

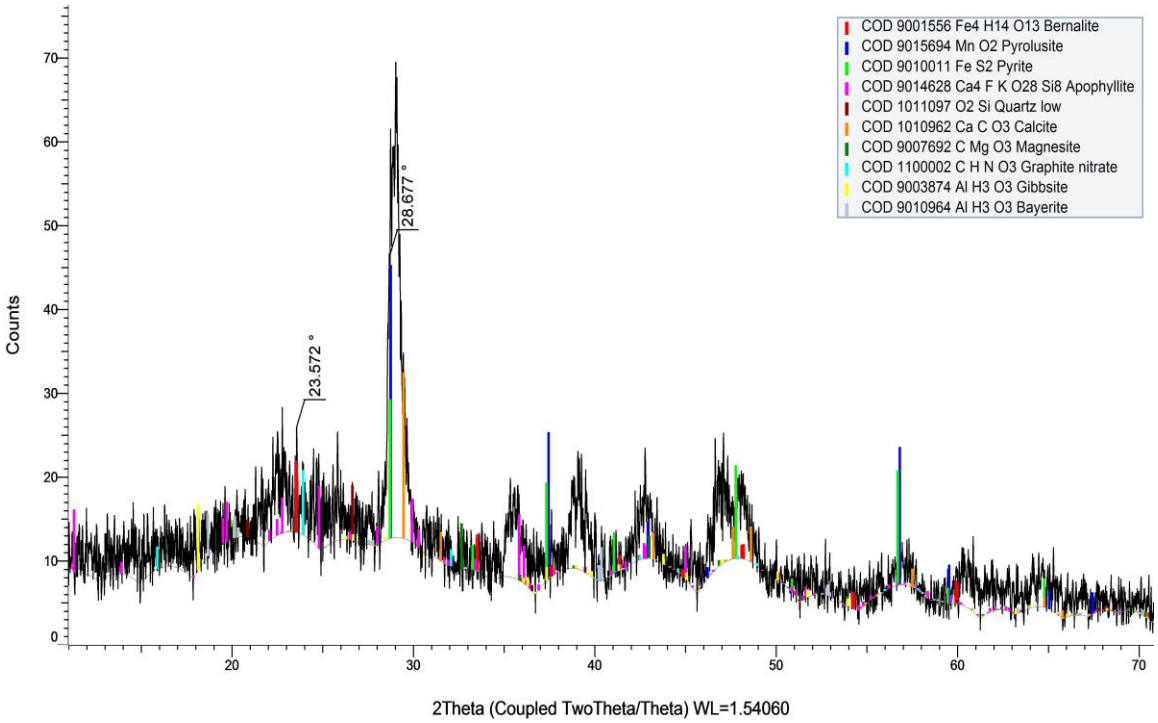

Index	Compound Name	Formula	Pattern #	I/Ic DB	S-Q
4	Apophyllite	Ca_4 F K O_{28} Si_8	COD 9014628	0.860	18.9 %
2	Pyrolusite	Mn O_2	COD 9015694	4.060	16.5 %
6	Calcite	$CaCO_3$	COD 1010962	3.820	10.7 %
3	Pyrite	FeS_2	COD 9010011	3.290	10.4 %
1	Bernalite	$Fe_4H_{14}O_{13}$	COD 9001556	1.780	9.8 %
9	Gibbsite	AlH_3O_3	COD 9003874	1.800	8.9 %
8	Graphite nitrate	$CHNO_3$	COD 1100002	11.610	8.2 %
10	Bayerite	AlH_3O_3	COD 9010964	1.400	7.5 %
7	Magnesite	$CMgO_3$	COD 9007692	1.910	5.9 %
5	Quartz low	O_2 Si	COD 1011097	4.430	3.1 %

APPENDIX 9: TEM IMAGES OF PJ 300: PJ 300RR: PJ 300MB RESPECTIVELY

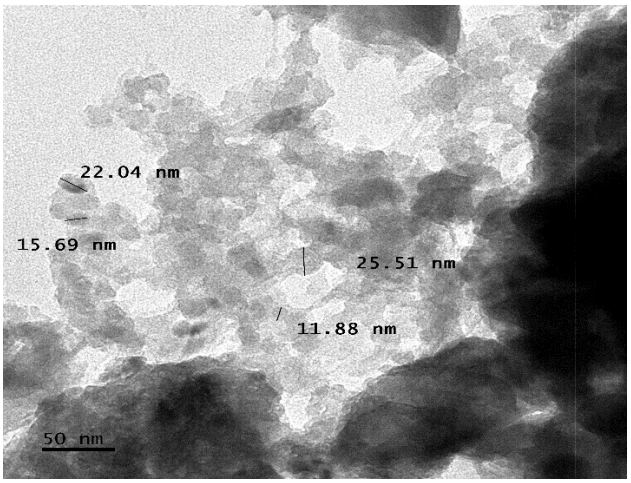

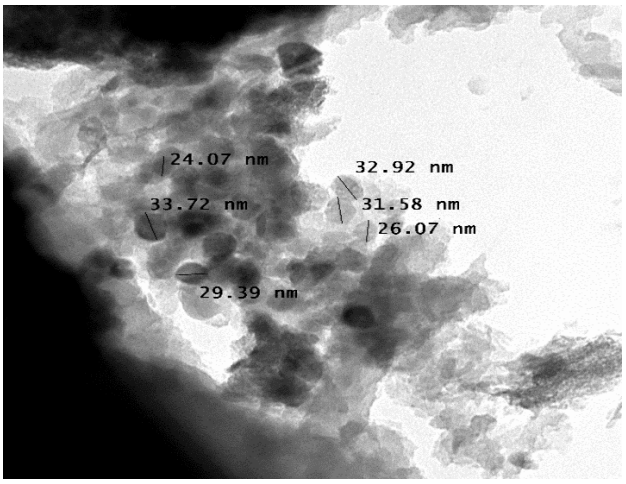

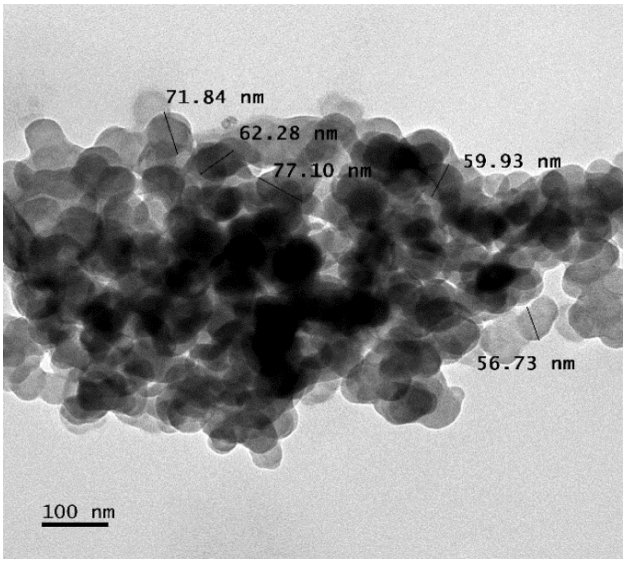

APPENDIX 10: TEM IMAGES OF PJ 500: PJ 500RR: PJ 500MB

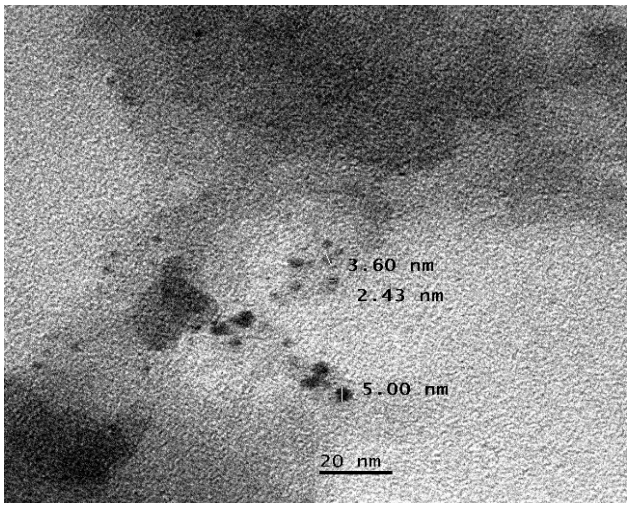

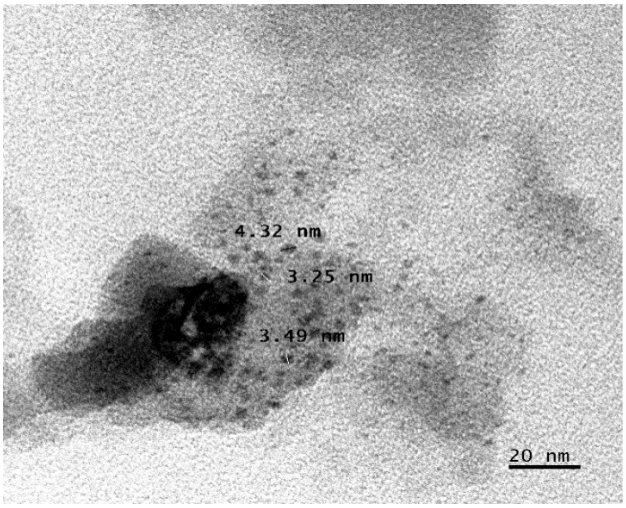

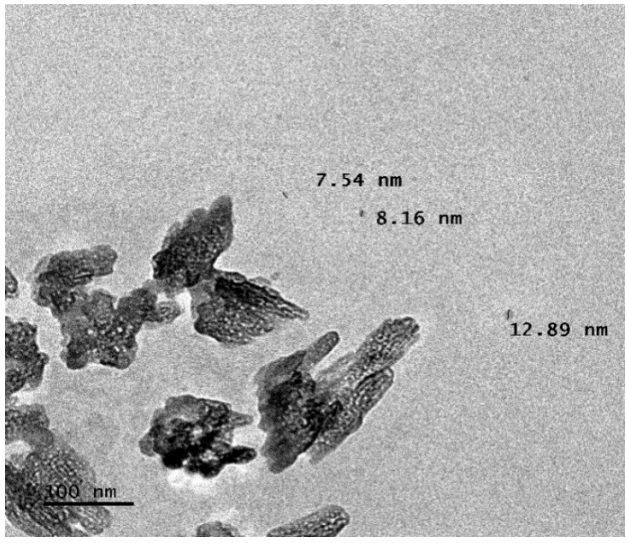

APPENDIX 11: TEM IMAGES OF AS 300: AS 300RR: AS 300MB

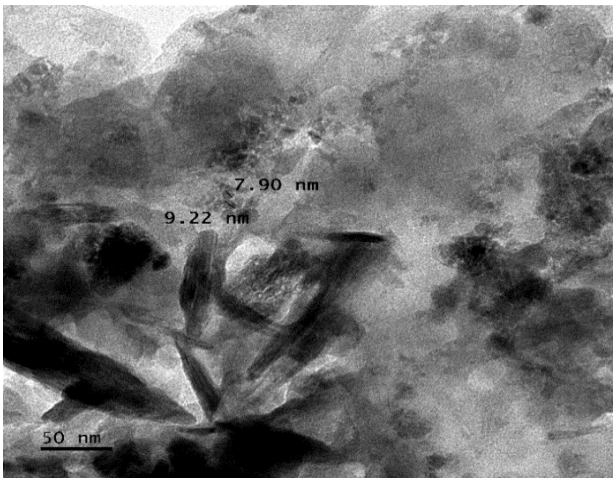

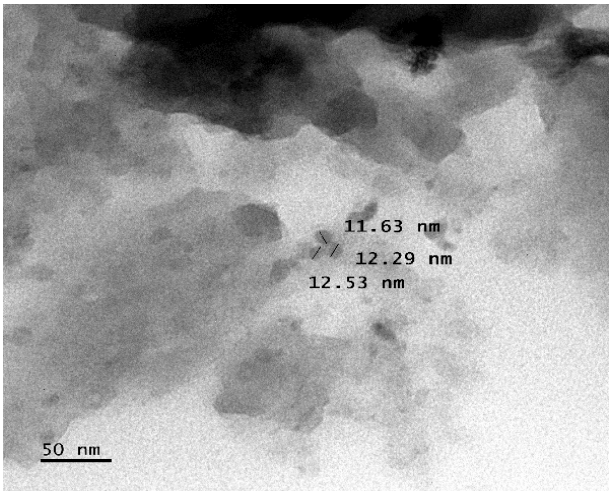

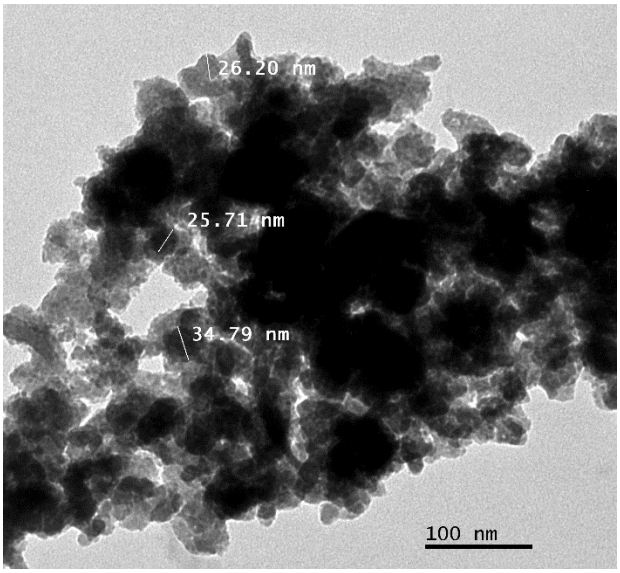

APPENDIX 12: TEM IMAGES OF AS 500: AS 500RR120: AS 300MB

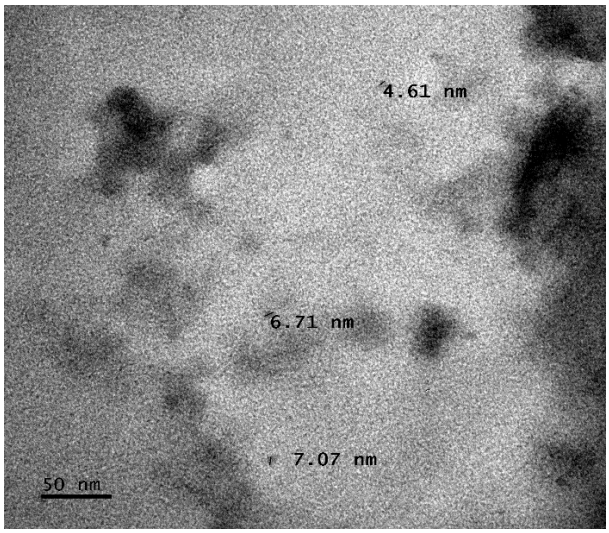

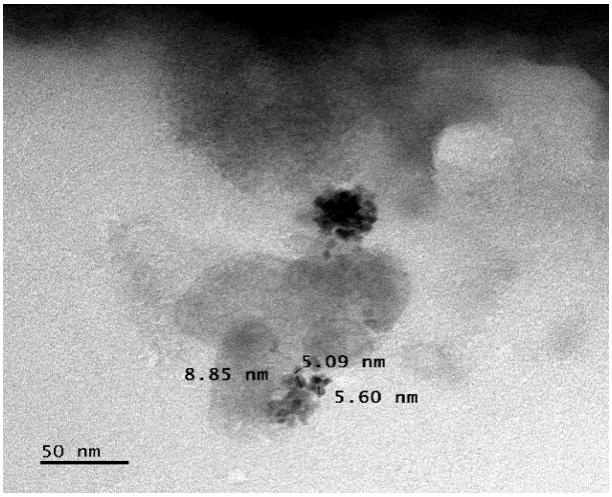

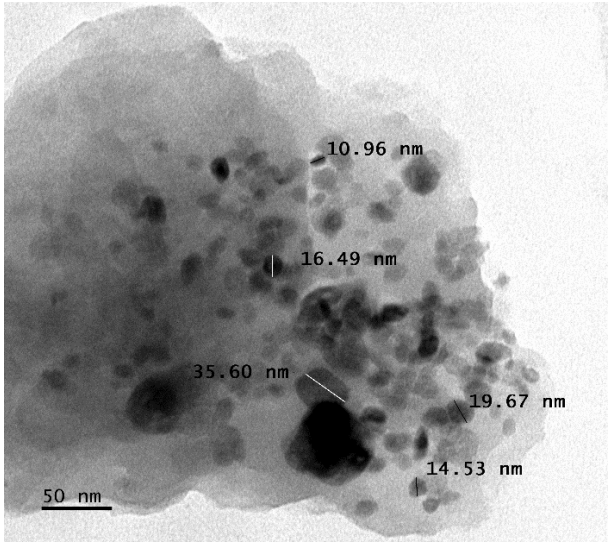

APPENDIX 13: PIECES OF DYED FABRIC

Dyed fabric of both *P. juliflora* and *A.succotrina*

APPENDIX 14: PREPARATION FOR LIGHT FASTNESS TESTS